UNIVERSITAT DE BARCELONA

Clues to the function of AWR effector proteins by expression on heterologous systems

Caracterització funcional de les proteïnes efectores AWR mitjançant l'expressió en sistemes heteròlegs

Crina Mihaela Popa

Facultat de Biologia

Departament de Genètica

Programa de doctorat: Biotecnologia

“Clues to the function of AWR effector proteins by expression on heterologous systems"

(Caracterització funcional de les proteïnes efectores AWR mitjançant l’expressió en sistemes heteròlegs)

Memòria presentada per Crina Mihaela Popa per tal d’optar al títol de Doctora expedit per la Universitat de Barcelona. Tesi doctoral realitzada sota la direcció del Dr. Marc Valls Matheu i la Dra. Núria Sánchez Coll al Departament de Genètica de la Facultat de Biologia (UB) i al Centre de Recerca en Agrigenòmica (CRAG).

Signatura dels Directors, Signatura de la doctoranda,

Dr. Marc Valls Matheu Dra. Núria Sánchez Coll Crina Mihaela Popa

Barcelona, Juliol 2015

ACKNOWLEDGEMENTS

CAST

(IN ORDER OF APPEARANCE)

MARC VALLS……BOSS NO.1/2

Encara me'n recordo del primer cop que vam parlar sobre el projecte del llevat. Un projecte quasi nou per tu i un món nou per mi. També me'n recordo del dia que em vas ensenyar a fer la primera transformació de llevat i restriar colònies de llevat en forma de 9 ☺. Gràcies per la oportunitat que em vas donar al lab BIOBACT (que de fet ha sigut el principi d'una nova etapa de la meva vida), per totes les coses que em vas ensenyar, per estar sempre pendent de mi i sobre tot pels ànims que em vas donar des del principi fins el final. Tot i que hauré tingut dies bons i de no tant bons, he gaudit molt amb aquest projecte i amb les moltes mudances de laboratori que vam fer ☺. I com em vas dir una vegada: Projects survive people, espero que aquest projecte també sobrevisqui d'una manera o altra.

MONTSERRAT SOLÉ……SIMPLY MONTSE

Montse, que et puc dir que no sàpigues? Me n'alegro molt que encara compartim laboratori, com al principi del meu Erasmus i després del meu doctorat. Això no pot ser una simple casualitat. Gràcies per tot el que em vas ensenyar al món del labo des del principi fins ara i gràcies per les converses que hem tingut durant tots aquests anys (sempre prenent infusions, clar!), per voler conèixer el meu món (el viatge a Romania!) i per deixar-me conèixer el teu.

ORIANE MITH……HÉRISSON

Oriane, le laboratoire BIOBACT avait pas été le même sans toi! Merci pour tous les jours nous avons partagé nos préoccupations au sujet de la science et de la vie et de me donner une autre vision, toujours optimiste.

FREDDY MONTEIRO……HIMSELF ☺

Gracias por todas las discusiones científicas que hemos tenido en el laboratorio, en los congresos, y los dibujos en papel de poyata sobre como clonar. Y gracias por mostrarme un trocito del jazz barcelonés.

MARINA, ESTHER, PILAR, SHEILA, FLORI, MARTA, ANNE, ISAAC……EQUIPO UB

Gràcies a tots per rebre´m al món UB i ensenyar-me'n una mica de Barcelona.

CRIS, LIDIA, SONIA, AARON, PATRICIA, MIREIA, MARCELO, ROSANY, RAQUEL, MARCEL……LAB ROSA

Gracias por recibirme en vuestro rinconcito de labo, y por todos los momentos divertidos. Cris, echo de menos los días en que a las 8 de la noche sólo estábamos tu y yo en el labo. También echo de menos la hora "pedorra" (no tengo ni idea como se escribe ☺).

ARES, MARIA, LLUISA, JUANJO Y CLARA……LAB VIRUS

Vecinos de experimentos, un placer compartir el laboratorio con vosotros, sobre todo las tardes con la radio a tope!

JOAQUIN ARIÑO……HIMSELF

Muchas gracias por todas las discusiones científicas y por guiar una parte de este proyecto. Gracias por estar siempre dispuesto a ayudarme y por "iniciarme" en el mundo TOR.

ASIER GONZALEZ, LAURA TATJER.....EQUIPO UAB

Asier, muchas gracias por enseñarme el mundo de las levaduras, aún me acuerdo del primer día que vimos células expresando *awr5* en el microscopio. Gracias por compartir conmigo todos tus conocimientos "levadurísticos". Laura, gracias por estar siempre pendiente de este proyecto y por ayudarme con todas las inquietudes y los "problemas" relacionados con las levaduras.

PABLO PÉREZ.....LIBRETITTA/SOSO 1

Me alegro mucho que hemos coincidido todos estos años, desde el principio y hasta el final (que lastima que no hemos podido hacer la fiesta final juntos!). Gracias por todos los momentos que hemos compartido hablando de ciencia o de la vida, y por todas las conversaciones en los viajes que hemos hecho (cuando los "sosos" estaban ocupados). Y estoy segura que aún nos esperan muchas aventuras en el "mundo ideal"!

LUIS MATÍAS.....EL DIVERTIDO 1

Luis, espero que consigamos ver Cuenca juntos en esta vida! Gracias por los ánimos en cuestiones científicas o en cosas de supervivencia (recuerdas el rafting???: NUNCA MAS!).

JORDI PERACAULA.....EL DIVERTIDO 2

Crec que els dos vam viure aquest projecte d'una manera diferent, però junts. Moltes gràcies per acompanyar-me en aquesta aventura i per donar-me sempre una visió diferent del "problema". I gràcies per les plaques que alguna vegada em vas preparar, pels dibuixos, per l'índex (:p) i per estar sempre "aquí".

PAOLA ZULUAGA.....LEIDI PAOLA

Paola, no voy a olvidar nunca las palabras "chévere" y "mi chandita"! Gracias por todas las discusiones científicas, por estar siempre pendiente de ayudarme en el labo y por tu optimismo. Aunque no te guste el sushi :p, he disfrutado mucho con las comidas juntas, las excursiones, las salidas de karaoke, la salida al gym jeje y todos los momentos del laboratorio.

NÚRIA SÁNCHEZ COLL.....BOSS NO.1/ 2

Me'n recordo molt bé del viatge a Japó quan vaig conèixer la Núria. Després vaig conèixer la Dra. Sánchez-Coll, posant per tot arreu coses de color rosa ☺. Moltes gràcies per totes les coses "de plantes" que em vas ensenyar, i per les noves perspectives que has donat al meu treball. Crec que aquest projecte no hagués estat el que és sense tu. I jo tampoc ☺ Després moltes gràcies per donar-me la oportunitat de formar part d'un nou projecte i d'aprendre mes coses, també de poder gaudir de temps, i no del temps a Suècia jeje. Gràcies pels ànims i per estar disponible a qualsevol hora per parlar sobre coses científiques o del món CRAG, pel karaoke a la muntanya (tenim vídeos jeje), les partides de Catan, pel sopar turc a Goteborg, pels moments a Sant Cugat o Mira-sol i pel que seguirà.

MITSUAKI TABUCHI.....HIMSELF

It's almost 3 years now since I have met you. I gladly remember the first days in your lab, all the yeast techniques you showed me and all the scientific discussions and drawings we shared. Thank you for always being there to help and for introducing me in a professional yeast environment. I will probably never forget the "Udon" ☺, and the trips we made, the barbecues and meals in your place, and all the amazing Japanese places and traditions you showed me. It was a lifetime experience.

MARINA PUIGVERT.....HERSELF

Marina, gràcies per ajudar-me amb tot el que he necessitat al laboratori. Gràcies pels ànims, pels moments de riure a l'hora de dinar (sense parar!), pels moments seriosos on vam intentar resoldre dilemes juntes (com per exemple: apuntar-me al SAF o no?jeje) i per tot el que seguirà. I a veure si et converteixes en la meva nova companya de gym ☺

HAIBIN LU.....HIMSELF

Haibin, thanks a lot for all the moments we shared. Remember the Chinese dinner on New Year's Eve? And the many times you brought delicious food to taste for lunch. Thank you also for all the scientific ideas you shared with me and for all the times you were there to help.

SERGIO GIL.....HIMSELF

Estic molt contenta d'haver pogut compartir una part del meu projecte amb tu i una mica del món TOR. Moltes gràcies per ajudar-me i per tots els moments compatits al labo i fora d'ell.

MARC PLANAS.....MARK STARK ☺

Gràcies per tots els moments divertits al labo i al P2 (així he après a infiltrar tomàquets estil high-throughput jeje). Ha sigut un plaer compartir la passió per GOT i després per Vikings. A veure que trobem en un futur.

SAÚL LEMA.....HIMSELF

Saúl, muchas gracias por todos los momentos que hemos compartido en el laboratorio y volviendo a casa en tren. Tengo que agradecerte por los infinitos stocks de glicerol y tú diciéndome: Aún estás haciendo experimentos? ☺

PEDRO COSTA.....PEDOR

Pedroooo, gràcies per tots els moments de riure sense parar, dels missatges/whatsapps d'ànims i totes les vegades que has estat allà per ajudar-me (no m'oblido de les minipreps jeje). Ara ja ho sé, quan tingui un problema, tenim el "Strong Women" grup.

CARMEN, MARIA JOSE, AGNESE, ROSANY, JUDIT, ARNAU.....EQUIPO GYM

Carmen, muchas gracias por ser mi primera compañera de gym, por los muchos momentos que hemos compartido en el CRAG y en Barcelona. Chiqui, gracias por las muchísimas veces que me sacaste las placas de levadura los fines de semana y por "iniciarme" en la clase de "spinning" ☺ Agnese, gracias por enseñarme como subir en una tela (es muy importante para acabar un doctorado!). Rosany, muchas gracias por todos los momentos que hemos compartido y "sudado" en el gym. Judit, primero tengo que agradecerte por los momentos que compartimos yendo en coche cada mañana al CRAG, perquè segurament tu parlaves més que jo pels matins. I després vam compartir (amb l'Arnau també) molts moments guais i intensos a les classes de "power" i "spinning". Moltes gràcies a tots dos pels ànims que m'heu donat sobre tot al final.

Gràcies Irma, Roger, Alba, Pol, thanks Aliki, Anthi for being always there to help or to have fun.

"TOT EL CRAG"

And I thank to all the "CRAG" people who contributed to this work, who were always there to help, every time I had a problem or every time I needed to talk about science or about "things". To all the people I shared the train with every morning and every evening. Ha estat una experiència molt "CRACK".

Și mulțumesc tuturor celor care au fost alături de mine necondiționat și dintotdeauna in toți acești ani. Mulțumesc, Adela, pentru tot timpul pe care l-am petrecut in Barcelona, in București, in Japonia, la Vama Veche, in Paris și oriunde am mai fost și o să mai mergem. Pentru nesfarșitele conversații in care vorbeam despre tot și nimic și pentru că ai fost mereu aproape. Multumesc Kuku, pentru energia pozitiva pe care mi-ai transmis-o de când ne-am cunoscut (in Barcelona!) și până acum, pentru nopțile cu Chino, pentru momentele spirituale (intotdeauna cu muzica). Multumesc Maria, pentru timpul pe care l-am petrecut in Sant Andreu, in Gracia, pentru rețetele noi de mancare (mai mult sau mai putin reușite:p), pentru momentele filozofice, pentru visele tale in care eu dormeam oriunde si pentru tot ce o să urmeze. Mulțumesc, Laura A. pentru că ești acolo oricând. Mulțumesc, Cristinutza, pentru optimismul pe care mi l-ai aratat in fiecare zi și pentru că te-ai gândit la mine. Mulțumesc, Alexandra Zuza, pentru toate mesajele

de incurajare pe care mi le-ai dat pe tot parcursul anilor ăștia; de abia aștept sa vin in Ro și sa mâncăm un orez cu lapte. Mulțumesc Irinuc, pentru toate clipele in care mi-ai alungat oboseala, pentru ca mi-ai transmis mereu energie si pentru tot timpul in care ai fost si vei fi aproape. Mulțumesc, Irina P., pentru toate poveștile pe care le-am avut pe drum spre casă și pentru multele momente de incurajare. Mulțumesc Cati, Crisulina și mulțumesc 12I ☺.

The end

Pentru tata, pentru inspiratia pe care mi-o transmite in fiecare zi

Pentru mama, pentru ca a fost si este mereu alaturi

Pentru Claudiu, Daciana, Tudor si Olivia, pentru toate lumile pe care mi le-au deschis

I per la Nala i el seu amo, que han mogut muntanyes dins meu.

INDEX

TABLE OF CONTENTS

INDEX ..... **v**

INTRODUCTION **1**

CHAPTER 1: MOLECULAR INSIGHTS INTO PLANT-PATHOGEN INTERACTION 3

CHAPTER 2: YEAST AS A HETEROLOGOUS MODEL SYSTEM TO UNCOVER TYPE III EFFECTOR FUNCTION 7

CHAPTER 3: TYPE III EFFECTORS IN *RALSTONIA SOLANACEARUM* 37

OBJECTIVES **41**

RESULTS **45**

CHAPTER 1: PHENOTYPIC CHARACTERIZATION OF AWR PROTEINS IN YEAST 47

CHAPTER2: IDENTIFICATION OF CELLULAR PROCESSES TARGETED BY AWR5 HETEROLOGOUS EXPRESSION IN YEAST 55

CHAPTER3: MOLECULAR MECHANISMS UNDERLYING AWR5-TRIGGERED INHIBITION OF THE YEAST TOR PATHWAY 61

CHAPTER4: IS AWR5 INHIBITING THE SAME KEY PROCESS *IN PLANTA*? 77

DISCUSSION **84**

CONCLUSIONS **97**

MATERIALS AND METHODS **101**

BIBLIOGRAPHY **115**

RESUM EN CATALÀ **137**

ANNEX **141**

INDEX

Acknowledgements i

INDEX ..... **v**

Table of contents vii

Index ix

Figures xiii

Tables xv

INTRODUCTION **1**

CHAPTER 1: MOLECULAR INSIGHTS INTO PLANT-PATHOGEN INTERACTION 3

CHAPTER 2: YEAST AS A HETEROLOGOUS MODEL SYSTEM TO UNCOVER TYPE III EFFECTOR FUNCTION 7

2.1 Approaches using yeast for T3E characterization 8

Heterologous expression of T3E in yeast 8

Testing known cellular processes/pathways 13

Effector repertoire screens 15

Phenotype suppressor screens 16

Synthetic lethality screens 17

Protein affinity purification and µLC-MS/MS 18

Screens for drugs inhibiting pathogen growth 19

Transcriptomic analyses using DNA microarrays 20

2.2 Conserved cellular processes targeted by bacterial T3E in yeast 21

Disruption of the cytoskeleton 24

Rho family of small GTPases: "favorite" targets of bacterial effector proteins 25

Inhibition of MAP kinase signaling 30

Modulation of pathogen-triggered cell death 31

Alteration of membrane structure and function 33

Perturbation of vesicle trafficking 34

CHAPTER 3: TYPE III EFFECTORS IN *RALSTONIA SOLANACEARUM* 37

OBJECTIVES **41**

RESULTS **45**

CHAPTER 1: PHENOTYPIC CHARACTERIZATION OF AWR PROTEINS IN YEAST 47

1.1. Expression of the *R. solanacearum awr* type III effectors in budding yeast causes growth inhibition 47

1.2. Characterization of the AWR5-dependent growth inhibition phenotype 50

CHAPTER2: IDENTIFICATION OF CELLULAR PROCESSES TARGETED BY AWR5 HETEROLOGOUS EXPRESSION IN YEAST 55
2.1. Expression of *awr5* mimics the transcriptional changes induced by the TORC1 inhibitor rapamycin 55
2.2. Effect of TORC1 activator cycloheximide on yeast cells expressing *awr5* 60
CHAPTER3: MOLECULAR MECHANISMS UNDERLYING AWR5-TRIGGERED INHIBITION OF THE YEAST TOR PATHWAY 61
3.1. Mutations in three genes involved in the TORC1 pathway rescue the yeast growth inhibition caused by AWR5 61
3.1.1. AWR5 impact on stress responses and NCR signalling 64
Mutation in Cdc55 attenuates AWR5-mediated transcriptional responses 67
Is PP2A subunit Cdc55 a direct target of AWR5? 70
3.1.2. AWR5 impact on protein and ribosome synthesis 72
3.2. *awr5* expression constitutively activates autophagy 73
3.3. Effect of *awr* genes expression on TORC1 downstream targets 75
CHAPTER4: IS AWR5 INHIBITING THE SAME KEY PROCESS IN PLANTA? 77
4.1. AWR5 alters the TOR pathway in plants 77
4.2. Effect of *awr5* expression on TOR downstream targets in *Arabidopsis thaliana* 79
4.3. Effect of *awr5* expression on TOR downstream targets in *Nicotiana benthamiana* 80
4.4. Role of AWR effector family in resistance to *Ralstonia solanacearum* in *Arabidopsis* plants with altered TOR levels 82
DISCUSSION 84
Challenges on the path to investigation of AWRs/AWR5 effector function 87
Yeast as a model system to decipher T3E function 89
At what level of the yeast TORC1 pathway is AWR5 acting? 90
The impact of AWR5 on the plant TOR pathway 93
CONCLUSIONS 97
MATERIALS AND METHODS 101
Plasmids, strains and gene cloning 103
Yeast strains and growth conditions 108
DNA microarray analysis 109
qRT-PCR 110
RNA-seq experiments 110
Protein assays 111
Plant material and growth conditions 112

Nitrate reductase assays....112
Pathogenicity assays *in planta*....113
BIBLIOGRAPHY....115
RESUM EN CATALÀ....137
ANNEX....141
Co-authored article 1:
"The *awr* gene family encodes a novel class of *Ralstonia solanacearum* type III effectors displaying virulence and avirulence activities"....143
Co-authored article 2:
"The plant metacaspase AtMC1 in pathogen-triggered programmed cell death and aging: functional linkage with autophagy"....157

FIGURES

FIGURE 1. Current view schematically depicting the cellular events underlying plant-microbe interactions 5

FIGURE 2. Schematic representation of the main processes targeted by T3Es in plant cells. 6

FIGURE 3: The most common phenotypes observed in *S. cerevisiae* upon T3E expression. 21

FIGURE 4. Yeast cellular processes targeted by bacterial type III effectors. 23

FIGURE 5. Full-length AWR5 causes growth inhibition in yeast when expressed from a high-copy-number plasmid. 48

FIGURE 6. Expression of *awr5* effector inhibits yeast growth. 49

FIGURE 7. Protein levels of the different AWR family members expressed in yeast. 49

FIGURE 8. Characterization of AWR-induced growth inhibition phenotype 50

FIGURE 9. *awr5* does not cause cell cycle arrest nor cell death in yeast. 52

FIGURE 10. AWR5-mediated yeast growth inhibition is not rescued by osmoprotection or respiration. 53

FIGURE 11. Expression of bacterial *awr5* in yeast mimics the transcriptomic changes caused by inhibition of the TORC1 pathway. 57

FIGURE 12. Transcriptional response of TORC1-related genes to *awr5* expression 58

FIGURE 13. Transcriptional response of *GLN1* and *GDH1* to *awr5* expression. 59

FIGURE 14. Effect of cycloheximide on yeast cells expressing *awr5*. 60

FIGURE 15. Schematic view of the Saccharomyces cerevisiae TORC1-regulated pathways 61

FIGURE 16. *cdc55, tpd3 and sch9* mutations suppress AWR5-induced yeast growth inhibition. 63

FIGURE 17. *cdc55* mutation attenuates AWR5-mediated growth inhibition. 64

FIGURE 18. Transcriptional response of GAP1 to awr5 expression. 65

FIGURE 19. Effect of *awr5* expression on yeast strains with altered levels of TORC1-regulated genes. 66

FIGURE 20. Correlation in gene expression data obtained by microarray hibridization vs RNA-seq. 67

FIGURE 21. Mutation of Cdc55 greatly attenuates AWR5 impact on the yeast transcriptional profile 69

FIGURE 22. Ratio between the repression caused by *awr5* expression in the wild type and cdc55 strains. 70

FIGURE 23. Co-immunoprecipitation of AWR5 and Cdc55 in yeast 71

FIGURE 24. Effect of *awr5* expression on Rps6 phosphorylation in wild-type and cdc55 mutant strains. 73

FIGURE 25. *awr5* expression induces constitutive autophagy, independently of Cdc55-PP2A activity 74

FIGURE 26. Transcriptional response of TORC1-related genes to awr effectors expression. 76

FIGURE 27. Interplay between AWR5 and TOR *in planta.* 78

FIGURE 28. Transcriptional response of *Arabidopsis thaliana* TOR-regulated genes to *awr5* expression. 79

FIGURE 29. Transcriptional response of nitrogen metabolism-related genes to *awr5* expression in *N. benthamiana.* 81

FIGURE 30. Pathogenicity test with *Ralstonia solanacearum* strains on *Arabidopsis thaliana* plants with altered levels of TOR. 83

TABLES

Table 1. Summary of methods used in characterization of type III effector function from plant and animal pathogens..... 9

Table 2. List of type III effectors from *Ralstonia solanacearum* studied *in planta* and their function. 38

Table 3. List of strains and plasmids used in this work..... 104

INTRODUCTION

CHAPTER 1:
MOLECULAR INSIGHTS INTO PLANT-PATHOGEN INTERACTION

The type III secretion system (T3SS) outlines the main virulence strategy of most gram-negative bacteria, consisting of a specialized molecular machinery, used to directly inject effector proteins inside host cells (Burkinshaw & Strynadka, 2014; Charro & Mota, 2015). Homologous type III secretion systems have been predominantly assigned to pathogens, including human-associated pathogen species of *Enterobacteriaceae* like *Yersinia, Shigella, Salmonella, Escherichia coli*, *Citrobacter,* bacteria from ɣ-proteobacteria group as *Vibrio cholerae* and *parahemolyticus,* and species from *Chlamydiaceae* group. However, T3SS can be also found inplant pathogens from ɣ-proteobacteria like *Pseudomonas syringae, Xanthomonas* pathovars, *Erwinia amylovora, Pantoea stewartii* and β-proteobacteria *Ralstonia solanacearum.* The T3SS presents a needle-like complex, consisting of a membrane-embedded basal structure and an external needle (Chatterjee *et al.*, 2013). When the needle tip complex gets in contact with the host cell, a translocon is assembled permitting translocation of type III effectors by creating a pore in the host membrane (see Figure 2).

Type III effectors (T3E) are of special interest in the context of host-pathogen interaction since they have a central role in virulence and disease by targeting key cellular processes (Deslandes & Rivas, 2012; Fraiture & Brunner, 2014; Zhou & Zhu, 2015). Bacterial effectors are often multifunctional proteins with different, but subtle activities and a wide array of virulence targets (Galan, 2009; Macho & Zipfel, 2015). Many effectors display multifunctionality, derived from their modular architecture, comprising domains that mediate distinct functions (Dean, 2011). T3Es like *Pseudomonas aeruginosa* ExoS and ExoT possess individual modules with different role/function on host cell morphology (Engel & Balachandran, 2009; Huber *et al.*, 2014; Rangel *et al.*, 2014). T3Es manipulate host cell pathways by mimicking the function of key host proteins or mediate their subcellular localization, by targeting plant-specific transcription factors, by inhibiting translation and metabolic stress pathways or exploiting a specific form of host-mediated fatty acid modification (Boyle & Martin, 2015; Dean, 2011; Kay *et al.*, 2007; Lemaitre & Girardin, 2013).

The functional study of T3Es from phytopathogenic bacteria has witnessed tremendous progress in the last years (Deslandes & Rivas, 2012; Marin & Ott, 2014). However, the

number of T3Es with an assigned function in planta only outlines the tip of the iceberg (Coll & Valls, 2013; Degrave *et al.*, 2015). The study of T3Es has been particularly complicated as these effectors belong to complex repertoires that feature internal redundancy, so the deletion of an individual T3E has little effect on virulence (Deslandes & Genin, 2014; Grant *et al.*, 2006; Kvitko *et al.*, 2009; Poh *et al.*, 2008). Effectors from *Ralstonia solanacearum* AWR family or AvrE superfamily of effectors from most type III-dependent phytobacteria have been shown to have overlapping effects and jointly contribute to disease development (Degrave *et al.*, 2015; Sole *et al.*, 2012). However, redundancy will eventually clear up as we enlarge our knowledge on biological assays that help eliminating the “lack of phenotype” problem.

Plant-pathogen interactions combine mutual attack and defense responses, illustrating a constant “dialogue” between the host cell and the invading pathogen. The zig-zag model proposed by Jones and Dangl in 2006 was extremely helpful in understanding molecular mechanism underlying plant-microbe interactions (Jones & Dangl, 2006). This divides plant immunity in two branches. On one side, plant cells recognize microbial/pathogen-associated molecular patterns (MAMPs/PAMPs) via extracellular pattern-recognition receptors (PRRs) and trigger PAMP-triggered immunity (PTI). The second branch, termed effector-triggered immunity (ETI) is activated when the plant resistance proteins recognize and respond to bacterial effectors, suppressing PTI. ETI leads to disease resistance, often accompanied by the hypersensitive response (HR), a form of programmed cell death (Jones & Dangl, 2006). This model describes a stepwise and permanent modulation of resistance and susceptibility from both sides: hosts and pathogens.

However, one of the criticisms faced by the zigzag model is that the conceptual division between PTI and ETI does not exist, and all the events take place at once (Thomma *et al.*, 2011). Others argue that the model does not take into account environmental factors like biotic and abiotic stresses that could influence the outcome of host-pathogen interactions (Pritchard & Birch, 2014). According to Pritchard & Birch (see Figure 1), activation of the host PTI leads to callose deposition -defined as a basal resistance against the pathogen-. Injection of a type III effector by the pathogen inside the host cell results in a reduction of callose deposition and increased pathogen growth. Under this circumstances both PTI and ETI can be active at the same time: the plant simultaneously produces callose and reduces the rate of effector translocation inside the cell. Moreover, resistance proteins that recognize specific effectors can also contribute to lowering pathogen levels by triggering HR. Actually, host resistance

mechanisms can modulate the levels of the pathogen inside plant cells at any given moment. Conversely, bacteria can reduce callose deposition and secrete more effectors to be translocated inside plant cell to manipulate host pathways (Pritchard & Birch, 2014). Importantly, this model can be adapted to either biotrophic, necrotrophic or symbiotic microbes.

During the last years, modelling and systems biology have contributed to expand our knowledge of plant-pathogen interactions. Particularly helpful have been whole-genome approaches and mathematical models of the host metabolic networks and central signaling pathways activated by pathogens attack (Kim *et al.*, 2014; Pathak *et al.*, 2013; Pinzon *et al.*, 2011; Sankar *et al.*, 2011). Still, the complexity of the plant-microbe interactions increases the need to develop a new model that can integrate the environmental context and its influence on host response in addition to the spatio-temporal regulation of pathogen growth and virulence (Pritchard & Birch, 2014).

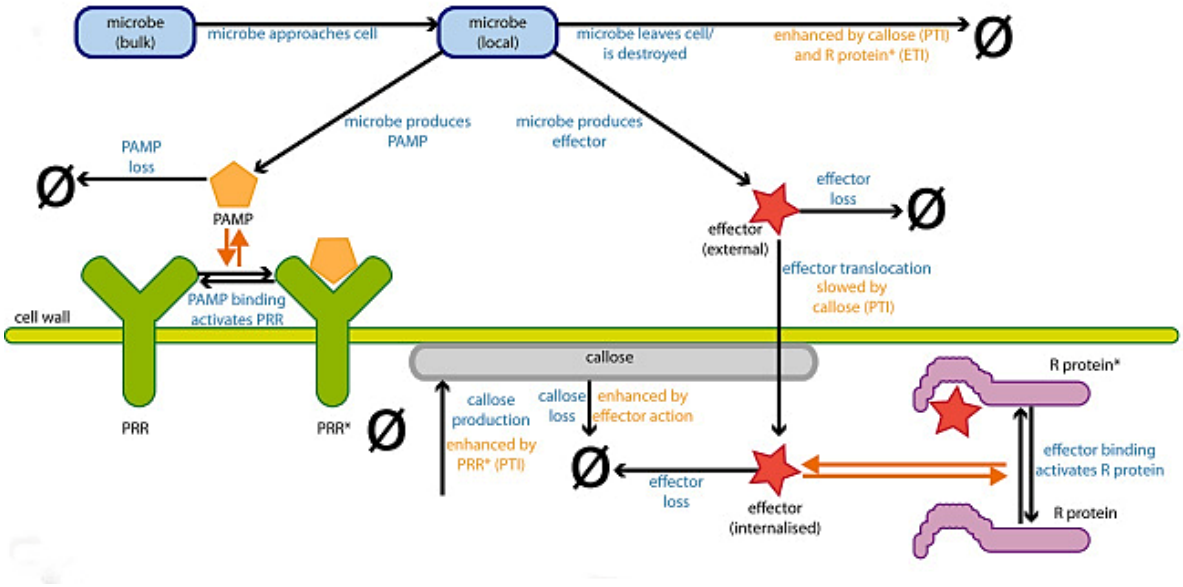

FIGURE 1. Current view schematically depicting the cellular events underlying plant-microbe interactions (Pritchard & Birch, 2014).

In addition to large-scale and mathematical approaches to study plant-pathogen interactions, it is essential to elucidate the function and targets of single T3Es to understand both pathogenesis and the immune response of the plant. So far, the plant pathogen with the best characterized effectome –effector collection- is *Pseudomonas syringae* (Dean, 2011; Lindeberg *et al.*, 2012). *P. syringae* different effectors have been shown to function as cysteine proteases, ubiquitin ligases, acetyltransferases, ADP-ribosyltransferases and kinase inhibitors (Deslandes & Rivas, 2012; Lewis *et al.*, 2009).

Nonetheless, great advances have been made to characterize type III effectors from other plant pathogens like *Xanthomonas* species (AvrAC, AvrBs3, XopD) and *Ralstonia solanacearum* (PopP2) (Figure 2), or to identify novel effector proteins important for bacterial virulence (Teper *et al.*, 2015). The study of T3E is being complicated by their redundancy or the hypersensitive response, which can mask effector activity. In addition, T3Es are often very toxic, causing host cell death and impeding monitoring of intracellular events, like the case of *Pseudomonas syringae* HopAA1-1 or XopX from *Xanthomonas euvesicatoria* (Munkvold *et al.*, 2008). These limitations, together with the premise that T3E target key cellular processes conserved among eukaryotes have appointed the need to use alternative approaches to investigate the functional roles of secreted effector proteins.

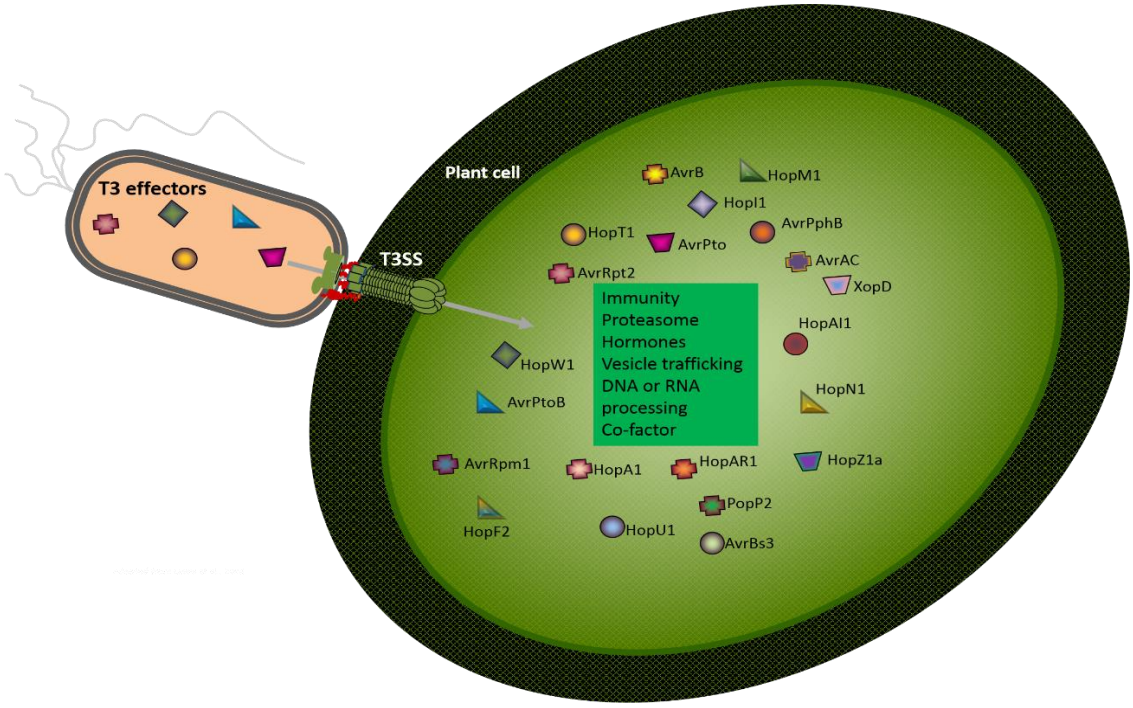

FIGURE 2. Schematic representation of the main processes targeted by T3Es in plant cells.

Examples of effector proteins from plant-associated bacteria injected inside host cells through the type III secretion system. Once inside host, T3Es interfere with plant immunity, hormone signalling, vesicle trafficking pathway, protein degradation or DNA and RNA processing. Adapted from (Deslandes & Rivas, 2012; Lewis *et al.*, 2009).

CHAPTER 2:
YEAST AS A HETEROLOGOUS MODEL SYSTEM TO UNCOVER TYPE III EFFECTOR FUNCTION

Heterologous expression in *Saccharomyces cerevisiae* has offered promising and effective strategies to investigate bacterial T3Es function. The observation that T3E altering central host pathways also target analogous processes in yeast has established this organism as a model system for studying effector function (Curak *et al.*, 2009). These studies are facilitated by the availability of unique databases and resources comprising genetic and phenotypic information on more than 6000 functionally annotated yeast genes (some reviewed in (Siggers & Lesser, 2008)) (Botstein & Fink, 2011; Koh *et al.*, 2015). Likewise, yeast provides powerful genomic and proteomic technologies that can be exploited to investigate subcellular localization, biochemical activity or cellular targets of T3E (Chong *et al.*, 2015; Howson *et al.*, 2005; Huh *et al.*, 2003; Suter *et al.*, 2006). For large-scale functional analysis of type III effectors, one can make use of yeast deletion collections (Giaever & Nislow, 2014) or overexpressing (Gelperin *et al.*, 2005; Sopko *et al.*, 2006), protein chips (Zhu *et al.*, 2000), or synthetic genetic arrays, comprising a global genetic interaction network that covers 75% of all genes in the budding yeast (Baryshnikova *et al.*, 2010a; Costanzo *et al.*, 2010). In addition, yeast has been used as a model organism for studying eukaryotic processes for more than 50 years (Duina *et al.*, 2014), therefore functional assays can be employed to screen for proteins altering conserved pathways (Sisko *et al.*, 2006; Slagowski *et al.*, 2008; Tabuchi *et al.*, 2009). Finally, yeast is emerging as a suitable alternative in gain-of-function analyses of T3E in plants, due to the absence of genes encoding for resistance proteins in its genome (Siamer *et al.*, 2014).

Different approaches using yeast systems biology have been widely exploited to investigate the function of bacterial effectors from animal pathogens, including species of bacteria from ɣ-proteobacteria group such as *Vibrio cholerae* and *parahemolyticus*, *Enterobacteriaceae* like*Yersinia, Shigella, Salmonella, Escherichia coli*, or *Citrobacter,* and species from *Chlamydiaceae* group (previously reviewed in (Curak *et al.*, 2009; Siggers & Lesser, 2008; Valdivia, 2004)). The current knowledge on type III effectors from plant pathogens *Pseudomonas syringae, Xanthomonas* pathovars, *Erwinia amylovora* and *Pantoea stewartii* obtained by using yeast as a model system will be discussed below.

2.1 Approaches using yeast for T3E characterization

The main challenge in the study of T3Es is not only elucidating their biological function, but identification of their physiological targets. As a start-up strategy, one can employ yeast two-hybrid screens (Uetz *et al.*, 2000) to determine host proteins targeted by T3Es. Nevertheless, because of the high toxicity of some type III effectors (for example *Yersinia* YopT or IpgB2 from *Shigella*), yeast transformants cannot be recovered (Alto *et al.*, 2006; Shao *et al.*, 2002). Alternative successful approaches have emerged and are currently being used to a better understanding of host-pathogen interactions.

Heterologous expression of T3E in yeast

Many research groups use inducible promoters to express bacterial effectors in yeast, as some of these proteins have proved to cause high toxicity on yeast cells. The "preferred" choice was the strong galactose-controlled *GAL1/10* promoter. With four exceptions (Arnoldo *et al.*, 2008; Siamer *et al.*, 2014; Stirling & Evans, 2006; Von Pawel-Rammingen *et al.*, 2000), all the other type III effectors studied in yeast were expressed under the control of *GAL1/10* promoter (see Table 1). This promoter system ensures strong expression of genes once the inducer galactose is added to the growing media. However, background or leaky expression of genes can be observed for *GAL1/10* system in the absence of induction (Belli *et al.*, 1998).

In some cases, strong expression of the effector may be limiting, as it can hinder screening for a particular phenotypic characteristics. In order to decrease expression levels of the bacterial effectors, weaker inducible promoters like *MET3* or *CUP1* can be used as an alternative (Arnoldo *et al.*, 2008; Von Pawel-Rammingen *et al.*, 2000). For instance, the use of *CUP1* promoter by Arnoldo and coworkers guaranteed optimal expression levels of *P. aeruginosa* ExoS for the drug inhibitor screen (Arnoldo *et al.*, 2008).

Alternatively, some groups successfully employed tetracycline-responsive promoters for the controlled expression of T3Es (Siamer *et al.*, 2014; Stirling & Evans, 2006) (S. Fujiwara *et al*., in press) (see Results, Chapter 1, this work). This activator-repressor dual system comprise regulatory DNA sequences from prokaryotes, allowing gene expression to be tightly regulated in response to concentrations of tetracycline or its analogues (Gossen & Bujard, 1992; Gossen *et al.*, 1995). In the Tet-Off system, expression of the gene is turned on in the absence of tetracycline or doxycycline.

Table 1. Summary of methods used in characterization of type III effector function from plant and animal pathogens.

Effector(s)	Organism	Approaches used in characterization	Phenotypes in yeast	References
YopE	*Yersinia spp.*	GTPase assays, effector point mutation analysis	Growth inhibition, GAP activity	(Von Pawel-Rammingen *et al.*, 2000)
YopE and SspA	*Yersinia spp./ Salmonella spp.*	subcellular localization, flow cytometry analyses, actin staining	Growth inhibition, disruption of actin cytoskeleton	(Lesser & Miller, 2001)
YopT	*Yersinia spp.*	suppressor screen, yeast two hybrid	Growth inhibition-Cytotoxicity	(Shao *et al.*, 2002)
SopE2 and SptP	*Salmonella typhimurium*	MAPK phosphorylation assays	SopE2 - Growth inhibition, Activation of Cdc42-dependent MAPK	(Rodriguez-Pachon *et al.*, 2002)
Exo U	*Pseudomonas aeruginosa*	fluorescence staining, functional mutational analysis	Growth inhibition-Cytotoxicity	(Rabin & Hauser, 2003)
AvrPtoB	*Pseudomonas syringae*	cell death assays	Suppression of oxidative stress-induced PCD	(Abramovitch *et al.*, 2003)
YopJ	*Yersinia spp.*	MAPK phosphorylation assays	Inhibition of MAPK signaling	(Yoon *et al.*, 2003)
ExoU	*Pseudomonas aeruginosa*	fluorescence staining, thin-layer chromatography of lipids, enzymatic assays	Cytotoxicity, Organelle membrane damage, Lipase activity	(Sato *et al.*, 2003)
YopM	*Yersinia pestis*	subcellular localization	Vesicle-trafficking dependent accumulation in the nucleus	(Skrzypek *et al.*, 2003)
ExoT	*Pseudomonas aeruginosa*	functional domain analysis	Growth inhibition, GAP domain and ADP domain toxic to yeast	(Garrity-Ryan *et al.*, 2004)
5 effectors	*Pseudomonas syringae*	viability assays	Suppression of Bax-induced PCD	(Jamir *et al.*, 2004)
YopM	*Yersinia pestis*	site-directed mutagenesis	Identification of critical residues for nuclear targeting	(Benabdillah *et al.*, 2004)
VopA	*Vibrio cholerae*	MAPK phosphorylation assays	Growth arrest, Block of MAPK signaling pathways	(Trosky *et al.*, 2004)
YopO/ YpkA	*Yersinia spp.*	viability assays, actin staining, indirect immunofluorescence	Growth inhibition-Cytotoxicity, Disruption of actin cytoskeleton	(Nejedlik *et al.*, 2004)
EspG	*EPEC / Citrobacter rodentium*	actin staining, indirect immunofluorescence	Loss of cytoplasmic microtubule structure	(Hardwidge *et al.*, 2005)
EspG, D, Map	*Enteropathogenic E. coli*	fluorescence staining, indirect immunofluorescence	Growth inhibition, Cell cycle alteration	(Rodriguez-Escudero *et al.*, 2005)
SigD/SopB	*Salmonella typhimurium*	fluorescence staining, functional domain analysis, enzymatic assays	Growth inhibition, Non-catalytic domain causes actin depolarization	(Aleman *et al.*, 2005)

Effector(s)	Organism	Approaches used in characterization	Phenotypes in yeast	References
Various effectors	*Enteropathogenic E. coli*	Protein affinity purification, µLC-MS/MS	Interaction of EspB, D, F, G, Map and Tir with host proteins	(Hardwidge *et al.*, 2006)
SigD/SopB	*Salmonella typhimurium*	subcellular localization, effector point mutation analysis, flow cytometry, indirect immunofluorescence, enzymatic assays, MAPK phosphorylation assays, protein affinity purification	Growth inhibition SigD R468A – cell cycle arrest, loss of growth polarity and septin ring assembly, downregulation of Cdc42-dependent MAPK pathway, co-purifies with Cdc42 G12V and Cdc24	(Rodriguez-Escudero *et al.*, 2006)
ExoS	*Pseudomonas aeruginosa*	site-directed mutagenesis, fluorescence staining, flow cytometry	Growth inhibition, Disruption of actin cytoskeleton and inhibition of DNA synthesis, both mediated by ADPRT domain	(Stirling & Evans, 2006)
Putative T3-associated proteins	*Chlamydia trachomatis*	screen for growth inhibition phenotypes	Growth inhibition	(Sisko *et al.*, 2006)
IpgB2	*Shigella flexneri*	pathogenic genetic screen, DNA microarray mRNA profiling, yeast two hybrid	Growth inhibition, Stimulation of Rho1p GTPase signalling	(Alto *et al.*, 2006)
OspF	*Shigella flexneri*	loss-of-function screen, MAPK phosphorylation assays, mRNA profiling	Inhibition of MAPK CWI signaling pathway	(Kramer *et al.*, 2007)
IpaH9.8	*Shigella flexneri*	functional domain analysis, enzymatic assays	E3 ubiquitin ligase for Ste7	(Rohde *et al.*, 2007)
CopN	*Chlamydia pneumoniae*	antivirulence drug screen, flow cytometry (FACS), fluorescence staining, phenotypic analysis of homologues	Growth inhibition-Cell cycle arrest, Disruption of microtubules, Identification of two CopN inhibitors	(Huang *et al.*, 2008)
IpaJ	*Shigella flexneri*	screen for growth inhibition phenotypes	Growth inhibition	(Slagowski *et al.*, 2008)
ExoS	*Pseudomonas aeruginosa*	phenotype suppressors screen, antivirulence drug screen, functional mutational analysis, in vitro enzymatic assays, kinetic analysis of enzymatic activity	Growth inhibition, Inactivation of yeast Ras2 by ADP-ribosylation, Exosin inhibits ExoS	(Arnoldo *et al.*, 2008)
WtsE	*Pantoea stewartii*	functional mutational analysis	Growth inhibition	(Ham *et al.*, 2008)
YspM	*Yersinia enterocolitica*	mutational analysis, phenotypic analysis of homologues	Growth inhibition	(Witowski *et al.*, 2008)

Effector(s)	Organism	Approaches used in characterization	Phenotypes in yeast	References
27 effectors	*P. syringae pv tomato dc3000*	effector repertoire screen, cell viability assays, indirect immunofluorescence, functional domain analysis	Cell death, Growth inhibition, Loss of respiration	(Munkvold *et al.*, 2008)
SteC, SseF	*Salmonella typhimurium*	screen for pathogenic proteins, fluorescence staining, MAPK phosphorylation assays	Growth inhibition, Alteration of actin cytoskeleton	(Aleman *et al.*, 2009)
HopAA1-1	*P. syringae pv tomato dc300*	functional domain analysis	Growth inhibition, Cell death	(Munkvold *et al.*, 2009)
Several effectors	*Yersinia enterocolitica Salmonella typhimurium*	CPY-Inv reporter system, Tet-off expression system	Growth inhibition, Vesicle trafficking damage	(Tabuchi *et al.*, 2009)
21 effectors	*X. euvesicatoria*	effector repertoire screen, functional mutational analysis	Cell cycle arrest & cell death, growth inhibition under stress	(Salomon *et al.*, 2011)
XopE2	*X. euvesicatoria*	synthetic lethality screen, lacZ reporter assays	Perturbation of ER-to-nucleus signaling (UPR response)	(Bosis *et al.*, 2011)
DspA/E	*Erwinia amylovora*	fluorescent staining, cell viability assays	Growth inhibition, Defects of actincytoskeleton, Endocytosis delay	(Siamer *et al.*, 2011)
VopX	*Vibrio cholerae*	screen for growth inhibition phenotypes	Growth inhibition, RLM1-dependent modulation of CWI MAPK signaling	(Alam *et al.*, 2011)
SopB/SigD	*Salmonella typhimurium*	fluorescence staining, functional mutational analysis, co-immunoprecipitation, MAPK phosphorylation assays	SigD R468A – Growth inhibition, Interaction with hCdc42, but not Rac1 in yeast	(Rodriguez-Escudero *et al.*, 2011)
29 effectors /HopX1	*P. syringae pv tomato*	effector repertoire screen, functional mutational analysis, lacZ reporter assays, subcellular localization	Growth inhibition under osmotic stress, HOG MAPK signaling inhibition	(Salomon *et al.*, 2012)
SteC	*Salmonella typhimurium*	suppressor screen, lacZ reporter assays, co-immunoprecipitation assays/fluorescent staining	Growth inhibition, Downregulation of MAPK mating and HOG pathways, Interaction with GEF Cdc24	(Fernandez-Pinar *et al.*, 2012)
SspH2	*Salmonella typhimurium*	cell cycle functional assays	No effect on cell viability or alteration of cell cycle	(Bhavsar *et al.*, 2013)
DspA/E	*Erwinia amylovora*	suppressor screen, actin staining, HPLC, cell labelling and thin-layer chromatography, phosphorylation assays	PP2A-Cdc55 dependent down-regulation of sphingolipid pathway	(Siamer *et al.*, 2014)

On the contrary, gene expression is turned on after addition of doxycycline in the Tet-On system. Main advantage of these systems, especially for Tet-On vectors, is the very low background or leaky expression of the genes, almost undetectable in the absence of induction (Belli *et al.*, 1998). Expression levels of the genes in Tet systems compare favorably to levels obtained from strong promoters, counting 70% of those achieved by the *GAL1* promoter (Gari *et al.*, 1997). In addition, the prokaryotic regulatory proteins act highly specific on their targets, avoiding pleiotropy (Harkin *et al.*, 1999). On the contrary, in the *GAL1* system, as regulation of gene expression requires a nutrient change, this might have pleiotropic effects on yeast metabolism. Thus, phenotypes observed might be a result of a shift in nutrient availability.

Strategies for optimization of gene expression control also include using different copy number plasmids, which allows tuning the concentrations of the inducers. A wide array of yeast vectors is now available for expression of heterologous proteins (Alberti *et al.*, 2007; Giuraniuc *et al.*, 2013; Tabuchi *et al.*, 2009), ranging from centromeric origin plasmids (low copy number – 1-3 copies) to 2µ vectors, which are maintained at a high copy number of 30-50. Low levels of heterologous expression allow highly sensitive screening conditions in high-throughput analyses (Salomon *et al.*, 2012; Slagowski *et al.*, 2008), avoiding non-specific phenotypes. Similarly, in co-localization studies, expression of T3Es from a low copy number vector permits distinction of specific subsets of yeast structures targeted by the T3E (see the case of *Salmonella* SspA (Lesser & Miller, 2001)). Targeted homologous recombination can be used to introduce a single gene copy and ensure stable expression of the effector (Ham *et al.*, 2008; Stirling & Evans, 2006) (see Results, Chapter 1, this work).

Gene expression control using different concentrations of the inducers also provides extra information on toxicity of T3Es. By modulating the amounts of repressing glucose or inducing galactose and counting viable yeast cells, Rabin and coworkers revealed a quantitative assay of ExoU toxicity, concluding that minimal expression of this T3E is sufficient to kill yeast (Rabin & Hauser, 2003).

Once expressed in the yeast heterologous system, T3E can be assessed subcellular localization by fusion to an epitope tag. These studies are facilitated by the availability of DNA-binding dyes for different yeast cellular compartments (DAPI, fluorescent rhodamine, Mitotracker). Moreover, co-localization studies and co-immunoprecipitation assays using yeast GFP clone collections or mRFP reporter strains (Huh *et al.*, 2003)

can also be performed, to decipher T3E localization patterns and/or its interactors. Finally, yeast offers many tools for rapid genetic manipulation, extremely helpful in effector functional mutations/domains analysis.

Testing known cellular processes/pathways

The yeast system has provided great knowledge on eukaryotic processes like cytoskeleton dynamics, MAPK signaling, vesicle trafficking, or cell cycle (Duina *et al.*, 2014). Experimental tools and resources emerging from these yeast studies have facilitated and contributed to identification of the precise target or conserved process affected by T3Es. For instance, many effector proteins were shown to affect cell cycle in yeast (Huang *et al.*, 2008; Rodriguez-Escudero *et al.*, 2005; Rodriguez-Escudero *et al.*, 2006; Salomon *et al.*, 2011). Using flow cytometry analyses and synchronization at a specific phase of cell cycle, one can determine the point where bacterial effectors are acting to induce growth arrest. Furthermore, staining of cell-cycle related structures using antibody markers helps monitoring progression and alteration of this process. For instance, staining of cells expressing *Chlamydia* CopN with anti-tubulin antibodies showed disruption of the spindle apparatus, required for mitosis (Huang *et al.*, 2008).

Similarly, plenty of tools are available to study yeast cytoskeleton dynamics. Fusion proteins like Cdc10-GFP allowed analysis of septin structures in the case of *E. coli* type III effectors Map and EspF, suggesting blocking of cell polarity (Rodriguez-Escudero *et al.*, 2005). Yeast presents a high conservation of cell polarity among eukaryotes (Park & Bi, 2007; Styles *et al.*, 2013), which permitted extensive research of this mechanism. Studies of bacterial effectors causing cell depolarization have used fluorescent markers to highlight yeast compartments. For instance, actin and related structures as cortical patches or actin cables can be visualized by staining with rhodamine-labeled phalloidin. Likewise, other processes like respiration or chitin biosynthesis can be studied using specific dyes: tetrazolium-based redox dyes (Sisko *et al.*, 2006) or calcuofluor-white staining (Rodriguez-Escudero *et al.*, 2005), respectively.

A significant group of T3E from animal (*Salmonella tyhphimurium, Yersinia spp., Shigella flexneri, Vibrio cholerae*) and plant pathogens (*Pseudomonas syringae)* target MAPK signaling pathways. Phosphorylation of MAP kinases in the four MAPK signaling pathways in yeast can be monitored using specific antibodies against the dually phosphorylated activation domain of mammalian p42/44 MAPK (Martin *et al.*, 2000). In addition, yeast *lacZ* reporter strains comprising regulatory elements responsive to activation of MAPK pathways can be used to gain insight on perturbation of these signaling pathways by T3E (Alam *et al.*, 2011).

Similarly, transcriptional reporters were successfully exploited to monitor vesicle trafficking. A reporter strain responsive to endoplasmic reticulum (ER) stress was employed to demonstrate *Xanthomonas* XopE2 failed to activate molecular signaling from ER to the nucleus (Bosis *et al.*, 2011). Also, alteration of endocytosis as a result of T3E action was detected using FM4-64, a vacuolar and endosomal fluorescent dye (Siamer *et al.*, 2011). In order to screen for pathogenic proteins altering host vesicle pathways a powerful resource is the yeast carboxypeptidase Y (CPY) - invertase (Inv) system (Shohdy *et al.*, 2005). In normal conditions, the CPY-INV hybrid protein is sequestered inside the vacuole, and as it cannot reach the surface, the cell cannot hydrolyze exogenous sugar. Perturbation of vesicle trafficking brings the hybrid protein to the surface and its secretion can be monitored by the formation of a brown precipitate, an indicator of sugar production. Later on, Tabuchi and coworkers adapted this system in a yeast strain isogenic to yeast deletion collections (Tabuchi *et al.*, 2009). Although developed for the first time to screen for *Legionella pneumophila* type IV effector proteins (Shohdy *et al.*, 2005), this system provides an excellent platform to be exploited in identification of type III effector proteins modulating host membrane trafficking.

Finally, biochemical activities of T3E have been also revealed using different enzymatic assays. For example, activity of T3E as RhoGTPases, either as GTPase activating proteins or guanine nucleotide exchange factors, can be evaluated by the percentage of GTP-bound (Lesser & Miller, 2001; Von Pawel-Rammingen *et al.*, 2000). Also, in the case of *Shigella* IpaH9.8, *in vitro* ubiquitination assays deciphered its biochemical activity as an E3 ubiquitin ligase for a MAPKK in the mating pathway (Rohde *et al.*, 2007). Lastly, ADP-ribosyltransferase assays were performed to monitor incorporation of ADP-ribose from *Pseudomonas aeruginosa* ExoS into its yeast interactor Ras2 by means of radioactive enzymatic substrates (Arnoldo *et al.*, 2008).

Effector repertoire screens

Most bacterial pathogens are estimated to deliver between 20-100 type III effector proteins inside host cells (Kenny & Valdivia, 2009). Many of these secreted proteins have been assigned a biological or biochemical function, but a great number of type III effector functions still need to be identified (Dean, 2011; Degrave *et al.*, 2015; Scholze & Boch, 2011). Yeast has emerged as a powerful resource in large-scale phenotypic analysis of bacterial effectors, as growth inhibition phenotypes in this organism were shown to be a result of alteration of eukaryotic conserved pathways by T3Es (Curak *et al.*, 2009).

The pioneer study using this approach revealed seven effector proteins from *Pseudomonas syringae* DC3000 strain inhibiting yeast growth (Munkvold *et al.*, 2008). For some of them that have been previously assigned an enzymatic function, this study by Munkvold and coworkers confirmed their role in virulence. Additionally, the screening discovered a previously uncharacterized effector, HopAA1-1. Further analysis showed expression of HopAA1-1 leads to cell death in both yeast and plants, confirming to a certain degree conservation of effector function across kingdoms (Munkvold *et al.*, 2009).

A similar approach has been employed to identify *Xanthomonas euvesicatoria* effectors inhibiting growth in yeast (Salomon *et al.*, 2011). This screening discovered additional effectors which inhibited growth under stress conditions. Analysis of phenotypes in the presence of various stressors has proved to be extremely helpful to identify cellular processes targeted by low toxicity type III effectors, yet showing crucial roles in pathogenesis (Salomon *et al.*, 2011). Effector repertoire screening under normal and stress conditions in *Pseudomonas syringae* plant pathogen confirmed six out of the seven effector proteins (Salomon *et al.*, 2012) showed to inhibit growth in a previous study (Munkvold *et al.*, 2008). Interestingly, five additional T3Es displayed growth inhibition phenotypes only in the presence of stressors. Among them, HopX1 was shown to have an important role in infection, by attenuating activation of MAPK signaling pathways (Salomon *et al.*, 2012).

Phenotype suppressor screens

Yeast deletion mutant collections provide unique resources used in large-scale phenotypic analyses to decipher biological functions, responses to stress and mechanisms of drug action (Giaever & Nislow, 2014). These collections comprise homozygous and heterozygous mutants deleted in all ~6000 known yeast ORFs, out of which ~5000 are non-essential genes. Based on this former observation, Tong and coworkers exploited yeast deletion strains to assess functional relationships between non-essential yeast genes and uncover potential redundant functions (Tong *et al.*, 2001). This approach, termed synthetic genetic array (SGA) analysis, consists of screening for mutations that either suppress or enhance the phenotype caused by other mutations.

SGA was applied to study T3E function. The ~5000 viable deletion yeast mutants were used to screen for growth defects associated to expression of T3Es. Tested T3Es are toxic to yeast cells, therefore those deletion mutants suppressing growth inhibition phenotype should uncover the corresponding target(s) of the T3E. In 2006, Alto and coworkers defined this technique as pathogenic genetic array (PGA) analysis, and exploited it to identify T3E *Shigella* IpgB2 modified processes in yeast. Likewise, two other groups employed yeast suppressor screens to uncover specific cellular processes targeted by *Shigella* OspF and DspA/E from *Erwinia amylovora*, respectively (Kramer *et al.*, 2007; Siamer *et al.*, 2014). In the case of DspA/E, as several deletion mutants were identified to suppress DspA/E-induced growth arrest, additional trials were performed to quantify growth recovery in liquid cultures by counting the number of viable cells. This assay provided information on the suppressor strength and increased the specificity of the screening (Siamer *et al.*, 2014).

Alternatively, one can use heterozygous essential gene knock-out library to unveil effector targets. This consists of identifying haploinsufficiency profiles that appear as a result of lowering the dosage of a gene from two copies to one copy (Suter *et al.*, 2006). Effector-induced haploinsufficiency is defined as hypersensitivity to effector expression, therefore corresponding gene(s) deleted in mutants selected as hypersensitive encode potential effector targets. While screens with homozygous deletions highlight genes important for effector function, haploinsufficiency is highly specific and is expected to uncover the primary target for the effector. So far, this strategy has not been used to study effector function; however, it is a powerful tool for future investigations in this field.

Conversely, available yeast overexpressing strains collections (Gelperin *et al.*, 2005; Sopko *et al.*, 2006) have been effectively used in phenotype suppressor screens to elucidate T3E function. This approach relies on the hypothesis that high amounts of effector targets should result in yeast growth recovery if the effector functions to inactivate these host proteins. The seminal work published by Shao and coworkers exploited a yeast gain-of-function screen to identify a Rho family of small GTPases as potential targets of the *Yersinia* effector YopT, suggesting that the cysteine protease function of YopT is conserved between animals and yeast (Shao *et al.*, 2002). Effector targets were shown to be conserved across kingdoms using the yeast methodology described above. Arnoldo and coworkers confirmed type III effector ExoS targets small GTPases from Ras superfamily in both mammals and yeast by overexpressing yeast homologues of *P. aeruginosa* ExoS human targets and screening for a growth rescue phenotype (Arnoldo *et al.*, 2008).

Similarly, gain-of-function screening using overexpressing yeast strains strengthened complementary findings on effector function. For instance, *Salmonella* SteC was shown to down-regulate the yeast MAPK mating pathway. Interestingly, the MAPK kinase in the mating pathway Cdc42 was found as a suppressor of SteC toxicity in yeast, confirming gain-of-function screening is a robust method to elucidate T3E molecular targets (Fernandez-Pinar *et al.*, 2012).

Synthetic lethality screens

Synthetic lethality screens have been successfully exploited to detect T3E-modified targets or organelles. This methodology implies screening for yeast deletion strains hypersensitive to the expression of the type III effector. Furthermore, specific pathways affected among these deletion strains, allegedly targeted by the T3E, can be deciphered using the yeast synthetic lethality interaction network, actually containing more than 10.000 genetic interactions between 2795 genes (Baryshnikova *et al.*, 2010b; Bosis *et al.*, 2011; Costanzo *et al.*, 2010). Synthetic lethality (SL) interactions were identified by SGA analysis and occurs if an allele of a gene combines with the allele of another gene to generate a double mutant phenotype (Costanzo *et al.*, 2010). Based on this observation, inviable double-mutant progenies show functional relationships between genes. SL interactions may include genes acting in the same pathway or genes from two parallel pathways, functionally interconnected (Tong *et al.*, 2001).

By screening for null alleles hypersensitive to expression of a bacterial effector, as the case of *Shigella* OspF, one can assess functional relationships between yeast genes

and T3Es toxicity (Kramer *et al.*, 2007). To identify pathways impaired among the 83 deletion strains found as hypersensitive to OspF expression, Kramer and coworkers proposed two types of analysis. First, statistical data-mining tool identified 25 gene ontologies, enriched among these strains, referring to four biological processes, including cell wall organization and biogenesis. Secondly, using existing SL interaction data, it was shown that OspF is congruent, therefore shares SL interaction partners (Ye *et al.*, 2005), with genes altered in cell wall biogenesis. Complementary assays confirmed OspF inhibited cell wall integrity MAPK signaling pathway in both mammals and yeast (Kramer *et al.*, 2007). Comparison of OspF loss-of-function screening results with analogous synthetic lethality data was extremely helpful in the identification of the cellular process altered by this T3E.

Some years later, Bosis and coworkers optimized this methodology, showing that an array of 90 deletion strains in the yeast collection covered the majority (69%) of the interacting genes (Bosis *et al.*, 2011). These strains were tested to predict host cellular process affected by *Xanthomonas* XopE2, a bacterial effector whose targets were previously unknown. The screen discovered 12 congruent genes involved in cell wall biogenesis and organization (Bosis *et al.*, 2011). Confirmation of this result with other functional assays showed that XopE2 affects the endoplasmic reticulum stress response. In addition, the deletion strains in the array were screened for hypersensitivity to the *Shigella* type III effector OspF. Interestingly, 13 genes congruent with OspF were found, out of which 8 genes were also described in the previous study (Kramer *et al.*, 2007). This finding appointed that less than 2% of the deletion strains in the yeast collection are sufficient to identify cellular processes altered by bacterial effectors.

Protein affinity purification and µLC-MS/MS

Interaction studies using type III effectors as baits have been complicated by the low concentration of these proteins inside infected host cells. Heterologous expression of T3Es in yeast oversteps these limitations, as it was shown that yeast supplies sufficient protein abundance for further analysis (Hardwidge *et al.*, 2006). In 2006, Hardwidge and coworkers performed proteomic analysis of *E. coli* T3E binding partners in yeast, providing important clues on effector activity inside hosts (Hardwidge *et al.*, 2006). For this, yeast proteins associated to *E. coli* effector proteins were isolated by affinity purification, followed by isotope-coded affinity tag labelling and µLC-MS/MS.

Importantly, proteomic analysis of yeast proteins enriched in the effector-containing samples correlated with phenotypes previously observed in yeast. For instance, yeast

cells expressing EspG showed actin depolarization and loss of coordination during bud development (Hardwidge *et al.*, 2005; Rodriguez-Escudero *et al.*, 2005). Correspondingly, EspG sample was enriched in Gpi17 and Elm1, two proteins regulating actin polarization and nuclear division (Hardwidge *et al.*, 2006). Another *E. coli* effector studied using this proteomic approach is Map, whose expression in yeast interferes with normal distribution of cortical actin and causes chitin enrichment of the cell wall (Rodriguez-Escudero *et al.*, 2005). As expected, Map co-purified with Sec6, a subunit of the exocyst complex, mediating polarized targeting of post-Golgi vesicles to the plasma membrane and Crh1, a cell wall protein localizing to chitin-rich areas (Hardwidge *et al.*, 2006; Jepson *et al.*, 2003). This is also consistent with findings in mammalian cells, where the T3E Map induces actin polymerization required for filopodia formation and bacterial entry (Jepson *et al.*, 2003).

Screens for drugs inhibiting pathogen growth

Yeast may be used to identify lead compounds that inhibit T3E activity and restore yeast growth, as it was the case in the screen for small molecule inhibitors of *Chlamydia pneumoniae* CopN effector protein and ExoS T3E from *Pseudomonas aeruginosa* (Huang *et al.*, 2008; Arnoldo *et al.*, 2008). In the context of host-pathogen interactions, discovery and development of natural or synthetic anti-virulence compounds emerged as a novel strategy to counteract drug resistance and host toxicity (Brown *et al.*, 2014; Su *et al.*, 2015; Xie *et al.*, 2014). Due to the high conservation in cellular and molecular mechanisms between yeast and human or plant cells, *Saccharomyces cerevisiae* has proven to be a powerful resource to identify and characterize small molecules inhibitors of pathogens growth (Hughes, 2002; Piotrowski *et al.*, 2015; Voisset & Blondel, 2014).

Using a phenotype-based chemical screening in yeast, Arnoldo and coworkers discovered 6 potential inhibitors against T3E ExoS toxicity (Arnoldo *et al.*, 2008). One of them, named exosin, also reduced ExoS cytotoxic effect in mammalian cells. In yeast, growth inhibitory effect caused by ExoS is mediated by its ADP ribosyltransferase activity (Stirling & Evans, 2006), therefore exosin was tested for modulation of ExoS enzymatic activity. Indeed, exosin was confirmed to act as a competitive inhibitor of ExoS ADP-ribosyltransferase activity *in vitro* (Arnoldo *et al.*, 2008). Moreover, this inhibitor molecule is only specific against ExoS, as it could not protect against infection with *P. aeruginosa* strains expressing other bacterial proteins like ExoT, ExoU or ExoY.

A chemical biology approach using yeast was also employed to elucidate role of T3E CopN in virulence caused by *Chlamydia pneumoniae* (Huang *et al.*, 2008). On the basis that expression of CopN severely affected yeast growth, Huang and coworkers screened a library of more than 40.000 small molecules for those able to restore this growth inhibition phenotype. The discovery of two drug inhibitors gave rise to "functional knock-outs" of CopN, exploited to demonstrate that this effector is required for intracellular growth and replication of *Chlamydia pneumoniae* (Huang *et al.*, 2008). Interestingly, small molecule inhibitors of *C. pneumoniae* CopN did not reduce toxicity after infection with *Chlamydia trachomatis*, showing that this method is highly specific and that these chemical compounds, including exosin, target a unique function of bacterial effectors (Huang *et al.*, 2008). In conclusion, yeast cell-based screening provided a successful alternative to study the role of CopN in disease, previously limited by the lack of tools for targeted gene disruption.

Transcriptomic analyses using DNA microarrays

Transcriptomic analyses in yeast have been exploited as complementary genome-screening procedures in confirmation of T3E activities already assessed by other techniques (Alto *et al.*, 2006; Kramer *et al.*, 2007). Gain-of-function screening of yeast cells expressing *Shigella* IpgB2 showed that this bacterial effector alters small GTPase Rho1 signaling (Alto *et al.*, 2006). To confirm this result and at the same time, discover other potential IpgB2 functions, Alto and coworkers performed mRNA profiling in yeast cells expressing IpgB2. Gene transcription profiles induced by expression of IpgB2 strongly correlated to those of yeast Rho1, proving IpgB2 GTPase mimicry activity (Alto *et al.*, 2006). Furthermore, comparison of IpgB2 profile with the transcriptional profile resulting from induction of another RhoGTPase Cdc42, showed that IpgB2 specifically activates Rho1-, but not Cdc42-dependent signaling. Similarly, *Shigella* OspF expression in yeast resulted in down-regulation of genes involved in the cell wall integrity pathway (Kramer *et al.*, 2007). This finding confirmed the fact OspF inhibits cell wall integrity MAPK signaling pathway, a result previously revealed by a loss-of-function screening.

Importantly, these studies were facilitated by the availability of a wide panoply of yeast transcriptomic profiles obtained in response to nutrient limitation or different environmental stresses (Brion *et al.*, 2015; de Groot *et al.*, 2007; Gasch *et al.*, 2000; Tai *et al.*, 2005). On this basis, mRNA profiling can also be used as a kick-off strategy in deciphering conserved processes or molecular targets of T3Es with unknown function. Genome-wide transcriptomic analysis of yeast cells expressing the T3E

AWR5 from the plant pathogen *Ralstonia solanacearum* revealed a profile reminiscent of inhibition of a central regulatory pathway conserved across kingdoms (see Results, Chapter 3, this work).

2.2 Conserved cellular processes targeted by bacterial T3E in yeast

Heterologous expression of T3Es in *S. cerevisiae* has resulted in a number of observable phenotypes, the most common of which is growth inhibition (Table 1 and Figure 3). This effect seems to be highly specific to T3Es, as inhibition of yeast growth was only observed for 9 out of 505 essential *Pseudomonas aeruginosa* ORFs (Arnoldo *et al.*, 2008) and 32 out of 216 ORFs tested from *Chlamydia trachomatis* (Sisko *et al.*, 2006). Likewise, between 6.5% and 8% genes from *Salmonella enterica* serovars affect yeast growth (Aleman *et al.*, 2009). On the contrary, toxicity is common amongst *Pseudomonas syringae* and *Vibrio cholerae* effectors, 7 and 11, respectively, out of 27 effectors tested inhibit growth in yeast (Alam *et al.*, 2011; Munkvold *et al.*, 2008). Moreover, screening for yeast growth inhibition phenotypes among *Shigella* translocated proteins was extremely helpful in identification of effector proteins, as IpaJ, previously missed by other experimental procedures (Slagowski *et al.*, 2008).

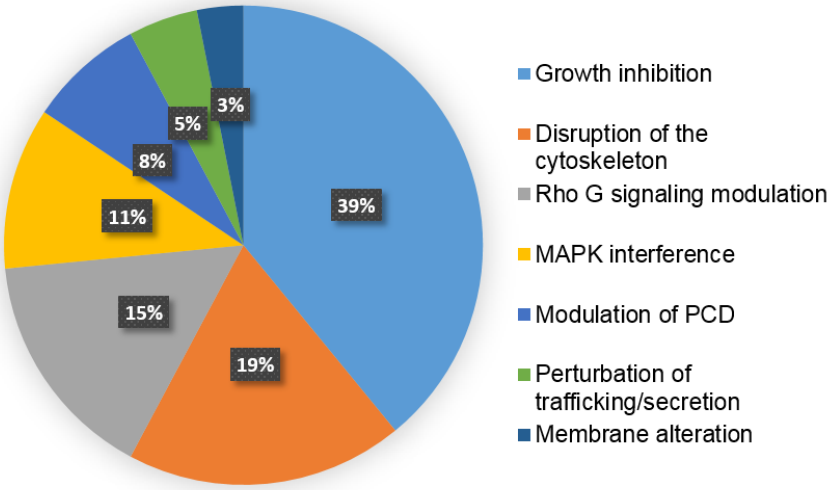

FIGURE 3: The most common phenotypes observed in *S. cerevisiae* upon T3E expression.

Growth inhibition is a rather unspecific phenotype that can be caused by alterations in a panoply of cellular activities. To narrow down and/or to increase the range of detection of the precise yeast process targeted by bacterial effectors, a number of assays have been performed, including analysis of cell morphology and budding, growth under stress conditions or in ethanol/glycerol plates to force respiration, among other observations (Munkvold *et al.*, 2008; Rodriguez-Pachon *et al.*, 2002; Salomon *et*

al., 2011). Importantly, growth under conditions that affect yeast cellular function, as for example salt or osmotic stress, has been shown to increase yeast sensitivity to effectors and helped identification of additional T3Es that caused toxicity. In a screen of *Shigella* effectors, 4 out of the 18 effectors tested showed growth inhibition phenotypes under normal conditions and 5 additional effectors inhibited yeast growth in presence of stress (Slagowski *et al.*, 2008). Similarly, screening of 21 T3Es from *Xanthomonas euvesicatoria* revealed 7 effectors affecting yeast growth under normal conditions and 7 more when applying different stressors (Salomon *et al.*, 2011). These analyses often traced the cause of growth inhibition to a specific arrest in cell cycle (Table 1). In other cases, toxicity was the indirect result of effector interferences with the cytoskeleton, organellar membranes or specific signaling pathways (see below), so that other phenotypes combine with growth arrest (Table 1).

Growth inhibition phenotypes have also been exploited to define the functional domains of bacterial effector proteins. For instance, the same domains or conserved aminoacid residues of *Yersinia* YopT, YopE, YopO (Nejedlik *et al.*, 2004; Shao *et al.*, 2002; Von Pawel-Rammingen *et al.*, 2000), *Shigella* IpgB2 (Alto *et al.*, 2006), *Pseudomonas aeruginosa* ExoT (Garrity-Ryan *et al.*, 2004), or *Xanthomonas euvesicatoria* XopE1 and XopE2 (Salomon *et al.*, 2011) are required to cause similar phenotypes in yeast and mammals. This indicates that the phenotype may be due to targeting of conserved eukaryotic processes. In a similar manner, these phenotypes led to the identification of functional differences between homologous T3Es of same or distinct species, extending the knowledge toolbox on effector function (Huang *et al.*, 2008; Witowski *et al.*, 2008). As an example, only YspM effector from *Yersinia enterocolitica* strain Y295, but not its homologue from *Y. enterocolitica* strain JB580, caused inhibition of yeast growth. This conveyed to the demonstration that toxicity toward eukaryotic cells is due to the presence of a conserved histidine domain (Witowski *et al.*, 2008).

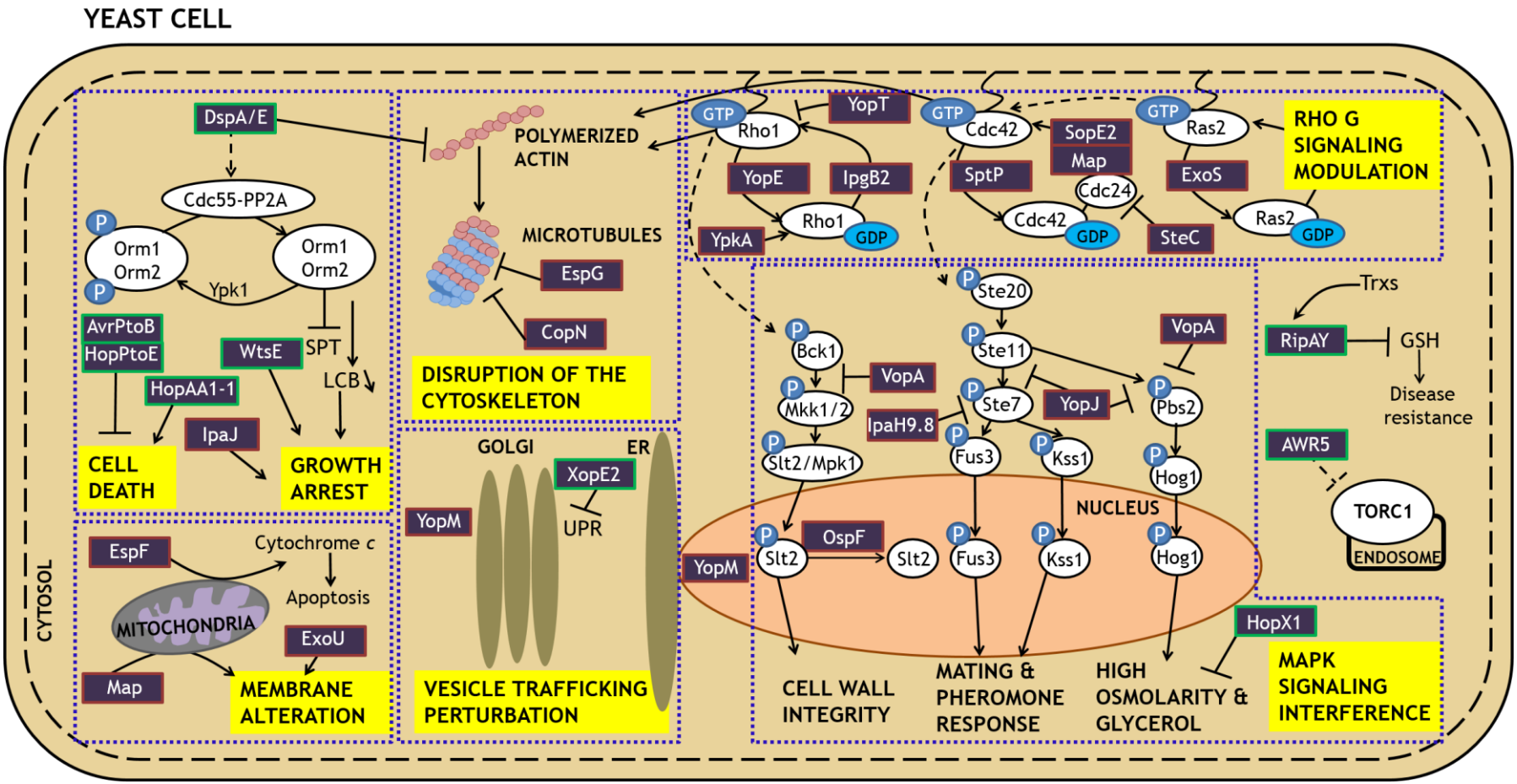

FIGURE 4. Yeast cellular processes targeted by bacterial type III effectors.

Effectors are marked by color-coded rectangles depending on species origin (plant-associated effectors in green, animal and animal-associated effectors in dark red). Arrows indicate activations and T symbols indicate inhibitions. P, phosphate group; UPR, unfolded protein response; SPT, serine palmitoyltransferase; LCB, long chain bases; GSH, glutathione; Trxs, thioredoxins. Other common abbreviations are given in the text.

Disruption of the cytoskeleton

Disruption and/or rearrangement of the cytoskeleton are common strategies that bacterial T3E employ in order to direct their entry into host cell and carry out their function (de Souza Santos & Orth, 2015; Jelenska *et al.*, 2014; Radhakrishnan & Splitter, 2012; Rottner *et al.*, 2005). Yeast has proven a very powerful resource to identify bacterial T3Es that affect host cytoskeletal function, due to the well-established knowledge and techniques related to yeast actin and microtubule dynamics (Mishra *et al.*, 2014; Styles *et al.*, 2013). 12 out of 37 T3E characterized in yeast target this process (Table 1).

Heterologous expression in yeast of DspA/E effector protein from the phytopathogen *Erwinia amylovora* was shown to cause defects in cell polarization and endocytosis delay, two processes that depend on a functional actin cytoskeleton (Siamer *et al.*, 2011). Interestingly, this plant-associated effector whose function and molecular mechanism were unknown is part of a T3E family that share a common WxxxE motif, required both for virulence and avirulence activities in plants (Ham *et al.*, 2009). In animals, the T3E WxxxE family present in several bacterial pathogens including *E. coli, Salmonella* or *Shigella* perturbs host actin cytoskeleton (Orchard & Alto, 2012). Exploiting a yeast suppressor screen, Siamer and coworkers found later on that mutant yeast strains impaired in sphingolipid biosynthesis restore the polarization defects seen after expression by DspA/E (Siamer *et al.*, 2014). This is not surprising as sphingolipids are linked to actin cytoskeleton organization by guaranteeing proper localization of actin regulators (Niles & Powers, 2014; Tabuchi *et al.*, 2006) and have been shown to play major roles in depolarization and repolarization of actin following salt stress in yeast (Balguerie *et al.*, 2002).

Other T3E proteins target microtubule cytoskeleton, preventing normal functioning of cell-cycle processes (Duro & Marston, 2015). Through monitoring cell-cycle progression in mammals and yeast, Huang and coworkers showed that *Chlamydia pneumoniae* CopN-expressing cells accumulated at the G2/M transition and presented a delay of host cell division (Huang *et al.*, 2008). Moreover, CopN expression resulted in abnormal microtubule spindles, indicating that nuclear division is affected. In mammalian cells, expression of CopN led to altered integrity of the microtubule network. CopN conserved its activity to induce a cell cycle block from yeast to mammals, a bacterial strategy also used by other T3E, as *P. aeruginosa* ExoT or *Salmonella* PheA, to redirect resources of the host cell to promote multiplication of the bacterium (Na *et al.*, 2015; Shafikhani & Engel, 2006).

Effector protein EspG from enteropathogenic bacteria *Escherichia coli* and *Citrobacter rodentium* was shown to disrupt native microtubule structure in both mammals and yeast (Hardwidge *et al.*, 2005; Rodriguez-Escudero *et al.*, 2005). The presence of a unique long microtubule extended along cell surface in yeast cells expressing EspG revealed that nuclear division was uncoupled from bud development (Hardwidge *et al.*, 2005). Interestingly, EspG can also perturb actin function. In mammalian cells, EspG induces formation of actin stress fibers. Yeast actin cytoskeleton is distinct from that of mammals, comprising three components: cortical patches, actin cables and actin rings (Mishra *et al.*, 2014). Expression of EspG in yeast resulted in mislocalized actin cortical patches. As a consequence, yeast cells expressing EspG lost their ability to control actin polarization. Expression in yeast of other two *E. coli* T3E, EspD and Map, also caused depolarization of cortical actin to different levels (Rodriguez-Escudero *et al.*, 2005). EspD blocked actin polarization to the bud, although to a less severe degree than reported for EspG. On the contrary, Map expression strongly interfered with cell polarity mechanism, leading to disruption of septins (Rodriguez-Escudero *et al.*, 2005), proteins required for actin ring assembly in yeast (Styles *et al.*, 2013). Expression of these effectors in yeast provided important clues on their function, suggesting an important link between actin cytoskeleton and disrupted microtubules. Besides cell cycle, Map and EspG have been shown to modulate G protein signaling (Alto *et al.*, 2006; Dong *et al.*, 2012; Hardwidge *et al.*, 2004; Matsuzawa *et al.*, 2004; Selyunin *et al.*, 2011), a pathway that connects microtubule network and actin dynamics (Mack & Georgiou, 2014).

Rho family of small GTPases: "favorite" targets of bacterial effector proteins

Many type III effector proteins have been shown to modulate activity of yeast Rho GTPases (Table 1 and Figure 4), either to facilitate bacterial invasion into host cell or to escape the phagocytosis and immune response (Lemichez & Aktories, 2013; Popoff, 2014).

The Rho-family GTPases belong to the Ras superfamily and function as molecular switches regulating membrane trafficking, actin dynamics, cell cycle or nuclear import (Croise *et al.*, 2014). In response to extracellular stimuli, these small G proteins cycle between an active GTP-bound state, usually anchored to the membrane and an inactive GDP-bound state, present in the cytoplasm (Iden & Collard, 2008). They are activated by guanine nucleotide exchange factors (GEFs), which catalyse the exchange of GDP for GTP. GTPase activating proteins (GAPs) act as negative regulators, accelerating their intrinsic GTPase activity and resulting in an inactive GDP-

bound GTPase and the shutdown of signaling. The inactive Rho GTPases are then sequestered into the cytosol by guanine nucleotide-dissociation inhibitors (GDIs), which inhibit the exchange of GDP for GTP and prevent their translocation to membranes (Buchsbaum, 2007; Goicoechea *et al.*, 2014; Tcherkezian & Lamarche-Vane, 2007). Importantly, Rho G proteins can be constitutively activated, as it was shown for 10 out of the 20 members of small GTPases in mammals, which are constitutively bound to GTP and therefore regulated by alternative mechanisms (Sadok & Marshall, 2014).

Bacterial T3E differently modulate Rho signaling, by mimicking GAPs and GEFs, therefore inhibiting or activating, respectively, small G signaling events. In mammals, *Yersinia* YopE T3E was shown to act as a Rho GAP protein, leading to inactivation of the Rho GTPase switch and disruption of actin microfilament stress fibers (Von Pawel-Rammingen *et al.*, 2000). In yeast, expression of YopE resulted in loss of actin cytoskeletal polarity, by the presence of cortical patches dispersed throughout the yeast cells, blocking bud formation and actin rings (Lesser & Miller, 2001). As Rho G proteins mediate budding pathway, yeast toxicity of YopE can be explained by alteration of the normal budding formation through inhibition of Rho proteins. Elucidating YopE function led to the discovery of a previously unknown role for Rho G proteins in actin polarization in yeast, observed with the formation of actin rings (Lesser & Miller, 2001).

Other bacterial T3E like *Shigella* IpgB2, *Escherichia coli* Map and *Salmonella* SopE2 and SifA activate Rho GTPases pathway, functioning as bacterial GEFs in both yeast and mammalian systems (Alto *et al.*, 2006; Rodriguez-Pachon *et al.*, 2002). Interestingly, structural studies comparing and contrasting bacterial and eukaryotic GEFs revealed that, although they are evolutionary distinct, they use the same residues to select and activate GTPases. Therefore, they share a similar biochemical strategy (Orchard & Alto, 2012). The mechanism of cellular invasion in *Salmonella* infection involves the time-dependent secretion of both GEF and GAP proteins. After injecting GEF SopE2 effector protein required for actin rearrangement and bacterial invasion, *Salmonella* secretes an antagonizing type III effector, SptP, which allows cell recovery and completion of bacterial internalization (Ly & Casanova, 2007; Van Engelenburg & Palmer, 2008; Zhou & Galan, 2001). SptP activity as a GAP is conserved in both yeast and mammals, down-regulating the GTPase Cdc42 and its dependent MAPK kinases after bacterial entry (Rodriguez-Pachon *et al.*, 2002).

Bacterial effectors also function by mimicking GDI factors and inhibiting Rho G signaling, without alteration in GDP/GTP exchange. For example, *Yersinia* effector

YpkA/YopO binds Rho GTPases Rac1 and RhoA in mammals, causing cytoskeletal disruption (Prehna *et al.*, 2006). Expression of YpkA/YopO in yeast was associated with disruption of actin and cytotoxicity, showing that YopO targets a conserved eukaryotic process (Nejedlik *et al.*, 2004). Rho GTPase proteins are highly conserved in eukaryotic cells from yeast to humans (Jaffe & Hall, 2005), and they are divided into three subfamilies: Cdc42, Rac, and Rho. Out of the six Rho GTPases described in *Saccharomyces cerevisiae* (Park & Bi, 2007), a large body of work focused on the study of two Rho G proteins: Cdc42, with a major role in yeast cell polarization and filamentous growth (Bi & Park, 2012; Cullen & Sprague, 2012; Meitinger *et al.*, 2014) and Rho1, activator of cell wall integrity pathway (Levin, 2011).

Salmonella SopE2 seems to modulate the activity of both yeast GTPases Rho1 and Cdc42. Expression of SopE2 stimulates signaling through the filamentation and mating pathway and also results in activation of the cell integrity pathway MAPK Slt2 (Rodriguez-Pachon *et al.*, 2002). The authors showed that there is a cross-regulation between filamentous growth and cell wall integrity pathway, by demonstrating that Cdc42 can induce Slt2 (MAPK) phosphorylation. In this case, study of a type III effector function in yeast has provided knowledge on regulation of MAPK signaling pathways. Moreover, yeast can be used to gain insight into the specificity of bacterial proteins for the different GTPases of the Rho subfamily. Additional studies have strengthened this statement. *Shigella* T3E IpgB2 functions as a GEF for Rho1 protein in yeast and for RhoA (homologue of Rho1) in mammalian cells (Alto *et al.*, 2006). Phosphatase-dead version of *Salmonella* SopB/SigD effector interacts with yeast Cdc42 and human Cdc42, but not Rac1, when co-expressed in *S. cerevisiae* (Rodriguez-Escudero *et al.*, 2006; Rodriguez-Escudero *et al.*, 2011). Cdc42 is highly conserved from yeast to humans at both the sequence (80 to 95% identity in the predicted amino acid sequence) and functional levels (Johnson, 1999). Another *Salmonella* effector SteC was shown to bind to *S. cerevisiae* Cdc24, the GEF for Cdc42, and also to *Schizosaccharomyces pombe* and human Cdc24 homologues (Fernandez-Pinar *et al.*, 2012). How bacterial effectors discriminate between various GTPase isoforms is still unknown.

Heterologous expression of these T3E in yeast also revealed and/or confirmed the roles of these proteins in cell cycle progression, including DNA replication, mitosis and cytokinesis. As commented before, the growth inhibition phenotype conferred by YopE expression in yeast is a result of inhibition of reorganization/polarization of the actin cytoskeleton (Lesser & Miller, 2001). The yeast actin cytoskeleton is polarized at several stages during the budding pathway, before bud formation and prior to

cytokinesis (Styles *et al.*, 2013). Synchronizing yeast at G1 phase of the cell cycle, Lesser and Miller showed YopE expression blocked bud formation and initiated the morphogenesis checkpoint, delaying mitosis. At later steps of the cell cycle, YopE expressing cells remained depolarized, but contrary to the phenotype seen in *Chlamydia* CopN-expressing yeast cells (Huang *et al.*, 2008)., these were able to reconstitute microtubule spindle, allowing nuclear division (Lesser & Miller, 2001). Similarly, expression of *E. coli* Map effector in yeast was marked by the presence of unbudded cells, suggesting loss of coordination between morphogenesis and nuclear events (Rodriguez-Escudero *et al.*, 2005). As Rho GTPases also regulate cell cycle, perturbation of this process by YopE and Map might be a consequence of their interaction with Rho G proteins, and not a direct effect of their activity.

Much work has focused on characterizing interaction between T3E and Rho GTPases, mediated via post-translational modifications. For example, *Yersinia* YopT cysteine protease recognizes and cleaves post-translational modified RhoGTPases, releasing them from the membrane. YopT-mediated inhibition of Rho G signaling seems to be conserved in yeast, as overexpression of Rho Cdc42 suppresses YopT-induced growth inhibition phenotype (Shao *et al.*, 2002).

P. aeruginosa T3E ExoS and ExoT are bi-functional enzymes, both containing N-terminal GAP domains and C-terminal ADP-ribosylation domains. In mammals, the two domains of ExoS and ExoT were shown to exert different effects on host cell morphology, although these effects might be interconnected. Expression of the GAP domain results mainly in disruption of the actin cytoskeleton and cell rounding, but not cytotoxicity (Huber *et al.*, 2014), while ADP-ribosylation domain causes cytotoxicity and cell death of mammalian cells (Barbieri *et al.*, 2001; Garrity-Ryan *et al.*, 2004) and is necessary for blocking bacterial internalization (Rangel *et al.*, 2014). In addition, ADP-ribosyltransferase (ADPRT) activity of both ExoS and ExoT can modify the catalytic arginine in their own GAP domain, leading to down-regulation of GAP activity (Riese *et al.*, 2002; Sun *et al.*, 2004). In yeast, both domains of ExoT are required for growth inhibition phenotype (Garrity-Ryan *et al.*, 2004). On the contrary, ADP-ribosylation domain of ExoS is the main responsible for toxicity in yeast, as only the ExoS ADP-ribosylation mutant, but not the mutant lacking ExoS GAP domain suppresses growth inhibition (Arnoldo *et al.*, 2008; Stirling & Evans, 2006). This might be explained by the different levels of ADPRT activity of ExoS and ExoT: the C-terminal of ExoT appears to possess minimal ADPRT activity *in vitro,* 0.2% compared to ExoS (Garrity-Ryan *et al.*, 2004). In addition, in yeast the main responsible for disruption of actin cytoskeleton it is the ADPRT domain of ExoS (Stirling & Evans, 2006).

By overexpressing yeast homologues of ExoS human targets, including members of Ras superfamily and cyclophilins, Arnoldo and coworkers found that Ras2, one of the two homologues of Ras protein in mammals, rescued ExoS-induced growth inhibition phenotype. This finding showed ExoS ADP-ribosylates identical targets in mammals and yeast, although the activity modulation of Ras proteins is thought to be a cumulative inhibitory effect to additional inactivation of unknown key protein(s) (Arnoldo *et al.*, 2008). Recently, it has been shown that the ribosyltransferase activity of ExoS modulates intracellular trafficking (Simon & Barbieri, 2014). Interestingly, targeting post-translational modified Rho GTPases is also linked to counter host immunity strategies or alter intracellular trafficking, which showcase new outcomes of the interaction effector - small GTPases other than the collapse of actin cytoskeleton (Nomura *et al.*, 2006; Simon & Barbieri, 2014; Woolery *et al.*, 2014).

Plant pathogen type III effectors also display conserved motifs or domains necessary for manipulating Rho G signaling. For example, *Pseudomonas syringae* DC3000 HopAA1-1 was shown to maintain the conserved arginine finger motif required for GAP activity of other T3Es as ExoS, YopE and SptP (Munkvold *et al.*, 2009). However, GAP-like domain is not required for HopAA1-1 function, since a mutation affecting the arginine motif had no effect on toxicity in yeast or virulence in tomato. Instead, introduction in HopAA1-1 GAP-like region of a polymorphism naturally found in its paralog, HopAA1-2 suppressed growth inhibition, suggesting that the phenotypes observed in yeast are the cumulative result of other interacting partners. This finding guided experiments in plants that showed HopAA1-1 functions redundantly with a chlorosis-promoting factor to cause lesion formation on host tomato (Munkvold *et al.*, 2009).

Bacterial effectors sharing conserved WxxxE motifs as for example *E. coli* Map, *Shigella* IpgB and *Salmonella* Sif family members act as GEFs and activate Rho G signaling, promoting lesion formation on hosts (Huang *et al.*, 2009; Orchard & Alto, 2012). The WxxxE motifs were reported to structurally mimic the active site of a GEF protein (Huang *et al.*, 2009). Plant-associated effectors WtsE from *Pantoea stewartii* and *P. syringae* AvrE require the same conserved WxxxE motifs to promote disease (Ham *et al.*, 2009). In addition, WtsE was shown to cause toxicity on yeast growth (Ham *et al.*, 2008). The activity of WtsE in yeast suggests that it may be targeting a fundamental process in eukaryotic cells. It is now known that WtsE affects phenylpropanoid metabolism in maize (Asselin *et al.*, 2015), but this might be a consequence of its still unknown activity in hosts. Rho GTPases in plants play an important role in host-pathogen interactions (Kawano *et al.*, 2014), so it would be

natural to speculate that plant-associated T3E have "learned" to manipulate this pathway, by either mimicking Rho GTPases or disrupting the host cytoskeleton and down-regulating related processes, as in the case of *Erwinia* DspA/E (Siamer *et al.*, 2014).

Inhibition of MAP kinase signaling

Inhibition of MAP kinase (MAPK) phosphorylation is a common outcome of the interaction of T3E with the eukaryotic cell signaling machinery. It has been observed for *Shigella* OspF (Kramer *et al.*, 2007) and IpaH9.8 (Rohde *et al.*, 2007), *Yersinia* YopJ (Yoon *et al.*, 2003), *Vibrio parahaemolyticus* VopA (Trosky *et al.*, 2004), *Vibrio cholerae* VopX (Alam *et al.*, 2011) and *Pseudomonas syringae* HopX1 effectors (Salomon *et al.*, 2012). By heterologous expression in yeast, these effectors were shown to inhibit specific steps in the four better-characterized MAPK signaling pathways in yeast (Chen & Thorner, 2007). These studies were possible since MAPK modules in both yeast and higher eukaryotes share similar regulated kinase cascades and cell surface receptors (Saito, 2010).

Shigella flexneri T3E OspF was shown to non-specifically inhibit activation of MAPK signaling pathways in yeast (Kramer *et al.*, 2007). In the cell wall integrity MAPK pathway, OspF inhibited the phosphorylation of Slt2/Mpk1 MAPK. This MAPK is activated during the cell cycle or under conditions that perturb yeast cell wall like depolarization of actin cytoskeleton (Levin, 2011). No alteration of yeast cytoskeleton was observed in response to OspF expression (Kramer *et al.*, 2007), suggesting this T3E targets downstream Rho1 (see Figure 4). In addition, expression of OspF impaired phosphorylation of MAPK Hog1, Fus3 and Kss1 (Kramer *et al.*, 2007). These MAPKs act in the yeast high osmolarity/glycerol (HOG) MAPK pathway, pheromone response and filamentous growth MAPK pathway, respectively. Correspondingly, studies in mammalian cells revealed that OspF is a MAPK phosphatase, capable of dephosphorylating host MAPKs in the nucleus (Arbibe *et al.*, 2007; Li *et al.*, 2007). Characterization of OspF in yeast is an excellent illustration of how the multiple genetic tools available for studying yeast MAPK signaling pathways (Furukawa & Hohmann, 2013) can be employed to uncover effector function. Similarly, expression of *P. syringae* HopX1 in yeast showed that this effector attenuated the activation of the HOG MAPK pathway under stress conditions, without alteration of Hog1 MAPK expression or its nuclear dynamics (Salomon *et al.*, 2012). Phenotypes caused by HopX1 expression in yeast were dependent on its intact enzymatic activity, as a mutation in HopX1 catalytic site constrained the ability of this effector to inhibit growth and

modulate HOG signaling under stress. This correlates to previous studies in plants showing the putative catalytic residues are crucial for HopX1 function (Nimchuk *et al.*, 2007). Importantly, in the case of OspF and HopX1 effectors, expression in yeast provided the first clues on their activity therefore engineering of yeast MAPK signaling pathways can provide a good start in deciphering effector function.

Other bacterial effectors operate upstream of the activation of the MAP kinase. For instance, the IpaH9.8 T3E from *Shigella flexneri* acts as an E3 ubiquitin ligase leading MAP kinase kinase (MAPKK) Ste7 to proteasomal degradation, diminishing phosphorylation of its MAPK targets and inhibiting the yeast pheromone response/mating MAPK pathway (Rohde *et al.*, 2007). Likewise, *Yersinia* YopJ inhibits both yeast pheromone response and HOG MAPK pathways, by preventing the activation of the MAPKK equivalent, that is Ste7 for the mating pathway and Pbs2 for the HOG pathway (Yoon *et al.*, 2003) (see Figure 4). YopJ also inhibits mammalian MAPK pathway (Orth *et al.*, 1999), therefore encodes an evolutionarily conserved activity.

VopA, another member of the YopJ-like family found in *Vibrio parahaemolyticus,* inhibits the HOG MAPK pathway and the cell wall integrity pathway, by preventing phosphorylation of MAPK Hog1 and Mpk1, respectively (Trosky *et al.*, 2004). Interestingly, unlike YopJ, VopA is able to induce a growth arrest phenotype in yeast, suggesting that, although the mechanism of MAPK inhibition is similar, the targets are distinct for each effector. Following studies in mammals showed VopA acts as an acetyltransferase, inhibiting the activity of activated MAPKK (Trosky *et al.*, 2007). Lastly, a novel T3E from *Vibrio cholerae,* VopX, was proposed to interact with components of the yeast cell wall integrity pathway as a strain deleted in Rlm1, a transcriptional activator acting in response to cell wall stress, rescued VopX-mediated growth inhibition phenotype (Alam *et al.*, 2011).

Modulation of pathogen-triggered cell death

Yeast may be used to identify T3Es that play a role in pathogen-triggered cell death, a typical outcome of the plant immune system after recognition of a pathogen effector. A screen using the type III effector repertoire of the plant pathogen *Xanthomonas euvesicatoria* revealed five T3Es that cause growth inhibition/cytotoxicity when expressed in yeast and cell death phenotypes in plants (Salomon *et al.*, 2011). For instance, expression of XopX and AvrRxo1 T3Es was cytotoxic to yeast and irreversibly arrested cells in the G0/1 phase of the cell cycle. Correspondingly, XopX and AvrRxo1 caused cell death in tomato and *Nicotiana benthamiana,* although

AvrRxo1 to a milder extent. Still, expression of XopB caused growth inhibition in yeast and a fast and confluent cell death in *N. benthamiana,* but not tomato plants. This suggests XopB triggers an HR-like cell death, probably because it is recognized by plant resistance proteins. Lastly, XopE1 and XopF2, which inhibited yeast growth less severely than XopX, determined sporadic cell death patches in tomato plants and chlorosis in *N. benthamiana* respectively. In addition, it was shown that the catalytic activity of XopE1 may be conserved across kingdoms, as it is required for growth inhibition phenotype in yeast and induction of chlorosis and cell death in plants (Salomon *et al.*, 2011). Using a similar repertoire screen of *P. syringae* effectors, Munkvold and coworkers showed expression of T3E HopAA1-1 leads to cell death in both yeast and plants (Munkvold *et al.*, 2008).

On the other hand, some bacterial T3E have evolved to escape plant recognition response by suppressing HR. As an example, *P. syringae* tyrosine phosphatase HopAO1 and cysteine protease HopN1 were shown to inhibit HR in plants, and for this, they require intact enzymatic activity (Bretz *et al.*, 2003; Espinosa *et al.*, 2003; Lopez-Solanilla *et al.*, 2004). Catalytic-site point mutations suppress growth inhibition caused by expression of wild-type effector in yeast, suggesting biochemical function of HopAO1 and HopN1 is conserved, although physiological consequences of their activity might be different in yeast and plants (Munkvold *et al.*, 2008).

Other plant pathogen effectors were shown to function as inhibitors of programmed cell death in both yeast and plants. For example, some *Pseudomonas syringae* effectors identified as HR suppressors *in planta* also suppress apotosis in yeast (Abramovitch *et al.*, 2003; Jamir *et al.*, 2004). In *N. benthamiana,* AvrPtoB T3E has the ability to suppress programmed cell death initiated by two R proteins as well as Bax-, a pro-apoptotic protein – induced cell death (Abramovitch *et al.*, 2003). In addition, AvrPtoB protected yeast from stress-induced programmed cell death, highlighting its activity as a eukaryotic cell death inhibitor. Likewise, screening for HR suppressors, Jamir and coworkers described five *Pseudomonas syringae* effectors, including AvrPtoB, able to completely block HR in plants. Interestingly, three of these effectors, AvrPphE$_{Pto}$, HopPtoE and HopPtoF suppress Bax-induced cell death in both plants and yeast, indicating the targets are likely to be conserved across kingdoms (Jamir *et al.*, 2004). Expression of these proteins in yeast opened the pathway to searching specific eukaryotic targets for type III effectors and enlarged comprehension of the molecular mechanism underlying plant-effector interaction.

Alteration of membrane structure and function

To ensure bacterial entry and survival inside host cells, many pathogenic bacteria inject T3E to induce cellular permeabilization and host membrane damage (Asrat *et al.*, 2014; Ham *et al.*, 2011). It is the case of *Pseudomonas aeruginosa* ExoU type III effector, a member of the phospholipases A2 (PLA_2) family of enzymes (Sato & Frank, 2004). Catalysis of membrane phospholipids by PLA_2 releases free fatty acids, involved in regulation of lipid remodeling, membrane disruption, signal transduction and pro-inflammatory response or cell death (Mouchlis *et al.*, 2015; Murakami *et al.*, 2011). ExoU was first defined as responsible for acute cytotoxicity in mammals (Finck-Barbancon *et al.*, 1997; Hauser *et al.*, 1998) and caused membrane damage to different organelles and fragmentation of the vacuole in yeast (Sato *et al.*, 2003). Moreover, similar N-terminal, internal and C-terminal domains were shown to be necessary for ExoU-mediated toxicity in both mammalian and yeast cells (Finck-Barbancon & Frank, 2001; Rabin & Hauser, 2003), strengthening the hypothesis ExoU might be acting through similar mechanism across kingdoms.

The phospholipase activity of ExoU was discovered by testing a series of inhibitors that affected the function of different cellular structures, including vacuolar biogenesis. Interestingly, phospholipase inhibitors suppressed ExoU-mediated yeast and mammalian cytotoxicity (Phillips *et al.*, 2003; Sato *et al.*, 2003). These results were also confirmed at the level of structure, as ExoU possessed a domain homologous to patatin (Sato *et al.*, 2003), an enzyme capable of hydrolyzing phospholipids and activated upon stress or pathogen attack (Holk *et al.*, 2002; La Camera *et al.*, 2009; Ramanadham *et al.*, 2015). *In vitro* enzymatic activity of ExoU was observed only in the presence of yeast extract, suggesting that ExoU could be activated or modified by a eukaryotic cell factor (Sato *et al.*, 2003). This is not surprising, as other bacterial type III effectors were shown to require activation by a host factor in order to carry out their enzymatic function. Plant-associated type III effector AvrRpt2 from *P. syringae* is a cysteine protease activated by a host cyclophilin, activation necessary for its protease activity in elimination of a plant protein (Coaker *et al.*, 2005). Similarly, enzymatic activation of ExoU requires binding of its C-terminal domain to ubiquitin or ubiquitin-modified proteins (Anderson *et al.*, 2011; Anderson *et al.*, 2013; Sato *et al.*, 2006). In the presence of ubiquitylated yeast superoxide dismutase and other ubiquitylated mammalian proteins, ExoU is activated as a phospholipase A2 and lyses infected cells (Anderson *et al.*, 2011; Sato *et al.*, 2006). In the case of *P. aeruginosa* ExoU, yeast constituted a guiding platform to define ExoU mechanism of activation and substrate specificity. Recent research described ExoU localizes to the plasma membrane, where

it hydrolyses a multifunctional phosphoinositide, causing disruption of host membrane integrity (Sato & Frank, 2014; Tyson *et al.*, 2015).

Perturbation of vesicle trafficking

In addition to manipulating the cytoskeleton and endomembrane system, intracellular pathogenic bacteria have learned to escape from phagosomal degradation by modulating host-vesicle trafficking (Baxt *et al.*, 2013; Brumell & Scidmore, 2007). Targeting these pathways by T3E was described to be a direct consequence of altering cellular processes like the cytoskeleton or G protein signalling, as for example *Erwinia amylovora* DspA/E or EspG from *Escherichia coli*, respectively. Yeast cells expressing DspA/E showed delayed endocytosis, due to defects in cell polarization (Siamer *et al.*, 2011). On the other hand, pathogenic *E. coli* modulates host vesicle pathways by injecting EspG, a type III effector displaying GAP activity for Rab1 G protein, therefore perturbing ER-to-Golgi trafficking (Dong *et al.*, 2012; Selyunin *et al.*, 2011).

In other cases, bacterial effectors exploit vesicular transport to their benefit, so that they can carry out their function inside hosts. For instance, *Yersinia pestis* YopM T3E depends on functional vesicle trafficking to localize to the nucleus in both yeast and mammalian cells (Benabdillah *et al.*, 2004; Skrzypek *et al.*, 2003). Yeast has been a robust model to study the intracellular trafficking of YopM and determine leucine-rich repeats (LRRs) in its structure necessary for nuclear translocation. Skrzypek and coworkers suggested that nuclear localization of YopM might be an indirect effect of interaction with proteins associated with the surfaces of vesicles or chaperones that can take it to the nucleus (Skrzypek *et al.*, 2003). Indeed, in mammals, YopM targets two kinases, Rsk1 and Prk2, involved in cell proliferation, apoptosis and translation, and down-regulates expression of several pro-inflammatory cytokines, although these two activities are not interdependent (Hofling *et al.*, 2014; McDonald *et al.*, 2003). Recent work has proven YopM also interacts with mammalian caspase-1, inhibiting host immune response and ensuring bacterial replication (LaRock & Cookson, 2012). These results show that bacterial effectors might have more than one target and/or interconnected activities inside host cells.

Other effectors were shown to target trafficking from the endoplasmic reticulum (ER) to the nucleus. Using an array of yeast deletion strains, Bosis and coworkers found that *Xanthomonas* XopE2 T3E affected the response to ER stress (Bosis *et al.*, 2011). More specifically, yeast cells expressing XopE2 failed to activate the unfolded protein response (UPR) after induction of ER stress. UPR is a quality control pathway comprising specific machinery working to maintain ER homeostasis and avoiding

overload of misfolded or underglycosylated proteins (Adhikari *et al.*, 2015; Mori, 2009). Interestingly, cells expressing XopE2 were highly sensitive to tunicamycin and 2-deoxy-D-glucose, two specific inhibitors of glycosylation in the ER (Bosis *et al.*, 2011). Altogether, these results show XopE2 alters UPR pathways, perturbing molecular signaling from the ER to the nucleus. It is not surprising that bacterial effectors have "learned" to subvert UPR signaling, escaping from phagocytic pathways and cell death, typically triggered by the host to protect the organism from cells that display misfolded proteins (Ron & Walter, 2007). Likewise, as commented before, yeast was described as a powerful resource in identification of pathogen effectors affecting vesicle trafficking pathways (Tabuchi *et al.*, 2009).

CHAPTER 3:
TYPE III EFFECTORS IN *RALSTONIA SOLANACEARUM*

Ralstonia solanacearum is emerging as a model system to study plant-pathogen molecular interactions and T3E function (Coll & Valls, 2013). This soil-borne bacterium is the causing agent of bacterial wilt and has been recently ranked as the second most important bacterial plant pathogen (Mansfield *et al.*, 2012). *R. solanacearum* has an enormous economic impact due to its wide geographical distribution and host range, high persistence and broad strain diversity. It infects more than 200 plant species, including important agricultural crops such as tomato and potato (Salanoubat *et al.*, 2002) and contains a large effector repertoire of largely unknown functions (Peeters *et al.*, 2013). Of more than 70 T3Es identified in the reference strain GMI1000 (Poueymiro & Genin, 2009; Mukaihara *et al.*, 2010), only 23 have been assigned a defined role *in planta* (Coll & Valls, 2013).

These effectors were shown to elicit or suppress plant defense, modulate host proteasome or function as TAL (transcription activator-like) effectors (Deslandes & Genin, 2014). *Ralstonia* TAL effectors (RipTALs) were shown to be structurally homologous to previously characterized *Xanthomonas* TAL effectors (de Lange *et al.*, 2013; Li *et al.*, 2013). Discovery of AvrBs3 effector family from *Xanthomonas spp.*, also called TAL effectors, constituted an outbreak in the field of plant-pathogen interactions, as these effectors can mimic eukaryotic transcription factors and modulate plant target genes (Boch & Bonas, 2010). These characteristics of TAL effectors offer fantastic genome-manipulation applications and are currently exploited for engineering of plants resistant to *Xanthomonas spp.* and *Ralstonia solanacearum* (Boch *et al.*, 2014; de Lange *et al.*, 2013; Li *et al.*, 2013).

Only in a few cases effector function has been elucidated and most of their plant targets remain unknown. In fact, PopP2 (RipP2) is the only effector from *Ralstonia solanacearum* for which a plant target is known. PopP2 displays auto-acetyltransferase activity suspected to be perceived by RRS1-R, a resistance protein from *Arabidopsis thaliana* (Deslandes *et al.*, 2003; Tasset *et al.*, 2010). Importantly, the functional characterization of PopP2 demonstrates for the first time a physical interaction between a plant-associated bacterial effector and its cognate resistance protein in the nucleus. Nevertheless, the precise molecular mechanisms by which PopP2 activates the plant

immune response are complex and involve cooperation of other interactors from both plant and pathogen side (Bernoux *et al.*, 2008; Williams *et al.*, 2014).

Table 2. List of type III effectors from *Ralstonia solanacearum* studied *in planta* and their function (Deslandes & Genin, 2014).

Effector	Relevant domain	Associated phenotypic trait	Function
RipA(1-5) (AWR1 to 5)		RipA2 contributes to pathogenicity and has necrogenic activity on tobacco RipA5 acts as a HR-like eliciting factor on some tobacco species	
RipG(1-8) (Gala1 to 8)	F box and leucine rich repeats	RipG2, RipG3, RipG6 and RipG7 collectively contribute to pathogenicity (tomato and *Arabidopsis)* RipG7 required for pathogenicity on *Medicago truncatula* RipG4 suppresses callose deposition (*Arabidopsis)*	Components of ubiquitin ligase complexes in host cells
RipH(1-3) (HLK1 to 3)		Collectively contribute to pathogenicity on tomato	
RipP1 (PopP1)	YopJ-like family of cysteine proteases	HR-eliciting factor on some *Petunia* genotypes and on tobacco species	
RipP2 (PopP2)	YopJ-like family of cysteine proteases	Avirulence factor on *Arabidopsis* genotypes carrying the RRS1-R resistance gene Tolerance in *Arabidopsis* also depends on the RRS1-RipP2 interaction Contribution to bacterial fitness on eggplant	Plant nuclear-localized and acetyltransferase activity
RipR (PopS)		Weak contribution to virulence (tomato) Suppression of salicylic acid-mediated defences (tomato)	
RipT	YopT-like family of cysteine proteases		Plant plasma membrane associated cysteine protease
RipAA (AvrA)		HR-eliciting factor on tobacco species Contribution to virulence (tomato, eggplant and *M. truncatula)*	
RipAF1	ADP-ribosyltransferase	Contribution to bacterial fitness on eggplant	
RipAX1 (Rip36)	Zinc-dependent protease	HR-eliciting factor on eggplant *S. torvum*	Putative protease
RipTAL1	TAL (transcription activator-like)		Plant nuclear-localized Transcription factor
RipV1, RipV2, RipAR, RipAW, RipBG	Ubiquitin-ligase		Putative ubiquitin-ligase
RipB, RipAV		Necrogenic activity on lettuce and tomato cultivars	

AWRs (named after a conserved alanine-tryptophan-arginine tryad and also called RipAs) are one of the multigenic families of five T3Es conserved in all *R. solanacearum* strains (Peeters *et al.*, 2013), with orthologues in other bacterial pathogens such as *Xanthomonas* strains, *Acidovorax avenae* or *Burkholderia* spp. (Sole *et al.*, 2012). A low protein similarity has also been described between AWRs and the *Xanthomonas oryzae pv. oryzae* effector XopZ, which was shown to be involved in virulence and suppression of host basal defence (Song & Yang, 2010). Translocation assays have proven AWRs as *bona fide R. solanacearum* type III secreted effectors (Cunnac *et al.*, 2004; Mukaihara *et al.*, 2010; Sole *et al.*, 2012). However, sequence information on AWR proteins gives no clue on their putative function. In a previous study, we showed that the AWR T3E family collectively contributes to *R. solanacearum* virulence, as a mutant bacterium devoid of all AWRs multiplies 50-fold less than the wild-type strain on eggplant and tomato plants (see annex (Sole *et al.*, 2012)). This is consistent with the fact that AWR family of belongs to the core effectome, defined as the minimal effector repertoire to cause disease (Deslandes & Genin, 2014).

Functional analysis of AWRs also demonstrated that their expression in different plant species triggers varying defense responses (annex (Sole *et al.*, 2012)). AWR proteins might be recognized in *Arabidopsis thaliana,* since the *Δawr1-5* strain infects faster than a wild-type strain. Also, heterologous expression of AWRs in *P. syringae* results in reduced growth compared to a wild-type strain, suggesting that some AWRs (except for AWR2) may be detected by plant proteins. Finally, *Agrobacterium*-mediated transient expression of AWRs in the leaves of non-host *Nicotiana benthamiana* plants induces a necrosis effect at different extents.

Functional analyses of each AWR showed that AWR5 had an important contribution in virulence and also caused the most dramatic responses in plants. In *N. benthamiana* plants, AWR5 induces an HR-like phenotype, as confirmed by trypan blue and DAB (diaminobenzidine) staining, for dead cells and cells producing H_2O_2, respectively, together with the up-regulation of HR-specific marker genes (see annex (Sole *et al.*, 2012)). In addition, we have recently found that *awr5* is one of the most highly expressed genes when *R. solanacearum* grows inside the plant host (Puigvert et al. unpublished), strengthening the hypothesis that AWR5 has an important role in infection.

These findings, together with the limitations encountered in AWR5 study, appointed us to characterization of this effector function by heterologous expression in yeast.

OBJECTIVES

The objectives of this thesis are detailed below:

Heterologous expression of AWR type III effectors in *Saccharomyces cerevisiae*

To investigate the function of AWR bacterial effectors in eukaryotic cells, we expressed the five *awr* genes from *Ralstonia solanacearum* GMI1000 in yeast, using different promoter systems.

Phenotypic characterization of AWR effector family in yeast

We aimed to evaluate the phenotypes caused by *awr* genes expression on yeast cells.

Effect of *awr5* expression on the physiology of the budding yeast

To understand the molecular basis of AWR5 effect on yeast physiology, we have used a genome-wide transcriptomic approach.

Identification of AWR5 molecular targets by heterologous expression in yeast

To further dissect the mechanism of action of AWR5 in heterologous systems, we applied gain-of-function approaches, to obtain information about the processes manipulated by the bacterial pathogen on yeast.

***In planta* validation of AWR5 impact on its targets**

In order to determine the degree of functional conservation of AWR5 in its natural context, we tested the impact of this effector protein on complementary plant processes.

RESULTS

CHAPTER 1:
PHENOTYPIC CHARACTERIZATION OF AWR PROTEINS IN YEAST

Background

Our first aim was to perform a yeast two-hybrid (Y2H) screening to identify plant proteins interacting with AWRs. We noticed that transformation of yeast cells with plasmids carrying *awr* genes had a very low efficiency when compared to the yeast cells transformation with the empty vector. This fact suggested a putative toxicity effect of AWRs on yeast growth.

1.1. Expression of the *R. solanacearum awr* type III effectors in budding yeast causes growth inhibition

To investigate the function of the AWR bacterial effectors in eukaryotic cells, we expressed the five *awr* genes from *R. solanacearum* GMI1000 in *S. cerevisiae.* In a first step, *awr*s were cloned in the high-copy number vector pAG426GAL, where they are transcribed from the strong galactose-inducible *GAL1* promoter. The resulting plasmids were introduced in yeast and the transformed strains grown overnight, then serially diluted and plated either in repressing media (glucose) or inducing media (galactose). It was observed that, except for AWR4, these effectors inhibited growth to different extents, as observed by the inability to form macroscopic colonies on inducing media (Fig. 5). AWR1, 2, 3 and 5 caused a strong toxicity upon induction, but AWR5 showed the most dramatic effect, inhibiting yeast growth even in non-inducing conditions. The phenotype seemed specific for AWR effectors, as it was not observed when a control gene (GFP) was expressed (Fig. 5).

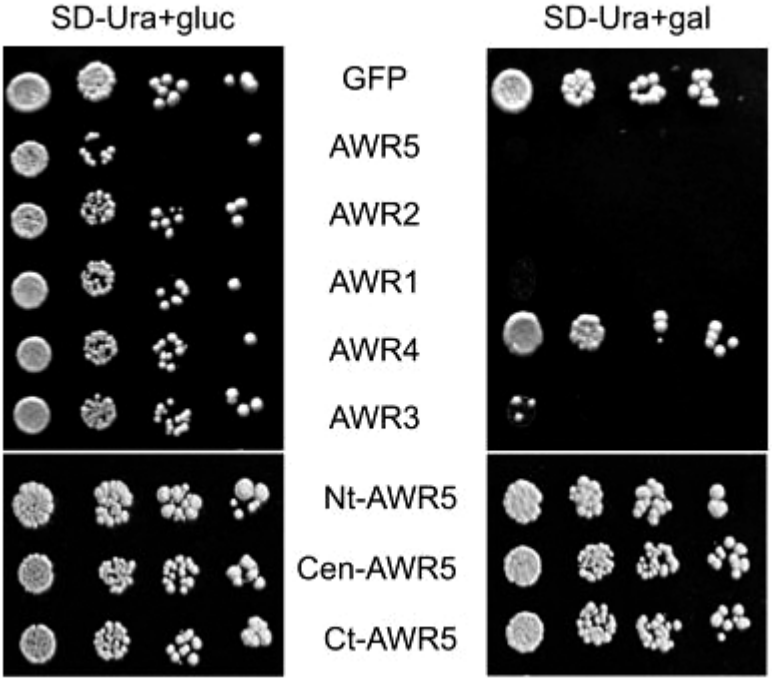

FIGURE 5. Full-length AWR5 causes growth inhibition in yeast when expressed from a high-copy-number plasmid.

Yeast strains bearing *awr* genes fused to GFP tag and the *awr5* effector gene N-terminal (Nt-AWR5), central (Cen-AWR5) and C-terminal (Ct-AWR5) fragments were subjected to serial 10-fold dilutions and spotted onto solid SD-Ura+gluc (glucose - repressing medium) and SD-Ura+gal (galactose - inducing medium). Photographs were taken after 2 days of growth.

The full-length AWR5 protein was required for functionality, as expression of split variants of AWR5 (N-terminal or C-terminal halves, or the central region) did not cause toxicity on yeast cells (Fig. 5). Importantly, these results correlated with the HR-like phenotypes observed in non-host plants (see Annex Figure 5A (Sole *et al.*, 2012)).

To evaluate the phenotype in more physiological conditions and ensure construct stability and tight control of effector transcription, we integrated the bacterial genes in the yeast genome under the control of a repressible Tet-Off promoter (Gossen & Bujard, 1992). When the resulting strains bearing *awr*s or a control *GUS* gene were plated in the absence of the repressor doxycycline, only expression of *awr5* reproduced the dramatic growth arrest (Fig. 6). Thus, we later concentrated on the characterization of the growth inhibition caused by *awr5* expression.

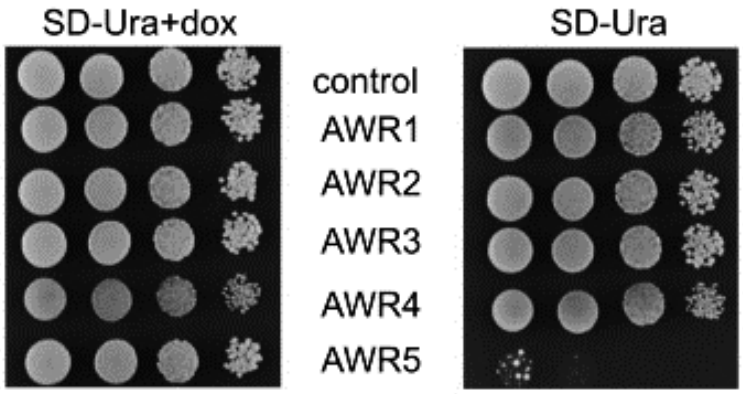

FIGURE 6. Expression of *awr5* effector inhibits yeast growth.

Growth on solid medium of yeast strains expressing *awr* effectors. Yeast strains bearing *awr* genes fused to GFP tag were subjected to serial 10-fold dilutions and spotted onto solid SD-Ura+doxycycline (repressing medium) and SD-Ura (inducing medium). Photographs were taken after 2 days of growth.

The absence of toxicity for AWR1, 2 and 4 could not be attributed to a lack of expression, as the full-length proteins were readily detected in yeast cells (Fig. 7).

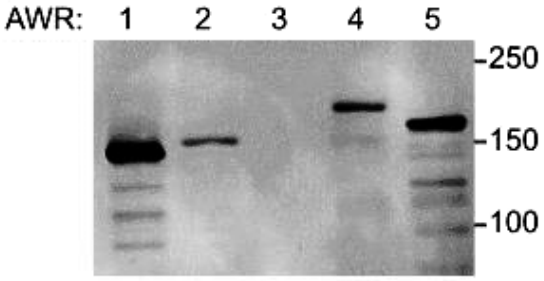

FIGURE 7. Protein levels of the different AWR family members expressed in yeast.

Total protein was extracted from yeast strains expressing AWR effectors fused to GFP and immunoblotted using anti-GFP antibody.

1.2. Characterization of the AWR5-dependent growth inhibition phenotype

Yeast growth inhibition was also apparent upon AWR5 production in liquid cultures, as indicated by a rapid stagnation of cell density over time (not shown) and a clear decrease in the number of viable cells (Fig. 8A). Growth inhibition kinetics paralleled with an increase in *awr5* RNA (Fig. 8C) and protein levels (Fig. 8B). Microscopic observation of strains producing AWR5 revealed the presence of budding cells at similar proportions to cells not producing the bacterial effector (Fig. 9A). Thus, it could be ruled out that this protein caused arrest in a particular step of the cell cycle.

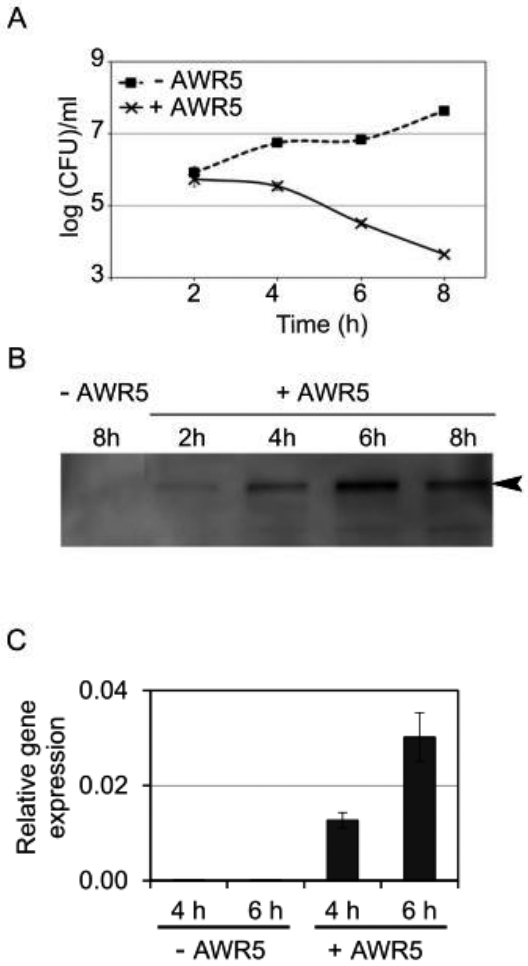

FIGURE 8. Characterization of AWR5-induced growth inhibition phenotype.

(A) Growth kinetics in liquid medium of yeast cells harboring *awr5*. Yeast cells harboring *awr5* were grown in SD-Ura+dox (-AWR5) and SD-Ura (+AWR5) liquid media and dispersed on SD-Ura+dox plates. The logarithm of colony forming units (CFU) per ml is shown over time. Error bars indicate standard errors for 2 biological replicates. (B) Immunoblot analysis of AWR5 protein levels. Total protein was extracted from cultures shown in figure 6 and immunoblotted using an anti-GFP antibody. The black arrowhead indicates AWR5-GFP protein. (C) qRT-PCR showing *awr5* expression levels relative to actin. Yeast strains bearing *awr5* gene were grown in SD-Ura+dox (-AWR5) and SD-Ura (+AWR5). *awr5* gene expression was tested at 4 and 6 hours after induction. Error bars represent standard errors of 2 independent clones. All experiments were performed at least three times, with similar results.

Expression of *awr5* caused strong growth inhibition but not cell death, as deduced from methylene blue staining of cells bearing *awr5* in the absence of doxycycline (Fig. 9A) and from counting of viable cells able to form colonies under *awr5* repression conditions after 6 h of *awr5* expression (Fig. 9B). Similarly, growth arrest in cells expressing *awr5* was not likely caused by defect in cell wall construction leading to cell lysis, since it was not eliminated by osmotic stabilization with 10% sorbitol (Fig. 10). In contrast, determination of cell size upon expression of *awr5* showed significant changes, visible after 8 h of induction, with AWR5-producing cells showing an average diameter of 4.96 ± 0.03 µm, while that of non-expressing cells was over 5.3 ± 0.06 µm ($p < 0.005$, Fig. 9C).

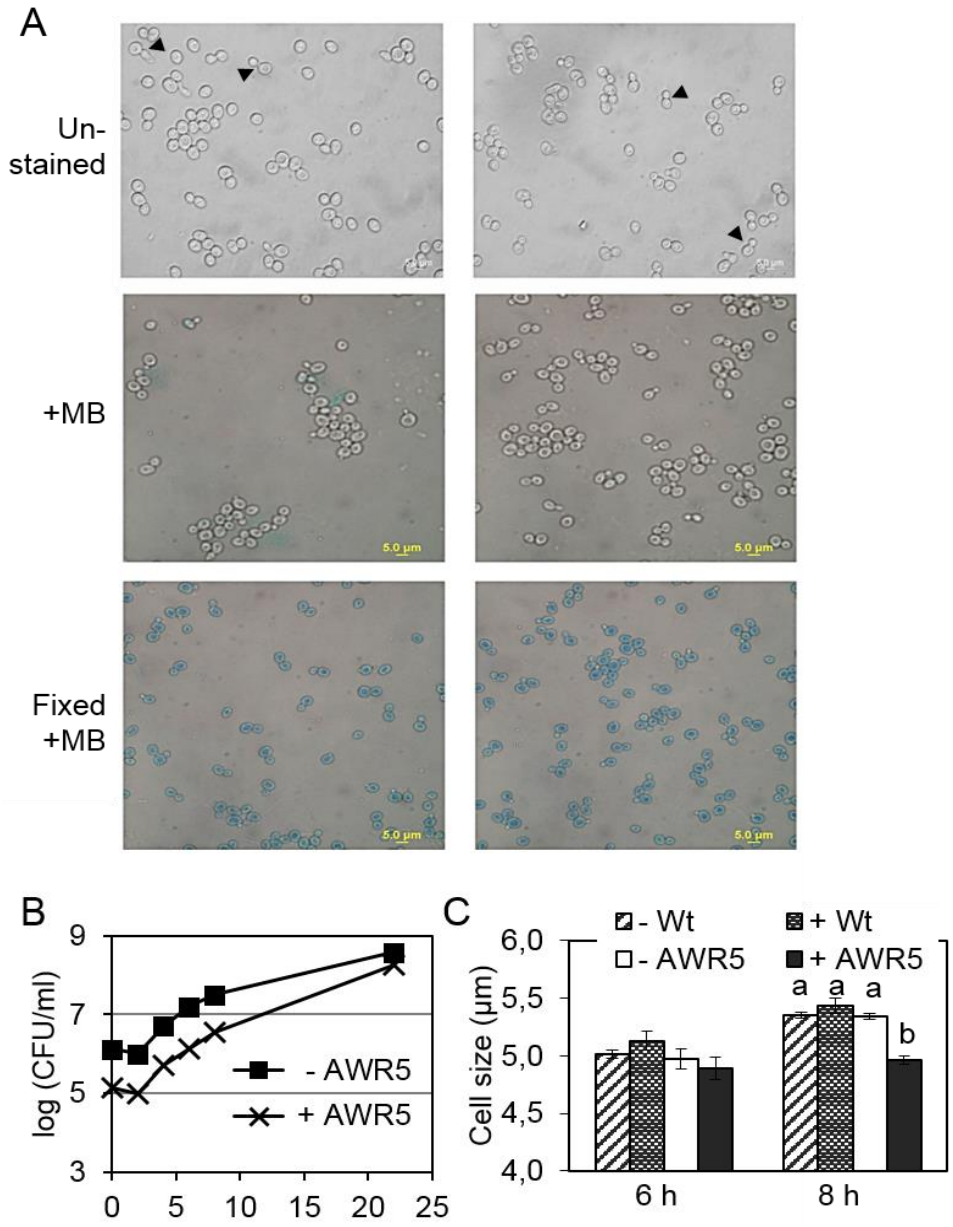

FIGURE 9. *awr5* does not cause cell cycle arrest nor cell death in yeast.

(A) Representative bright field microscope pictures of cells bearing *awr5* grown for 6 hours in SD-Ura+dox (-AWR5) in SD-Ura (+AWR5). Upper panel: unstained cells. Middle panel: Cells stained with methylene blue. Lower panel: Cells fixed with formaldehyde before methylene blue staining. Black arrows indicate budding yeast cells. Bars correspond to 5 µm. (B) Growth curves under repressing conditions (SD-Ura+dox) of the yeast strain harboring *awr5* that had been previously been grown in SD-Ura+dox (repression of *awr5*) or SD-Ura (induction of *awr5*). Yeast counts were measured by spotting culture dilutions on SD-Ura+dox plates. The logarithm of colony forming units (CFU) per ml is shown over time. A representative curve is shown for each condition. (C) Expression of AWR5 diminishes yeast cell size. Strains bearing AWR5 were grown in YPD+dox (repression, -AWR5) or YPD (induction, +AWR5) for 6 and 8 hours. Cell size was analyzed with a Scepter Handheld Automated Cell Counter (Merck Millipore) and compared to that of the wildtype strain with (-Wt) and without doxycycline (+Wt). Letters at 8 hpi indicate a statistically significant difference following post-ANOVA Tuckey test (P<0.001).

Previous reports studying effectors from *Pseudomonas syringae* or *Xanthomonas euvesicatoria* had shown that some of them caused growth arrest when yeast was forced to respire (Munkvold *et al.*, 2008). To verify if respiration affected AWR5 toxicity in yeast, we grew serial dilutions of the strain producing this protein or a control gene (β-glucuronidase, *GUS*) onto solid medium containing the non-fermentable carbon sources ethanol and glycerol. The toxic effect due to AWR5 was maintained under these conditions (Fig. 10). As observed in Figure 10, the toxic effect due to AWR5 was maintained under these conditions.

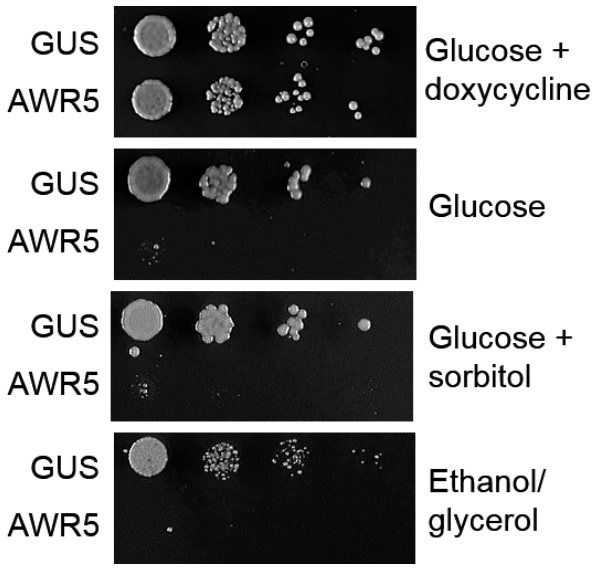

FIGURE 10. AWR5-mediated yeast growth inhibition is not rescued by osmoprotection or respiration.

Serial tenfold dilutions of strains bearing *awr5* or a control gene (*GUS)* were spotted onto solid SD-Ura medium containing glucose and doxycycline (repressing conditions), or on plates without doxycyline (*awr5* inducing conditions) supplemented either with: glucose, glucose and sorbitol (osmoprotectant) or ethanol/glycerol (carbon sources that force respiration). Photographs of representative plates out of several replicas were taken after 2 days of growth.

In summary, we established that production of the full-length AWR5 protein in yeast targeted a cellular process leading to a growth inhibition and decreased cell size, but not involving an evident cell cycle arrest or cell death.

CHAPTER2:
IDENTIFICATION OF CELLULAR PROCESSES TARGETED BY AWR5 HETEROLOGOUS EXPRESSION IN YEAST

2.1. Expression of *awr5* mimics the transcriptional changes induced by the TORC1 inhibitor rapamycin

To understand the molecular basis of *awr5* toxicity in yeast and to highlight putative functional targets, we considered the identification of possible changes at the mRNA level caused by expression of the effector. To this end, we carried out a genome-wide transcriptomic analysis using DNA microarrays in yeast cells with *awr5* expression induced for 2, 4 and 6 h. This time-course was selected according to the previously characterized growth effect (Figure 8A). DNA microarray analysis yielded 3763 genes with valid data for all 3 time-points. We observed that induction of *awr5* expression produced relevant time-dependent changes in the transcriptomic profile that, in most cases, could be observed after 4 and 6 h of induction. The mRNA level of 766 genes was modified at least 2-fold, with 319 genes induced and 447 repressed. The functional assignment of induced genes revealed a striking excess of genes subjected to nitrogen catabolite repression (NCR) (Godard *et al.*, 2007), such as *MEP2*, *GAP1*, *DAL5*, *CPS1* or *DUR1,2*, whereas among the repressed genes there was a vast excess of genes encoding ribosomal proteins or involved in ribosome biogenesis. This profile was reminiscent of that reported by several laboratories for inhibition of the TORC1 pathway (Hughes Hallett *et al.*, 2014).

The TOR complex 1 (TORC1) is involved in the regulation of cell growth in response to nutrient availability and stress conditions by controlling diverse cellular processes, including transcriptional activation, ribosome biogenesis or autophagy (Smets *et al.*, 2010). This complex contains the Tor1 or Tor2 protein kinases (Loewith & Hall, 2011) and can be inhibited by the drug rapamycin. We took advantage of recent work by the collaborating laboratory of Joaquin Ariño that had generated the transcriptomic profile in response to 1 h of exposure to rapamycin (Gonzalez *et al.*, 2013). Combination of this data with that obtained here after *awr5* expression yielded 2774 genes with expression information in both conditions. Figure 11 shows the correspondence

between changes produced in response to *awr5* with those caused by rapamycin. Whereas the correlation was relatively poor shortly after *awr5* induction (correlation coefficient = 0.401), the similarity between both responses became evident after 4 h and, particularly, after 6 h of *awr5* induction (correlation coefficients 0.569 and 0.739, respectively). We then selected among the 766 genes whose expression changed at least 2-fold those with data for the rapamycin treatment (596 genes) and subjected this set of genes to clustering analysis. Figure 11 clearly documents that the time-dependent transcriptional response to expression of *awr5* matches that provoked by rapamycin treatment (correlation coefficient of 0.872 when compared with *awr5* data after 6 h of expression). It can be observed that clusters 1 and 2 -and to some extent also cluster 3- are enriched in induced genes related to metabolism of nitrogen (mostly amino acids), whereas regarding the repressed genes, cluster 5 includes genes involved in translation and cluster 6 is enriched in genes encoding ribosomal proteins or members of the RiBi (ribosome biogenesis) regulon. All these results indicate that expression of bacterial *awr5* in yeast triggers a response that mimics the inhibition of the TORC1 pathway.

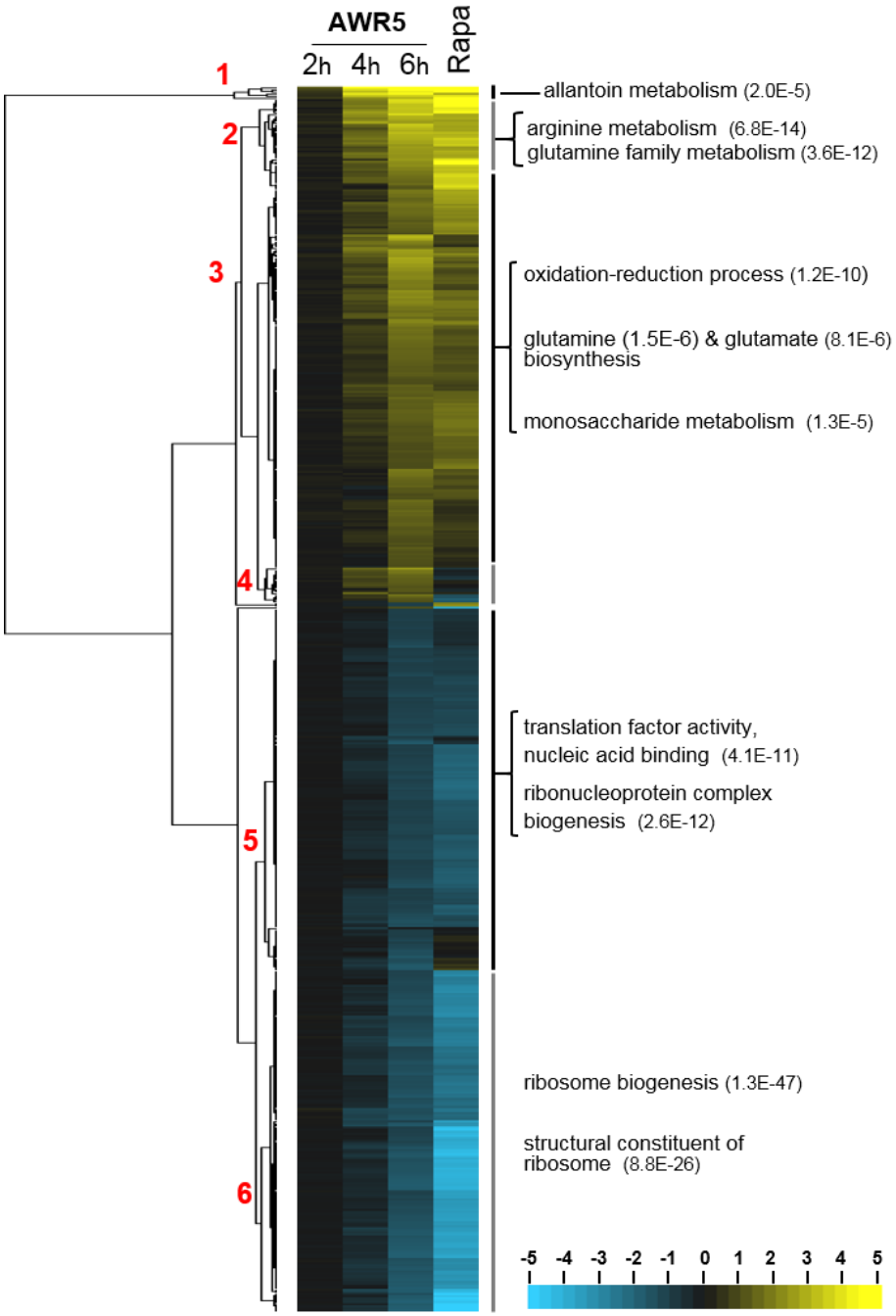

FIGURE 11. Expression of bacterial *awr5* in yeast mimics the transcriptomic changes caused by inhibition of the TORC1 pathway.

The set of 596 genes presenting at least 2-fold changes in mRNA levels upon expression of *awr5* and with valid data for the rapamycin treatment (1 h; 200 ng/ml rapamycin) were clustered (Euclidean distance, average linkage) using Cluster 3.0 software (de Hoon *et al.*, 2004) and are represented with the Java Treeview software, version 1.1.6r4 (Saldanha, 2004). Numbers in red denote selected clusters referred to in the main text and number between parentheses designate the p-value for the indicated GO annotations.

These transcriptome data were validated by performing quantitative RT-PCR analysis on a subset of genes from different TORC1-regulated pathways, which showed altered expression levels in response to *awr5* (Fig. 12A). As expected, *awr5* expression resulted in a decrease of the levels of the TOR-activated *STM1* and *NSR1* genes, which are involved in yeast growth (Homma *et al.*, 2003; Van Dyke *et al.*, 2013). In contrast, the levels of the TOR-repressed *GAP1* and *MEP2*, which control nitrogen catabolite repression (Conway *et al.*, 2012), increased in response to *awr5* expression. Similar results were obtained when promoter activity was measured using fusions to the β-galactosidase reporter: *awr5* expression resulted in increased *GAP1* and *MEP2* promoter output (Fig. 12B).

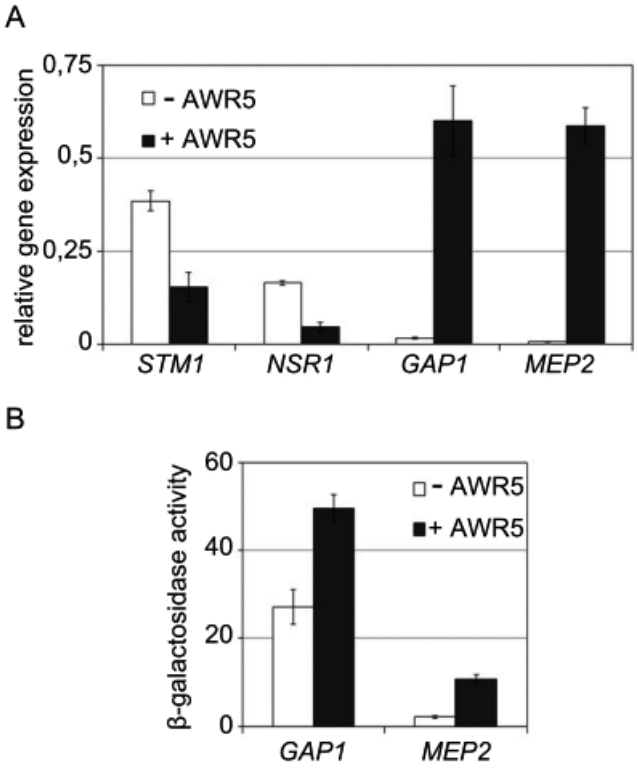

FIGURE 12. Transcriptional response of TORC1-related genes to *awr5* expression.

(A) qRT-PCR experiments showing relative gene expression of TORC1 downstream targets. Gene expression of nitrogen catabolite repression (NCR)-sensitive *GAP1* and *MEP2* and ribosomal biogenesis *STM1* and *NSR1* genes was tested in yeast strains expressing *awr5* (+AWR5) 6 hours after induction. Error bars represent standard errors from 2 biological replicates. (B) β-galactosidase activities from yeast cells bearing *awr5*. Promoter activities of *GAP1* and *MEP2* were determined 6 hours after growth in SD-Ura+dox (-AWR5) and SD-Ura (+AWR5). Data represent the means and standard errors of 4 independent clones. All assays were repeated at least twice with similar results.

In parallel, we also tested promoter activity of *GLN1* and *GDH1* fused to the β-galactosidase reporter strains. Transcriptomic analyses showed that *GLN1* and *GDH1* were induced after *awr5* expression, although to a lower level than *MEP2* and *GAP1*. This resembled the transcriptional changes induced by treatment with rapamycin in which expression of plasma membrane permeases *MEP2* and *GAP1* is rapidly induced more than 10-fold, whereas induction of *GLN1* and *GDH1* occurrs to lower levels (Cardenas *et al.*, 1999; Hardwick *et al.*, 1999). Moreover, in the case of *GLN1*, expression reaches its maximum at 1 hour after rapamycin induction, and at 2 hours expression returns to the original level (Cardenas *et al.*, 1999). Differences in fold-induction after rapamycin treatment were also seen at the level of promoter activity of these NCR-regulated genes (Gonzalez *et al.*, 2013). No significant change in *GLN1* and *GDH1* promoter activity was observed six hours after *awr5* expression (Figure 13), indicating AWR5-mediated induced expression of *GLN1* and *GDH1* genes showed by the transcriptomic data is not detectable at the level of the promoter activity.

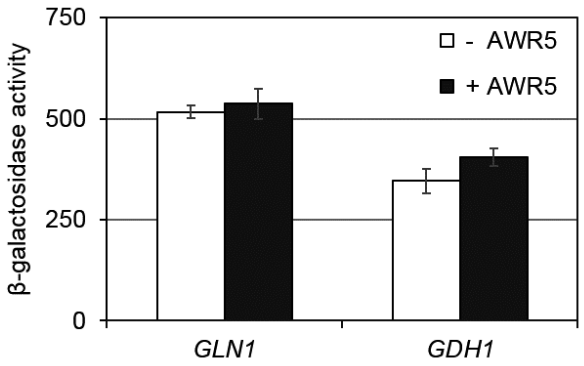

FIGURE 13. Transcriptional response of *GLN1* and *GDH1* to *awr5* expression.

β-galactosidase activities from yeast cells bearing *awr5*. Promoter activities of *GLN1* and *GDH1* were determined 6 hours after growth in SD-Ura+dox (-AWR5) and SD-Ura (+AWR5). Data represent the mean and standard errors of 3 independent clones. All assays were repeated at least twice with similar results.

2.2. Effect of TORC1 activator cycloheximide on yeast cells expressing *awr5*

To better characterize AWR5 impact on TORC1 pathway in yeast, we studied the effect of the protein biosynthesis inhibitor cycloheximide on yeast cells expressing *awr5.* Contrary to rapamycin, cycloheximide has been previously shown to cause a strong increase in TORC1 activity, probably by boosting the levels of free intracellular amino-acids (Binda *et al.*, 2009; Urban *et al.*, 2007). Thus, we hypothesized that cycloheximide treatment would revert the effect caused by AWR5. However, AWR5-mediated TORC1 pathway inhibition could not be reverted by cycloheximide (Figure 14). A previous study demonstrated that simultaneous treatment with cycloheximide and rapamycin still shows an inhibitory effect on TORC1 activity (MacGurn *et al.*, 2011). So, if AWR5 expression resembles rapamycin treatment, it might be possible that it prevails on the effect of cycloheximide.

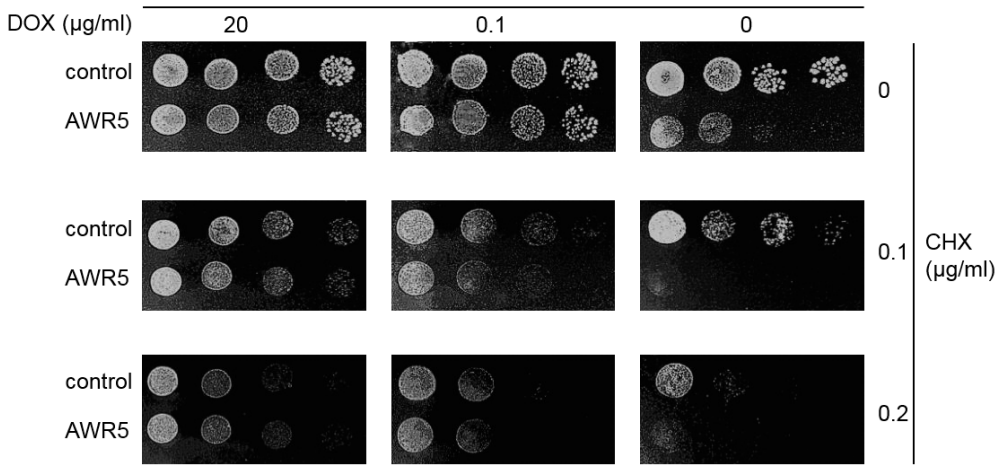

FIGURE 14. Effect of cycloheximide on yeast cells expressing *awr5.*

Yeast strains bearing AWR5 effector or a control gene (*GUS*) were spotted in 1:10 dilution series on solid SD-Ura plates containing different concentrations of doxycycline (DOX: 20, 0.1 and 0 µg/ml) and cycloheximide (CHX: 0, 0.1, 0.2 µg/ml). Photographs were taken after 3 days of growth.

CHAPTER3:
MOLECULAR MECHANISMS UNDERLYING AWR5-TRIGGERED INHIBITION OF THE YEAST TOR PATHWAY

In the previous chapters, we have shown heterologous expression of AWR5 in *S. cerevisiae* resulted in dramatic growth inhibition of yeast cells caused by inhibition of the central regulatory TOR pathway. Thus, we focused on a close analysis of the TORC1 pathway in yeast to better understand molecular mechanisms underlying AWR5-mediated toxicity.

3.1. Mutations in three genes involved in the TORC1 pathway rescue the yeast growth inhibition caused by AWR5

The TORC1 protein complex regulates the transition between growth and quiescence in response to nutrient status and can be inhibited by rapamycin. TORC1 acts by controlling three major cell components: the kinase Sch9, Tap42, its associated phosphatases and the ATG1 complex (Conrad *et al.*, 2014; Zaman *et al.*, 2008).

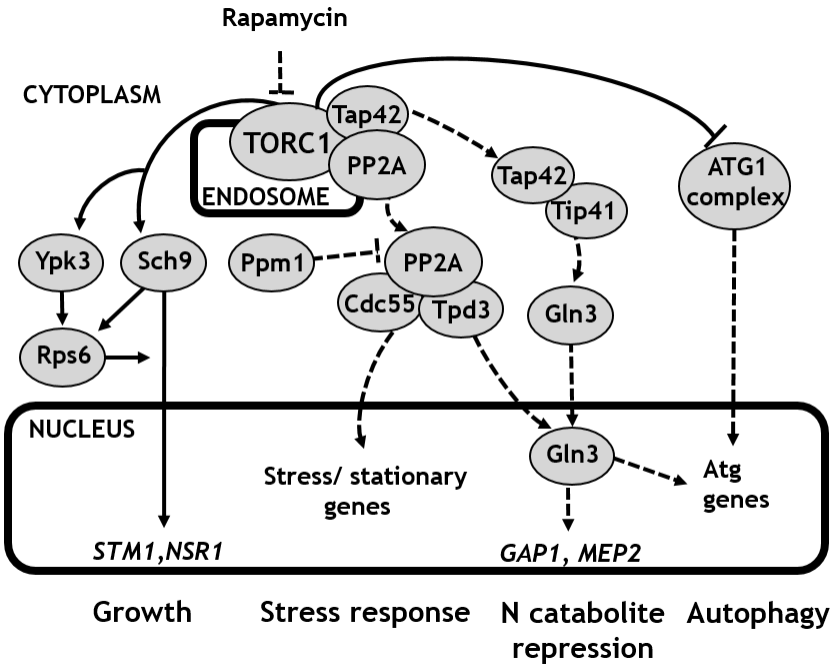

FIGURE 15. Schematic view of the Saccharomyces cerevisiae TORC1-regulated pathways.

The TORC1 complex is a central growth regulator, controlling the balance between growth and quiescence. Continuous and dotted lines represent, respectively, signaling events regulated by active and inactive TORC1.

Active TORC1 directly phosphorylates Sch9 -the orthologue of the mammalian S6 kinase-, which induces RiBi genes, such as *STM1* and *NSR1*, to increase translation and promote growth (Urban *et al.*, 2007) (Figure 15). In addition, when TORC1 is active, the essential downstream regulatory protein, Tap42, is phosphorylated and associates with the catalytic subunits of the PP2A and PP2A-like phosphatases, which are retained in membranes interacting with TORC1 (Aronova *et al.*, 2007; Kunz *et al.*, 2000). Finally, active TORC1 can inhibit autophagy by phosphorylation of ATG13, which prevents association with the ATG1 kinase and subsequent autophagy induction (Kamada *et al.*, 2010). On the contrary, when TORC1 is inactivated by rapamycin treatment or nitrogen starvation, Tap42 and the PP2A and PP2A-like phosphatases are released to the cytosol and activated, allowing expression of stress genes and NCR genes such as *GAP1* and *MEP2* (Conrad *et al.*, 2014; Zaman *et al.*, 2008) (Figure 15). This gene reprogramming takes place through PP2A/Sit4-mediated de-phosphorylation and subsequent translocation of Gln3 to the nucleus and PP2A-mediated inhibition of nuclear export of the Msn2/4 factors (Gonzalez *et al.*, 2009). Our gene expression analyses and biochemical characterizations showed that the bacterial effector AWR5 interferes with the TORC1-regulated pathways, repressing ribosome biogenesis and translation and activating autophagy and stress responses. In order to ascertain which point of these pathways was targeted by AWR5 we analyzed yeast strains with altered levels of different genes mediating TORC1 signaling.

In yeast, TORC1 modulates stress responses and nitrogen catabolite repression mostly by controlling the activity of several phosphatases, such as protein phosphatase 2A (PP2A) or Sit 4, often by modifying their interaction with regulatory subunits (Fig. 15, (Loewith & Hall, 2011)). Interestingly, the strains mutated in the PP2A regulatory or scaffold subunits *CDC55* or *TPD3* did not show AWR5-triggered growth inhibition. In addition, mutation in *SCH9*, the yeast kinase required for TORC1-dependent regulation of growth and mass accumulation (Urban *et al.*, 2007), also rescued toxicity caused by AWR5 (Fig. 16).

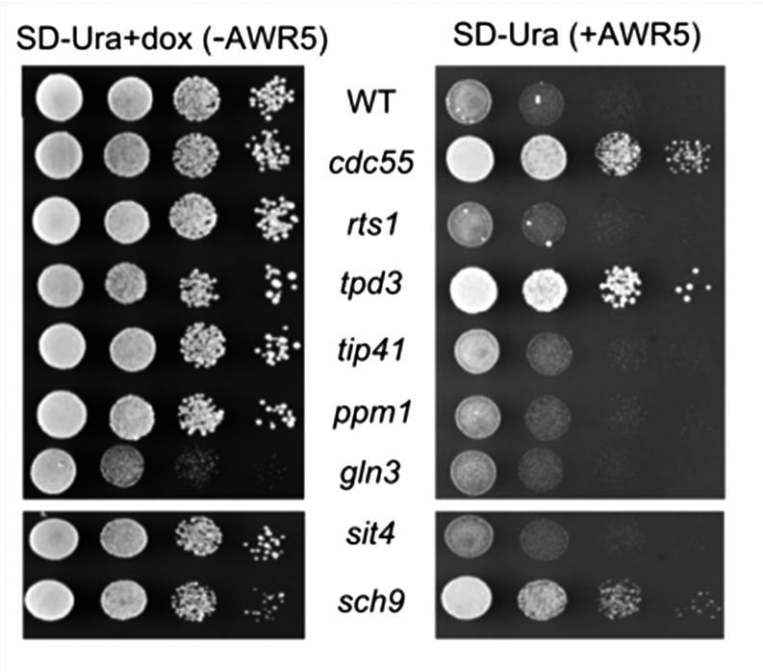

FIGURE 16. *cdc55, tpd3* and *sch9* mutations suppress AWR5-induced yeast growth inhibition.

Growth on solid medium of control (Wt) and TORC1-related yeast mutants containing plasmid carrying *awr5*. Serial 10-fold dilutions were spotted onto solid SD-Ura+doxycycline (-AWR5) and SD-Ura (+AWR5). Photographs were taken after 2 days of growth.

Since genes deleted in the phenotype suppressor strains modulate independent cellular processes, we divided the following experiments in two sections. The first part of the work was meant to provide clues on AWR5-triggered responses on signaling controlled by Tap42 and PP2A complexes. Secondly, we evaluated AWR5 impact on protein and ribosome synthesis and the cell growth pathway.

3.1.1. AWR5 impact on stress responses and NCR signalling

As mutations in the *CDC55* or *TPD3* genes rescued AWR5-triggered growth inhibition, this indicated that these PP2A subunits are essential for AWR5 to cause its phenotype and might be directly targeted by the effector. These results were also corroborated by evaluating growth kinetics in *cdc55* mutant yeast strains expressing *awr5.* Figure 17 shows *cdc55* mutation attenuates the decrease in number of viable cells observed after *awr5* expression.

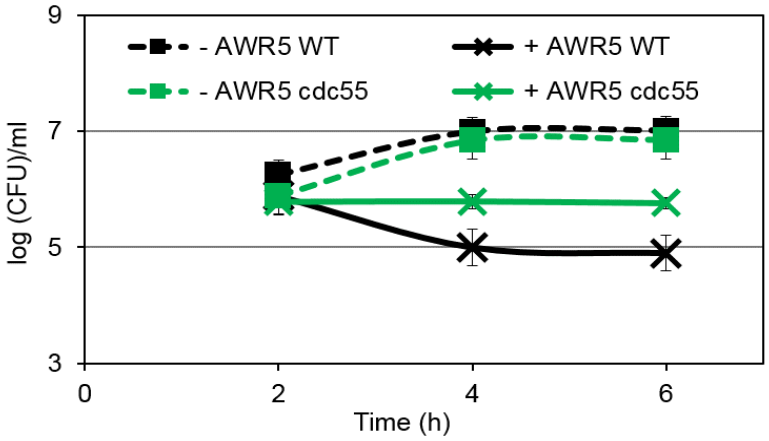

FIGURE 17. *cdc55* mutation attenuates AWR5-mediated growth inhibition.

Growth kinetics in liquid medium of wild-type (WT) and *cdc55* mutant yeast cells harboring *awr5*. Yeast cells harboring *awr5* were grown in SD-Ura+dox (-AWR5) and SD-Ura (+AWR5) liquid media and dispersed on SD-Ura+dox plates. The logarithm of colony forming units (CFU) per ml is shown over time. Error bars indicate standard errors for 2 biological replicates.

Next, we tested promoter activity of *GAP1* fused to the β-galactosidase reporter in wild type and *cdc55* mutant strains. Our results clearly showed that Cdc55 was required for the increase in *GAP1* promoter activity that occurs in response to *awr5* expression (Fig. 18). On the contrary, effect of AWR5 on *GAP1* activity was not dependent on Tip41 or Ppm1, as increased promoter levels were still observed in *tip41* and *ppm1* mutant strains (Fig. 18). In the *gln3* mutant yeast strain, *GAP1* showed very low promoter levels independent of *awr5* expression, therefore the results obtained are not significant.

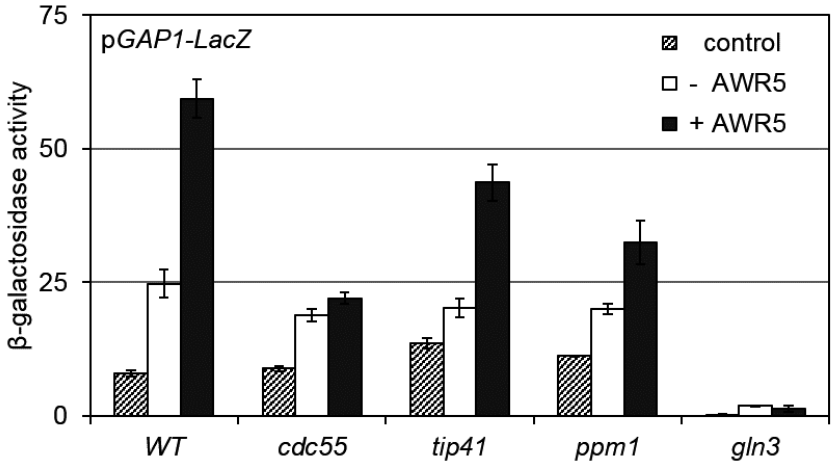

FIGURE 18. Transcriptional response of GAP1 to awr5 expression.

GAP1 promoter activities from plasmid *pGAP1-LacZ* in wild-type (WT) and mutant *cdc55, tip41, ppm1* and *gln3* yeast cells bearing *awr5* or a control gene (*GFP*). β-galactosidase activity was measured 6 hours after growth in SD-Ura+dox (-AWR5) and SD-Ura (+AWR5). Values represent the means and standard errors of 4 independent clones. All experiments were performed three times with similar results.

AWR5-mediated growth inhibition could not be rescued by overexpression or conditional mutation of the two redundant genes (*pph21, 22*) encoding the PP2A catalytic subunits (Fig. 19A and 19B). Thus, the effector does not seem to target these subunits. Alteration in genes related to NCR or stress response signaling through the TORC1 pathway did not show reversion of AWR5-mediated growth inhibition. Indeed, mutants *rts1*, *tip41*, *ppm1* and *gln3* and an overexpressor of *SIT4* had no effect (Fig. 19B)

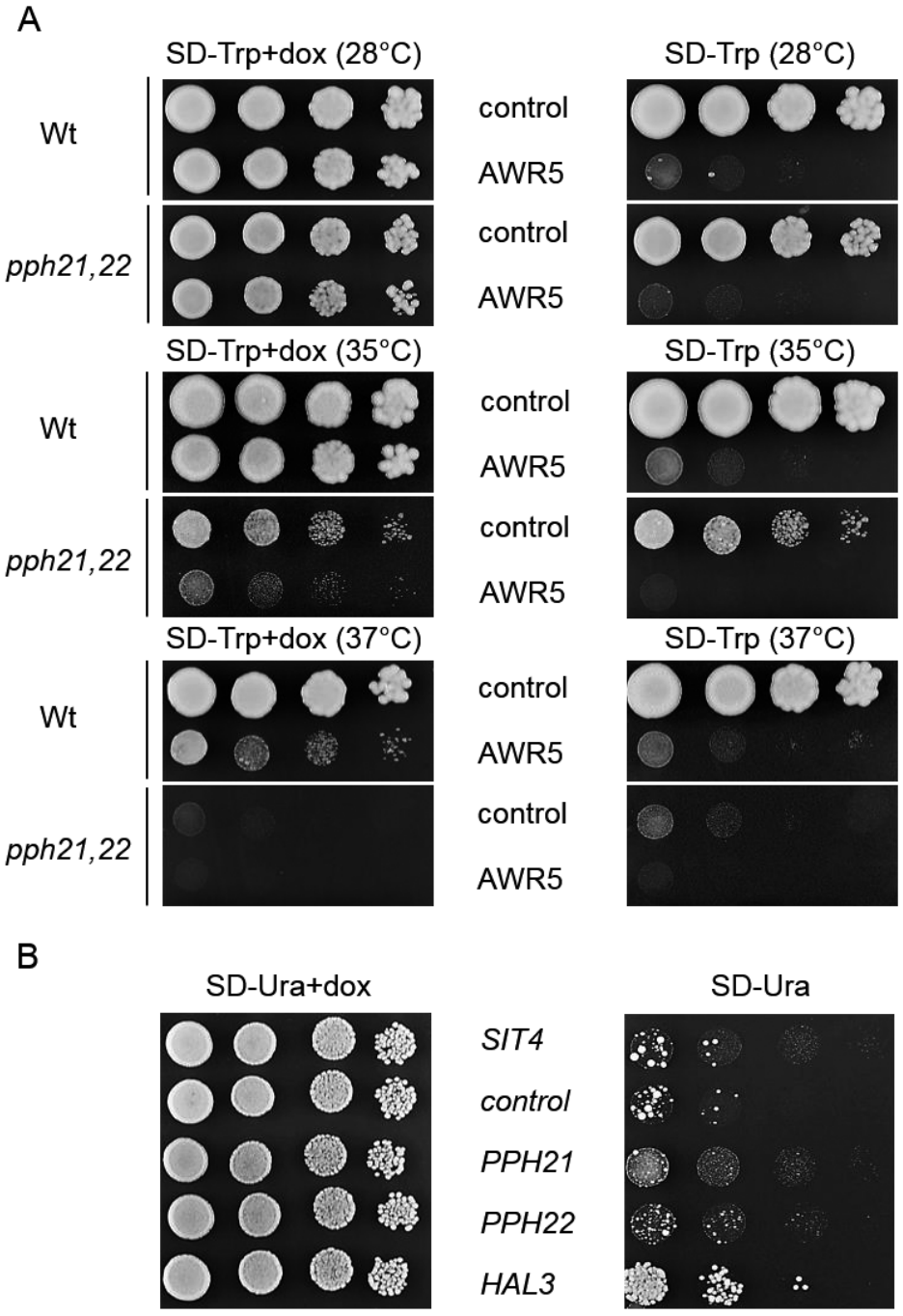

FIGURE 19. Effect of awr5 expression on yeast strains with altered levels of TORC1-regulated genes.

(A) Growth of a wild-type (Wt) and a temperature-conditional *pph21, 22* double mutant expressing *awr5* or carrying an empty vector. Serial 10-fold dilutions were spotted onto solid SD-Trp+doxycycline (repressing medium) and SD-Trp (inducing medium) and plates were incubated at different temperatures (28, 35 and 37°C). (B) Growth of yeast strains expressing *awr5* and overexpressing different TORC1-regulated genes. Serial 10-fold dilutions were spotted onto solid SD-Ura+doxycycline (repression of *awr5*) and SD-Ura (*awr5* expression). All photographs were taken after 3 days of growth.

Interestingly, overexpressing *HAL3* seemed to partially revert the AWR5-triggered growth inhibition phenotype. *HAL3* is a negative regulator of *PPZ1* (de Nadal *et al.*, 1998), a phosphatase shown to modulate different cellular processes in yeast. Among other functions, Ppz1 is involved in regulation of Gln3 phosphorylation, being required for its cytoplasmic localization (Hirasaki *et al.*, 2011). In addition, Ppz1 modulates cellular salt homeostasis, as the *ppz1* mutant was shown to have an increased sodium tolerance (Posas *et al.*, 1995). Overexpression of *HAL3* mimics deletion of *PPZ1,* therefore, the partial recovery of growth observed in yeast *HAL3* strains expressing *awr5* is puzzling but could be attributed to the different state of the cell, in this case more adapted and resistant to stress.

Mutation in Cdc55 attenuates AWR5-mediated transcriptional responses

To determine whether *Cdc55* was required for downstream AWR5-mediated responses, we carried out a new transcriptomic analysis, in this case by direct sequencing of RNAs (RNA-seq) in wild type and *cdc55* cells expressing *awr5* for 6 h. Analysis of the wild type strain showed a response congruent with that observed previously using DNA microarrays, with a correlation coefficient of 0.63 in the genes detected as induced by both methodologies (Fig. 20).

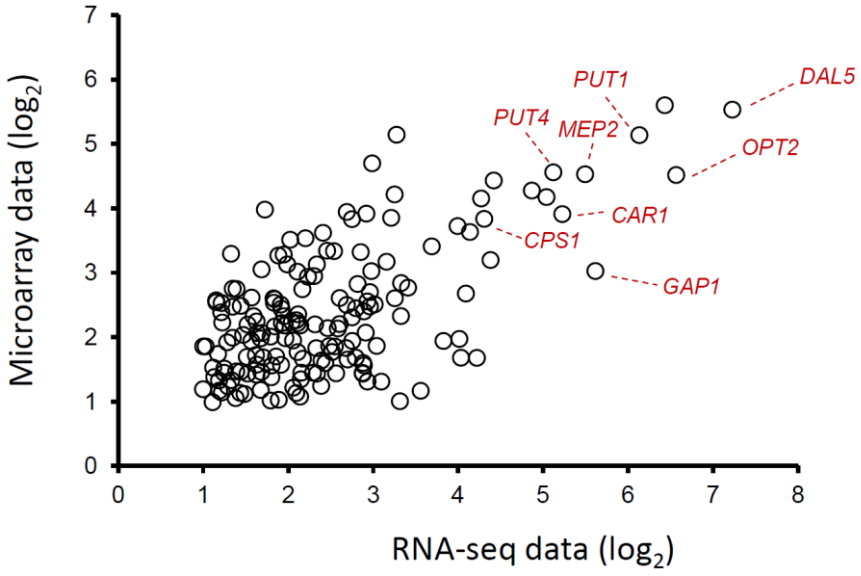

FIGURE 20. Correlation in gene expression data obtained by microarray hibridization vs RNA-seq.

Expression ratios for genes induced genes upon *awr5* expression compared to non-expressing conditions are represented for both methodologies. Key genes mentioned in the text are labelled with their names.

In addition, among the top 25 most induced genes detected by microarray analysis, 13 were also ranked as such by RNA-seq. Comparison of the profiles of the wild type and the *cdc55* strains after 6 h of *awr5* induction showed that mutation in *Cdc55* dramatically attenuated the transcriptomic effects caused by *awr5* expression. As illustrated in Figure 21A, 512 genes were induced in the wild type strain upon *awr5* expression and only 212 in the *cdc55* strain (of which only 144 were also induced in wild type cells). This effect was particularly evident in repressed genes, since the *cdc55* mutation affected almost 90% of the genes repressed by *awr5* expression in the wild type strain. The attenuation of the transcriptional response to AWR5 could clearly be observed by plotting the 100 genes showing highest induction (Fig. 21B, upper panel) or repression (Fig. 21B, lower panel) in wild-type cells and comparing to their expression in *cdc55* cells. It was notorious that many of the highly induced genes, which belong to the NCR and the mitochondrial retrograde pathways, decreased their expression in the absence of the regulatory subunit of PP2A. Indeed, 26 out of 28 NCR and *RTG* genes (Dilova *et al.*, 2002) ranking as top 100 induced decreased their expression more than 50% in *cdc55* cells.

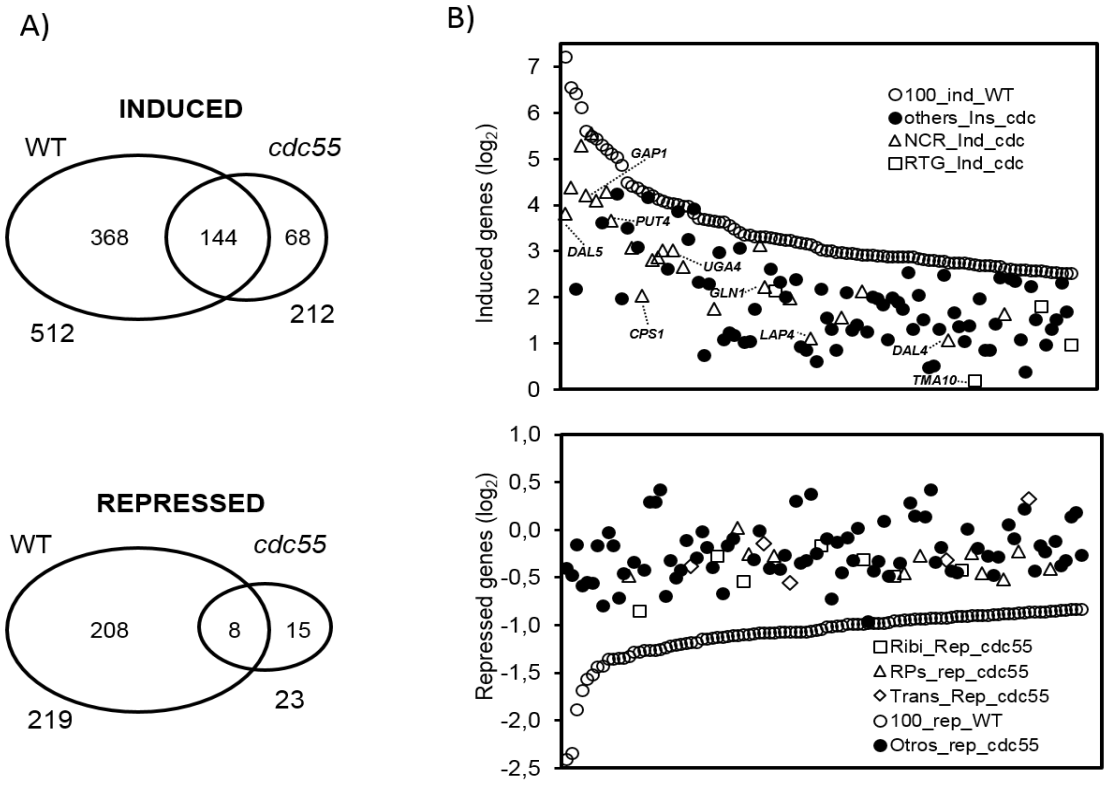

FIGURE 21. Mutation of Cdc55 greatly attenuates AWR5 impact on the yeast transcriptional profile.

(A) Venn diagram showing the number of genes whose expression was considered to be induced (top) or repressed (bottom) by expression of AW5 in wild-type and *cdc55* cells for a set of 5732 genes with valid data for both strains. (B) Plots of the log2 values for the changes in the level of expression induced by expression of AW5 in both wild-type (open circles) and *cdc55* strains for the 100 most upregulated (top) and 100 most downregulated (bottom) genes in the wild-type strain (open circles). Symbols for the expression values for the *cdc55* strain are depicted as follows. For the induced genes: open triangles, the NCR family, as defined previously (Godard *et al.*, 2007); the RTG group (open squares) comprises the genes described as documented targets for the Rtg1 or Rtg3 transcription factors as defined in (Gonzalez *et al.*, 2009). Genes not included in these categories are designated as “others” (closed circles). The genes downregulated in the wild-type strain are classified into one of three possible families: Ribi regulon (closed squares), ribosomal proteins (open triangles), protein translation (open diamonds), and others (closed circles), as defined in (Gonzalez *et al.*, 2009).

Similarly, a significant number of genes whose expression was decreased in response to AWR5, were clearly no longer repressed in *cdc55* cells. However, the effect was not homogeneous. For instance the transcripts showing little or no change in *awr5*-induced repression upon deletion of *cdc55* are largely enriched in genes involved in ribosome biogenesis and rRNA processing (Figure 22). This could be expected, as TOR-regulated expression of these genes is mostly PP2A-independent.

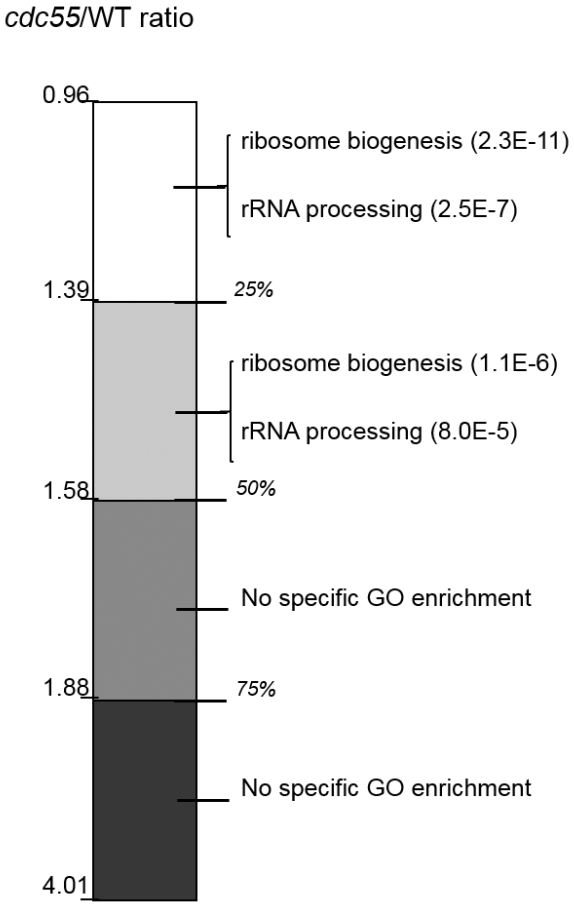

FIGURE 22. Ratio between the repression caused by *awr5* expression in the wild type and cdc55 strains.

The ratio was calculated for 219 genes found to be repressed in the wild type strain. Genes were ranked according to this ratio and the rank divided into quartiles. Gene Ontology analysis was performed for each quartile using the SGD YeastMine tool and relevant results are shown on the right. p-values are shown in parentheses.

Is PP2A subunit Cdc55 a direct target of AWR5?

To determine whether AWR5 interacted with Cdc55, we carried out co-immunoprecipitation experiments with yeast cells co-expressing endogenous HA-tagged Cdc55 and AWR5-GFP. As shown in Figure 23, AWR5-GFP was not able to specifically pull down 3HA-Cdc55 from yeast extracts.

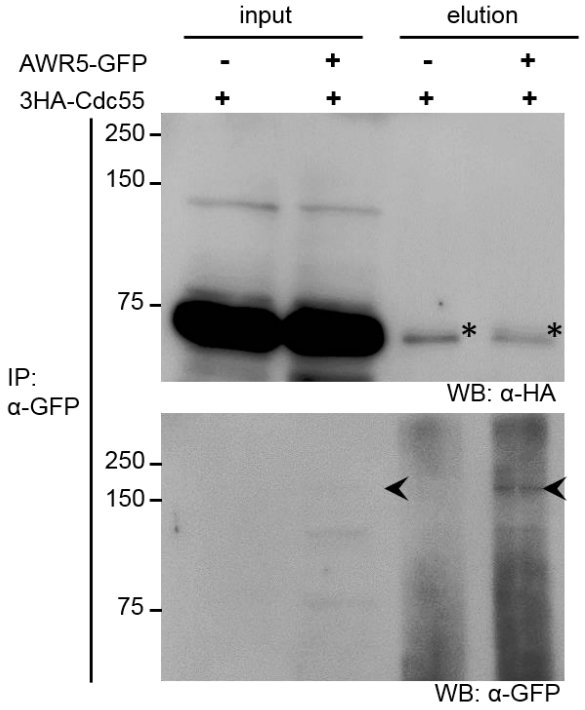

FIGURE 23. Co-immunoprecipitation of AWR5 and Cdc55 in yeast.

Protein extracts from yeast cells co-expressing HA-Cdc55 and AWR5-GFP were immunoprecipitated with anti-GFP-coupled magnetic beads. Crude extract (input) and eluate (elution) were analyzed by SDS-polyacrylamide gel electrophoresis (SDS-PAGE) with anti-HA (top) or anti-GFP (bottom) immunoblot. The asterisk denotes nonspecific cross-reacting bands; arrowheads are ~163 kDa, the expected apparent molecular mass of AWR5-GFP. WB, Western Blot. Experiments were performed three times with similar results.

Taken together, our results indicate that the inability to form PP2A complexes containing Cdc55 not only neutralizes the severe growth defect caused by expression of *awr5*, but also substantially minimizes the transcriptional alterations derived from such expression. However, no specific interaction was detected between AWR5 and PP2A-Cdc55 subunit, further supporting the notion that the PP2A complex might indirectly mediate the phenotype caused by the AWR5 effector.

3.1.2. AWR5 impact on protein and ribosome synthesis

In order to decipher the mechanisms underlying AWR5-mediated down-regulation of protein and ribosome synthesis, we analysed phosphorylation of Rps6 in yeast cells expressing *awr5.* Rps6 is a component of protein and ribosome synthesis signalling and its phosphorylation status was proven to be a valuable readout of TORC1-dependent signalling in both yeast and mammals (Gonzalez *et al.*, 2015; von Manteuffel *et al.*, 1997). In yeast cells, inhibition of TORC1 by both rapamycin treatment and nitrogen starvation resulted in decreased Rps6 phosphorylation levels (Gonzalez *et al.*, 2015) (Figure 15).

Taking advantage of a commercially available antibody shown to detect endogenous Rps6 phosphorylation in yeast, we have observed *awr5* expression does not affect Rps6 total protein levels or its level of phosphorylation in wild-type strains (Figure 24). This implies that, contrary to our expectations, AWR5-mediated TORC1 inhibition does not lead to a decrease in Rps6 phosphorylation or that this is not detectable in our experiments. Next, we tested phosphorylation of this ribosomal protein in *cdc55* mutant strains expressing *awr5.* Cells lacking Cdc55 seemed to have slightly lower amounts of phosphorylated Rps6 upon induction of *awr5* expression, but this is probably due to low levels of total Rps6 proteins in comparison to wild-type strains (Figure 24). In addition, since lower amounts of total Rps6 protein were observed independently of *awr5* expression, differences in Rps6 phosphorylation in mutant *cdc55* might be a result of pleiotropic effects.

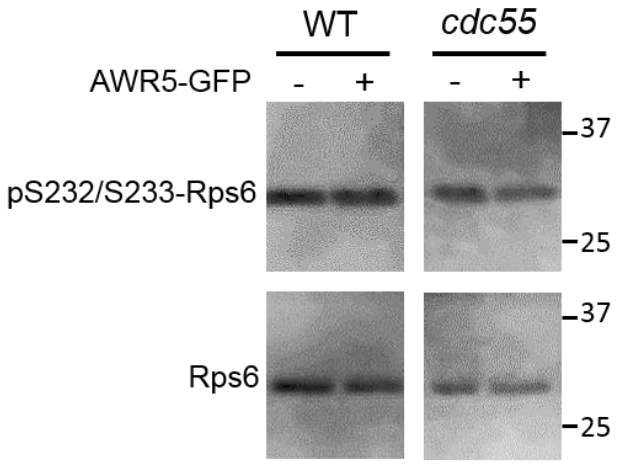

FIGURE 24. Effect of *awr5* expression on Rps6 phosphorylation in wild-type and *cdc55* mutant strains.

Immunoblot analysis of Rps6 phosphorylation in wild-type (WT) and *cdc55* mutant strains. Total protein was extracted from the indicated strains at 6 hours after growth in SD-Ura+dox (-AWR5) and SD-Ura (+AWR5) and immunoblotted using anti-phospho-S6 and anti-RPS6 antibodies.

We have not tested AWR5 impact on phosphorylation of Rps6 in mutant *sch9* strain, as it was shown this event was unaffected in cells lacking Sch9 upon nitrogen starvation (Gonzalez *et al.*, 2015).

3.2. *awr5* expression constitutively activates autophagy

It is known that TORC1 regulates autophagy in yeast via inhibition of the ATG1 complex (Fig. 15 and (Kamada *et al.*, 2000)). Our microarray data showed that expression of *awr5* increased the expression of diverse autophagy genes, such as *ATG8* or *ATG14,* which indicates activation of this process. In order to confirm whether autophagy was affected by *awr5* expression, autophagic flux was monitored in yeast cells constitutively expressing *GFP-ATG8* (Fig. 25). Proteolysis of GFP-ATG8 in the vacuole during autophagy results in the accumulation of the GFP moiety. Hence, detection of free GFP levels by western blot analysis can be used as readout of the autophagic rate (Cheong & Klionsky, 2008). Expression of *awr5* led to a dramatic accumulation of GFP in yeast cells, indicating an increased autophagic flux (Fig. 25A). As a control, we subjected yeast cells to nitrogen starvation, which resulted, as expected, in an increase of free GFP levels (Fig. 25B).

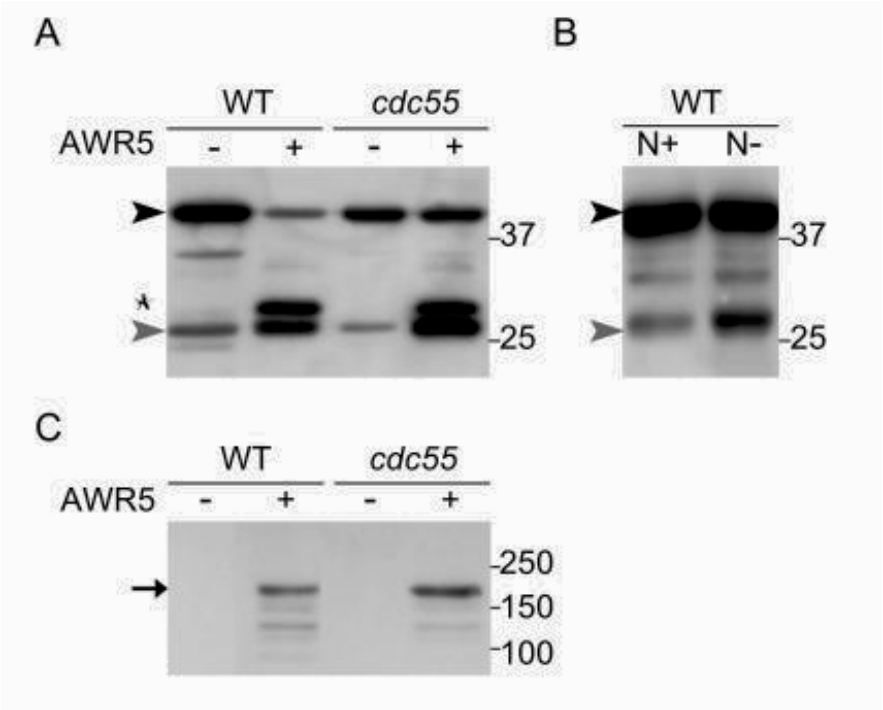

FIGURE 25. *awr5* expression induces constitutive autophagy, independently of Cdc55-PP2A activity.

(A) Immunodetection of GFP-ATG8 processing in wild-type and mutant *cdc55* yeast strains expressing *awr5*. Wild-type (WT) and mutant *cdc55* yeast cells bearing *awr5* gene were grown in SD-Ura+dox (-AWR5) and SD-Ura (+AWR5). Total protein extracts were immunoblotted using anti-GFP antibody. The black and the grey arrowhead indicate, respectively, GFP-ATG8 fusion protein and cleaved GFP. The asterisk denotes a degradation product of AWR5-GFP protein. (B) Wild-type cells carrying GFP-ATG8 grown in nitrogen-rich (N+) or nitrogen-depleted (N-) medium were used as a control of GFP-ATG8 processing and induction of autophagy in N- conditions. (C) AWR5 protein levels in wild-type and mutant *cdc55* yeast cells. Total protein was extracted and immunoblotted using anti-GFP antibody. The black arrow indicates AWR5-GFP protein. All experiments were performed at least three times, with similar results.

Interestingly, free GFP levels in *awr5*-expressing cells were higher than in nitrogen-starved cells, indicating that AWR5 is a stronger autophagy inducer. Next, we tested whether Cdc55 was involved in AWR5-triggered autophagy in yeast. Although GFP-ATG8 levels were slightly higher in *cdc55* mutant cells expressing *awr5*, autophagy was similarly induced in both strains (Fig. 25A). *awr5* expression was analyzed and similar levels were detected in wild type and *cdc55* mutant cells (Fig. 25C). These findings indicated that AWR-mediated autophagy induction occurs independently of Cdc55 in yeast.

3.3. Effect of *awr* genes expression on TORC1 downstream targets

Characterization of AWR effector proteins *in planta* had demonstrated that the type III effectorsof this family are important for bacterial multiplication and act redundantly on pathogenicity towards hosts (Sole *et al.*, 2012). In addition, most AWRs caused toxicity in yeast. Thus, we next explored whether the modes of action of other AWRs resembled those of AWR5. To this end, we tested if gene expression of *GAP1* and *MEP2* was also altered by other members of AWR family.

As seen in Figure 26, yeast cells expressing AWR2 and AWR4 effectors exhibit higher levels of *GAP1* and *MEP2* in comparison to non-inducing conditions. This resembled the transcriptional response to *awr5* expression, suggesting that targeting of TORC1 pathway might be conserved among AWR2, AWR4 and AWR5. On the contrary, *GAP1* and *MEP2* showed very low expression in yeast cells transformed with AWR1 and AWR3, and even lower after these effectors expression was induced (Figure 26). Altogether, these data strengthen the hypotesis that effectors from the same family might affect central processes inside host and lead to similar cellular outcomes in spite of not sharing the same molecular targets.

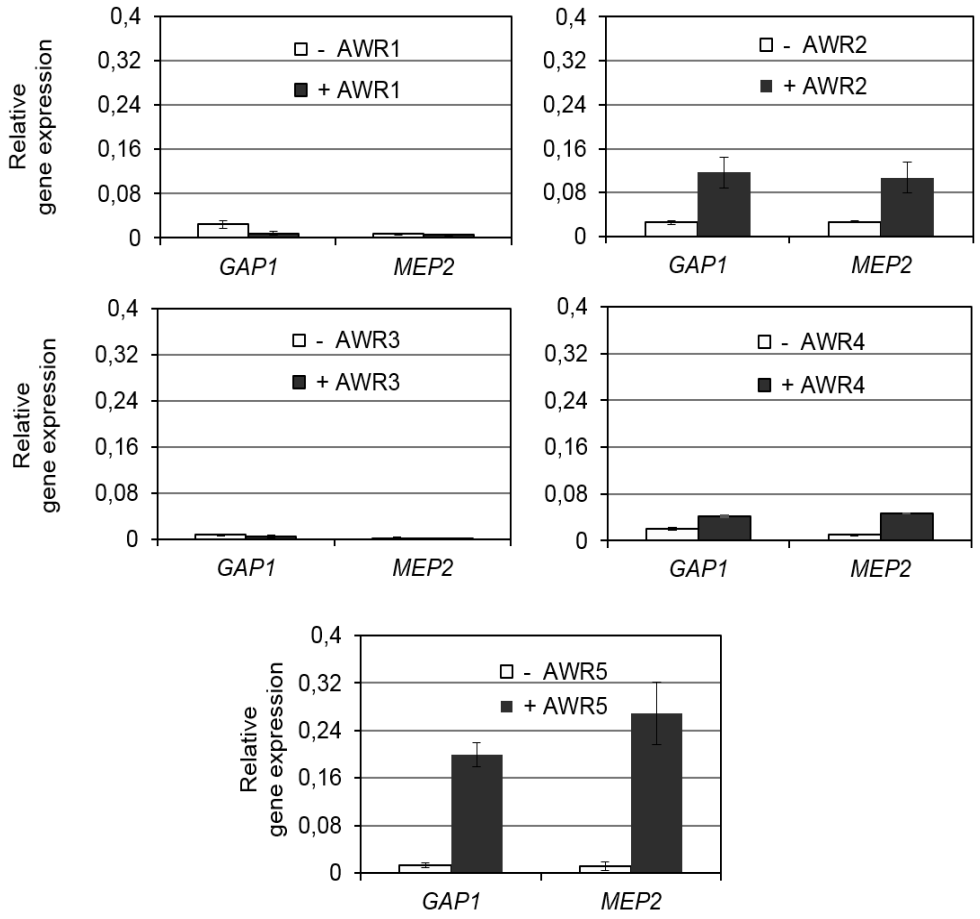

FIGURE 26. Transcriptional response of TORC1-related genes to awr effectors expression.

Gene expression of NCR-sensitive (*GAP1* and *MEP2*) genes was tested in yeast strains expressing different members of AWR family 6 hours after induction. Error bars represent standard errors from 2 biological replicates.

CHAPTER4:
IS AWR5 INHIBITING THE SAME KEY PROCESS *IN PLANTA?*

4.1. AWR5 alters the TOR pathway in plants

Since heterologous expression of a T3E from *R. solanacearum* in yeast altered the TORC1 pathway, it was plausible that the effector had a similar effect in its natural context, i.e. when translocated inside plant cells. In plants, it has been shown that TOR silencing results in activation of nitrogen recycling activities and reduces primary nitrogen assimilation, measured by nitrate reductase activity (Ahn *et al.*, 2011; Bi *et al.*, 2007). In order to test whether *awr5* expression resulted in TOR inhibition in plants we thus used nitrate reductase activity as readout. Transient expression of *awr5* in *Nicotiana benthamiana* leaves resulted in a significant reduction of nitrate reductase activity compared to the control (GUS) (Fig. 27A). Leaky expression of *awr5* prior to induction may account for the slightly lower nitrate reductase activity values in leaves transformed with *awr*5. Thus, our data indicate that AWR5 may target the TOR pathway in both plants and yeast through a conserved mechanism.

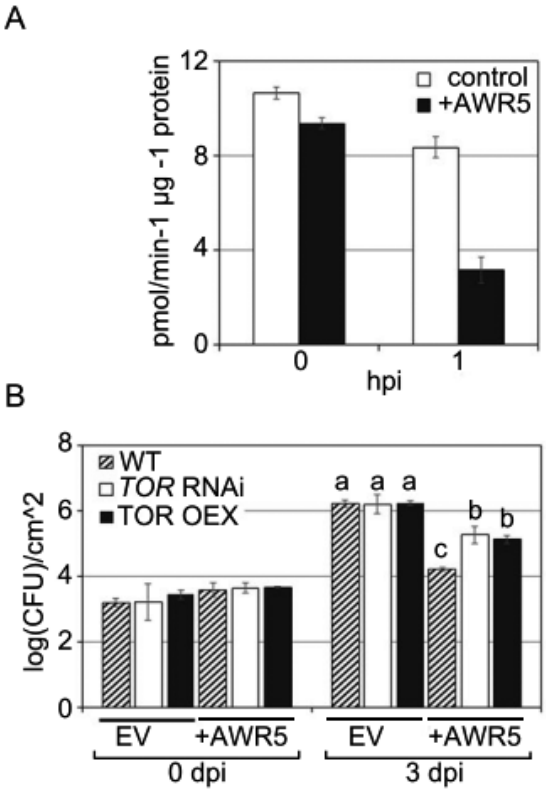

FIGURE 27. Interplay between AWR5 and TOR in planta.

(A) Effect of *awr5* transient expression on nitrate reductase (NR) activity in *Nicotiana benthamiana*. Full leaves of *N. benthamiana* were agroinfiltrated with constructs bearing *awr5* or a control gene (*GUS*). Total protein extracts were used to determine NR activity at 0 and 1 hour post-induction (hpi). Error bars indicate standard errors of 2 biological replicates. (B) Multiplication of *Pseudomonas syringae* DC3000 in *Arabidopsis thaliana* plants with altered levels of TOR. Strains bearing an empty vector (EV) or the same vector with *awr5* (+AWR5) were inoculated at 5 x 10^5 CFU/ml on leaves of *A. thaliana* Col-0 (Wt), TOR silenced (*TOR* RNAi) and TOR overexpressing (TOR OEX) plants. Bacterial growth is represented as the logarithm of recovered CFU per square centimeter at 0 and 3 days post inoculation (dpi). Values represent the mean of three biological replicates. Letters at 3 dpi indicate a statistically significant difference following post-ANOVA Tuckey test (P<0.001). All experiments were repeated twice with similar results.

We previously showed that AWR5 restricts bacterial growth in *Arabidopsis thaliana* plants infected with a *Pseudomonas syringae pv.* tomato DC3000 strain heterologously expressing the effector (Sole *et al.*, 2012). To determine whether the AWR5 effect on bacterial growth was mediated by TOR, *Arabidopsis* TOR silenced and TOR overexpressing plants (TOR OEX, *TOR* RNAi (Deprost *et al.*, 2007)) were infected with *P. syringae* DC3000 carrying *awr5* (+AWR5) or an empty vector (EV) and growth was recorded at 0 and 3 days. The growth restriction effect caused by AWR5 was significantly reduced in TOR overexpressing and *TOR* RNAi lines (Fig. 27B), indicating that normal levels of TOR kinase are required for AWR5-mediated phenotype observed in *Arabidopsis* plants.

4.2. Effect of *awr5* expression on TOR downstream targets in *Arabidopsis thaliana*

TOR silencing in *Arabidopsis thaliana* causes an increase in nitrogen recycling genes such as *GS1* (glutamine synthethase) and *GDH* (glutamate dehydrogenase) and down-regulation of nitrogen assimilatory genes (Deprost *et al.*, 2007). Recent studies have shown depletion of Tap46, the plant homolog of Tap42, reproduced transcriptional responses underlying TOR inactivation *in planta* (Ahn *et al.*, 2011). In *Tap46* RNAi plants, gene expression of *GS1* (cytosolic glutamine synthethase) and *GDH* was up-regulated, whereas *GOGAT* (glutamate synthase), playing a role in nitrogen assimilation, showed decreased levels.

In order to assess AWR5 effect on gene expression of TOR-regulated targets *in planta*, we performed quantitative RT-PCR analysis at 0 and 1 day after infection of *Arabidopsis* plants with *P. syringae* DC3000 carrying *awr5* (+AWR5) or an empty vector (EV).

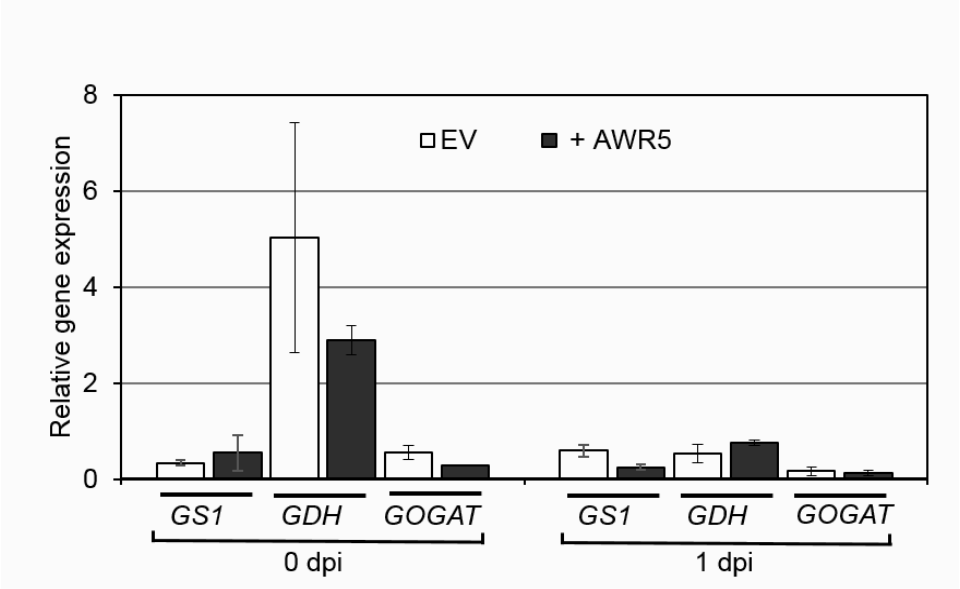

FIGURE 28. Transcriptional response of *Arabidopsis thaliana* TOR-regulated genes to *awr5* expression.

qRT-PCR showing *GS1, GDH* and *GOGAT* expression levels relative to tubulin. *Pseudomonas syringae* DC3000 strains bearing an empty vector (EV) or the same vector with *awr5* (+AWR5) were inoculated at 5 x 10^5 CFU/ml in *A. thaliana* Col-0 plants. Gene expression levels of *GS1, GDH* and *GOGAT* were analysed at 0 and 1 day post inoculation (dpi). Error bars represent standard errors of 2 independent clones. All experiments were performed at least two times, with similar results.

Relative gene expression levels of *GS1, GDH* and *GOGAT* seem to decrease at day 1 post-inoculation, moreover no significant differences were observed after *awr5* expression in comparison to their levels in plants inoculated with control strains (Figure 28). In conclusion, our results show *awr5* expression does not influence expression of TOR-regulated genes controlling nitrogen metabolism in *Arabidopsis thaliana.*

4.3. Effect of *awr5* expression on TOR downstream targets in *Nicotiana benthamiana*

Previously, we have showed transient expression of *awr5* leads to decrease of nitrate reductase activity in *N. benthamiana* leaves. This prompted us to investigate effect of AWR5 on TOR-regulated genes related to nitrogen metabolism in *N. benthamiana.*

Since no metabolic profiles are available in *N. benthamiana*, we first selected *Arabidopsis* genes shown to have a differential expression in response to TOR inhibition for which we could find homologous in *N. benthamiana*. These were *ASN2* (asparagine synthethase) and *NAP14* (non-intrinsic ABC protein 14 – role in ATP-binding), shown to be down-regulated, and *NIT4* (nitrilase 4) and *GDH1* (glutamate dehydrogenase 1), induced after TOR repression (Caldana *et al.*, 2013; Deprost *et al.*, 2007).

Next, we transiently expressed *awr5* in *Nicotiana benthamiana* leaves and performed quantitative RT-PCR analysis at 0 and 6 hours after induction. It is worth remarking, in the case of *ASN2* and *NAP14*, we detected different responses in gene expression between the two biological replicates we tested, that is why results are represented and interpreted for each of the replicates (Figure 29).

No significant changes in *ASN2* gene expression were detected 6 hours after *awr5* expression in both biological replicates tested. If any effect, this could refer to slightly more increased levels of *ASN2* in replica 2, which would be contradictory with transcriptional profiles seen after inhibition of TOR kinase. In the case of *NAP14*, similar gene expression levels were observed in both biological replicates before *awr5* induction. Six hours post-induction, *NAP14* showed significant lower levels in replica 1 in comparison to replica 2. This might insinuate that *NAP14* is down-regulated in replica 1 after *awr5* transient expression. However, since *NAP14* showed different transcriptional response between the two biological replicates in more than one experiment, we qualified this gene as not suitable for testing AWR5-mediated TOR inhibition *in planta.* Finally, *awr5* expression did not cause any major effect on *GDH1* and *NIT4* levels of expression.

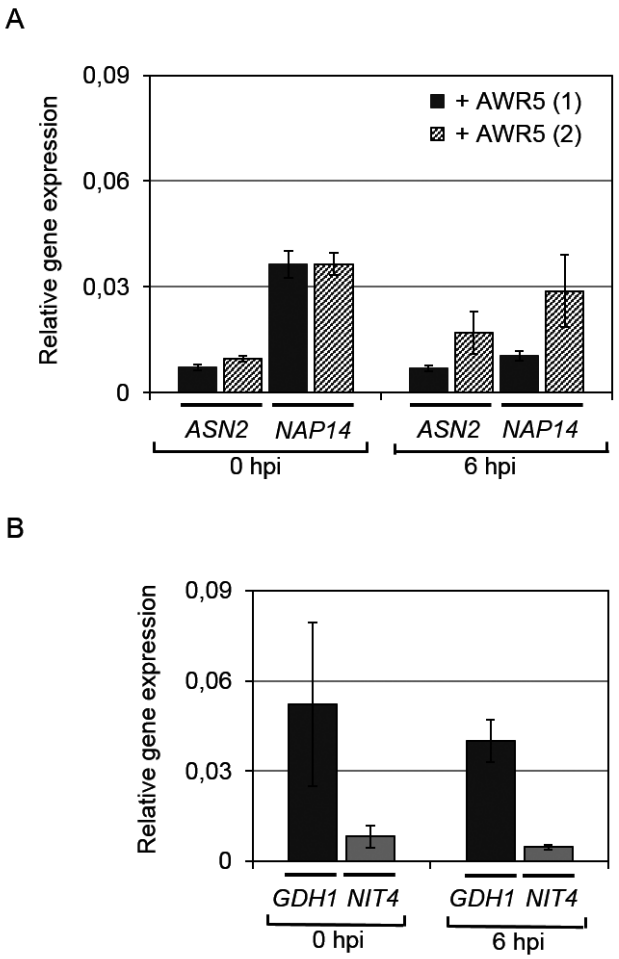

FIGURE 29. Transcriptional response of nitrogen metabolism-related genes to *awr5* expression in *N. benthamiana*.

(A) qRT-PCR showing *ASN2* and *NAP14* expression levels relative to PP2A. Full leaves of *N. benthamiana* were agroinfiltrated with constructs bearing *awr5*. Two biological replicates (two leaves from different plants) were used for RNA extraction at 0 and 6 hours post-induction (hpi) (+ AWR5 (1); + AWR5 (2)). Error bars indicate standard errors of 2 technical replicates. (B) qRT-PCR showing *GDH1* and *NIT4* expression levels relative to PP2A. Full leaves of *N. benthamiana* were agroinfiltrated with constructs bearing *awr5*. Two biological replicates (two leaves from different plants) were used for RNA extraction at 0 and 6 hours post-induction (hpi). Error bars indicate standard errors of 2 biological replicates. All assays were repeated twice with similar results.

In conclusion, we did not detect major changes on transcriptional response of genes related to nitrogen metabolism after *awr5* transient expression in *N. benthamiana.*

4.4. Role of AWR effector family in resistance to *Ralstonia solanacearum* in *Arabidopsis* plants with altered TOR levels

We have previously showed that expression of AWRs in different plant species triggers varying defense responses, which indicates that they play a dual role in both virulence and plant recognition (Sole *et al.*, 2012). To determine whether the effect of AWRs on disease/resistance was mediated by TOR, *Arabidopsis* TOR silenced and TOR overexpressing plants (TOR OEX, *TOR* RNAi, (Deprost *et al.*, 2007)) were infected with *R. solanacearum* strains devoid of all *awrs* (*Δawr1-5*) and disease symptoms were recorded over time. GMI1000 strain showed slightly increased virulence on *Arabidopsis* plants with altered levels of TOR, especially on lines with TOR silenced (Figure 30, upper panel). Although not significant, this result is surprising, as previous studies have shown that TOR silencing lines are more resistant in response to pathogens like *Xanthomonas oryzae pv. oryzae,* necrotrophs and hemibiotrophic fungi as *Verticillium* (David Mackey, personal communication). However, increased virulence of the *R. solanacearum* reference strain GMI1000 in TOR silenced plants may be attributed to a decreased capacity of the plant immune system to recognize bacteria. As previously mentioned, the AWR effector family might be recognized in *Arabidopsis thaliana,* as the mutant *Δawr1-5* multiplied faster than wild-type GMI1000 strain (Sole *et al.*, 2012). Therefore, assuming that the TOR pathway is targeted by one or more members of the AWR family, an alteration in the plant TOR kinase levels could interfere in recognition of these effector proteins by the plant.

Interestingly, the increased virulence shown by *R. solanacearum* devoid of all *awrs* was suppressed in plants with altered levels of TOR. This could again indicate that normal TOR levels are required for AWR recognition, positioning TOR or an upstream regulator as a potential AWR target. Alternatively, normal TOR levels could be required to sense a cellular/metabolic alteration caused upon injection of certain AWR effectors into the cell (Figure 30, lower panel).

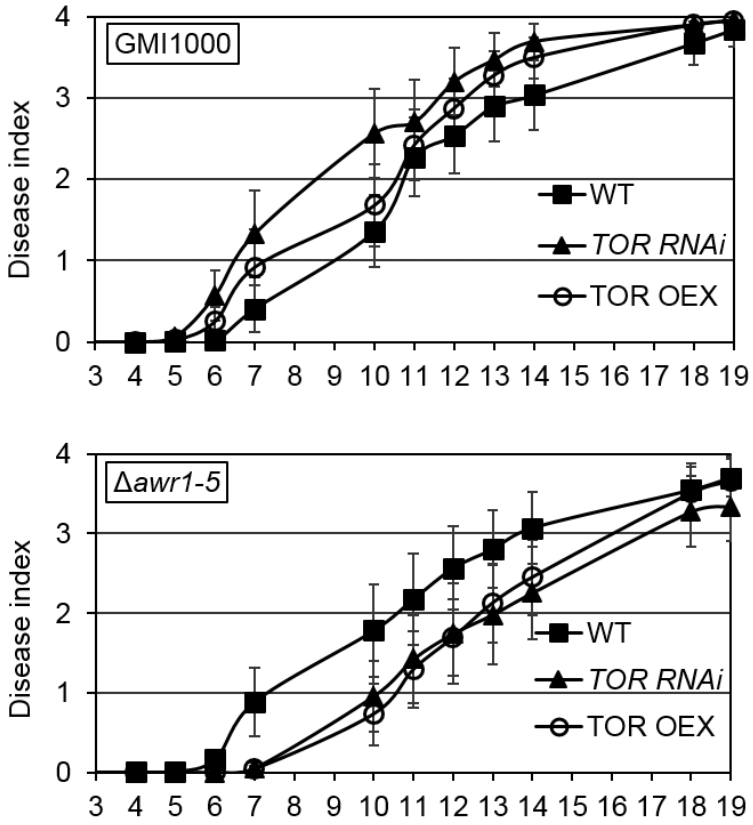

FIGURE 30. Pathogenicity test with *Ralstonia solanacearum* strains on *Arabidopsis thaliana* plants with altered levels of TOR.

Ralstonia solanacearum strain GMI1000 (upper panel) and *Δawr1-5* multiple mutant strain (lower panel) were root-inoculated at 10^8 CFU/ml in *Arabidopsis thaliana* Col-0 (Wt), TOR silenced (*TOR* RNAi) and TOR overexpressing (TOR OEX) plants. Disease progression was annotated daily according to wilting symptoms appearance: no wilting (0), 25% wilted leaves (1), 50% (2), 75% (3), and dead plant (4). Values represent mean of 24 biological replicates and their standard error. All experiments were repeated twice with similar results.

Earlier we have shown that in yeast, the ability to alter the TORC1 pathway was conserved among AWR2, 4 and 5. Our plant pathogenicity results might indicate that, consistent with what we found in yeast, effectors from the AWR family might also act co-operatively to affect central TOR-mediated processes inside host plants that modulate defense responses.

DISCUSSION

Challenges on the path to investigation of AWRs/AWR5 effector function

Ralstonia solanacearum contains one of the largest bacterial effector repertoire, comprising about 70 type III effectors, out of which more than the half still have an unknown function (Coll & Valls, 2013). To fill this knowledge gap, we previously analyzed the AWR multigenic family of effectors *in planta*, showing that these proteins are important for *R. solanacearum* virulence, and may also be detected by the plant surveillance system (see annex (Sole *et al.*, 2012)). These findings have special interest in the context of plant-pathogen interactions. Therefore, in this work we aimed to deepen our knowledge on the mechanism of action of AWR effectors in their natural environment or by expression on heterologous systems.

Awrs are conserved genes widespread in the *Ralstonia solanacearum* species complex and also present in other plant and animal pathogens. However, BLAST comparison of AWR protein or gene sequences to the recent databanks returned no similarity to characterized proteins or motifs with predicted biochemical function. Moreover, structure prediction based on sequence motif analysis performed with Hhpred Bioinformatics Toolkit (Max-Planck Institute for Developmental Biology) retrieved no statistically relevant hits for any of the AWR effectors. Considering this, it may be more informative to focus on knowledge derived from AWR homologs in other pathogens, since effectors from the same family in different pathogens have shown conserved function. For instance, *Pseudomonas syringae* HopZ1a and PopP2 from *Ralstonia solanacearum,* both belonging to YopJ family of effectors, require the same residues for their activity and association to host proteins (Ma *et al.*, 2015). Nevertheless, significant similarities for AWR proteins outside the *R. solanacearum* species were only found at the level of protein sequence and homologs found (i.e., XopZ (Song & Yang, 2010)) are quite divergent from those of *Ralstonia* (Sole *et al.*, 2012). As an alternative, a recent approach to study effector proteins with unknown function relies on identification of positive selection sites among effector paralogs (Peeters *et al.*, 2013). This approach was used to understand functional relationship between structure and function of *Ralstonia* effector RipG7, since the positively selected sites seem to correlate with the virulence function of specific alleles (Wang et al., unpublished). Interestingly, AWR5 is one of the *R. solanacearum* effectors under strong positive diversifying selection at the protein level (Peeters *et al.*, 2013).

In the case of AWRs, and especially for AWR5, effector toxicity hampered most gain-of-function analyses of these effector proteins *in planta*. First, we encountered difficulties in obtaining *Arabidopsis* transgenic lines expressing *awr* effectors, in spite of

using inducible promoters. To overcome this and study the effect of each *awr in planta*, these genes were successfully expressed in *P. syringae,* an *Arabidopsis* pathogen naturally lacking them. Second, the hypersensitive response observed after transient expression of AWR5 in *N. benthamiana* interfered with phenotype interpretation. To overcome this hurdle, expression of AWR5 under the control of an inducible promoter and short induction times proved to be helpful. In addition, heterologous expression of AWR5 in *Saccharomyces cerevisiae* emerged as a promising and robust strategy to find clues on its role in *R. solanacearum* pathogenicity.

In parallel with characterization of AWRs in yeast, we performed proteomic analysis of AWR5 binding partners in *N. benthamiana.* This technique has been extremely successful in unravelling novel secreted factors from pathogens like *Salmonella* (Niemann *et al.*, 2011) or for determining posttranslational modifications of the *R. solanacearum* effector PopP2 (Tasset *et al.*, 2010). In our case, *awr5* and the control gene *avrA* fused to GFP were expressed by means of transient *Agrobacterium* transformation in *N. benthamiana* plants. Setting up the production of AWR5 in *N. benthamiana* was extremely laborious due to the high insolubility of this protein. Actually, only treatment with 0.2% of the detergent NP-40 allowed the partial solubilization of AWR5 from plant. This was not surprising considering the size of this protein (1240 aminoacids), which indicates that the insolubility might be due to its accumulation within aggregates when the plant cell cannot ensure its proper folding (Khachatoorian *et al.*, 2015).

However, after effector production in *N. benthamiana*, plant proteins associated to AWR5 and AvrA effectors were isolated by immunoaffinity purification and eluted protein complexes were analyzed by LC-MS/MS and peptide spectrum matching. Unexpectedly, the list of candidate interactors for both proteins AWR5 and AvrA was mostly enriched in highly abundant proteins (e.g., chloroplastic enzymes), or common hits (probably false positives). Consequently we were not able to select for any relevant interactor.

Considering all the above-discussed limitations, we have mainly concentrated on the characterization of this effector family by expression in *Saccharomyces cerevisiae*. Findings on AWR effector function in yeast were then tested in plant systems.

Yeast as a model system to decipher T3E function

In this work we have produced *R. solanacearum* AWR effectors in yeast and have found that AWR5 impacts the TORC1 pathway, an essential component of eukaryotic cells. The premise for using *Saccharomyces cerevisiae* was that this organism carries out most eukaryotic processes and, unlike host cells where T3E are naturally injected, yeast lacks resistance components that counteract and mask effector function (Duina *et al.*, 2014). As an example of these resistance reactions, we have previously showed that transient expression of AWRs in *Nicotiana spp.* caused different levels of necrosis, especially strong after *awr5* expression. Similarly, these effectors inhibited yeast growth to different extents, and AWR5 showed the most dramatic effect. Interestingly, other studies on type III effector function showed correlation of phenotypes between yeast and plants. For example, the same effectors from *Xanthomonas euvesicatoria* that inhibited growth in yeast (XopX, AvrRxo1, XopB, XopE1, XopF2) also caused phenotypes, such as chlorosis and cell death, when expressed in either host or non-host plants (Salomon *et al.*, 2011). Likewise, expression of DspA/E effector from *Erwinia amylovora* caused cell death in *N. benthamiana* and growth arrest in yeast (Oh *et al.*, 2007; Siamer *et al.*, 2014). Thus, yeast may offer valuable clues on effector function, since phenotypes caused by these proteins are truly a consequence of effector activity, and not a response to effector recognition.

For all this, a number of studies have successfully used *S. cerevisiae* as a model to identify T3E targets (Curak *et al.*, 2009). Toxicity -ranging from growth arrest to cell death- is the most common phenotype observed in these studies. However, this is not a widespread phenomenon when *R. solanacearum* T3E are expressed in yeast, as only 6 out of 36 effectors representing the repertoire of strain GMI1000 caused substantial growth inhibition (this work and S. Fujiwara *et al*., in press). Interestingly, four out of the six toxic T3E encode AWR proteins, suggesting a distinct function for this effector family in bacterial-host interactions. Cell growth inhibition caused by T3E has been traced back to interference on vesicle trafficking (Siamer *et al.*, 2011), disruption of the cytoskeleton (Nejedlik *et al.*, 2004) or MAP Kinase alteration (Fernandez-Pinar *et al.*, 2012), providing important clues on T3E function. In the case of AWR5, we show that it targets a novel cellular process, namely, the TORC1 pathway.

We took advantage of the very well established resources and functional assays for studying eukaryotic processes in yeast (Botstein & Fink, 2011). First, expression under the control of a Tet-off promoter permitted monitoring the subtle effects of *awr5*

expression over time. Second, functional assays testing viability or cell death and measuring of cell size provided fast and essential clues on characterization of AWR5-mediated growth arrest. Finally, the extensive information available on yeast TORC1 pathway helped carry out functional analysis of AWR5 and decipher molecular mechanisms underlying inhibition of this central regulatory pathway.

At what level of the yeast TORC1 pathway is AWR5 acting?

As mentioned before, most TORC1-controlled effects occur through two major branches, mediated by i) the Sch9 kinase and ii) by complexes of Tap42 and the phosphatases (mainly PP2A and Sit4). The wide transcriptomic impact of AWR5 on all TORC1-controlled pathways, mimicking the effect of rapamycin or nitrogen starvation, could be explained by assuming that AWR5 would target one or multiple hits upstream of the Sch9 and PP2A complex. The most likely scenario is that AWR5 would exert its function directly or indirectly inhibiting TORC1 upstream of PP2A, thus causing Sch9 inhibition, autophagy activation and the release of Tap42 and PP2A phosphatase subunits. That would explain why *awr5* expression triggers a dual response in yeast: down-regulation of translation and ribosome biosynthesis and induction of genes related to metabolism of nitrogen.

The observation that deletion of two components of the PP2A heterotrimeric forms- *CDC55* and *TPD3*- abolishes the dramatic growth defect of cells expressing *awr5* might indicate that the formation of this heterotrimer is essential for the negative effect of AWR5 to take place. In this regard, it is worth noting that deletion of *TPD3* and of *CDC55* yields yeast cells resistant to rapamycin, whereas that of *RTS1* does not. Moreover, it has been proposed that an active TORC1 pathway promotes the association of Tap42 with PP2A catalytic subunits Pph21/22 to form complexes necessary for sustaining cell growth, whereas Cdc55 and Tpd3 would inhibit such association (Jiang & Broach, 1999). Therefore, it is conceivable that AWR5 could be acting upstream PP2A by promoting an abnormally stable formation of the Cdc55-Tpd3-PP2Ac complex, thus preventing functional Tap42-PP2Ac interactions. This is consistent with the effect we observed at the level of *GAP1* promoter activity after *awr5* expression, suggesting that in the absence of Cdc55, Tap42 association with Pph21/22 leads to decreased levels of *GLN3*-regulated genes expression in order to permit promotion of cell growth (Figure 18). Deletion of *TPD3* should lead to similar *GAP1* promoter activities after *awr5* expression, since Cdc55 and Tpd3 are both required for the association with Pph21/22 to occur.

Interestingly, during the course of this work, the *cdc55* mutant has been also isolated in a screen for suppressors of the yeast growth inhibition caused by the *Erwinia amylovora* T3E DspA (Siamer *et al.*, 2014). This could suggest that the PP2A phosphatase has evolved as a cellular hub, targeted by different pathogens to interfere with plant host cell homeostasis. However, DspA caused a specific alteration of the yeast sphingolipid biosynthesis, showing no overlap with AWR5-triggered phenotypes other than the Cdc55-dependent growth inhibition. In addition, AWR5 still caused its toxicity on strains with mutations in the small GTPase *rho2* and in the sphingolipid biosynthesis gene *sur1* (data not shown), which strongly supressed DspA-triggered growth defects (Siamer *et al.*, 2014). All these data support a different mode of action for these two T3Es, only sharing Cdc55 as an intermediate in signal transduction.

Furthermore, we have showed that disruption of *SCH9* also suppressed the AWR5-triggered growth inhibition phenotype. Cells lacking *SCH9* display enhanced stress responses and reduced levels of oxidative stress (Qie *et al.*, 2015). As seen in Figure 16, cells lacking *SCH9* seemed to recover at a lower level than those lacking either *Cdc55* or *TPD3* after *awr5* expression, suggesting that growth recovery might be a result of abnormal stress responses. Nevertheless, the fact that Sch9 might be needed for the AWR5-mediated phenotype cannot be disregarded, as this kinase is the major signaling molecule (although not the only one) of TORC1-regulated ribosome biosynthesis and cell-size control pathway (Urban *et al.*, 2007). Sch9 is considered the functional ortholog of S6 kinase (S6K), the best characterized target of TORC1 in mammals. Ribosomal protein S6 (S6) is directly phosphorylated by mammalian S6K to promote transcription of genes involved in ribosome biogenesis (Chauvin *et al.*, 2014). Still, in *Saccharomyces cerevisiae*, data validating Rps6 (the yeast equivalent of S6) as a substrate of Sch9 is rather controversial. Although Sch9 was shown to phosphorylate Rps6 *in vitro* (Urban *et al.*, 2007), recent studies reported that active TORC1 stimulated Rps6 phosphorylation independently of Sch9 through regulation of the Ypk3 kinase activity (Gonzalez *et al.*, 2015) (Figure 15). In addition, the role of Rps6 protein in maintaining global translation is not clear and other Sch9 substrates like Dot6, Tod6 and Stb3 might drive transcription of ribosome biogenesis genes and genes encoding ribosomal proteins through this pathway (Huber *et al.*, 2011). Therefore, the fact that we could not detect differences in Rps6 phosphorylation status after *awr5* expression might be indicative of a situation in which factors other than Rps6 are strictly required for the AWR5 effect downstream Sch9, namely down-regulation of protein and ribosome synthesis.

In addition, the AWR5 effect on nitrogen metabolism is inconsistent with a scenario where this bacterial protein would exclusively target Sch9, since *GLN3*-regulated genes *GLN1* and *GAP1* do not show dependence on Sch9 (Urban *et al.*, 2007). Instead, a situation in which AWR5 would function at the level of TORC1 to inhibit Sch9 and activate Tap42/PP2A-controlled pathways is more plausible. This is congruent with the observation that deletion of *CDC55* only normalizes the expression of specific subsets of genes altered by *awr5* expression (i.e. NCR genes but not ribosomal protein encoding genes) and the fact that AWR5-mediated autophagy promotion was not dependent on Cdc55.

The notion of a single target is reinforced by the consideration that only a limited number of T3E molecules are injected into the host cell to exert their function. Along this line, it is remarkable that minimal leaky expression of *awr5* from a tet-off promoter in the presence of the repressor doxycycline substantially limits yeast growth. In addition, the reduced size of yeast cells expressing *awr5,* a phenotype also observed after rapamycin treatment, point to the impact of a growth regulatory pathway (Du *et al.*, 2012) (Figure 9).

Alternatively, AWR5 could act upstream TORC1, simulating a stress situation to which this kinase would respond by negatively regulating growth. TORC1 pathway responds to different nutrient and metabolic cell conditions and activates different gene expression programs in accordance with the needs of the cell. Moreover, in certain stress/starvation circumstances, there is a crosstalk between TORC1 and other pathways like Rho1, MAPK Hog1, AMP-activated protein kinase Snf1 or Protein Kinase A (PKA) signaling (Hughes Hallett *et al.*, 2014). For instance, in nitrogen and amino acid starvation conditions, binding of Gtr1, Gtr2 (components of the EGO complex) and Rho1 GTPases to TORC1 leads on one side, to down-regulation of Sch9-dependent protein and ribosome synthesis genes and on the other side to induction of PP2A-dependent genes involved in nitrogen assimilation and amino acid synthesis (Stracka *et al.*, 2014). Thus, similar TORC1-mediated responses observed after treatment with rapamycin also occur in oxidative and heat stress (Hughes Hallett *et al.*, 2014). Another signaling molecule modulating TORC1 activity is Mtl1, a transmembrane protein acting in the cell wall integrity pathway (Sundaram *et al.*, 2015). Upon glucose deprivation or in quiescence (including rapamycin treatment), Mtl1 transmits the signal through the CWI pathway to inactivate TORC1, which in turn inhibits Sch9 (Sundaram *et al.*, 2015). Therefore, it is also possible that AWR5 modulates state transitions of the cell, by causing metabolic alterations or by interacting with TORC1 partners which will alternatively bind this kinase complex or transmit signaling to prevent its activation. We

speculate that this hypothesis might as well apply to AWR2 or AWR4, whose expression caused similar transcriptional responses at the level of TORC1 downstream targets as *awr5* expression. Additional experiments testing direct interaction with TORC1 or the effect of AWR proteins on interconnected pathways mediating TORC1 activity will allow pointing to a specific event to explain effector-mediated phenotypes in yeast.

The impact of AWR5 on the plant TOR pathway

TOR functions are conserved across kingdoms; in plants TOR is also a master regulator of the cell, controlling the switch between stress and growth (Xiong & Sheen, 2014). Our data clearly supports the idea that AWR5 alters the TOR pathway in plants.

First, *awr5* expression *in planta* results in nitrate reductase activity inhibition. This enzyme has a central role in nitrogen metabolism and its inhibition has been previously linked to TOR deficiency and activated nitrogen recycling (Ahn *et al.*, 2011). Noteworthy, even a minimal escape in *awr5* expression visibly impacted plant nitrate reductase activity, similar to what was observed in yeast growth inhibition assays. This strengthens the notion of a conserved AWR function as an extremely efficient modulator of the TOR pathway in disparate eukaryotic contexts. In addition, the bacterial growth inhibition caused by T3SS-mediated delivery of AWR5 into the plant host cells was partially suppressed by both silencing and overexpression of TOR kinase (Figure 27). Our interpretation is that AWR5 causes a TOR-mediated homeostatic imbalance resulting in a stress situation that may resolve as acclimation, tightly linked to activation of defense responses (Karpinski *et al.*, 2013). Induction of defense would render the plant less vulnerable to infection, as we observed after inoculation with bacteria expressing *awr5*.

Whether induction of the hypersensitive response is a cause or a consequence of effector recognition is still a matter of debate (Coll *et al.*, 2011). Recognition of AWR5 could account for the minor changes caused by *awr5* expression on TOR-regulated targets in *Arabidopsis thaliana* or *Nicotiana benthamiana* (Figure 28 and 29). In this scenario, plant responses triggered after AWR5 recognition would mask effector activity and its role in virulence. This would also explain the increased virulence of the *Ralstonia solanacearum* strain devoid of all *awrs* in *Arabidopsis thaliana* plants. The fact that *R. solanacearum* is more virulent in plants with altered TOR levels indicate that in fact, TOR might be required for recognition (Figure 30).

As an alternative hypothesis, AWR effectors might be causing a cellular/metabolic alteration in the host, similar to our previous interpretation of AWR function in yeast. In this case, the host plant might respond through induction of stress responses, including defense. In the context of *Ralstonia solanacearum* infection it remains a mystery why a bacterial T3E would mimic the effect of nitrogen starvation on infected tissues. Interestingly, there are several instances in the literature showing modulation of the host metabolism by T3Es. For example, the *R. solanacearum* effector RipTPS was shown to possess trehalose-6-phosphate synthase activity (Poueymiro *et al.*, 2014). Furthermore, group A *Streptococcus* enhances its growth by activation of asparagine metabolism via ER stress induction in mammalian cells (Baruch *et al.*, 2014). Since ER stress responses are intimately connected with TOR signaling (Crespo, 2012), it is tempting to speculate that AWR5 modulates the TOR pathway to induce ER stress responses and stimulate growth by an analogous mechanism to the one proposed in *Streptococcus*. Interestingly enough, in the case of infection with the human pathogen *Pseudomonas entomophila,* hyperactivation of the stress pathways lead to inhibition of protein synthesis by the host. The cellular damage caused by this pathogen was sensed by two stress kinases that transmitted signals towards inhibition of translation through different pathways, including inactivation of TOR kinase (Lemaitre & Girardin, 2013).

It is tempting to speculate that AWR5-mediated inhibition of TOR (nitrogen recycling, autophagy, inhibition of protein synthesis) might be beneficial for the bacterium during its necrotrophic phase, as it would facilitate cell dismissal and enhanced nutrient availability. Alternatively, considering that TOR-suppressed plants have an extended life span (Ren *et al.*, 2012), one could think that AWR5 might strategically inhibit TOR to ensure availability of nutritional supplies. By simulating a calorie restriction state, the bacteria would take profit of consuming secondary intermediates, accumulated by the cells as alternate nutrients and energy source for survival when TOR is inhibited (Ren *et al.*, 2012). Still, AWR5 would target upstream regulators of TOR pathway, such as still-unknown plant homologues of the yeast EGO complex or its mammalian counterpart SEA complex, shown to mediate amino-acid dependent activation of TOR (Dokudovskaya & Rout, 2015; Stracka *et al.*, 2014).

In our case, it would be interesting to determine if TOR activity is really inhibited after *awr5* expression *in planta* or if AWR5 protein directly targets TOR kinase and prevents its activation. For this, a sensitive *in vivo* cellular assay was recently established in *Arabidopsis thaliana* for monitoring endogenous TOR activity, based on the phosphorylation of its conserved S6 kinase (Xiong & Sheen, 2012). Hence, deciphering

AWR5 target(s) will help to further uncover its role in virulence and/or resistance and set up the basis to study the other members of this family. Noteworthy, AWR2-mediated phenotypes in *Arabidopsis thaliana* and yeast suggest this effector protein has an important role in *Ralstonia* infection, although in a distinct context than AWR5. This may be attributed to the fact that *Ralstonia* might use particular combinations of effectors depending on the host (Cunnac *et al.*, 2004; Kvitko *et al.*, 2009). Alternatively, these two effectors might have different impacts in a particular host process, in this case on TOR pathway.

The impact of AWRs upstream the TOR pathway constitutes a significant advance in the context of plant-pathogen interactions. Firstly, it is the first report where a bacterial type III effector modulates such a central and conserved regulatory pathway, integrating responses to a wide variety of signals. In addition, the resemblance between AWR5 expression and rapamycin treatment may constitute the basis for genome-manipulation applications, since this compound has been showed to induce pathways regulating host and pathogen metabolism (Gordon *et al.*, 2015).

In summary, taking advantage of the yeast system, we have characterized the impact of AWR effector family on the physiology of this model organism. In the case of AWR5, we have unveiled a new T3E function that is highly conserved through evolution as it targets TOR, a central regulator of cellular homeostasis and metabolism. Our work opens the avenues for future research aimed at mechanistically understanding the benefit of this function for the bacteria and whether it can be targeted to design new sustainable strategies to fight infection.

CONCLUSIONS

From the main objectives followed in this work we extract the conclusions listed below:

Heterologous expression of AWR type III effectors in *Saccharomyces cerevisiae*

1. All *awr* genes have been successfully transcribed in yeast from episomic or genome-integrated constructs. All full-length proteins, except for AWR3, have been detected in yeast cells.

Phenotypic characterization of AWR effector family in yeast

2. Strong expression of AWR1, 2, 3 and 5 (*GAL1* promoter, episomal constructs) inhibits yeast growth. AWR5 caused the strongest toxicity still apparent at low expression levels (monocopy integration into the yeast genome under Tet-Off promoter).

3. Production of the full-length AWR5 protein in yeast leads to a growth inhibition and reduced cell size, but not to an apparent cell cycle arrest or cell death.

Effect of *awr5* expression on the physiology of the budding yeast

4. Expression of bacterial *awr5* in yeast mimics the transcriptional changes caused by inhibition of the TORC1 pathway by rapamycin or nitrogen starvation.

5. AWR5-mediated yeast growth inhibition is not rescued by treatment with the TORC1 activator cycloheximide.

Identification of AWR5 molecular targets by heterologous expression in yeast

6. Mutations in three genes (*CDC55, TPD3, SCH9)* involved in the TORC1 pathway rescue the yeast growth inhibition caused by AWR5.

7. Cdc55 is required for AWR5-mediated growth inhibition phenotype and its downstream transcriptional responses.

8. *awr5* expression induces constitutive autophagy, independently of Cdc55-PP2A activity and does not interfere with Rps6 protein levels or its degree of phosphorylation.

9. Targeting of TORC1 pathways may be conserved among AWR2, AWR4 and AWR5, since their expression in yeast leads to similar downstream transcriptional responses.

***In planta* validation of AWR5 impact on its targets**

10. *Agrobacterium*-mediated transient expression of *awr5* in *Nicotiana benthamiana* results in a significant reduction of nitrate reductase activity, indicating AWR5 may target the TOR pathway *in planta* through a conserved mechanism.

11. Normal levels of the TOR kinase are required for the *Pseudomonas syringae* growth restriction effect caused by heterologously expressed *awr5* in *Arabidopsis thaliana* plants.

12. *Ralstonia solanacearum* is more virulent on *Arabidopsis* plants with altered levels of TOR compared to Col-0 plants.

13. Alterations in the plant TOR kinase levels lead to suppression of the increased virulence of a *R. solanacearum* strain devoid of all *awrs* in *Arabidopsis thaliana.*

MATERIALS AND METHODS

Plasmids, strains and gene cloning

All strains and plasmids used in this study are described in Table 3. For heterologous expression of *awr*s under the control of the galactose inducible promoter (*GAL1*), expression vectors were constructed by recombining entry clones carrying each of the *awr* ORFs into the Gateway destination vector pAG426GAL-ccdb-HA (Alberti *et al.*, 2007) through a Gateway LR reaction (Invitrogen, Waltham, Massachusetts, USA). For expression of *awr5* fragments in yeast, N-terminal (1368 bp) and C-terminal (1821 bp) halves of *awr5* as well as a central (1425 bp) fragment overlapping them were amplified from genomic DNA. PCR fragments were introduced to the final vector pAG426GAL-ccdb-HA by Gateway recombination and transformed into *Escherichia coli*.

For integration of the *awr* genes fused to a C-terminal GFP tag at the locus of *URA3* gene in the yeast chromosome, each of them was cloned by Gateway recombination or ligation into the integrative vector pYI-GWY, a *URA3* plasmid in which the heterologous genes are under the control of a Tet-off promoter created in this study. pYI-GWY was constructed by cloning *Kpn*I/*Sac*I fragment from pMT735 (Tabuchi *et al.*, 2009) into the same sites of the yeast integrative vector YIplac211 (Gietz & Sugino, 1988). Following linearization with *Bst*BI that cuts inside in *URA3* cassette, pYI-GWY derivatives carrying genes *awr1* to *awr5* were integrated into the yeast chromosome by double recombination into the *URA3* locus in yeast. To this end, the wild type strain JA-100 containing a *ura3* point mutation was used as recipient, giving rise to uracyl autotrophs after *awr* integration. For expression of *awr5* gene in the ***cdc55Δ*** mutant yeast strain, cloning was performed in two steps. Firstly, a *cdc55Δ::KanMX4* cassette from the ***cdc55Δ*** strain in the BY4741 background was amplified and subsequently introduced into the genome of strain JA-100. Secondly, the *awr5* gene fused to the C-terminal GFP was integrated into the newly constructed *cdc55* strain as described above.

To measure promoter activity, the *GAP1* promoter was cloned from the *URA3* yeast shuttle vector YEp357 (Gonzalez *et al.*, 2009) into the yeast vector YEp367R (Myers *et al.*, 1986), endowed with a *LEU2* marker and the plasmid transformed into the yeast strain carrying *awr5*::GFP inside the URA3 ORF. For construction of a 2µ origin vector with the *TRP1* selection marker expressing *awr5*, a *Kpn*I/*Sac*I digested fragment from pMT735-*awr5* was cloned into the same sites of the vector YEplac112 (Gietz & Sugino, 1988).

Table 3. List of strains and plasmids used in this work.

Name	Description	Background/Source
Plasmids for expression of AWRs genes and AWR5 fragments under control of galactose promoter		
pAG426GAL-ccdb-HA	Renamed pGAL; 2 µ pGAL1-GWY-HA URA3 CmR AmpR	(Alberti *et al.*, 2007)
pDONR207	Gateway™ entry vector, CmR GmR	Invitrogen
pDONR-Nterm *awr5*	pDONR207 containing N-terminal fragment of AWR5 from *R. solanacearum* GMI1000 GmR	This study
pDONR-Cen *awr5*	pDONR207 containing central fragment of AWR5 from *R. solanacearum* GMI1000 GmR	This study
pDONR-Cterm *awr5*	pDONR207 containing C-terminal fragment of AWR5 from *R. solanacearum* GMI1000 GmR	This study
pGAL-Nterm *awr5*-HA	pGAL bearing N-terminal fragment of AWR5 from *R. solanacearum* GMI1000 URA3 AmpR	This study
pGAL-Cen *awr5*-HA	pGAL bearing central fragment of AWR5 from *R. solanacearum* GMI1000 URA3 AmpR	This study
pGAL-Cterm *awr5*-HA	pGAL bearing C-terminal fragment of AWR5 from *R. solanacearum* GMI1000 URA3 AmpR	This study
pDONR-*awr5*	pDONR207 containing AWR5 from *R. solanacearum* GMI1000 GmR	(Sole *et al.*, 2012)
pENTR-*awr4*	pENTR/SD/D-Topo containing AWR4 from R. solanacearum GMI1000 KmR	(Monteiro *et al.*, 2012)
pDONR-*awr3*	pDONR207 containing AWR3 from *R. solanacearum* GMI1000 GmR	(Sole *et al.*, 2012)
pENTR-*awr2*	pENTR/SD/D-Topo containing AWR2 from R. solanacearum GMI1000 KmR	(Monteiro *et al.*, 2012)
pDONR-*awr1*	pDONR207 containing AWR1 from *R. solanacearum* GMI1000 GmR	(Sole *et al.*, 2012)
pDONR-*gfp*	pDONR201 containing *green fluorescent* control gene KmR	F. Monteiro *et al.* unpublished
pGAL-*awr5*	pGAL destination vector expressing AWR5 from *R. solanacearum* GMI1000 URA3 AmpR	This study
pGAL-*awr4*	pGAL destination vector expressing AWR4 from *R. solanacearum* GMI1000 URA3 AmpR	This study
pGAL-*awr3*	pGAL destination vector expressing AWR3 from *R. solanacearum* GMI1000 URA3 AmpR	This study
pGAL-*awr2*	pGAL destination vector expressing AWR2 from *R. solanacearum* GMI1000 URA3 AmpR	This study
pGAL-*awr1*	pGAL destination vector expressing AWR1 from *R. solanacearum* GMI1000 URA3 AmpR	This study
pGAL-*gfp*	pGAL destination vector expressing *gfp* control gene URA3 AmpR	This study
Plasmids for integration of AWRs into yeast genome		
YIplac211	Yeast integrative vector URA3 AmpR	(Gietz & Sugino, 1988)

pMT735	CEN pTet-off GFP tag URA3 CmR AmpR	(Tabuchi *et al.*, 2009)
pDONR-*awr5*	pDONR207 containing AWR5 (no stop) from *R. solanacearum* GMI1000 GmR	(Sole *et al.*, 2012)
pMT735-*awr5*	pMT735 destination vector expressing AWR5 from *R. solanacearum* GMI1000 URA3 AmpR	This study
pMT735-*awr1*	pMT735 destination vector expressing AWR1 from *R. solanacearum* GMI1000 URA3 AmpR	This study
pMT735-*awr3*	pMT735 destination vector expressing AWR3 from *R. solanacearum* GMI1000 URA3 AmpR	(Tabuchi *et al.*, 2009)
pYI-GWY	Kpn I-Sac I fragment from pMT735 cloned into YIplac211 same sites URA3 CmR AmpR	This study
pYI-*awr1*	Kpn I-Sac I fragment from pMT735-*awr1* cloned into YIplac211 same sites URA3 AmpR	This study
pYI-*awr3*	Kpn I-Sac I fragment from pMT735-*awr3* cloned into YIplac211 same sites URA3 AmpR	This study
pYI-*awr5*	Kpn I-Sac I fragment from pMT735-*awr5* cloned into YIplac211 same sites URA3 AmpR	This study
pYI-*awr2*	pYI-GWY destination vector expressing AWR2 from *R. solanacearum* GMI1000 URA3 AmpR	This study
pYI-*awr4*	pYI-GWY destination vector expressing AWR4 from *R. solanacearum* GMI1000 URA3 AmpR	This study

Plasmids for autophagy and β galactosidase assays

pRS415-ATG8-GFP	pRS415 ATG8-GFP *CEN LEU2* AmpR	(Shimobayashi *et al.*, 2010)
YEp367R	Yeast shuttle vector for construction of *lacZ* fusions (*LEU2*, AmpR)	(Myers *et al.*, 1986)
YEp357-*pGAP1*	YEp357 carrying PromGAP1(-968 to +21)::lacZ cloned Kpn I-XbaI URA3 AmpR	(Gonzalez *et al.*, 2009)
YEp357-*pGLN1*	YEp357 carrying PromGLN1(-853 to +21)::lacZ cloned Kpn I-XbaI URA3 AmpR	(Gonzalez *et al.*, 2009)
YEp357-*pGDH1*	YEp357 carrying PromGDH1(-904 to +21)::lacZ cloned EcoR I-XbaI URA3 AmpR	(Gonzalez *et al.*, 2009)
YEp367R-*pGAP1*	YEp367R carrying a fusion between lacZ gene and *GAP1* promoter LEU2 AmpR	This study
YEp367R-*pGLN1*	YEp367R carrying a fusion between lacZ gene and *GLN1* promoter LEU2 AmpR	This study
YEp367R-*pGDH1*	YEp367R carrying a fusion between lacZ gene and *GDH1* promoter LEU2 AmpR	This study
YCplac111-*pMEP2*	Yeast shuttle vector YCplac111 carrying Prom*MEP2*(-828 to +27)::lacZ LEU2 AmpR	(Marini *et al.*, 1997)

Plasmids for growth assays of TOR-related mutants

pMT921	pMT735 inverse PCR self-ligated plasmid; CEN pTet-off GFP tag URA3 AmpR	(Tabuchi *et al.*, 2009)
pMT830	2μ pTet-off, GFP tag URA3 CmR AmpR	(Tabuchi *et al.*, 2009)
pMT830-*awr5*	pMT830 destination vector expressing AWR5 from *R. solanacearum* GMI1000 URA3 AmpR	This study
YEplac112	2μ TRP1 AmpR	(Gietz & Sugino, 1988)
YEplac112-*awr5*	2μ YEplac112 Tet-Off promoter::AWR5::GFP TRP1 AmpR	This study

Plasmids for overexpression of TOR-related genes		
YEplac181-PPH21	2µ plasmid for *PPH21* gene expression under its own promoter (*LEU2*, AmpR)	(Munoz *et al.*, 2003)
YEplac181-PPH22	2µ plasmid for *PPH22* gene expression under its own promoter (*LEU2*, AmpR)	(Munoz *et al.*, 2003)
YEplac181-SIT4	2µ plasmid for *SIT4* gene expression under its own promoter (*LEU2*, AmpR)	(Munoz *et al.*, 2003)
YEp351-HAL3	2µ plasmid for *HAL3* gene expression under its own promoter (*LEU2*, AmpR)	(Ferrando *et al.*, 1995)
Plasmids for overexpression of TOR-related genes		
pMDC7-*citrine*	Gateway destination vector, estradiol-inducible, Ct-YFPv/HA tag CmR SpR	E. Washington et al., unpublished
pMDC7-*awr5*	pMDC7 containing AWR5 from *R. solanacearum* GMI1000 SpR	(Sole *et al.*, 2012)
pMDC7-*gus*	pMDC7 containing the *beta-glucuronidase* control gene SpR	(Sole *et al.*, 2012)
pEDV6	Gateway destination vector for effector gene fusion to AvrRPS4 N-terminus (1-137). RPS4 promoter, HA tag RifR GmR	(Song & Yang, 2010)
pEDV6-*awr*5	pEDV6 vector carrying *R. solanacearum* GMI1000 AWR5, GmR	(Sole *et al.*, 2012)
Yeast strains		
BY4741	*MATa his3Δ0 leu2Δ0 met15Δ0 ura3Δ0*	(Winzeler *et al.*, 1999)
JA-100	*MATa ura3-52 leu2-3,112 trp1-1 his4 can-1^r*	(de Nadal *et al.*, 1998)
JA-*awr5*	JA-100 *AWR5::GFP::URA3*	This study
JA-*awr4*	JA-100 *AWR4::GFP::URA3*	This study
JA-*awr3*	JA-100 *AWR3::GFP::URA3*	This study
JA-*awr2*	JA-100 *AWR2::GFP::URA3*	This study
JA-*awr1*	JA-100 *AWR1::GFP::URA3*	This study
gln3Δ	BY4741 *gln3Δ::kanMX4*	EUROSCARF
tip41Δ	BY4741 *tip41Δ::kanMX4*	EUROSCARF
ppm1Δ	BY4741 *ppm1Δ::kanMX4*	EUROSCARF
cdc55Δ	BY4741 *cdc55Δ::kanMX4*	EUROSCARF
rts1Δ	BY4741 *rts1Δ::kanMX4*	EUROSCARF
tpd3Δ	BY4741 *tpd3Δ::kanMX4*	EUROSCARF
sit4Δ	BY4741 *sit4Δ::kanMX4*	EUROSCARF
sch9Δ	BY4741 *sch9Δ::kanMX4*	EUROSCARF

W303-1A	*MAT*a *leu2-3,112 trp1-1 can1-100 ura3-1 ade2-1 his3-11,15*	(Thomas & Rothstein, 1989)
DEY172-2B	*W303-1A pph22-172::URA3 pph21A1::HIS3*	(Evans & Stark, 1997)
3HA-Cdc55	W303 *3HA::CDC55*	W303, (Queralt & Uhlmann, 2008)
cdc55Δ	JA-100 *MATa cdc55Δ::kanMX4*	JA-100, This study
cdc55Δ AWR5-GFP	JA-100 *MATa cdc55Δ::kanMX4 AWR5::GFP::URA3*	JA-100, This study
***Agrobacterium tumefaciens* strains**		
GV3101 *awr5*	GV3101 expressing AWR5-YFP-HA RifR GmR SpR	GV3101, This study
GV3101 *gus*	GV3101 expressing GUS-YFP-HA RifR GmR SpR	GV3101, This study
***Pseudomonas syringae* strains**		
DC3000	*P.syringae* pv. tomato DC3000 strain, RifR	(Cunnac *et al.*, 2004)
3000-*awr5*	DC3000 expressing RPS4N-HA-AWR5, RifR GmR	(Sole *et al.*, 2012)
***Ralstonia solanacearum* strains**		
GMI1000	*R. solanacearum* strain Phylotype I	(Boucher *et al.*, 1987)
Δ*awr1-5*	GMI1000 Δ*awr1-5* mutant, GmR	(Sole *et al.*, 2012)
***E. coli* strains**		
MACH 1	*ΔrecA1398 endA1 tonA Φ80ΔlacM15 ΔlacX74 hsdR($r_K^-m_K^+$)*	Invitrogen
DB3.1	*F- gyrA462 endA1 glnV44 Δ(sr1-recA) mcrBmrr hsdS20(r_B^-, m_B^-) ara14 galK2 lacY1 proA2 rpsL20(Smr) xyl5 Δleu mtl1, Smr*	Invitrogen

To verify gene integration in the yeast genome, cells were treated with lyticase (Sigma-Aldrich, Buchs, Switzerland) for 30 mins at 37°C, followed by centrifugation for 2 mins/max speed. PCR amplifications were performed from the resulting supernatant using primers corresponding to genomic and episomal regions.

Yeast strains and growth conditions

Yeast strains were grown in either rich YPD (Yeast Peptone Dextrose) medium or synthetic defined (SD) medium (Sherman, 2002), containing yeast nitrogen base w/o aminoacids (BD Difco) with 2% glucose, 2% raffinose, or 2% galactose as carbon sources. SD Media were supplemented with a yeast synthetic drop-out without histidine, leucine, tryptophan and uracil (Sigma-Aldrich, Buchs, Switzerland) adding the necessary requirements to select for auxotrophies. The ethanol-glycerol medium was equivalent to synthetic defined (SD) medium with 3% ethanol and 3% glycerol and supplemented with yeast synthetic drop-out. Doxycycline was used at 0.1, 15, or 20 µg/ml. The latter concentration was used unless otherwise indicated. All yeast transformations were performed by the lithium acetate transformation method (Gietz *et al.*, 1992).

For expression of *awrs* or their fragments under the control of the galactose promoter, yeast cells were grown for 2 days in SD-Ura + raffinose 2%, then diluted to optical density at 600 nm of 0.4 in water and plated either in repressing media (glucose) or inducing media (galactose) to monitor the effects of AWRs in cell growth/viability. For standard growth inhibition experiments on plates, strains were incubated overnight with shaking in selective medium with doxycycline 20 µg/ml. Cultures were then normalized to OD_{600}=0.1-0.2 and incubated until exponential phase. 1 OD_{600} of cells were then harvested, washed 2 times with sterile water, re-suspended in 1 ml water and 10-fold serially diluted in water four times. Each suspension (5 or 10 µl) was dropped either in non-inducing media (+doxycycline) or inducing media (no doxycycline) onto agar plates and then incubated for 2-3 days before photographs were taken.

To test growth viability in liquid media over time and for sample harvesting for RNA isolation, yeast strains were grown overnight in rich YPD medium with doxycycline 15µg/ml (repressing conditions), then normalized to OD_{600}=0.05 and grown for 2, 4, 6 or 8 hours in YPD+dox (non-inducing conditions) and YPD (inducing conditions). Similar growth conditions were carried out for protein extraction and beta-galactosidase assays, using selective medium in this case.To test viability of yeast cells expressing *awr5* after doxycycline addition, strains were grown overnight in either SD-Ura+dox (non-inducing conditions) or SD-Ura (inducing). Cells were recovered and normalized

to OD_{600} =0.05 and grown in liquid in SD-Ura+dox. Samples were harvested at different time points, serially 10-fold diluted and plated onto solid SD-Ura+dox and incubated for 2 days at 28°C until colonies were counted.

For microscopic analyses, yeast strains bearing *awr5* grown for 8 hours in SD-Ura+dox and SD-Ura were visualised in bright field at 100x under a fluorescence microscope (Axiophot, Zeiss, Oberkochen, Germany), equipped with a Digital color camera DP70 Olympus. For methylene blue staining, yeast cells carrying *awr5* were harvested at 6 hours after induction and stained for 5 minutes with a 0.01% methylene blue solution in glycine buffer. In parallel, the same cells were fixed with formaldehyde 37% for 10 mins before methylene blue addition as a positive staining control. Images were obtained using a Dapi 395-440/ FT 460 /LP470 filterset.

To measure yeast cell size, three independent replicates of wild-type yeast strains (JA-100) and strains bearing *awr5* were grown overnight in YPD medium with and without doxycycline (15µg/ml). Next day, cultures were normalized to OD_{600}=0.05 and grown in liquid either in YPD+dox or YPD during 6 and 8 hours. 50 µl of each culture were diluted in the same volume of PBS1x and analyzed with a Scepter Handheld Automated Cell Counter (Merck Millipore, Darmstadt, Germany).

To measure induction of autophagy, wild-type and *cdc55Δ* strains carrying *awr5* and ATG8-GFP were grown overnight in selective media +doxycycline. Cultures were then normalized to an OD_{600}=0.2, grown until exponential phase, normalized again to OD_{600}=0.05 and finally grown overnight with or without dox until samples were harvested. For autophagy induction after nitrogen starvation JA-100 cells were grown overnight in SD medium without ammonium sulfate (BD Difco, Franklin Lakes, NJ, USA) and 2% glucose. Yeast cells were incubated at 28-30°C, unless otherwise stated.

DNA microarray analysis

Aliquots of the same samples harvested to test viability of cells expressing *awr5* in liquid media at 2, 4 and 6 hours after induction were used for microarray analysis. RNA was extracted using the yeast RiboPure™ RNA Purification Kit (Ambion, Carlsbad, CA, USA) according to the manufacturer's protocol and quantified. For microarray hybridization, total RNA (8 *µ*g) was employed for cDNA synthesis and labelling using the indirect labelling kit (CyScribe Post-Labeling kit; GE Healthcare, Wauwatosa, WI, USA) with Cy3–dUTP and Cy5–dUTP fluorescent nucleotides. The cDNA obtained was dried, re-suspended in hybridization buffer and evaluated with a Nanodrop spectrophotometer (Nanodrop Technologies, Thermo Scientific, Waltham, MA, USA). The combined fluorescently labelled cDNAs were hybridized to yeast genomic

microchips constructed in our laboratory by arraying 6014 different PCR-amplified open reading frames from *S. cerevisiae* (Alberola *et al.*, 2004). Microarrays were processed as described previously (Hegde *et al.*, 2000), scanned with a ScanArray 4000 apparatus (Packard BioChip Technologies, Perkin Elmer, Waltham, MA, USA) and the output was analysed using GenePix Pro 6.0 software. Data collected from 2 biological replicates (with dye swap) after 2, 4 and 6 h of doxycycline removal (thus triggering expression of *awr5*) were combined. Genes were considered induced or repressed by AWR5 expression when the minus/plus doxycycline ratio was ≥ 2.0 or ≤ 0.5, respectively, for both biological replicates. All data has been added to the Gene Expression Omnibus (GEO) database under number XXX (available upon publication).

qRT-PCR

Two independent biological replicas of the strain carrying *awr5* grown in inducing and non-inducing conditions were harvested at 4 and 6 hours after induction and subjected to RNA extraction to quantify *awr5* mRNA levels, whereas of *GAP1, MEP2, STM1* and *NSR1* levels were only tested from samples obtained 6 h after induction. RNA was extracted from the samples (RiboPure^{TM} RNA Purification Kit, yeast; Ambion, Carlsbad, CA, USA) and quantified. 2 µg of total RNA were subjected to retro-transcription with anchored oligo-$(dT)_{18}$ primers (Transcriptor first strand cDNA synthesis kit; Roche, Basel, Switzerland).

Plant RNA was obtained from 2-week old *Arabidopsis* plants and from leaves of 3 to 4 week-old *N. benthamiana* plants. RNA was extracted using TRIzol (Life Technologies) according to the manufacturer's instructions. RNA was treated 30 minutes with Ambion TURBO DNase (Life Technologies) to eliminate DNA contamination. 2 µg of total RNA was reverse transcribed as described above. For quantitative real-time PCR, a Light Cycler 480 (Roche, Basel, Switzerland) with SYBR Green chemistry was used with three technical replicas. Actin was used as a housekeeping gene to normalize samples for yeast qRT-PCR assays, whereas for plant qRT-PCRs, tubulin and protein phosphatase 2A (PP2A) was used.

RNA-seq experiments

For RNA-seq experiments, total RNA was extracted from wild type and *cdc55* cultures carrying *awr5* grown in non-inducing and inducing conditions for 6 hours. Libraries were prepared with the QuantSeq 3' mRNA kit (Lexogen, Greenland, NH, USA) using 0.5 µg of total RNA purified as above. Sequencing was performed in an Illumina MiSeq machine with Reagent Kit v3 (single end, 80-125 nt/read). Two biological replicates were sequenced, obtaining a total number of 8.4-12.9 million reads per condition.

Mapping of fastq files to generate SAM files was carried out with the Bowtie2 software (Langmead & Salzberg, 2012) in local mode (95.1-97.3% mapped reads). The SAM files were analyzed with the SeqMonk software (http://www.bioinformatics.bbsrc.ac.uk/projects/seqmonk). Mapped reads were counted using CDS probes (extended 100 nt downstream the open reading frame because the library is biased towards the 3'-end of mRNAs) and corrected for the largest dataset. Raw data was subjected to diverse filters to remove sequences with a low number of reads.

Protein assays

For immunoblots, 30 or 40 OD_{600} units from overnight yeast cultures grown in non-inducing or inducing conditions were resuspended in 500 µl of extraction buffer (50 mM Tris-HCl pH7.5, 1 mM EDTA, 0.1% Nonidet P-40, 1% glycerol, with complete protease inhibitor (Roche, Basel, Switzerland) and subjected to 10 cycles of 1 minute sonication and 1 minute pauses. Supernatants were recovered after centrifugation at 500 g for 10 min at 4°C. 125 µg of total protein extracts were separated on 7.5% polyacrylamide gels and immunoblot was performed using anti-GFP mouse monoclonal antibody (clone B-2; Santa Cruz Biotechnology, Dallas, TX, USA).

For co-immunoprecipitation assays, yeast cells expressing 3HA-tagged Cdc55 transformed with the plasmid bearing *awr5* were lysed in the same buffer described above. Supernatants were incubated with 50 µl of magnetic µMACS Microbeads (µMACS GFP Isolation Kit, Miltenyi Biotec) conjugated to an anti-GFP monoclonal antibody at a dilution of 1 mg/ml for 2 hours at 4°C. Beads were washed and eluted according to the manufacturer's instructions and assayed by Western Blotting with anti-GFP mouse monoclonal antibody (clone B-2; Santa Cruz Biotechnology, Dallas, TX, USA) and anti-HA rat monoclonal antibody (clone 3F10, Roche, Basel, Switzerland).

For detection of total Rps6 and pRps6, 50 ml from yeast cultures grown for 6 hours in non-inducing or inducing conditions were pelleted and cells were resuspended in 100 µl of lysis buffer -50 mM Tris-HCl pH7.5, 150 mM NaCl, 15% glycerol, 0.5% Tween-20, phosphatase inhibitor mixture (PPi; 10 mM NaF, 10 mM NaN_3, 10 mM *p*-nitrophenyl phosphate, 10 mM sodium pyrophosphate, and 10 mM β-glycerophosphate), 1 mM phenylmethylsulfonyl fluoride (PMSF), and EDTA-free protease inhibitor cocktail (Roche)-. One volume of glass beads was added, and cells were broken by vigorous shaking in a FastPrep (5 times for 45 s each at setting 5.5, with intervals of 3 minutes on ice). Unbroken cells and debris were removed by centrifugation at 500 x g for 3 min. 10 µg of total protein extracts were separated on 10% polyacrylamide gels and

transferred to nitrocellulose membranes (GE Healthcare). Membranes were blocked with 5% BSA for 1 h at room temperature and incubated for 1 h at room temperature or overnight at 4°C with the respective antibodies, followed by the secondary antibodies. Antibodies are as follows: phosphor-Ser235/Ser236-S6 (#2211, Cell Signaling Technology), RPS6 (#ab40820, Abcam), goat anti-rabbit IgG-HRP (Santa Cruz Biotechnology).

Beta-galactosidase activity was measured from 2 ml of cultures pelleted 6 hours after induction. Cells were resuspended in 100µl of Z buffer and mixed to 900 µl of Z buffer with 0.05M ß-mercaptoethanol, 40 µl of chloroform and 20 µl of SDS 0.1%. After incubation for 15 minutes at 30°C, 200µl of ONPG (Fluka) was added. The reaction was stopped with 500 µl of Na_2CO_3, the reaction time was recorded and the optical density at 420nm and 550nm were measured to calculate beta-galactosidase activity (Miller units) as described (Reynolds *et al.*, 2001).

Plant material and growth conditions

For all experiments, *Arabidopsis thaliana* plants were germinated, transplanted 10 days after sowing and grown for two additional weeks in short-day conditions at 20-22°C and 55% humidity. Wild type (Wt) Columbia 0, TOR overexpressor G548 from the Gabi collection (TOR OEX) and TOR RNAi-silenced 35-7 (*TOR* RNAi) (Deprost *et al.*, 2007) were used. 3 to 4-week-old *N. benthamiana* plants were used for transient expression experiments.

Nitrate reductase assays

To measure Nitrate reductase activity, *N. benthamiana* plants were treated two times a week with 2mM-15mM KNO_3, then, transient *Agrobacterium*-mediated transformation was performed as previously described (Sole *et al.*, 2012). Protein expression was induced by painting the leaves 14 hours post-infiltration with 20 µM estradiol and Silwet L-77 adjuvant. Whole leaves (1g) were harvested at 0 and 1 hour post-induction and homogenized in 3 ml of 0.1 M HEPES-KOH, pH 7.5, 3% polyvinylpolypyrrolidone, 1 mM EDTA and 10 mM cysteine. The extracts were filtered through four layers of Miracloth (Merk Millipore, Billerica, USA) and centrifuged for 15 minutes at 30,000xg at 4°C. The assay mixture (2 ml) contained 25 mM HEPES-KOH, 10 mM KNO_3, 0.4 mM NADH (Sigma). The reaction was initiated by addition of 200 µl of enzyme extract and terminated by rapid addition of 1 ml of 1% sulphanilamide (Fluka) and 1 ml of 0.02% N-(1-naphtyl)-ethylene-diamine dihydrochloride (Sigma) in 3N HCl. Moles of nitrite present in the reaction were determined using a standard solution at 0.01 M of sodium

nitrite. Nitrate reductase activity was expressed as picomoles of nitrite produced per minute per µg of protein (adapted after (Reed & Hageman, 1980)).

Pathogenicity assays *in planta*

Arabidopsis leaves were hand inoculated with *Pseudomonas syringae* strains at $5x10^5$ CFU/ml with a 1-ml blunt syringe. Leaves were recovered and homogenized in 200 µl of $MgCl_2$ 10 mM. For each strain, three biological replicates were taken at time zero and 3 days post inoculation (each containing four 5 mm diameter discs from independent leaves). Bacterial suspensions were serially 10-fold diluted, and plated in the presence of antibiotics. Colony forming units (CFUs) were counted and bacterial growth calculated as the recovered CFU per square centimeter with respect to the original inoculums. Results were validated with the one-way analysis of variance test (Tukey post-analysis test) with the R-3.2.0 software statistics package.

For *Ralstonia solanacearum* pathogenicity test, 5-week old *Arabidopsis* plants in Jiffy-7 peat pellets were root-cut, incubated with *Ralstonia* solution at 10^8 CFU/ml for 30 minutes and transferred to chamber again. Symptom appearance was recorded independently for each plant according to a wilting scale (0: no wilting, 1: 25% wilted leaves, 2: 50%, 3: 75%, 4: death).

BIBLIOGRAPHY

Abramovitch, R. B., Kim, Y. J., Chen, S., Dickman, M. B. & Martin, G. B. (2003). Pseudomonas type III effector AvrPtoB induces plant disease susceptibility by inhibition of host programmed cell death. *EMBO J* **22**, 60-69.

Adhikari, H., Vadaie, N., Chow, J., Caccamise, L. M., Chavel, C. A., Li, B., Bowitch, A., Stefan, C. J. & Cullen, P. J. (2015). Role of the unfolded protein response in regulating the mucin-dependent filamentous-growth mitogen-activated protein kinase pathway. *Mol Cell Biol* **35**, 1414-1432.

Ahn, C. S., Han, J. A., Lee, H. S., Lee, S. & Pai, H. S. (2011). The PP2A regulatory subunit Tap46, a component of the TOR signaling pathway, modulates growth and metabolism in plants. *Plant Cell* **23**, 185-209.

Alam, A., Miller, K. A., Chaand, M., Butler, J. S. & Dziejman, M. (2011). Identification of Vibrio cholerae type III secretion system effector proteins. *Infect Immun* **79**, 1728-1740.

Alberola, T. M., Garcia-Martinez, J., Antunez, O., Viladevall, L., Barcelo, A., Arino, J. & Perez-Ortin, J. E. (2004). A new set of DNA macrochips for the yeast Saccharomyces cerevisiae: features and uses. *Int Microbiol* **7**, 199-206.

Alberti, S., Gitler, A. D. & Lindquist, S. (2007). A suite of Gateway cloning vectors for high-throughput genetic analysis in Saccharomyces cerevisiae. *Yeast* **24**, 913-919.

Aleman, A., Rodriguez-Escudero, I., Mallo, G. V., Cid, V. J., Molina, M. & Rotger, R. (2005). The amino-terminal non-catalytic region of Salmonella typhimurium SigD affects actin organization in yeast and mammalian cells. *Cell Microbiol* **7**, 1432-1446.

Aleman, A., Fernandez-Pinar, P., Perez-Nunez, D., Rotger, R., Martin, H. & Molina, M. (2009). A yeast-based genetic screen for identification of pathogenic Salmonella proteins. *FEMS Microbiol Lett* **296**, 167-177.

Alto, N. M., Shao, F., Lazar, C. S. & other authors (2006). Identification of a bacterial type III effector family with G protein mimicry functions. *Cell* **124**, 133-145.

Anderson, D. M., Schmalzer, K. M., Sato, H., Casey, M., Terhune, S. S., Haas, A. L., Feix, J. B. & Frank, D. W. (2011). Ubiquitin and ubiquitin-modified proteins activate the Pseudomonas aeruginosa T3SS cytotoxin, ExoU. *Mol Microbiol* **82**, 1454-1467.

Anderson, D. M., Feix, J. B., Monroe, A. L., Peterson, F. C., Volkman, B. F., Haas, A. L. & Frank, D. W. (2013). Identification of the major ubiquitin-binding domain of the Pseudomonas aeruginosa ExoU A2 phospholipase. *J Biol Chem* **288**, 26741-26752.

Arbibe, L., Kim, D. W., Batsche, E., Pedron, T., Mateescu, B., Muchardt, C., Parsot, C. & Sansonetti, P. J. (2007). An injected bacterial effector targets chromatin access for transcription factor NF-kappaB to alter transcription of host genes involved in immune responses. *Nat Immunol* **8**, 47-56.

Arnoldo, A., Curak, J., Kittanakom, S. & other authors (2008). Identification of small molecule inhibitors of Pseudomonas aeruginosa exoenzyme S using a yeast phenotypic screen. *PLoS Genet* **4**, e1000005.

Aronova, S., Wedaman, K., Anderson, S., Yates, J., 3rd & Powers, T. (2007). Probing the membrane environment of the TOR kinases reveals functional interactions

between TORC1, actin, and membrane trafficking in Saccharomyces cerevisiae. *Mol Biol Cell* **18**, 2779-2794.

Asrat, S., de Jesus, D. A., Hempstead, A. D., Ramabhadran, V. & Isberg, R. R. (2014). Bacterial pathogen manipulation of host membrane trafficking. *Annu Rev Cell Dev Biol* **30**, 79-109.

Asselin, J. A., Lin, J., Perez-Quintero, A. L. & other authors (2015). Perturbation of maize phenylpropanoid metabolism by an AvrE family type III effector from Pantoea stewartii. *Plant Physiol* **167**, 1117-1135.

Balguerie, A., Bagnat, M., Bonneu, M., Aigle, M. & Breton, A. M. (2002). Rvs161p and sphingolipids are required for actin repolarization following salt stress. *Eukaryot Cell* **1**, 1021-1031.

Barbieri, A. M., Sha, Q., Bette-Bobillo, P., Stahl, P. D. & Vidal, M. (2001). ADP-ribosylation of Rab5 by ExoS of Pseudomonas aeruginosa affects endocytosis. *Infect Immun* **69**, 5329-5334.

Baruch, M., Belotserkovsky, I., Hertzog, B. B. & other authors (2014). An extracellular bacterial pathogen modulates host metabolism to regulate its own sensing and proliferation. *Cell* **156**, 97-108.

Baryshnikova, A., Costanzo, M., Dixon, S., Vizeacoumar, F. J., Myers, C. L., Andrews, B. & Boone, C. (2010a). Synthetic genetic array (SGA) analysis in Saccharomyces cerevisiae and Schizosaccharomyces pombe. *Methods Enzymol* **470**, 145-179.

Baryshnikova, A., Costanzo, M., Kim, Y. & other authors (2010b). Quantitative analysis of fitness and genetic interactions in yeast on a genome scale. *Nat Methods* **7**, 1017-1024.

Baxt, L. A., Garza-Mayers, A. C. & Goldberg, M. B. (2013). Bacterial subversion of host innate immune pathways. *Science* **340**, 697-701.

Belli, G., Gari, E., Piedrafita, L., Aldea, M. & Herrero, E. (1998). An activator/repressor dual system allows tight tetracycline-regulated gene expression in budding yeast. *Nucleic Acids Res* **26**, 942-947.

Benabdillah, R., Mota, L. J., Lutzelschwab, S., Demoinet, E. & Cornelis, G. R. (2004). Identification of a nuclear targeting signal in YopM from Yersinia spp. *Microb Pathog* **36**, 247-261.

Bernoux, M., Timmers, T., Jauneau, A., Briere, C., de Wit, P. J., Marco, Y. & Deslandes, L. (2008). RD19, an Arabidopsis cysteine protease required for RRS1-R-mediated resistance, is relocalized to the nucleus by the Ralstonia solanacearum PopP2 effector. *Plant Cell* **20**, 2252-2264.

Bhavsar, A. P., Brown, N. F., Stoepel, J. & other authors (2013). The Salmonella type III effector SspH2 specifically exploits the NLR co-chaperone activity of SGT1 to subvert immunity. *PLoS Pathog* **9**, e1003518.

Bi, E. & Park, H. O. (2012). Cell polarization and cytokinesis in budding yeast. *Genetics* **191**, 347-387.

Bi, Y. M., Wang, R. L., Zhu, T. & Rothstein, S. J. (2007). Global transcription profiling reveals differential responses to chronic nitrogen stress and putative nitrogen regulatory components in Arabidopsis. *BMC Genomics* **8**, 281.

Binda, M., Peli-Gulli, M. P., Bonfils, G., Panchaud, N., Urban, J., Sturgill, T. W., Loewith, R. & De Virgilio, C. (2009). The Vam6 GEF controls TORC1 by activating the EGO complex. *Mol Cell* **35**, 563-573.

Boch, J. & Bonas, U. (2010). Xanthomonas AvrBs3 family-type III effectors: discovery and function. *Annu Rev Phytopathol* **48**, 419-436.

Boch, J., Bonas, U. & Lahaye, T. (2014). TAL effectors--pathogen strategies and plant resistance engineering. *New Phytol* **204**, 823-832.

Bosis, E., Salomon, D. & Sessa, G. (2011). A simple yeast-based strategy to identify host cellular processes targeted by bacterial effector proteins. *PLoS One* **6**, e27698.

Botstein, D. & Fink, G. R. (2011). Yeast: an experimental organism for 21st Century biology. *Genetics* **189**, 695-704.

Boucher, C. A., Van Gijsegem, F., Barberis, P. A., Arlat, M. & Zischek, C. (1987). Pseudomonas solanacearum genes controlling both pathogenicity on tomato and hypersensitivity on tobacco are clustered. *J Bacteriol* **169**, 5626-5632.

Boyle, P. C. & Martin, G. B. (2015). Greasy tactics in the plant-pathogen molecular arms race. *J Exp Bot* **66**, 1607-1616.

Bretz, J. R., Mock, N. M., Charity, J. C., Zeyad, S., Baker, C. J. & Hutcheson, S. W. (2003). A translocated protein tyrosine phosphatase of Pseudomonas syringae pv. tomato DC3000 modulates plant defence response to infection. *Mol Microbiol* **49**, 389-400.

Brion, C., Pflieger, D., Friedrich, A. & Schacherer, J. (2015). Evolution of intraspecific transcriptomic landscapes in yeasts. *Nucleic Acids Res* **43**, 4558-4568.

Brown, J. C., Nelson, J., VanderSluis, B. & other authors (2014). Unraveling the biology of a fungal meningitis pathogen using chemical genetics. *Cell* **159**, 1168-1187.

Brumell, J. H. & Scidmore, M. A. (2007). Manipulation of rab GTPase function by intracellular bacterial pathogens. *Microbiol Mol Biol Rev* **71**, 636-652.

Buchsbaum, R. J. (2007). Rho activation at a glance. *J Cell Sci* **120**, 1149-1152.

Burkinshaw, B. J. & Strynadka, N. C. (2014). Assembly and structure of the T3SS. *Biochim Biophys Acta* **1843**, 1649-1663.

Caldana, C., Li, Y., Leisse, A., Zhang, Y., Bartholomaeus, L., Fernie, A. R., Willmitzer, L. & Giavalisco, P. (2013). Systemic analysis of inducible target of rapamycin mutants reveal a general metabolic switch controlling growth in Arabidopsis thaliana. *Plant J* **73**, 897-909.

Cardenas, M. E., Cutler, N. S., Lorenz, M. C., Di Como, C. J. & Heitman, J. (1999). The TOR signaling cascade regulates gene expression in response to nutrients. *Genes Dev* **13**, 3271-3279.

Coaker, G., Falick, A. & Staskawicz, B. (2005). Activation of a phytopathogenic bacterial effector protein by a eukaryotic cyclophilin. *Science* **308**, 548-550.

Coll, N. S., Epple, P. & Dangl, J. L. (2011). Programmed cell death in the plant immune system. *Cell Death Differ* **18**, 1247-1256.

Coll, N. S. & Valls, M. (2013). Current knowledge on the Ralstonia solanacearum type III secretion system. *Microb Biotechnol* **6**, 614-620.

Conrad, M., Schothorst, J., Kankipati, H. N., Van Zeebroeck, G., Rubio-Texeira, M. & Thevelein, J. M. (2014). Nutrient sensing and signaling in the yeast Saccharomyces cerevisiae. *FEMS Microbiol Rev* **38**, 254-299.

Conway, M. K., Grunwald, D. & Heideman, W. (2012). Glucose, nitrogen, and phosphate repletion in Saccharomyces cerevisiae: common transcriptional responses to different nutrient signals. *G3 (Bethesda)* **2**, 1003-1017.

Costanzo, M., Baryshnikova, A., Bellay, J. & other authors (2010). The genetic landscape of a cell. *Science* **327**, 425-431.

Crespo, J. L. (2012). BiP links TOR signaling to ER stress in Chlamydomonas. *Plant Signal Behav* **7**, 273-275.

Croise, P., Estay-Ahumada, C., Gasman, S. & Ory, S. (2014). Rho GTPases, phosphoinositides, and actin: a tripartite framework for efficient vesicular trafficking. *Small GTPases* **5**, e29469.

Cullen, P. J. & Sprague, G. F., Jr. (2012). The regulation of filamentous growth in yeast. *Genetics* **190**, 23-49.

Cunnac, S., Boucher, C. & Genin, S. (2004). Characterization of the cis-acting regulatory element controlling HrpB-mediated activation of the type III secretion system and effector genes in Ralstonia solanacearum. *J Bacteriol* **186**, 2309-2318.

Curak, J., Rohde, J. & Stagljar, I. (2009). Yeast as a tool to study bacterial effectors. *Curr Opin Microbiol* **12**, 18-23.

Charro, N. & Mota, L. J. (2015). Approaches targeting the type III secretion system to treat or prevent bacterial infections. *Expert Opin Drug Discov* **10**, 373-387.

Chatterjee, S., Chaudhury, S., McShan, A. C., Kaur, K. & De Guzman, R. N. (2013). Structure and biophysics of type III secretion in bacteria. *Biochemistry* **52**, 2508-2517.

Chauvin, C., Koka, V., Nouschi, A. & other authors (2014). Ribosomal protein S6 kinase activity controls the ribosome biogenesis transcriptional program. *Oncogene* **33**, 474-483.

Chen, R. E. & Thorner, J. (2007). Function and regulation in MAPK signaling pathways: lessons learned from the yeast Saccharomyces cerevisiae. *Biochim Biophys Acta* **1773**, 1311-1340.

Cheong, H. & Klionsky, D. J. (2008). Biochemical methods to monitor autophagy-related processes in yeast. *Methods Enzymol* **451**, 1-26.

Chong, Y. T., Koh, J. L., Friesen, H., Duffy, K., Cox, M. J., Moses, A., Moffat, J., Boone, C. & Andrews, B. J. (2015). Yeast Proteome Dynamics from Single Cell Imaging and Automated Analysis. *Cell* **161**, 1413-1424.

de Groot, M. J., Daran-Lapujade, P., van Breukelen, B., Knijnenburg, T. A., de Hulster, E. A., Reinders, M. J., Pronk, J. T., Heck, A. J. & Slijper, M. (2007). Quantitative proteomics and transcriptomics of anaerobic and aerobic yeast cultures reveals post-transcriptional regulation of key cellular processes. *Microbiology* **153**, 3864-3878.

de Hoon, M. J., Imoto, S., Nolan, J. & Miyano, S. (2004). Open source clustering software. *Bioinformatics* **20**, 1453-1454.

de Lange, O., Schreiber, T., Schandry, N., Radeck, J., Braun, K. H., Koszinowski, J., Heuer, H., Strauss, A. & Lahaye, T. (2013). Breaking the DNA-binding code of Ralstonia solanacearum TAL effectors provides new possibilities to generate plant resistance genes against bacterial wilt disease. *New Phytol* **199**, 773-786.

de Nadal, E., Clotet, J., Posas, F., Serrano, R., Gomez, N. & Arino, J. (1998). The yeast halotolerance determinant Hal3p is an inhibitory subunit of the Ppz1p Ser/Thr protein phosphatase. *Proc Natl Acad Sci U S A* **95**, 7357-7362.

de Souza Santos, M. & Orth, K. (2015). Subversion of the cytoskeleton by intracellular bacteria: lessons from Listeria, Salmonella and Vibrio. *Cell Microbiol* **17**, 164-173.

Dean, P. (2011). Functional domains and motifs of bacterial type III effector proteins and their roles in infection. *FEMS Microbiol Rev* **35**, 1100-1125.

Degrave, A., Siamer, S., Boureau, T. & Barny, M. A. (2015). The AvrE superfamily: ancestral type III effectors involved in suppression of pathogen-associated molecular pattern-triggered immunity. *Mol Plant Pathol*.

Deprost, D., Yao, L., Sormani, R., Moreau, M., Leterreux, G., Nicolai, M., Bedu, M., Robaglia, C. & Meyer, C. (2007). The Arabidopsis TOR kinase links plant growth, yield, stress resistance and mRNA translation. *EMBO Rep* **8**, 864-870.

Deslandes, L., Olivier, J., Peeters, N., Feng, D. X., Khounlotham, M., Boucher, C., Somssich, I., Genin, S. & Marco, Y. (2003). Physical interaction between RRS1-R, a protein conferring resistance to bacterial wilt, and PopP2, a type III effector targeted to the plant nucleus. *Proc Natl Acad Sci U S A* **100**, 8024-8029.

Deslandes, L. & Rivas, S. (2012). Catch me if you can: bacterial effectors and plant targets. *Trends Plant Sci* **17**, 644-655.

Deslandes, L. & Genin, S. (2014). Opening the Ralstonia solanacearum type III effector tool box: insights into host cell subversion mechanisms. *Curr Opin Plant Biol* **20**, 110-117.

Dilova, I., Chen, C. Y. & Powers, T. (2002). Mks1 in concert with TOR signaling negatively regulates RTG target gene expression in S. cerevisiae. *Curr Biol* **12**, 389-395.

Dokudovskaya, S. & Rout, M. P. (2015). SEA you later alli-GATOR - a dynamic regulator of the TORC1 stress response pathway. *J Cell Sci* **128**, 2219-2228.

Dong, N., Zhu, Y., Lu, Q., Hu, L., Zheng, Y. & Shao, F. (2012). Structurally distinct bacterial TBC-like GAPs link Arf GTPase to Rab1 inactivation to counteract host defenses. *Cell* **150**, 1029-1041.

Du, W., Halova, L., Kirkham, S., Atkin, J. & Petersen, J. (2012). TORC2 and the AGC kinase Gad8 regulate phosphorylation of the ribosomal protein S6 in fission yeast. *Biol Open* **1**, 884-888.

Duina, A. A., Miller, M. E. & Keeney, J. B. (2014). Budding yeast for budding geneticists: a primer on the Saccharomyces cerevisiae model system. *Genetics* **197**, 33-48.

Duro, E. & Marston, A. L. (2015). From equator to pole: splitting chromosomes in mitosis and meiosis. *Genes Dev* **29**, 109-122.

Engel, J. & Balachandran, P. (2009). Role of Pseudomonas aeruginosa type III effectors in disease. *Curr Opin Microbiol* **12**, 61-66.

Espinosa, A., Guo, M., Tam, V. C., Fu, Z. Q. & Alfano, J. R. (2003). The Pseudomonas syringae type III-secreted protein HopPtoD2 possesses protein tyrosine phosphatase activity and suppresses programmed cell death in plants. *Mol Microbiol* **49**, 377-387.

Evans, D. R. & Stark, M. J. (1997). Mutations in the Saccharomyces cerevisiae type 2A protein phosphatase catalytic subunit reveal roles in cell wall integrity, actin cytoskeleton organization and mitosis. *Genetics* **145**, 227-241.

Fernandez-Pinar, P., Aleman, A., Sondek, J., Dohlman, H. G., Molina, M. & Martin, H. (2012). The Salmonella Typhimurium effector SteC inhibits Cdc42-mediated signaling through binding to the exchange factor Cdc24 in Saccharomyces cerevisiae. *Mol Biol Cell* **23**, 4430-4443.

Ferrando, A., Kron, S. J., Rios, G., Fink, G. R. & Serrano, R. (1995). Regulation of cation transport in Saccharomyces cerevisiae by the salt tolerance gene HAL3. *Mol Cell Biol* **15**, 5470-5481.

Finck-Barbancon, V., Goranson, J., Zhu, L., Sawa, T., Wiener-Kronish, J. P., Fleiszig, S. M., Wu, C., Mende-Mueller, L. & Frank, D. W. (1997). ExoU expression by Pseudomonas aeruginosa correlates with acute cytotoxicity and epithelial injury. *Mol Microbiol* **25**, 547-557.

Finck-Barbancon, V. & Frank, D. W. (2001). Multiple domains are required for the toxic activity of Pseudomonas aeruginosa ExoU. *J Bacteriol* **183**, 4330-4344.

Fraiture, M. & Brunner, F. (2014). Killing two birds with one stone: trans-kingdom suppression of PAMP/MAMP-induced immunity by T3E from enteropathogenic bacteria. *Front Microbiol* **5**, 320.

Fujiwara, S., Ohnishi, K., Kitagawa, T., Popa, C., Kawazoe, T., Valls, M., Genin, S., Nakamura, K., Kuramitsu, Y., Tanaka, N. & Tabuchi, M. (2015). RipAY, a plant pathogen effector protein exhibits robust γ-glutamyl cyclotransferase activity when stimulated by eukaryotic thioredoxins. *In press.*

Furukawa, K. & Hohmann, S. (2013). Synthetic biology: lessons from engineering yeast MAPK signalling pathways. *Mol Microbiol* **88**, 5-19.

Galan, J. E. (2009). Common themes in the design and function of bacterial effectors. *Cell Host Microbe* **5**, 571-579.

Gari, E., Piedrafita, L., Aldea, M. & Herrero, E. (1997). A set of vectors with a tetracycline-regulatable promoter system for modulated gene expression in Saccharomyces cerevisiae. *Yeast* **13**, 837-848.

Garrity-Ryan, L., Shafikhani, S., Balachandran, P. & other authors (2004). The ADP ribosyltransferase domain of Pseudomonas aeruginosa ExoT contributes to its biological activities. *Infect Immun* **72**, 546-558.

Gasch, A. P., Spellman, P. T., Kao, C. M., Carmel-Harel, O., Eisen, M. B., Storz, G., Botstein, D. & Brown, P. O. (2000). Genomic expression programs in the response of yeast cells to environmental changes. *Mol Biol Cell* **11**, 4241-4257.

Gelperin, D. M., White, M. A., Wilkinson, M. L. & other authors (2005). Biochemical and genetic analysis of the yeast proteome with a movable ORF collection. *Genes Dev* **19**, 2816-2826.

Giaever, G. & Nislow, C. (2014). The yeast deletion collection: a decade of functional genomics. *Genetics* **197**, 451-465.

Gietz, D., St Jean, A., Woods, R. A. & Schiestl, R. H. (1992). Improved method for high efficiency transformation of intact yeast cells. *Nucleic Acids Res* **20**, 1425.

Gietz, R. D. & Sugino, A. (1988). New yeast-Escherichia coli shuttle vectors constructed with in vitro mutagenized yeast genes lacking six-base pair restriction sites. *Gene* **74**, 527-534.

Giuraniuc, C. V., MacPherson, M. & Saka, Y. (2013). Gateway vectors for efficient artificial gene assembly in vitro and expression in yeast Saccharomyces cerevisiae. *PLoS One* **8**, e64419.

Godard, P., Urrestarazu, A., Vissers, S., Kontos, K., Bontempi, G., van Helden, J. & Andre, B. (2007). Effect of 21 different nitrogen sources on global gene expression in the yeast Saccharomyces cerevisiae. *Mol Cell Biol* **27**, 3065-3086.

Goicoechea, S. M., Awadia, S. & Garcia-Mata, R. (2014). I'm coming to GEF you: Regulation of RhoGEFs during cell migration. *Cell Adh Migr* **8**, 535-549.

Gonzalez, A., Ruiz, A., Casamayor, A. & Arino, J. (2009). Normal function of the yeast TOR pathway requires the type 2C protein phosphatase Ptc1. *Mol Cell Biol* **29**, 2876-2888.

Gonzalez, A., Casado, C., Arino, J. & Casamayor, A. (2013). Ptc6 is required for proper rapamycin-induced down-regulation of the genes coding for ribosomal and rRNA processing proteins in S. cerevisiae. *PLoS One* **8**, e64470.

Gonzalez, A., Shimobayashi, M., Eisenberg, T., Merle, D. A., Pendl, T., Hall, M. N. & Moustafa, T. (2015). TORC1 promotes phosphorylation of ribosomal protein S6 via the AGC kinase Ypk3 in Saccharomyces cerevisiae. *PLoS One* **10**, e0120250.

Gordon, E. B., Hart, G. T., Tran, T. M. & other authors (2015). Inhibiting the Mammalian target of rapamycin blocks the development of experimental cerebral malaria. *MBio* **6**.

Gossen, M. & Bujard, H. (1992). Tight control of gene expression in mammalian cells by tetracycline-responsive promoters. *Proc Natl Acad Sci U S A* **89**, 5547-5551.

Gossen, M., Freundlieb, S., Bender, G., Muller, G., Hillen, W. & Bujard, H. (1995). Transcriptional activation by tetracyclines in mammalian cells. *Science* **268**, 1766-1769.

Grant, S. R., Fisher, E. J., Chang, J. H., Mole, B. M. & Dangl, J. L. (2006). Subterfuge and manipulation: type III effector proteins of phytopathogenic bacteria. *Annu Rev Microbiol* **60**, 425-449.

Ham, H., Sreelatha, A. & Orth, K. (2011). Manipulation of host membranes by bacterial effectors. *Nat Rev Microbiol* **9**, 635-646.

Ham, J. H., Majerczak, D., Ewert, S., Sreerekha, M. V., Mackey, D. & Coplin, D. (2008). WtsE, an AvrE-family type III effector protein of Pantoea stewartii subsp. stewartii, causes cell death in non-host plants. *Mol Plant Pathol* **9**, 633-643.

Ham, J. H., Majerczak, D. R., Nomura, K., Mecey, C., Uribe, F., He, S. Y., Mackey, D. & Coplin, D. L. (2009). Multiple activities of the plant pathogen type III effector proteins WtsE and AvrE require WxxxE motifs. *Mol Plant Microbe Interact* **22**, 703-712.

Hardwick, J. S., Kuruvilla, F. G., Tong, J. K., Shamji, A. F. & Schreiber, S. L. (1999). Rapamycin-modulated transcription defines the subset of nutrient-sensitive signaling pathways directly controlled by the Tor proteins. *Proc Natl Acad Sci U S A* **96**, 14866-14870.

Hardwidge, P. R., Rodriguez-Escudero, I., Goode, D., Donohoe, S., Eng, J., Goodlett, D. R., Aebersold, R. & Finlay, B. B. (2004). Proteomic analysis of the intestinal epithelial cell response to enteropathogenic Escherichia coli. *J Biol Chem* **279**, 20127-20136.

Hardwidge, P. R., Deng, W., Vallance, B. A., Rodriguez-Escudero, I., Cid, V. J., Molina, M. & Finlay, B. B. (2005). Modulation of host cytoskeleton function by the enteropathogenic Escherichia coli and Citrobacter rodentium effector protein EspG. *Infect Immun* **73**, 2586-2594.

Hardwidge, P. R., Donohoe, S., Aebersold, R. & Finlay, B. B. (2006). Proteomic analysis of the binding partners to enteropathogenic Escherichia coli virulence proteins expressed in Saccharomyces cerevisiae. *Proteomics* **6**, 2174-2179.

Harkin, D. P., Bean, J. M., Miklos, D. & other authors (1999). Induction of GADD45 and JNK/SAPK-dependent apoptosis following inducible expression of BRCA1. *Cell* **97**, 575-586.

Hauser, A. R., Kang, P. J. & Engel, J. N. (1998). PepA, a secreted protein of Pseudomonas aeruginosa, is necessary for cytotoxicity and virulence. *Mol Microbiol* **27**, 807-818.

Hegde, P., Qi, R., Abernathy, K. & other authors (2000). A concise guide to cDNA microarray analysis. *Biotechniques* **29**, 548-550, 552-544, 556 passim.

Hirasaki, M., Horiguchi, M., Numamoto, M., Sugiyama, M., Kaneko, Y., Nogi, Y. & Harashima, S. (2011). Saccharomyces cerevisiae protein phosphatase Ppz1 and protein kinases Sat4 and Hal5 are involved in the control of subcellular localization of Gln3 by likely regulating its phosphorylation state. *J Biosci Bioeng* **111**, 249-254.

Hofling, S., Scharnert, J., Cromme, C., Bertrand, J., Pap, T., Schmidt, M. A. & Ruter, C. (2014). Manipulation of pro-inflammatory cytokine production by the bacterial cell-penetrating effector protein YopM is independent of its interaction with host cell kinases RSK1 and PRK2. *Virulence* **5**, 761-771.

Holk, A., Rietz, S., Zahn, M., Quader, H. & Scherer, G. F. (2002). Molecular identification of cytosolic, patatin-related phospholipases A from Arabidopsis with potential functions in plant signal transduction. *Plant Physiol* **130**, 90-101.

Homma, T., Iwahashi, H. & Komatsu, Y. (2003). Yeast gene expression during growth at low temperature. *Cryobiology* **46**, 230-237.

Howson, R., Huh, W. K., Ghaemmaghami, S. & other authors (2005). Construction, verification and experimental use of two epitope-tagged collections of budding yeast strains. *Comp Funct Genomics* **6**, 2-16.

Huang, J., Lesser, C. F. & Lory, S. (2008). The essential role of the CopN protein in Chlamydia pneumoniae intracellular growth. *Nature* **456**, 112-115.

Huang, Z., Sutton, S. E., Wallenfang, A. J., Orchard, R. C., Wu, X., Feng, Y., Chai, J. & Alto, N. M. (2009). Structural insights into host GTPase isoform selection by a family of bacterial GEF mimics. *Nat Struct Mol Biol* **16**, 853-860.

Huber, A., French, S. L., Tekotte, H. & other authors (2011). Sch9 regulates ribosome biogenesis via Stb3, Dot6 and Tod6 and the histone deacetylase complex RPD3L. *EMBO J* **30**, 3052-3064.

Huber, P., Bouillot, S., Elsen, S. & Attree, I. (2014). Sequential inactivation of Rho GTPases and Lim kinase by Pseudomonas aeruginosa toxins ExoS and ExoT leads to endothelial monolayer breakdown. *Cell Mol Life Sci* **71**, 1927-1941.

Hughes Hallett, J. E., Luo, X. & Capaldi, A. P. (2014). State transitions in the TORC1 signaling pathway and information processing in Saccharomyces cerevisiae. *Genetics* **198**, 773-786.

Hughes, T. R. (2002). Yeast and drug discovery. *Funct Integr Genomics* **2**, 199-211.

Huh, W. K., Falvo, J. V., Gerke, L. C., Carroll, A. S., Howson, R. W., Weissman, J. S. & O'Shea, E. K. (2003). Global analysis of protein localization in budding yeast. *Nature* **425**, 686-691.

Iden, S. & Collard, J. G. (2008). Crosstalk between small GTPases and polarity proteins in cell polarization. *Nat Rev Mol Cell Biol* **9**, 846-859.

Jaffe, A. B. & Hall, A. (2005). Rho GTPases: biochemistry and biology. *Annu Rev Cell Dev Biol* **21**, 247-269.

Jamir, Y., Guo, M., Oh, H. S., Petnicki-Ocwieja, T., Chen, S., Tang, X., Dickman, M. B., Collmer, A. & Alfano, J. R. (2004). Identification of Pseudomonas syringae type III

effectors that can suppress programmed cell death in plants and yeast. *Plant J* **37**, 554-565.

Jelenska, J., Kang, Y. & Greenberg, J. T. (2014). Plant pathogenic bacteria target the actin microfilament network involved in the trafficking of disease defense components. *Bioarchitecture* **4**, 149-153.

Jepson, M. A., Pellegrin, S., Peto, L., Banbury, D. N., Leard, A. D., Mellor, H. & Kenny, B. (2003). Synergistic roles for the Map and Tir effector molecules in mediating uptake of enteropathogenic Escherichia coli (EPEC) into non-phagocytic cells. *Cell Microbiol* **5**, 773-783.

Jiang, Y. & Broach, J. R. (1999). Tor proteins and protein phosphatase 2A reciprocally regulate Tap42 in controlling cell growth in yeast. *EMBO J* **18**, 2782-2792.

Johnson, D. I. (1999). Cdc42: An essential Rho-type GTPase controlling eukaryotic cell polarity. *Microbiol Mol Biol Rev* **63**, 54-105.

Jones, J. D. & Dangl, J. L. (2006). The plant immune system. *Nature* **444**, 323-329.

Kamada, Y., Funakoshi, T., Shintani, T., Nagano, K., Ohsumi, M. & Ohsumi, Y. (2000). Tor-mediated induction of autophagy via an Apg1 protein kinase complex. *J Cell Biol* **150**, 1507-1513.

Kamada, Y., Yoshino, K., Kondo, C., Kawamata, T., Oshiro, N., Yonezawa, K. & Ohsumi, Y. (2010). Tor directly controls the Atg1 kinase complex to regulate autophagy. *Mol Cell Biol* **30**, 1049-1058.

Karpinski, S., Szechynska-Hebda, M., Wituszynska, W. & Burdiak, P. (2013). Light acclimation, retrograde signalling, cell death and immune defences in plants. *Plant Cell Environ* **36**, 736-744.

Kawano, Y., Kaneko-Kawano, T. & Shimamoto, K. (2014). Rho family GTPase-dependent immunity in plants and animals. *Front Plant Sci* **5**, 522.

Kay, S., Hahn, S., Marois, E., Hause, G. & Bonas, U. (2007). A bacterial effector acts as a plant transcription factor and induces a cell size regulator. *Science* **318**, 648-651.

Kenny, B. & Valdivia, R. (2009). Host-microbe interactions: bacteria. *Curr Opin Microbiol* **12**, 1-3.

Khachatoorian, C., Ramirez, R. A., Hernandez, F., Serna, R. & Kwok, E. Y. (2015). Overexpressed Arabidopsis Annexin4 accumulates in inclusion body-like structures. *Acta Histochem* **117**, 279-287.

Kim, Y., Tsuda, K., Igarashi, D., Hillmer, R. A., Sakakibara, H., Myers, C. L. & Katagiri, F. (2014). Mechanisms underlying robustness and tunability in a plant immune signaling network. *Cell Host Microbe* **15**, 84-94.

Koh, J. L., Chong, Y. T., Friesen, H., Moses, A., Boone, C., Andrews, B. J. & Moffat, J. (2015). CYCLoPs: A Comprehensive Database Constructed from Automated Analysis of Protein Abundance and Subcellular Localization Patterns in Saccharomyces cerevisiae. *G3 (Bethesda)* **5**, 1223-1232.

Kramer, R. W., Slagowski, N. L., Eze, N. A., Giddings, K. S., Morrison, M. F., Siggers, K. A., Starnbach, M. N. & Lesser, C. F. (2007). Yeast functional genomic screens lead to identification of a role for a bacterial effector in innate immunity regulation. *PLoS Pathog* **3**, e21.

Kunz, J., Schneider, U., Howald, I., Schmidt, A. & Hall, M. N. (2000). HEAT repeats mediate plasma membrane localization of Tor2p in yeast. *J Biol Chem* **275**, 37011-37020.

Kvitko, B. H., Park, D. H., Velasquez, A. C., Wei, C. F., Russell, A. B., Martin, G. B., Schneider, D. J. & Collmer, A. (2009). Deletions in the repertoire of Pseudomonas syringae pv. tomato DC3000 type III secretion effector genes reveal functional overlap among effectors. *PLoS Pathog* **5**, e1000388.

La Camera, S., Balague, C., Gobel, C., Geoffroy, P., Legrand, M., Feussner, I., Roby, D. & Heitz, T. (2009). The Arabidopsis patatin-like protein 2 (PLP2) plays an essential role in cell death execution and differentially affects biosynthesis of oxylipins and resistance to pathogens. *Mol Plant Microbe Interact* **22**, 469-481.

Langmead, B. & Salzberg, S. L. (2012). Fast gapped-read alignment with Bowtie 2. *Nat Methods* **9**, 357-359.

LaRock, C. N. & Cookson, B. T. (2012). The Yersinia virulence effector YopM binds caspase-1 to arrest inflammasome assembly and processing. *Cell Host Microbe* **12**, 799-805.

Lemaitre, B. & Girardin, S. E. (2013). Translation inhibition and metabolic stress pathways in the host response to bacterial pathogens. *Nat Rev Microbiol* **11**, 365-369.

Lemichez, E. & Aktories, K. (2013). Hijacking of Rho GTPases during bacterial infection. *Exp Cell Res* **319**, 2329-2336.

Lesser, C. F. & Miller, S. I. (2001). Expression of microbial virulence proteins in Saccharomyces cerevisiae models mammalian infection. *Embo J* **20**, 1840-1849.

Levin, D. E. (2011). Regulation of cell wall biogenesis in Saccharomyces cerevisiae: the cell wall integrity signaling pathway. *Genetics* **189**, 1145-1175.

Lewis, J. D., Guttman, D. S. & Desveaux, D. (2009). The targeting of plant cellular systems by injected type III effector proteins. *Semin Cell Dev Biol* **20**, 1055-1063.

Li, H., Xu, H., Zhou, Y., Zhang, J., Long, C., Li, S., Chen, S., Zhou, J. M. & Shao, F. (2007). The phosphothreonine lyase activity of a bacterial type III effector family. *Science* **315**, 1000-1003.

Li, L., Atef, A., Piatek, A. & other authors (2013). Characterization and DNA-binding specificities of Ralstonia TAL-like effectors. *Mol Plant* **6**, 1318-1330.

Lindeberg, M., Cunnac, S. & Collmer, A. (2012). Pseudomonas syringae type III effector repertoires: last words in endless arguments. *Trends Microbiol* **20**, 199-208.

Loewith, R. & Hall, M. N. (2011). Target of rapamycin (TOR) in nutrient signaling and growth control. *Genetics* **189**, 1177-1201.

Lopez-Solanilla, E., Bronstein, P. A., Schneider, A. R. & Collmer, A. (2004). HopPtoN is a Pseudomonas syringae Hrp (type III secretion system) cysteine protease effector that suppresses pathogen-induced necrosis associated with both compatible and incompatible plant interactions. *Mol Microbiol* **54**, 353-365.

Ly, K. T. & Casanova, J. E. (2007). Mechanisms of Salmonella entry into host cells. *Cell Microbiol* **9**, 2103-2111.

Ma, K. W., Jiang, S., Hawara, E., Lee, D., Pan, S., Coaker, G., Song, J. & Ma, W. (2015). Two serine residues in Pseudomonas syringae effector HopZ1a are required for acetyltransferase activity and association with the host co-factor. *New Phytol*.

MacGurn, J. A., Hsu, P. C., Smolka, M. B. & Emr, S. D. (2011). TORC1 regulates endocytosis via Npr1-mediated phosphoinhibition of a ubiquitin ligase adaptor. *Cell* **147**, 1104-1117.

Mack, N. A. & Georgiou, M. (2014). The interdependence of the Rho GTPases and apicobasal cell polarity. *Small GTPases* **5**, 10.

Macho, A. P. & Zipfel, C. (2015). Targeting of plant pattern recognition receptor-triggered immunity by bacterial type-III secretion system effectors. *Curr Opin Microbiol* **23**, 14-22.

Mansfield, J., Genin, S., Magori, S. & other authors (2012). Top 10 plant pathogenic bacteria in molecular plant pathology. *Mol Plant Pathol* **13**, 614-629.

Marin, M. & Ott, T. (2014). Intrinsic disorder in plant proteins and phytopathogenic bacterial effectors. *Chem Rev* **114**, 6912-6932.

Marini, A. M., Soussi-Boudekou, S., Vissers, S. & Andre, B. (1997). A family of ammonium transporters in Saccharomyces cerevisiae. *Mol Cell Biol* **17**, 4282-4293.

Martin, H., Rodriguez-Pachon, J. M., Ruiz, C., Nombela, C. & Molina, M. (2000). Regulatory mechanisms for modulation of signaling through the cell integrity Slt2-mediated pathway in Saccharomyces cerevisiae. *J Biol Chem* **275**, 1511-1519.

Matsuzawa, T., Kuwae, A., Yoshida, S., Sasakawa, C. & Abe, A. (2004). Enteropathogenic Escherichia coli activates the RhoA signaling pathway via the stimulation of GEF-H1. *EMBO J* **23**, 3570-3582.

McDonald, C., Vacratsis, P. O., Bliska, J. B. & Dixon, J. E. (2003). The yersinia virulence factor YopM forms a novel protein complex with two cellular kinases. *J Biol Chem* **278**, 18514-18523.

Meitinger, F., Khmelinskii, A., Morlot, S. & other authors (2014). A memory system of negative polarity cues prevents replicative aging. *Cell* **159**, 1056-1069.

Mishra, M., Huang, J. & Balasubramanian, M. K. (2014). The yeast actin cytoskeleton. *FEMS Microbiol Rev* **38**, 213-227.

Monteiro, F., Sole, M., van Dijk, I. & Valls, M. (2012). A chromosomal insertion toolbox for promoter probing, mutant complementation, and pathogenicity studies in Ralstonia solanacearum. *Mol Plant Microbe Interact* **25**, 557-568.

Mori, K. (2009). Signalling pathways in the unfolded protein response: development from yeast to mammals. *J Biochem* **146**, 743-750.

Mouchlis, V. D., Bucher, D., McCammon, J. A. & Dennis, E. A. (2015). Membranes serve as allosteric activators of phospholipase A2, enabling it to extract, bind, and hydrolyze phospholipid substrates. *Proc Natl Acad Sci U S A* **112**, E516-525.

Mukaihara, T., Tamura, N. & Iwabuchi, M. (2010). Genome-wide identification of a large repertoire of Ralstonia solanacearum type III effector proteins by a new functional screen. *Mol Plant Microbe Interact* **23**, 251-262.

Munkvold, K. R., Martin, M. E., Bronstein, P. A. & Collmer, A. (2008). A survey of the Pseudomonas syringae pv. tomato DC3000 type III secretion system effector repertoire reveals several effectors that are deleterious when expressed in Saccharomyces cerevisiae. *Mol Plant Microbe Interact* **21**, 490-502.

Munkvold, K. R., Russell, A. B., Kvitko, B. H. & Collmer, A. (2009). Pseudomonas syringae pv. tomato DC3000 type III effector HopAA1-1 functions redundantly with chlorosis-promoting factor PSPTO4723 to produce bacterial speck lesions in host tomato. *Mol Plant Microbe Interact* **22**, 1341-1355.

Munoz, I., Simon, E., Casals, N., Clotet, J. & Arino, J. (2003). Identification of multicopy suppressors of cell cycle arrest at the G1-S transition in Saccharomyces cerevisiae. *Yeast* **20**, 157-169.

Murakami, M., Taketomi, Y., Miki, Y., Sato, H., Hirabayashi, T. & Yamamoto, K. (2011). Recent progress in phospholipase A(2) research: from cells to animals to humans. *Prog Lipid Res* **50**, 152-192.

Myers, A. M., Tzagoloff, A., Kinney, D. M. & Lusty, C. J. (1986). Yeast shuttle and integrative vectors with multiple cloning sites suitable for construction of lacZ fusions. *Gene* **45**, 299-310.

Na, H. N., Yoo, Y. H., Yoon, C. N. & Lee, J. S. (2015). Unbiased Proteomic Profiling Strategy for Discovery of Bacterial Effector Proteins Reveals that Salmonella Protein PheA Is a Host Cell Cycle Regulator. *Chem Biol* **22**, 453-459.

Nejedlik, L., Pierfelice, T. & Geiser, J. R. (2004). Actin distribution is disrupted upon expression of Yersinia YopO/YpkA in yeast. *Yeast* **21**, 759-768.

Niemann, G. S., Brown, R. N., Gustin, J. K. & other authors (2011). Discovery of novel secreted virulence factors from Salmonella enterica serovar Typhimurium by proteomic analysis of culture supernatants. *Infect Immun* **79**, 33-43.

Niles, B. J. & Powers, T. (2014). TOR complex 2-Ypk1 signaling regulates actin polarization via reactive oxygen species. *Mol Biol Cell* **25**, 3962-3972.

Nimchuk, Z. L., Fisher, E. J., Desveaux, D., Chang, J. H. & Dangl, J. L. (2007). The HopX (AvrPphE) family of Pseudomonas syringae type III effectors require a catalytic triad and a novel N-terminal domain for function. *Mol Plant Microbe Interact* **20**, 346-357.

Nomura, K., Debroy, S., Lee, Y. H., Pumplin, N., Jones, J. & He, S. Y. (2006). A bacterial virulence protein suppresses host innate immunity to cause plant disease. *Science* **313**, 220-223.

Oh, C. S., Martin, G. B. & Beer, S. V. (2007). DspA/E, a type III effector of Erwinia amylovora, is required for early rapid growth in Nicotiana benthamiana and causes NbSGT1-dependent cell death. *Mol Plant Pathol* **8**, 255-265.

Orchard, R. C. & Alto, N. M. (2012). Mimicking GEFs: a common theme for bacterial pathogens. *Cell Microbiol* **14**, 10-18.

Orth, K., Palmer, L. E., Bao, Z. Q., Stewart, S., Rudolph, A. E., Bliska, J. B. & Dixon, J. E. (1999). Inhibition of the mitogen-activated protein kinase kinase superfamily by a Yersinia effector. *Science* **285**, 1920-1923.

Park, H. O. & Bi, E. (2007). Central roles of small GTPases in the development of cell polarity in yeast and beyond. *Microbiol Mol Biol Rev* **71**, 48-96.

Pathak, R. K., Taj, G., Pandey, D., Arora, S. & Kumar, A. (2013). Modeling of the MAPK machinery activation in response to various abiotic and biotic stresses in plants by a system biology approach. *Bioinformation* **9**, 443-449.

Peeters, N., Carrere, S., Anisimova, M., Plener, L., Cazale, A. C. & Genin, S. (2013). Repertoire, unified nomenclature and evolution of the Type III effector gene set in the Ralstonia solanacearum species complex. *BMC Genomics* **14**, 859.

Phillips, R. M., Six, D. A., Dennis, E. A. & Ghosh, P. (2003). In vivo phospholipase activity of the Pseudomonas aeruginosa cytotoxin ExoU and protection of mammalian cells with phospholipase A2 inhibitors. *J Biol Chem* **278**, 41326-41332.

Pinzon, A., Rodriguez, R. L., Gonzalez, A., Bernal, A. & Restrepo, S. (2011). Targeted metabolic reconstruction: a novel approach for the characterization of plant-pathogen interactions. *Brief Bioinform* **12**, 151-162.

Piotrowski, J. S., Okada, H., Lu, F. & other authors (2015). Plant-derived antifungal agent poacic acid targets beta-1,3-glucan. *Proc Natl Acad Sci U S A* **112**, E1490-1497.

Poh, J., Odendall, C., Spanos, A., Boyle, C., Liu, M., Freemont, P. & Holden, D. W. (2008). SteC is a Salmonella kinase required for SPI-2-dependent F-actin remodelling. *Cell Microbiol* **10**, 20-30.

Popoff, M. R. (2014). Bacterial factors exploit eukaryotic Rho GTPase signaling cascades to promote invasion and proliferation within their host. *Small GTPases* **5**.

Posas, F., Camps, M. & Arino, J. (1995). The PPZ protein phosphatases are important determinants of salt tolerance in yeast cells. *J Biol Chem* **270**, 13036-13041.

Poueymiro, M. & Genin, S. (2009). Secreted proteins from Ralstonia solanacearum: a hundred tricks to kill a plant. *Curr Opin Microbiol* **12**, 44-52.

Poueymiro, M., Cazale, A. C., Francois, J. M., Parrou, J. L., Peeters, N. & Genin, S. (2014). A Ralstonia solanacearum type III effector directs the production of the plant signal metabolite trehalose-6-phosphate. *MBio* **5**.

Prehna, G., Ivanov, M. I., Bliska, J. B. & Stebbins, C. E. (2006). Yersinia virulence depends on mimicry of host Rho-family nucleotide dissociation inhibitors. *Cell* **126**, 869-880.

Pritchard, L. & Birch, P. R. (2014). The zigzag model of plant-microbe interactions: is it time to move on? *Mol Plant Pathol* **15**, 865-870.

Qie, B., Lyu, Z., Lyu, L. & other authors (2015). Sch9 regulates intracellular protein ubiquitination by controlling stress responses. *Redox Biol* **5**, 290-300.

Queralt, E. & Uhlmann, F. (2008). Separase cooperates with Zds1 and Zds2 to activate Cdc14 phosphatase in early anaphase. *J Cell Biol* **182**, 873-883.

Rabin, S. D. & Hauser, A. R. (2003). Pseudomonas aeruginosa ExoU, a toxin transported by the type III secretion system, kills Saccharomyces cerevisiae. *Infect Immun* **71**, 4144-4150.

Radhakrishnan, G. K. & Splitter, G. A. (2012). Modulation of host microtubule dynamics by pathogenic bacteria. *Biomol Concepts* **3**, 571-580.

Ramanadham, S., Ali, T., Ashley, J. W., Bone, R. N., Hancock, W. D. & Lei, X. (2015). Calcium-Independent Phospholipases A2 (iPLA2s) and their Roles in Biological Processes and Diseases. *J Lipid Res*.

Rangel, S. M., Logan, L. K. & Hauser, A. R. (2014). The ADP-ribosyltransferase domain of the effector protein ExoS inhibits phagocytosis of Pseudomonas aeruginosa during pneumonia. *MBio* **5**, e01080-01014.

Reed, A. J. & Hageman, R. H. (1980). Relationship between Nitrate Uptake, Flux, and Reduction and the Accumulation of Reduced Nitrogen in Maize (Zea mays L.): I. GENOTYPIC VARIATION. *Plant Physiol* **66**, 1179-1183.

Ren, M., Venglat, P., Qiu, S. & other authors (2012). Target of rapamycin signaling regulates metabolism, growth, and life span in Arabidopsis. *Plant Cell* **24**, 4850-4874.

Reynolds, A., Lundblad, V., Dorris, D. & Keaveney, M. (2001). Yeast vectors and assays for expression of cloned genes. *Curr Protoc Mol Biol* **Chapter 13**, Unit13 16.

Riese, M. J., Goehring, U. M., Ehrmantraut, M. E., Moss, J., Barbieri, J. T., Aktories, K. & Schmidt, G. (2002). Auto-ADP-ribosylation of Pseudomonas aeruginosa ExoS. *J Biol Chem* **277**, 12082-12088.

Rodriguez-Escudero, I., Hardwidge, P. R., Nombela, C., Cid, V. J., Finlay, B. B. & Molina, M. (2005). Enteropathogenic Escherichia coli type III effectors alter cytoskeletal function and signalling in Saccharomyces cerevisiae. *Microbiology* **151**, 2933-2945.

Rodriguez-Escudero, I., Rotger, R., Cid, V. J. & Molina, M. (2006). Inhibition of Cdc42-dependent signalling in Saccharomyces cerevisiae by phosphatase-dead SigD/SopB from Salmonella typhimurium. *Microbiology* **152**, 3437-3452.

Rodriguez-Escudero, I., Ferrer, N. L., Rotger, R., Cid, V. J. & Molina, M. (2011). Interaction of the Salmonella Typhimurium effector protein SopB with host cell Cdc42 is involved in intracellular replication. *Mol Microbiol* **80**, 1220-1240.

Rodriguez-Pachon, J. M., Martin, H., North, G., Rotger, R., Nombela, C. & Molina, M. (2002). A novel connection between the yeast Cdc42 GTPase and the Slt2-mediated cell integrity pathway identified through the effect of secreted Salmonella GTPase modulators. *J Biol Chem* **277**, 27094-27102.

Rohde, J. R., Breitkreutz, A., Chenal, A., Sansonetti, P. J. & Parsot, C. (2007). Type III secretion effectors of the IpaH family are E3 ubiquitin ligases. *Cell Host Microbe* **1**, 77-83.

Ron, D. & Walter, P. (2007). Signal integration in the endoplasmic reticulum unfolded protein response. *Nat Rev Mol Cell Biol* **8**, 519-529.

Rottner, K., Stradal, T. E. & Wehland, J. (2005). Bacteria-host-cell interactions at the plasma membrane: stories on actin cytoskeleton subversion. *Dev Cell* **9**, 3-17.

Sadok, A. & Marshall, C. J. (2014). Rho GTPases: masters of cell migration. *Small GTPases* **5**, e29710.

Saito, H. (2010). Regulation of cross-talk in yeast MAPK signaling pathways. *Curr Opin Microbiol* **13**, 677-683.

Salanoubat, M., Genin, S., Artiguenave, F. & other authors (2002). Genome sequence of the plant pathogen Ralstonia solanacearum. *Nature* **415**, 497-502.

Saldanha, A. J. (2004). Java Treeview--extensible visualization of microarray data. *Bioinformatics* **20**, 3246-3248.

Salomon, D., Dar, D., Sreeramulu, S. & Sessa, G. (2011). Expression of Xanthomonas campestris pv. vesicatoria type III effectors in yeast affects cell growth and viability. *Mol Plant Microbe Interact* **24**, 305-314.

Salomon, D., Bosis, E., Dar, D., Nachman, I. & Sessa, G. (2012). Expression of Pseudomonas syringae type III effectors in yeast under stress conditions reveals that HopX1 attenuates activation of the high osmolarity glycerol MAP kinase pathway. *Microbiology* **158**, 2859-2869.

Sankar, M., Osmont, K. S., Rolcik, J., Gujas, B., Tarkowska, D., Strnad, M., Xenarios, I. & Hardtke, C. S. (2011). A qualitative continuous model of cellular auxin and brassinosteroid signaling and their crosstalk. *Bioinformatics* **27**, 1404-1412.

Sato, H., Frank, D. W., Hillard, C. J. & other authors (2003). The mechanism of action of the Pseudomonas aeruginosa-encoded type III cytotoxin, ExoU. *EMBO J* **22**, 2959-2969.

Sato, H. & Frank, D. W. (2004). ExoU is a potent intracellular phospholipase. *Mol Microbiol* **53**, 1279-1290.

Sato, H., Feix, J. B. & Frank, D. W. (2006). Identification of superoxide dismutase as a cofactor for the pseudomonas type III toxin, ExoU. *Biochemistry* **45**, 10368-10375.

Sato, H. & Frank, D. W. (2014). Intoxication of host cells by the T3SS phospholipase ExoU: PI(4,5)P2-associated, cytoskeletal collapse and late phase membrane blebbing. *PLoS One* **9**, e103127.

Scholze, H. & Boch, J. (2011). TAL effectors are remote controls for gene activation. *Curr Opin Microbiol* **14**, 47-53.

Selyunin, A. S., Sutton, S. E., Weigele, B. A., Reddick, L. E., Orchard, R. C., Bresson, S. M., Tomchick, D. R. & Alto, N. M. (2011). The assembly of a GTPase-kinase signalling complex by a bacterial catalytic scaffold. *Nature* **469**, 107-111.

Shafikhani, S. H. & Engel, J. (2006). Pseudomonas aeruginosa type III-secreted toxin ExoT inhibits host-cell division by targeting cytokinesis at multiple steps. *Proc Natl Acad Sci U S A* **103**, 15605-15610.

Shao, F., Merritt, P. M., Bao, Z., Innes, R. W. & Dixon, J. E. (2002). A Yersinia effector and a Pseudomonas avirulence protein define a family of cysteine proteases functioning in bacterial pathogenesis. *Cell* **109**, 575-588.

Sherman, F. (2002). Getting started with yeast. *Methods Enzymol* **350**, 3-41.

Shimobayashi, M., Takematsu, H., Eiho, K., Yamane, Y. & Kozutsumi, Y. (2010). Identification of Ypk1 as a novel selective substrate for nitrogen starvation-triggered proteolysis requiring autophagy system and endosomal sorting complex required for transport (ESCRT) machinery components. *J Biol Chem* **285**, 36984-36994.

Shohdy, N., Efe, J. A., Emr, S. D. & Shuman, H. A. (2005). Pathogen effector protein screening in yeast identifies Legionella factors that interfere with membrane trafficking. *Proc Natl Acad Sci U S A* **102**, 4866-4871.

Siamer, S., Patrit, O., Fagard, M., Belgareh-Touze, N. & Barny, M. A. (2011). Expressing the Erwinia amylovora type III effector DspA/E in the yeast Saccharomyces cerevisiae strongly alters cellular trafficking. *FEBS Open Bio* **1**, 23-28.

Siamer, S., Guillas, I., Shimobayashi, M., Kunz, C., Hall, M. N. & Barny, M. A. (2014). Expression of the bacterial type III effector DspA/E in Saccharomyces cerevisiae down-regulates the sphingolipid biosynthetic pathway leading to growth arrest. *J Biol Chem* **289**, 18466-18477.

Siggers, K. A. & Lesser, C. F. (2008). The Yeast Saccharomyces cerevisiae: a versatile model system for the identification and characterization of bacterial virulence proteins. *Cell Host Microbe* **4**, 8-15.

Simon, N. C. & Barbieri, J. T. (2014). Exoenzyme S ADP-ribosylates Rab5 effector sites to uncouple intracellular trafficking. *Infect Immun* **82**, 21-28.

Sisko, J. L., Spaeth, K., Kumar, Y. & Valdivia, R. H. (2006). Multifunctional analysis of Chlamydia-specific genes in a yeast expression system. *Mol Microbiol* **60**, 51-66.

Skrzypek, E., Myers-Morales, T., Whiteheart, S. W. & Straley, S. C. (2003). Application of a Saccharomyces cerevisiae model to study requirements for trafficking of Yersinia pestis YopM in eucaryotic cells. *Infect Immun* **71**, 937-947.

Slagowski, N. L., Kramer, R. W., Morrison, M. F., LaBaer, J. & Lesser, C. F. (2008). A functional genomic yeast screen to identify pathogenic bacterial proteins. *PLoS Pathog* **4**, e9.

Smets, B., Ghillebert, R., De Snijder, P., Binda, M., Swinnen, E., De Virgilio, C. & Winderickx, J. (2010). Life in the midst of scarcity: adaptations to nutrient availability in Saccharomyces cerevisiae. *Curr Genet* **56**, 1-32.

Sole, M., Popa, C., Mith, O., Sohn, K. H., Jones, J. D., Deslandes, L. & Valls, M. (2012). The awr gene family encodes a novel class of Ralstonia solanacearum type III effectors displaying virulence and avirulence activities. *Mol Plant Microbe Interact* **25**, 941-953.

Song, C. & Yang, B. (2010). Mutagenesis of 18 type III effectors reveals virulence function of XopZ(PXO99) in Xanthomonas oryzae pv. oryzae. *Mol Plant Microbe Interact* **23**, 893-902.

Sopko, R., Huang, D., Preston, N. & other authors (2006). Mapping pathways and phenotypes by systematic gene overexpression. *Mol Cell* **21**, 319-330.

Stirling, F. R. & Evans, T. J. (2006). Effects of the type III secreted pseudomonal toxin ExoS in the yeast Saccharomyces cerevisiae. *Microbiology* **152**, 2273-2285.

Stracka, D., Jozefczuk, S., Rudroff, F., Sauer, U. & Hall, M. N. (2014). Nitrogen source activates TOR (target of rapamycin) complex 1 via glutamine and independently of Gtr/Rag proteins. *J Biol Chem* **289**, 25010-25020.

Styles, E., Youn, J. Y., Mattiazzi Usaj, M. & Andrews, B. (2013). Functional genomics in the study of yeast cell polarity: moving in the right direction. *Philos Trans R Soc Lond B Biol Sci* **368**, 20130118.

Su, P. W., Yang, C. H., Yang, J. F., Su, P. Y. & Chuang, L. Y. (2015). Antibacterial Activities and Antibacterial Mechanism of Polygonum cuspidatum Extracts against Nosocomial Drug-Resistant Pathogens. *Molecules* **20**, 11119-11130.

Sun, J., Maresso, A. W., Kim, J. J. & Barbieri, J. T. (2004). How bacterial ADP-ribosylating toxins recognize substrates. *Nat Struct Mol Biol* **11**, 868-876.

Sundaram, V., Petkova, M. I., Pujol-Carrion, N., Boada, J. & de la Torre-Ruiz, M. A. (2015). Tor1, Sch9 and PKA downregulation in quiescence rely on Mtl1 to preserve mitochondrial integrity and cell survival. *Mol Microbiol* **97**, 93-109.

Suter, B., Auerbach, D. & Stagljar, I. (2006). Yeast-based functional genomics and proteomics technologies: the first 15 years and beyond. *Biotechniques* **40**, 625-644.

Tabuchi, M., Audhya, A., Parsons, A. B., Boone, C. & Emr, S. D. (2006). The phosphatidylinositol 4,5-biphosphate and TORC2 binding proteins Slm1 and Slm2 function in sphingolipid regulation. *Mol Cell Biol* **26**, 5861-5875.

Tabuchi, M., Kawai, Y., Nishie-Fujita, M., Akada, R., Izumi, T., Yanatori, I., Miyashita, N., Ouchi, K. & Kishi, F. (2009). Development of a novel functional high-throughput screening system for pathogen effectors in the yeast Saccharomyces cerevisiae. *Biosci Biotechnol Biochem* **73**, 2261-2267.

Tai, S. L., Boer, V. M., Daran-Lapujade, P., Walsh, M. C., de Winde, J. H., Daran, J. M. & Pronk, J. T. (2005). Two-dimensional transcriptome analysis in chemostat cultures. Combinatorial effects of oxygen availability and macronutrient limitation in Saccharomyces cerevisiae. *J Biol Chem* **280**, 437-447.

Tasset, C., Bernoux, M., Jauneau, A., Pouzet, C., Briere, C., Kieffer-Jacquinod, S., Rivas, S., Marco, Y. & Deslandes, L. (2010). Autoacetylation of the Ralstonia solanacearum effector PopP2 targets a lysine residue essential for RRS1-R-mediated immunity in Arabidopsis. *PLoS Pathog* **6**, e1001202.

Tcherkezian, J. & Lamarche-Vane, N. (2007). Current knowledge of the large RhoGAP family of proteins. *Biol Cell* **99**, 67-86.

Teper, D., Burstein, D., Salomon, D., Gershovitz, M., Pupko, T. & Sessa, G. (2015). Identification of novel Xanthomonas euvesicatoria type III effector proteins by a machine-learning approach. *Mol Plant Pathol*.

Thomas, B. J. & Rothstein, R. (1989). Elevated recombination rates in transcriptionally active DNA. *Cell* **56**, 619-630.

Thomma, B. P., Nurnberger, T. & Joosten, M. H. (2011). Of PAMPs and effectors: the blurred PTI-ETI dichotomy. *Plant Cell* **23**, 4-15.

Tong, A. H., Evangelista, M., Parsons, A. B. & other authors (2001). Systematic genetic analysis with ordered arrays of yeast deletion mutants. *Science* **294**, 2364-2368.

Trosky, J. E., Mukherjee, S., Burdette, D. L., Roberts, M., McCarter, L., Siegel, R. M. & Orth, K. (2004). Inhibition of MAPK signaling pathways by VopA from Vibrio parahaemolyticus. *J Biol Chem* **279**, 51953-51957.

Trosky, J. E., Li, Y., Mukherjee, S., Keitany, G., Ball, H. & Orth, K. (2007). VopA inhibits ATP binding by acetylating the catalytic loop of MAPK kinases. *J Biol Chem* **282**, 34299-34305.

Tyson, G. H., Halavaty, A. S., Kim, H., Geissler, B., Agard, M., Satchell, K. J., Cho, W., Anderson, W. F. & Hauser, A. R. (2015). A novel phosphatidylinositol 4,5-bisphosphate binding domain mediates plasma membrane localization of ExoU and other patatin-like phospholipases. *J Biol Chem* **290**, 2919-2937.

Uetz, P., Giot, L., Cagney, G. & other authors (2000). A comprehensive analysis of protein-protein interactions in Saccharomyces cerevisiae. *Nature* **403**, 623-627.

Urban, J., Soulard, A., Huber, A. & other authors (2007). Sch9 is a major target of TORC1 in Saccharomyces cerevisiae. *Mol Cell* **26**, 663-674.

Valdivia, R. H. (2004). Modeling the function of bacterial virulence factors in Saccharomyces cerevisiae. *Eukaryot Cell* **3**, 827-834.

Van Dyke, N., Chanchorn, E. & Van Dyke, M. W. (2013). The Saccharomyces cerevisiae protein Stm1p facilitates ribosome preservation during quiescence. *Biochem Biophys Res Commun* **430**, 745-750.

Van Engelenburg, S. B. & Palmer, A. E. (2008). Quantification of real-time Salmonella effector type III secretion kinetics reveals differential secretion rates for SopE2 and SptP. *Chem Biol* **15**, 619-628.

Voisset, C. & Blondel, M. (2014). [Chemobiology at happy hour: yeast as a model for pharmacological screening]. *Med Sci (Paris)* **30**, 1161-1168.

von Manteuffel, S. R., Dennis, P. B., Pullen, N., Gingras, A. C., Sonenberg, N. & Thomas, G. (1997). The insulin-induced signalling pathway leading to S6 and initiation factor 4E binding protein 1 phosphorylation bifurcates at a rapamycin-sensitive point immediately upstream of p70s6k. *Mol Cell Biol* **17**, 5426-5436.

Von Pawel-Rammingen, U., Telepnev, M. V., Schmidt, G., Aktories, K., Wolf-Watz, H. & Rosqvist, R. (2000). GAP activity of the Yersinia YopE cytotoxin specifically targets the Rho pathway: a mechanism for disruption of actin microfilament structure. *Mol Microbiol* **36**, 737-748.

Williams, S. J., Sohn, K. H., Wan, L. & other authors (2014). Structural basis for assembly and function of a heterodimeric plant immune receptor. *Science* **344**, 299-303.

Winzeler, E. A., Shoemaker, D. D., Astromoff, A. & other authors (1999). Functional characterization of the S. cerevisiae genome by gene deletion and parallel analysis. *Science* **285**, 901-906.

Witowski, S. E., Walker, K. A. & Miller, V. L. (2008). YspM, a newly identified Ysa type III secreted protein of Yersinia enterocolitica. *J Bacteriol* **190**, 7315-7325.

Woolery, A. R., Yu, X., LaBaer, J. & Orth, K. (2014). AMPylation of Rho GTPases subverts multiple host signaling processes. *J Biol Chem* **289**, 32977-32988.

Xie, J. L., Polvi, E. J., Shekhar-Guturja, T. & Cowen, L. E. (2014). Elucidating drug resistance in human fungal pathogens. *Future Microbiol* **9**, 523-542.

Xiong, Y. & Sheen, J. (2012). Rapamycin and glucose-target of rapamycin (TOR) protein signaling in plants. *J Biol Chem* **287**, 2836-2842.

Xiong, Y. & Sheen, J. (2014). The role of target of rapamycin signaling networks in plant growth and metabolism. *Plant Physiol* **164**, 499-512.

Ye, P., Peyser, B. D., Pan, X., Boeke, J. D., Spencer, F. A. & Bader, J. S. (2005). Gene function prediction from congruent synthetic lethal interactions in yeast. *Mol Syst Biol* **1**, 2005 0026.

Yoon, S., Liu, Z., Eyobo, Y. & Orth, K. (2003). Yersinia effector YopJ inhibits yeast MAPK signaling pathways by an evolutionarily conserved mechanism. *J Biol Chem* **278**, 2131-2135.

Zaman, S., Lippman, S. I., Zhao, X. & Broach, J. R. (2008). How Saccharomyces responds to nutrients. *Annu Rev Genet* **42**, 27-81.

Zhou, D. & Galan, J. (2001). Salmonella entry into host cells: the work in concert of type III secreted effector proteins. *Microbes Infect* **3**, 1293-1298.

Zhou, Y. & Zhu, Y. (2015). Diversity of bacterial manipulation of the host ubiquitin pathways. *Cell Microbiol* **17**, 26-34.

Zhu, H., Klemic, J. F., Chang, S. & other authors (2000). Analysis of yeast protein kinases using protein chips. *Nat Genet* **26**, 283-289.

RESUM EN CATALÀ

El patogen vegetal *Ralstonia solanacearum* és l'agent causant del marciment bacterià, una malaltia devastadora amb una àmplia distribució geogràfica i un extens ventall d'hostes que té un enorme impacte econòmic a nivell mundial. Per tal de causar malaltia, *R. solanacearum* injecta un conjunt de proteïnes efectores de tipus III (T3Es) als seus hostes. Tant a *R. solanacearum* com a altres patògens bacterians, pocs T3Es han sigut caracteritzats funcionalment. Utilitzant el llevat com a sistema model, demostrem que l'expressió de la família de T3Es *awr* provoca una inhibició del creixement de les cèl·lules del llevat en diferents graus segons l'efector, éssent AWR5 el que mostra l'efecte més dramàtic. L'expressió de la proteïna AWR5 en llevat resulta en la inhibició del creixement i la reducció de la mida de la cèl·lula, sense aturar el cicle cel·lular o la mort cel·lular. A més, hem demostrat que l'AWR5 és un inhibidor de la via TOR (*target of rapamycin*), un regulador central en eucariotes que integra els estímuls cel·lulars i prioritza creixement o resposta a estrés. L'expressió heteròloga d'*awr5* en llevat causa una inducció de l'autofàgia acoblada a canvis transcriptòmics massius, que recorden a la inhibició de la via TOR per rapamicina o per manca de nitrogen.

La fosfatasa PP2A i la kinasa SCH9 són dos components essencials de la via TOR. L'observació que la deleció de dos components de la forma heterotrimèrica PP2A -*CDC55* i *TPD3*- i la mutació en *SCH9* aboleixen els defectes de creixement en cèl·lules que expressen awr5 indiquen que AWR5 podria exercir la seva funció directa o indirectament mitjançant la inhibició de la via TOR, aigües amunt de PP2A i Sch9. En base als perfils transcripcionals d'AWR2 i AWR4, similars als d'AWR5, especulem que aquests efectors actuarien de forma similar, inhibint la via. També presentem evidència que l'AWR5 té un efecte sobre la via TOR *in planta*, ja que aquest efector causa una reducció en l'activitat nitrat reductasa, regulada per la via TOR. A més a més, la inhibició del creixement bacterià causada pel lliurament d'AWR5 en les cèl·lules hostes també està mediada per TOR. El nostre treball demostra que el llevat és un model molt efectiu per descobrir noves funcions dels T3Es i revela no només un nou mode d'acció per T3Es sinó també una nova diana de virulència que podria estar conservada entre els regnes biològics.

ANNEX

MPMI Vol. 25, No. 7, 2012, pp. 941–953. http://dx.doi.org/10.1094/MPMI-12-11-0321.

e-Xtra*

The *awr* Gene Family Encodes a Novel Class of *Ralstonia solanacearum* Type III Effectors Displaying Virulence and Avirulence Activities

Montserrat Solé,[1] Crina Popa,[1] Oriane Mith,[1] Kee Hoon Sohn,[2] Jonathan D. G. Jones,[2] Laurent Deslandes,[3] and Marc Valls[1]

[1]Dept. Genètica, Universitat de Barcelona, Av. Diagonal 643 Annex, 08028 Barcelona, and Centre de Recerca Agrigenòmica, Edifici CRAG, Campus UAB, 08193 Bellaterra, Catalonia, Spain; [2]The Sainsbury Laboratory, John Innes Centre, Norwich Research Park, Norwich NR4 7UH, U.K.; [3]Laboratoire des Interactions Plantes Micro-organismes, UMR CNRS-INRA 2594/441, 31320 Castanet Tolosan, France

Submitted 23 December 2011. Accepted 4 March 2012.

We present here the characterization of a new gene family, *awr,* found in all sequenced *Ralstonia solanacearum* strains and in other bacterial pathogens. We demonstrate that the five paralogues in strain GMI1000 encode type III-secreted effectors and that deletion of all *awr* genes severely impairs its capacity to multiply in natural host plants. Complementation studies show that the AWR (alanine-tryptophan-arginine tryad) effectors display some functional redundancy, although AWR2 is the major contributor to virulence. In contrast, the strain devoid of all *awr* genes (Δ*awr1-5)* exhibits enhanced pathogenicity on *Arabidopsis* plants. A gain-of-function approach expressing AWR in *Pseudomonas syringae* pv. *tomato* DC3000 proves that this is likely due to effector recognition, because AWR5 and AWR4 restrict growth of this bacterium in *Arabidopsis*. Transient overexpression of AWR in nonhost tobacco species caused macroscopic cell death to varying extents, which, in the case of AWR5, shows characteristics of a typical hypersensitive response. Our work demonstrates that AWR, which show no similarity to any protein with known function, can specify either virulence or avirulence in the interaction of *R. solanacearum* with its plant hosts.

Bacterial pathogens have been extraordinarily useful to characterize the mechanisms of virulence and plant defense. Plant infection and colonization by bacterial pathogens often requires the injection of so-called effector proteins into host cells through the type III secretion system (T3SS) (Buttner and He 2009; Galan and Collmer 1999; Marlovits and Stebbins 2009). This molecular syringe is present in gram-negative bacterial pathogens or mutualists that interact with animals or plants (He et al. 2004; Preston 2007). In phytopathogenic bacteria, a cluster of 20 to 25 hypersensitive response (HR) and pathogenicity (*hrp*) genes encodes the T3SS that is essential for virulence because T3SS-deficient mutants cannot elicit HR or cause disease on resistant or susceptible plants, respectively (Alfano and Collmer 2004).

Bacterial effectors contribute to the establishment or development of disease (Hogenhout et al. 2009; Lewis et al. 2009), although the mechanisms by which effectors function inside plant cells are not fully understood. Type III-secreted effectors (T3E) from phytopathogens of the genera *Pseudomonas* and *Xanthomonas* have been widely studied and shown to interfere with plant signal transduction by acting as proteases, phosphatases, ubiquitin ligases, ribosyltransferases, and phosphothreonine lyases (Dean 2011; Hann et al. 2010; Zhou and Chai 2008).

During coevolution with microbes, plants have developed innate immune mechanisms to counterattack invading pathogens (Cui et al. 2009; Jones and Dangl 2006). Two main layers of defense responses have been described: pathogen-associated molecular pattern (PAMP)-triggered immunity (PTI) and effector-triggered immunity (ETI). PTI consists of a general resistance directed toward invading microbes and is activated upon detection of PAMP molecules via pattern recognition receptors (Segonzac and Zipfel 2011). ETI represents a stronger version of this defense. ETI usually culminates in the elicitation of the plant HR, a localized programmed cell death associated with strong race- or cultivar-specific resistance (Coll et al. 2011; Tsuda and Katagiri 2010). One of the main roles of effectors is the suppression or modulation of PTI or ETI (Block et al. 2008; Lewis et al. 2009; Stavrinides et al. 2008). The amplitude of disease resistance or susceptibility for a specific plant–pathogen interaction thus depends on four variables: i) the PTI plant response, ii) the interference of PTI by bacterial effectors, iii) the ETI, and iv) the capacity of some effectors to suppress ETI (Jones and Dangl 2006). Heterologous expression of bacterial T3E in different pathosystems and characterization of the resulting phenotype can provide important clues to both their function and plant defense mechanisms.

Ralstonia solanacearum is the causal agent of bacterial wilt on more than 200 plant species from 50 botanical families, including economically important crops such as potato, tomato, tobacco, banana, and eggplant (Boucher et al. 1987; Hayward 2000). The bacterium has a strong impact in tropical and subtropical agriculture because of its unusually wide host range, its high persistence and aggressiveness, and the lack of resistant crop varieties (Hong et al. 2005). The sequencing of *R. solanacearum* GMI1000 (Salanoubat et al. 2002) led to the identification of 70 putative T3E (Mukaihara et al. 2010;

Corresponding author: M. Valls; Telephone: +34 93 4021499; Fax: +34 93 4034420; E-mail: marcvalls@ub.edu

*The *e*-Xtra logo stands for "electronic extra" and indicates that three supplementary tables and three supplementary figures are published online.

Poueymiro et al. 2009). The only two *R. solanacearum* effectors that have been attributed a biochemical function thus far are the GALA effectors, which mimic plant E3 ubiquitin ligases (Angot et al. 2006) and the YopJ-like protein PopP2, which functions as acetyltransferase (Tasset et al. 2010). PopP2 was pinpointed as the GMI1000 avirulence (Avr) protein recognized by the RRS1-R resistance (R) protein of the *Arabidopsis thaliana* resistant accession Nd-1 (Deslandes et al. 2003). In addition, AvrA and PopP1 effectors are also known to trigger plant defense responses. AvrA was shown to be an avirulence determinant of various *R. solanacearum* strains in *Nicotiana tabacum* (Carney and Denny 1990; Robertson et al. 2004) and recent reports have also suggested a role in pathogenicity (Macho et al. 2010; Turner et al. 2009). PopP1 was described as a host-specificity factor that behaves as a typical avirulence gene in *Petunia* spp. (Lavie et al. 2002) and that plays a minor contribution to the HR in tobacco plants (Poueymiro et al. 2009).

Among the T3E candidates in *R. solanacearum*, there is a multigenic family called AWR for the alanine-tryptophan-arginine tryad found in a highly conserved region in their primary sequence. AWR are long polypeptides of 1,063 to 1,330 amino acids. Strain GMI1000 contains five *awr* genes (*Rsc2139, Rsp0099, Rsp0846, Rsp0847*, and *Rsp1024*) that we have called here *awr1, awr2, awr3, awr4*, and *awr5*, respectively. Except for *awr1*, these genes are present in all *R. solanacearum* phylotypes (Guidot et al. 2007) and their transcriptional activation requires HrpB, a master regulator of the T3SS (Cunnac et al. 2004a). AWR2 was one of only two T3E whose disruption in GMI1000 showed delayed disease symptom development on tomato, indicating an important role in bacterial pathogenesis (Cunnac et al. 2004a).

In this work, we sought to characterize the contribution of AWR to *R. solanacearum* interactions with plant hosts. Our data indicate that the AWR gene family collectively contributes to bacterial virulence and that some members are recognized in nonhost plants.

RESULTS AND DISCUSSION

AWR: a T3E family conserved in various plant and animal pathogens.

Genomic analysis of the *awr* genes in *R. solanacearum* GMI1000 showed some interesting features: i) four of the *awr* genes (*awr2* to *awr5*) are borne by the megaplasmid whereas *awr1* is located on the chromosome; ii) *awr3* and *awr4* lie side by side and adjacent to the *hrp* gene cluster; iii) *awr2* and *awr5* are placed near alternative codon usage regions, often indicative of genes that have been acquired by lateral gene transfer (Arnold et al. 2003; Guidot et al. 2007); and iv) the chromosomal paralogue *awr1* encodes the only protein whose translocation was not detected in previous studies, although the gene seems functional because it has not accumulated any missense mutations. Pairwise analysis of AWR protein sequences from GMI1000 revealed that they all shared high identity and similarity (19 to 53% and 27 to 62%, respectively). A survey of all available sequences in databases was performed to search for AWR orthologs. These comparisons revealed homologous genes or proteins with varying degrees of similarity in all sequenced strains of *R. solanacearum*, including phylotypes I (GMI1000, RS1000, and OE1-1), II (CFBP2957, IPO1609, Molk2, and UW551), III (CMR15), and IV (PSI07). We confirmed that genes *awr2*, *awr3*, *awr4*, and *awr5* are present in all *R. solanacearum* strains whose genome has been entirely sequenced. AWR2, AWR3, and AWR4 are present even in *R. syzygii*, a related strain included in the *R. solanacearum* phylotype IV. This was in agreement with comparative genomic hybridization analyses of 12 *R. solanacearum* strains representative of all phylotypes, where these four AWR were considered core effector proteins, emphasizing their functional importance (Guidot et al. 2007). In contrast, AWR1 is absent from phylotypes II, III, and IV.

Significant similarities to AWR outside the *R. solanacearum* species were only detected with protein sequences and not at the DNA level. This is not unexpected because DNA sequences among distantly related species may differ considerably whereas protein regions important for the function are conserved. Related proteins were identified in other bacterial plant pathogens or symbionts such as several sequenced *Xanthomonas* strains, two *Acidovorax avenae* strains, and some *Burkholderia* spp. Surprisingly, AWR homologous proteins were also found in the animal pathogen *Burkholderia pseudomallei* (Supplementary Table S1). Interestingly enough, among AWR homologues in *Xanthomonas oryzae* pv. *oryzae* is XopZ (named secXoO here), which was recently shown to be involved in virulence and inhibition of basal defense (Song and Yang 2010). However, this protein is quite divergent from those of *R. solanacearum* and is more related to *Pseudomonas syringae* HopAS1, not considered in our studies because it did not appear as a BLAST result of AWR. To identify the most conserved regions, all proteins that showed a significant similarity to AWR (*e* value < 0.01 with a sequence coverage ≥30% or sequence identity ≥20% with higher *e* values) were aligned using the MAFFT program (Katoh et al. 2002) and edited with GBlocks (Castresana 2000). Interestingly, pairwise similarity between AWR was comparable with that of their putative counterparts in other species. Sequence conservation extended all along the polypeptide sequence, showing some scattered highly conserved regions. A domain containing the AWR tripeptide—after which the protein family was named—was especially apparent as remarkably well-conserved not only in *Ralstonia* but also in *Burkholderia* spp. (Supplementary Fig. S1).

To better understand the relationships between different AWR, we constructed a phylogenetic tree based on sequence similarities using a Bayesian estimation of phylogenies (MrBAYES) (Fig. 1A). The tree obtained was rooted in the *Xanthomonas* sequences, which correspond to γ-proteobacteria, more distantly related to the rest of β-proteobacterial sequences. The tree showed that maximal diversification of AWR was found in *R. solanacearum* strains, whose five proteins appeared as distinct branches (Fig. 1A). Interestingly, AWR from different strains clustered together in orthologous groups rather than with the other paralogues from the same strain. This indicates that they correspond to ancestral effectors that emerged before *R. solanacearum* speciation. Three clades were observed among *R. solanacearum* AWR, containing the sequences of AWR 3 and 4, 1 and 2, and 5. The observations that i) AWR3 and AWR4 form twin branches in the phylogenetic tree, ii) they are placed side by side in the genome, and iii) they show the highest identity and similarity values strengthen the hypothesis that these genes emerged from a recent duplication event. Molk2 and UW551 strains harbor an extra *awr* gene that has been called AWR6 (Poueymiro and Genin 2009). According to our tree, these effectors (t3e2RsM and pawrRsU) correspond to a second copy of AWR5. This extra AWR5 is also present in IPO1609 strain RSIPO_01281 but not in the other phylotype II strain, CFBP 2957. The tree also clarified the phylogenetic relationships of AWR-related proteins found in other species. For instance, the AWR present in *Xanthomonas* spp., where the tree was rooted, is highly related to the common ancestor of the family. Similarly, the AWR found in strains of the human pathogen *B. pseudomallei* form a distinct ancestral clade. *A. avenae* pv. *citruli* contains two AWR: one in a basal branch close to *Xanthomonas* proteins

and the other (hyp1AaC and hypAaA) related to *R. solanacearum* sequences. Finally, an effector closely related to the AWR3/4 ancestor is present in plant pathogens from the *Burkholderia* genus (e.g., hyp1 Bg), which carry a copy of AWR1 (e.g., hyp2 Bg) as well, an effector otherwise restricted to the *R. solanacearum* phylotype I.

Based on all of these observations, we proposed an evolutionary model for AWR (Fig. 1B), in which the origin of these effectors preceded the splitting of β- and γ-proteobacteria (Naum et al. 2009; Tayeb et al. 2008; Wu and Eisen 2008). From this origin, the gene family experienced several duplications or deletions in the γ-proteobacteria lineage. This explains the presence of an ancestor for *awr3* and *awr4* in several *Burkholderia* spp. and suggests that *awr1* appeared as a recent duplication of *awr2*. The model also includes two recent horizontal gene transfer events that took place from *R. solanacearum* toward plant pathogens or symbionts of the genera *Acidovorax* and *Burkholderia*. The well-known instability of the *R. solanacearum* genome (Guidot et al. 2009) and the fact that *Burkholderia* spp. and *A. avenae* share the same soil habitat (Attree and Attree, 2001; Ham et al. 2010; Viallard et al. 1998; Willems et al. 1992) render these gene transfers very likely. The evolutionary model results in five AWR members in each *Ralstonia* strain, except in UW551 and Molk5, where an extra duplication event in *awr5* gave rise to *awr6*.

Finally, we performed BLAST comparisons of AWR protein or gene sequences with the databanks, and no similarity to characterized proteins or motifs with predicted biochemical function was found. Prediction analysis for sequence motifs was performed with INTERPRO Scan software, which analyzes different data sources using the protein sequences or consensus sequences derived from the most conserved domains. Three-dimensional structure predictions using PHYRE were also performed and rendered no statistically relevant hits for any of the AWR proteins.

Thus, *awr* genes are conserved genes widespread in *R. solanacearum*, with orthologs present in other bacterial pathogens, but their sequence information gives no clue to their function.

AWR are bona fide T3E.

Previous studies demonstrated that *awr* genes, except for *awr1*, were transcriptionally regulated by the T3SS master regulator *hrpB* (Cunnac et al. 2004a). In addition, AWR2 from GMI1000 or the homologues of AWR3, AWR4, and AWR5 in phylotype I strain RS1000 were shown to be translocated into the plant cell using the *cyaA* reporter system (Cunnac et al. 2004a; Mukaihara and Tamura 2009). In order to confirm the type-III dependent secretion of the effectors from GMI1000, we took advantage of a novel tool that allows stable production

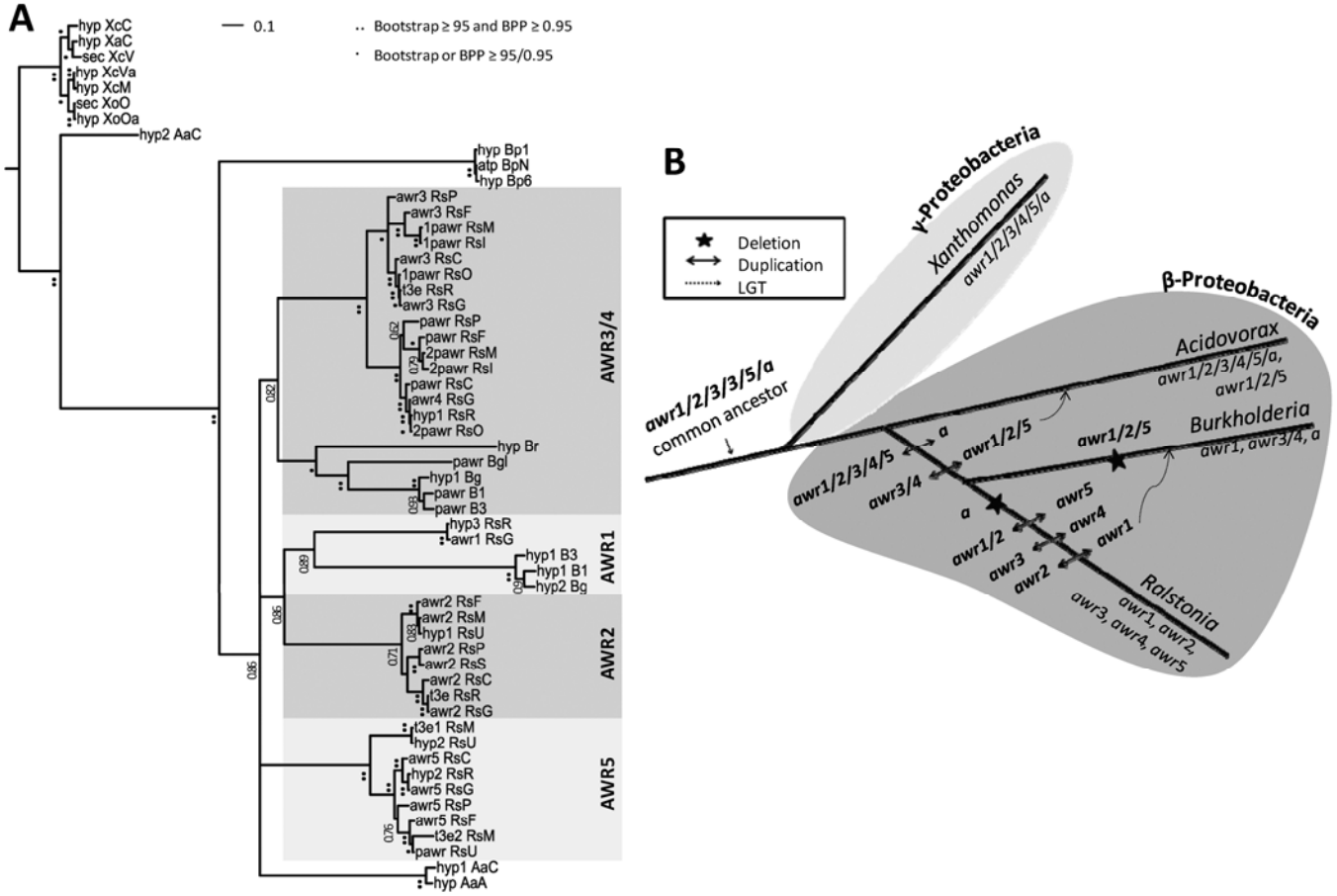

Fig. 1. Evolutionary relationships between *awr* genes. **A,** Rooted phylogenetic tree of the *awr* gene family. The tree was constructed, according to the Bayesian inference, from those sequences obtained by BLAST for each GMI1000 alanine-tryptophan-arginine tryad (AWR). Sequences were named after acronyms of the protein annotation in the original databanks followed the species they belonged to; that is, t3e (type 3 effector), hyp (hypothetical protein), awr (awr protein), pawr (putative awr protein), atp (atp-binding protein), sec (secreted protein), Rs (*Ralstonia solanacearum*), Xa (*Xanthomonas axonopodis*), Xc (*X. campestris*), Xo (*X. oryzae*), Aa (*Acidovorax avenae*), Bp (*Burkholderia pseudomallei*), Br (*B. rhizoxinica*), Bg (*B. graminis*), Bgl (*B. glumae*), and B (*Burkholderia* spp.). Numbers in branch nodes correspond to the BPP value and branch lengths indicate sequence divergence. **B,** Model of *awr* evolution in the gram-negative bacterial lineage. The model represents the most plausible evolutionary scenario, taking into account the phylogenetic relationships amongst bacteria and minimizing the number of gene duplications and losses. *Xanthomonas* and *Acidovorax* spp. contain the sequence considered more related to the ancestral form. Gene duplications are represented as arrows, deletions by stars, and putative horizontal gene transfers by discontinuous lines.

of tagged proteins in *R. solanacearum* (Monteiro et al. 2012). We fused the hemagglutinin (HA) sequence to the 3′ end of the *awr* coding sequences under the control of the strong *eps* promoter and introduced the constructs in the genome of the wild-type GMI1000 strain or its T3SS-deficient counterpart (*hrpV*⁻) by recombination. Next, we grew the strains under type III–inducing conditions and evaluated AWR expression inside the bacterium and their secretion to the culture medium. Thus, total bacterial protein extracts and concentrated proteins from the culture medium were obtained and subjected to immunoblot analysis using an anti-HA antibody. Distinct band sizes corresponding to the different expressed effectors could be distinguished in cell lysates of both strains (Fig. 2). Although full-length AWR were produced in *R. solanacearum,* the protein was detected in the medium from the wild-type strain but not from the *hrpV* mutant, thereby demonstrating that secretion was dependent on a functional T3SS. These results confirmed that AWR2, AWR3, AWR4, and AWR5 were secreted via the T3SS, as previously described using the CyA reporter assay (Cunnac et al. 2004b; Mukaihara and Tamura 2009). In addition, our data demonstrate that, contrary to what had been reported, AWR1 is also secreted to the medium and, thus, can be considered a genuine T3E protein (Fig. 2).

AWR effectors jointly contribute to the pathogenicity of *R. solanacearum* GMI1000.

A previous study showed that disruption of a single *awr* gene slightly affects bacterial pathogenicity. To better evaluate the combined contribution of the whole gene family in pathogenicity, we constructed a mutant of *R. solanacearum* GMI1000 devoid of all *awr* members. To this end, we used a recently adapted methodology for precise excision of DNA sequences in the *R. solanacearum* genome that allows the generation of cumulative mutations (Angot et al. 2006; Marx and Lidstrom 2002). Consecutive deletion of all five *awr* genes resulted in strain Δ*awr1-5* and each of the intermediate mutants (Δ*awr3,4*; Δ*awr3-5*; and Δ*awr2-5*). These mutant strains were tested for virulence in the host plants tomato (ecotypes 'Marmande' and 'Hawaii 7996') and eggplant 'Zebrina'. Bacterial multiplication was measured in the leaves, because this methodology was shown to be more sensitive and quantitative than plant disease scoring (Macho et al. 2010). The wild-type strain GMI1000 and a nonpathogenic *hrp* regulation mutant were used as references in this experiment. GMI1000 (wild type) multiplied 1,000 to 10,000 times at 3 days postinoculation (dpi) in infected plants, depending on the host, whereas *hrpG* multiplied a maximum of 1.5 $\log_{10}$ (Fig. 3). The bacterium grew to a similar extent in the hosts tomato (Marmande) and eggplant but much less in the tomato Hawaii 7996, known to be tolerant to the disease (Wang et al. 2000). In eggplant, the multiplication capacity of the quintuple *awr* mutant and all its intermediates was significantly reduced compared with the wild-type strain, except for the mutant deleted for AWR3 and AWR4 (Δ*awr3,4)*, whose growth was only slightly affected (Fig. 3A). The mutant devoid of all AWR multiplied 50-fold less than the wild-type strain, demonstrating an important role of AWR in pathogenicity. The whole gene family was key for bacterial progression in planta, because consecutive deletions exerted an additive effect in the phenotype. These phenotypes are specific for plant colonization, because none of the tested strains was affected in growth in culture media (data not shown). Similar results were obtained in tomato (Fig. 3B). In contrast, when the effects of single *awr* deletion mutations on virulence were compared, no significant differences were observed (Supplementary Fig. S2), except for AWR2, which had

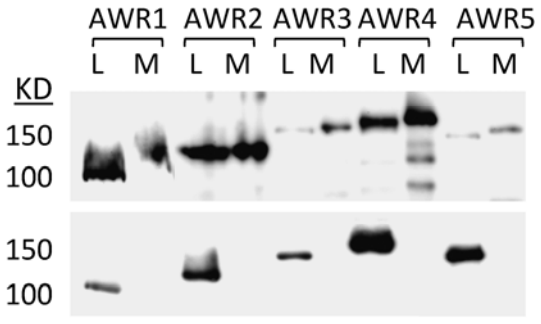

Fig. 2. Secretion assay of alanine-tryptophan-arginine tryad (AWR) effectors in *Ralstonia solanacearum* GMI1000. Immunodetection of protein extracts from bacterial lysates (L) or culture media of strains bearing different AWR effector genes fused to the hemagglutinin (HA) epitope tag. The wild-type GMI1000 was used to test protein secretion in the medium and the *hrpV*⁻ mutant to verify that secretion was type III secretion system specific. AWR proteins were detected with an anti-HA antibody.

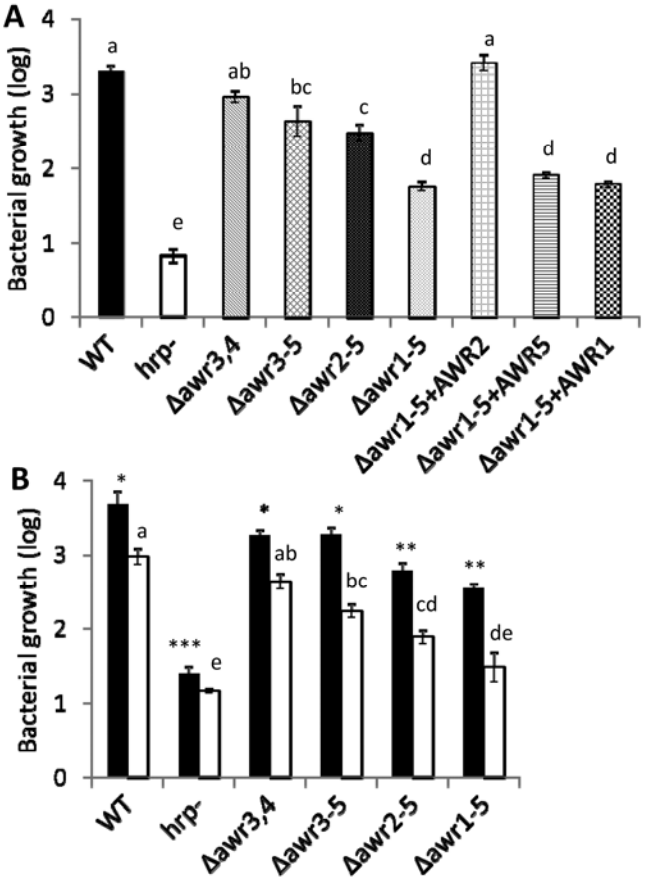

Fig. 3. Bacterial growth of alanine-tryptophan-arginine tryad (AWR) deletion mutants and their complemented strains on host plants. The wild-type *Ralstonia solanacearum* GMI1000 (WT), its hypersensitive response and pathogenicity (*hrp*)-deficient counterpart (*hrpG*⁻), and AWR mutant strains of mutant complemented strains were infiltrated at 10^5 CFU/ml on leaves and recovered 3 days later (4 days for tomato 'Hawaii 7796') to monitor bacterial growth. Bacterial multiplication is represented as the logarithm of recovered CFU per square centimeter with respect to the original inoculum. Values represent the mean of eight biological replicates and their standard errors which were obtained in two independent assays. Statistically significant groups (letters and asterisks) were calculated using a one-way analysis of variance and a Tukey test ($P < 0.05$). A "–" sign between numbers indicates that the intermediate *awr* genes are also deleted (i.e., Δ*awr1-5* is the quintuple deletion mutant strain). A "+" indicates complementation with the gene following the sign. **A,** *R. solanacearum* growth curves in eggplant 'Zebrina'. **B,** *R. solanacearum* growth curves in tomato 'Marmande' (black bars) and 'Hawaii 7796' (white bars).

been previously shown to contribute to pathogenicity. To confirm the described phenotypes and better determine the contribution of each gene to bacterial fitness in planta, the quintuple mutant was complemented by sequentially introducing into its genome a single copy of *awr1*, *awr2*, or *awr5*. The strain bearing only *awr2* restored bacterial multiplication to almost wild-type levels, whereas addition of *awr1* or *awr5* to the quintuple mutant did not affect bacterial growth in the plant (Fig. 3A, right-most bars). These data correlate with the phenotypes of the single mutants and support a major role of *awr2* in *R. solanacearum* virulence, with some functional redundancy of its paralogues.

Some AWR effectors constrain *R. solanacearum* pathogenicity on *Arabidopsis*.

To better understand the role of AWR effectors in *R. solanacearum* virulence, in planta multiplication assays were also carried out in the alternative host *Arabidopsis thaliana* accession Col-0. Surprisingly, the strains deleted of four or five AWR multiplied much better than wild-type strain in Col-0 whereas growth of the wild type was almost undetectable (data not shown). Thus, contrary to what was observed in other hosts, the absence of AWR seemed to render the bacterium more proficient for multiplication in *Arabidopsis*. Because an advantage in multiplication often causes an increase in pathogenicity, we then performed the classical pathogenicity tests to better analyze these phenotypes (Fig. 4A). Plants were root inoculated with either the wild-type GMI1000 or Δ*awr1*-5 mutant and development of wilting symptoms was recorded daily. Disease scoring showed increased virulence of the Δ*awr1*-5 strain compared with the wild strain, accelerating symptom appearance for approximately 2 days. Similar results were obtained with the Δ*awr1-4* strain (not shown). This suggested that the presence of AWR effectors was limiting the capacity of the bacterium to multiply and cause disease in *Arabidopsis*. To better characterize this effect, we designed a gain-of-function assay introducing *awr* genes in *P. syringae* DC3000, an *Arabidopsis* pathogen naturally lacking them. AWR were heterologously expressed using the pEDV6 system and bacterial growth of the resulting strains was measured in Col-0 leaves (Fabro et al. 2011; Sohn et al. 2007). As expected, expression of several AWR effectors in this pathosystem caused a restriction in bacterial multiplication (Fig. 4B). This was particularly apparent when AWR4 and AWR5 were present, whereas AWR1 and AWR3 caused only a mild impact on pathogen progression. By contrast, the strain expressing AWR2 exhibited increased fitness in planta. These results support the previous observation that AWR2 plays a major role in virulence which, on natural hosts, is aided by a collective contribution of its paralogues. In addition, several AWR also seem to trigger specific plant recognition responses in *A. thaliana*, which is not a natural host for *R. solanacearum*, despite having been isolated from other crucifers. The same results were obtained when the effectors were expressed in the less virulent *P. syringae* pv. DC3000 derivative lacking the conserved effector locus instead of the wild type (not shown). Other studies have shown disparate responses of effector proteins on *Arabidopsis* and tomato plants (Lin et al. 2008; Milling et al. 2011). Unsurprisingly, *Arabidopsis* is a tremendous source of plant resistance toward pathogens and its study led to the discovery of the R protein, RRS1 (resistance to *R. solanacearum* 1) that confers resistance to *R. solanacearum* expressing PopP2 (Deslandes et al. 2003).

Transient expression of AWR in *N. benthamiana* causes different levels of necrosis.

To determine whether AWR bacterial effectors are recognized in resistant plants, we used *Agrobacterium*-mediated transient expression (hereafter, agroinfiltration) of AWR from an estradiol-inducible vector. We agroinfiltrated and scored for macroscopic cell death phenotypes in *N. benthamiana, N. tabacum*, and *N. glutinosa* plants, which are resistant to strain GMI1000. AWR5 production resulted in a rapid and marked

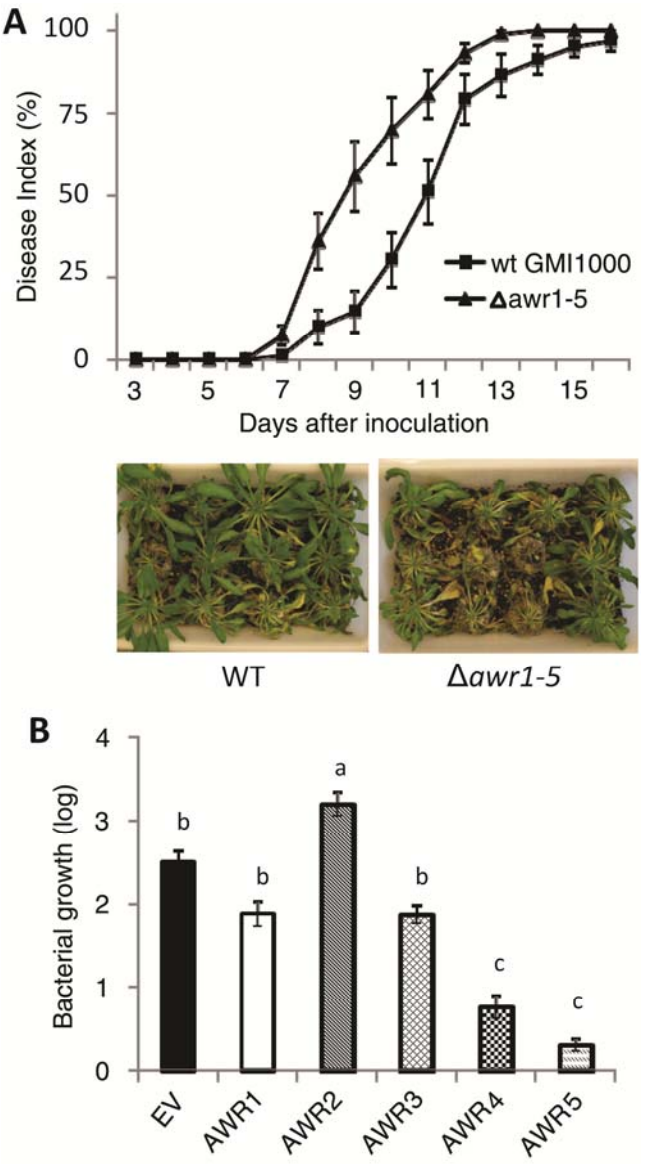

Fig. 4. Effect of alanine-tryptophan-arginine tryads (AWR) on bacterial pathogenicity on *Arabidopsis thaliana*. **A,** Pathogenicity test on *A. thaliana* Col-0 plants with the *Ralstonia solanacearum* Δ*awr1-5* multiple mutant strain and the control strain GMI1000 (WT). Plants were root inoculated and disease progression annotated daily according to wilting symptoms appearance: no wilting (0), 25% wilted leaves (1), 50% (2), 75% (3), and dead plant (4). Values represent the mean of 12 biological replicas and their standard errors. Representative pictures were taken 10 days postinfection. Differences were statistically significant according to Student's *t* test at $P < 0.01$. The assay was repeated three times with similar results. **B,** Multiplication in *A. thaliana* Col-0 plants of *Pseudomonas syringae* DC3000 heterologously expressing AWR effectors. Strain DC3000 bearing the pEDV3 empty vector (EV), its hypersensitive response and pathogenicity (*hrp*)-deficient variant (*hrcC*), and the strains that express each AWR were inoculated on leaves at 5×10^5 CFU/ml and recovered 3 days later to monitor bacterial growth. Bacterial multiplication is represented as the logarithm of recovered CFU per square centimeter with respect to the original inocula. Values represent the mean of four biological replicates. Statistically significant groups were calculated using a one-way analysis of variance with a Tukey test ($P < 0.01$). The experiment was repeated three times with similar results.

necrosis in *N. benthamiana* leaves, and AWR1 and AWR2 produced a milder and less clear necrosis phenotype (Fig. 5A). Leaves expressing one of the two other AWR were indistinguishable from control leaves expressing β-glucuronidase (GUS) with the same inducible system. The full-length AWR5 protein was required for correct function or folding to trigger plant responses, because production of N- or C-terminal or central protein fragments was insufficient to cause the necrosis phenotype (not shown). The rapid onset (approximately 24 h) and the extent of the necrosis caused by AWR5 were reminiscent of that produced by the AvrA effector, known to trigger an HR in *Nicotiana* spp. (Fig. 5A, left) (Poueymiro et al. 2009).

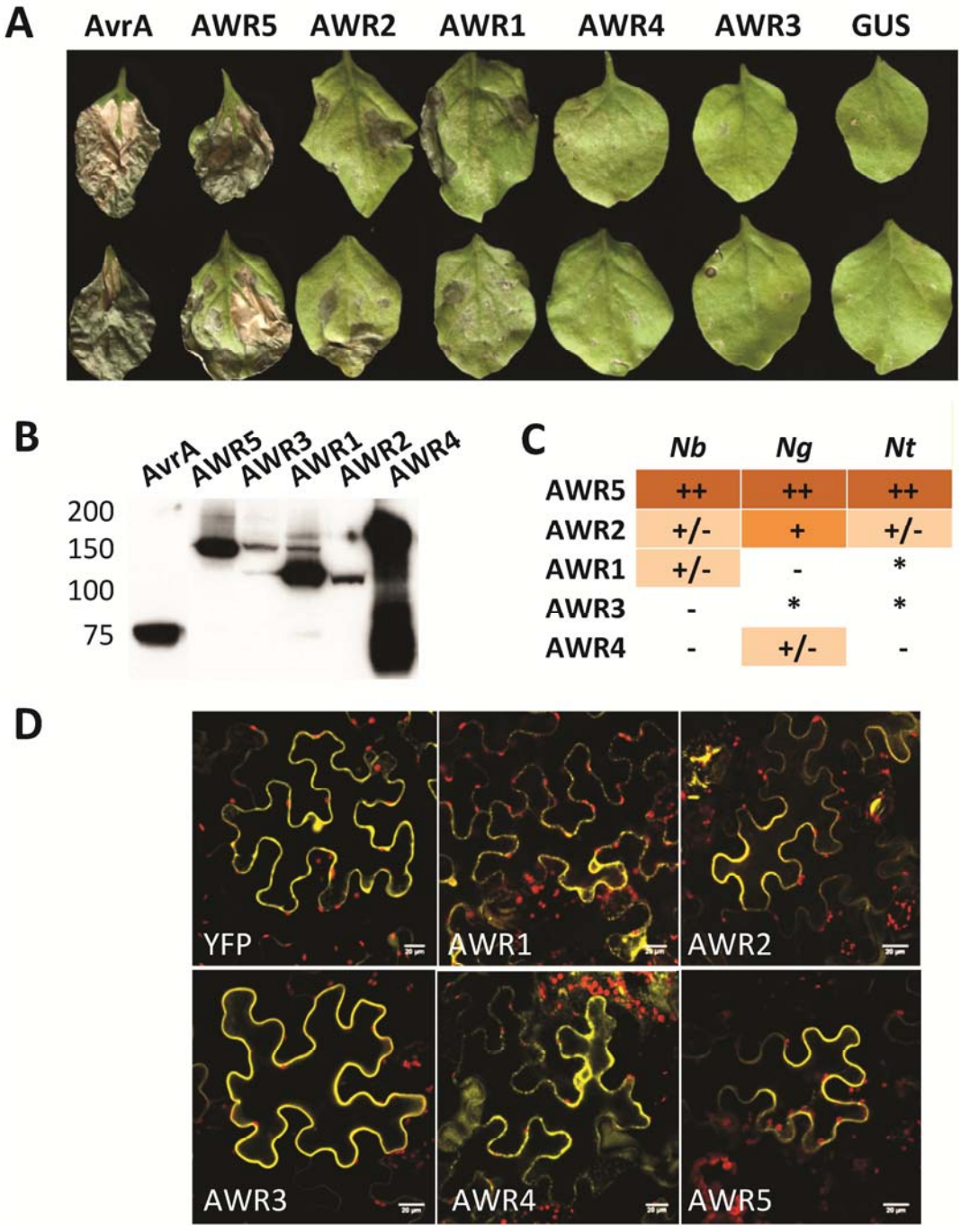

Fig. 5. Effects of AWR (alanine-tryptophan-arginine tryad) transient expression on nonhost *Nicotiana* plants. **A,** Photograph of representative *Nicotiana benthamiana* leaves expressing AWR or control proteins. Transient expression was performed using *Agrobacterium tumefaciens* as a vector to transfer estradiol-inducible constructs from pAMP-PAT-derived plasmids. Full leaves were agroinfiltrated with the each construct. Pictures were taken 4 days after inoculation. The experiment was repeated four times with the same results. **B,** Immunoblotting of proteins transiently produced in *N. benthamiana* under an estradiol-inducible promoter. Hemagglutinin (HA)-tagged proteins from total leaf extracts obtained at 6 to 8 h postinduction were immunodetected using an anti-HA antibody. **C,** Summary chart of the phenotypes caused by transient expression of AWR in *N. benthamiana* (*Nb*), *N. tabacum* (*Nt*), and *N. glutinosa* (*Ng*) plants. Average phenotypes observed from eight independent leaves are shown in a semiquantitative scale: ++ = massive macroscopic necrosis, + = clear necrosis variable in size and intensity, +/– = minor necrosis present in only some infiltrated leaves, – = appearance indistinguishable from control β-glucuronidase -expressing plants, and * = not tested. **D,** AWR subcellular localization in *N. benthamiana.* Fluorescence confocal microscopy images of the 525- to 550-nm (AWR-YFPv, yellow) and 610- to 700-nm (chloroplasts, red) spectra obtained after excitation with a 514-nm light. Pictures of representative cells expressing the bacterial effectors taken at 8 h postinduction are shown. As a reference, notice the cytoplasmatic and nuclear localization of the control yellow fluorescent protein (YFP). Bars correspond to 20 μm.

Accumulation levels of all transiently expressed proteins were checked by immunoblot. Although proteins were expressed at different levels, it was clear that phenotypical responses triggered by AWR were not related to differences in their relative expression. Bands corresponding to the expected full-size proteins were detected for all constructs at 8 h postinduction (Fig. 5B). Phenotypical responses caused by AWR were also evaluated in two other nonhost tobacco species to check their specificity. The results are presented in Figure 5C in a semiquantitative scale. The phenotypes caused by AWR5 and AWR2 were apparent in all backgrounds and even stronger in *N. tabacum*. AWR1 and AWR4 showed minor necrosis on *N. benthamiana* and *N. glutinosa*, respectively (Fig. 5C). AWR3 had no macroscopic effect in any case, in spite of being readily detected by

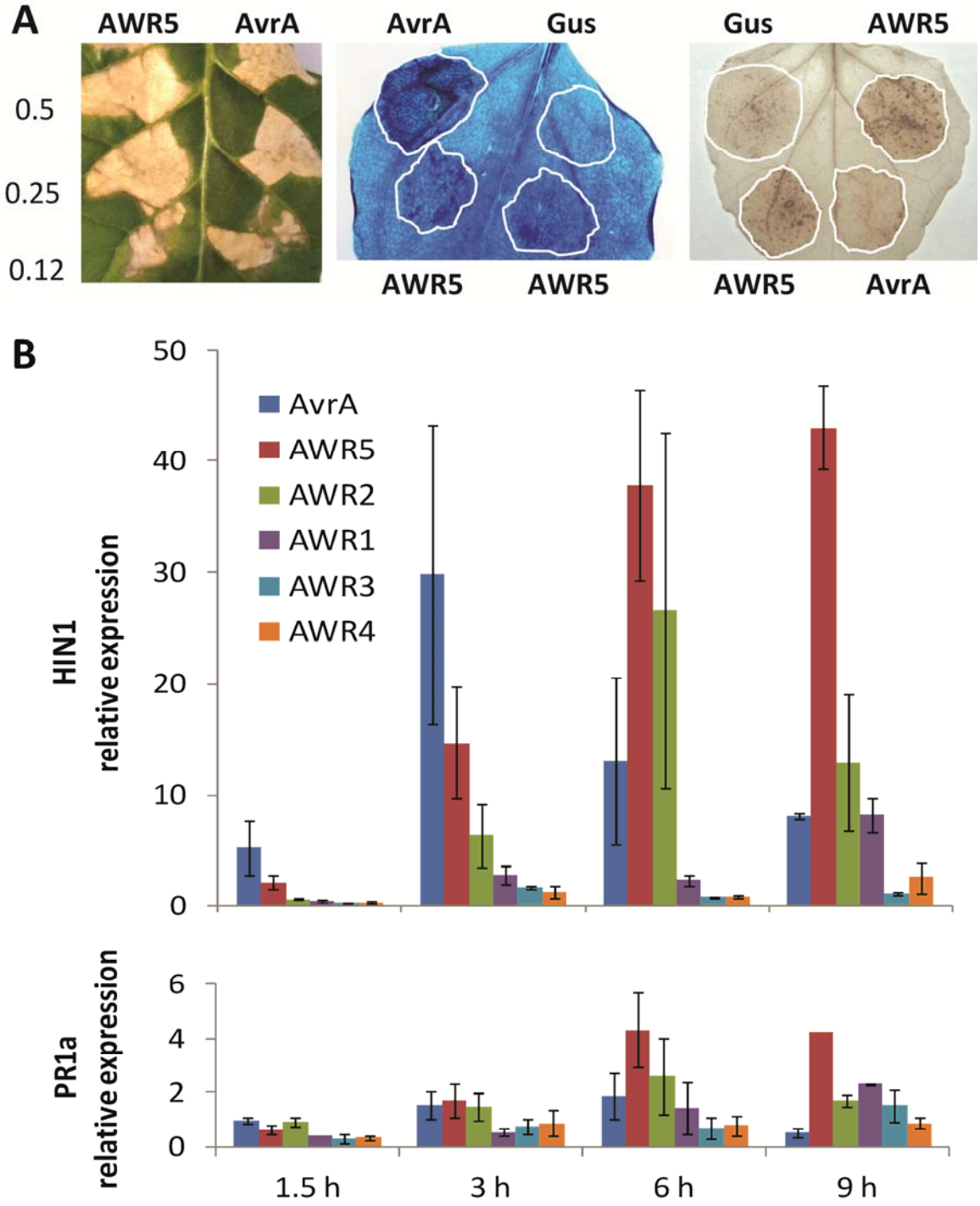

Fig. 6. Cell death phenotype caused by AWR5 is comparable with a hypersensitive response (HR). **A,** Pictures of *Nicotiana tabacum* leaves 48 h after infiltration with various concentrations of *Agrobacterium tumefaciens* bearing the *awr5* and *avrA* genes (left). Left numbers indicate bacterial optical density at 600 nm of the inocula. Trypan blue staining of dead cells 26 h postinduction of agroinfiltrated leaf areas (central panel); GUS = β-glucuronidase. Diaminobenzidine staining of agroinfiltrated leaves showing H_2O_2 production at 8 h postinduction (right). **B,** AWR5 triggers an early induction of specific HR plant markers. Expression of *HIN1* (HR-specific gene) and *PR1a* (defense marker) was evaluated from RNA samples extracted at different time points from *N. benthamiana* leaves agroinfiltrated with constructs producing each AWR. Gene expression was normalized by the housekeeping gene tubulin and represented as fold-induction with respect to basal levels in control samples transiently expressing the GUS gene. Values shown are the mean of two biological replicates and their standard error.

Western blot. It is worth mentioning that AWR5, which displays the strongest impact on plant physiology, is the one causing a major growth restriction when expressed in *P. syringae*. Interestingly, AWR2 and AWR5 are the only family members that have a very minor impact, if any, when ectopically overexpressed in tomato host plants (Supplementary Fig. S3). This reinforces the idea that the cell death produced in resistant plants is due to recognition and not a consequence of AWR function in planta. Such diversity in plant responses to AWR is surprising considering their similarity in the primary protein sequence. Similar results using other bacterial effectors have been described, further supporting the diverse host responses to AWR. A recent report where effector candidates from *X. campestris*, *P. syringae*, and *R. solanacearum* were transiently overexpressed in various plant species demonstrated that, although one-third produced visible phenotypes in at least one accession, none of them caused a reaction in all plants tested (Wroblewski et al. 2009). HR-like phenotypes have been interpreted as a programmed cell death elicited by avirulence factors, although recent publications discuss whether this HR might be a cause or a consequence of cascade signaling downstream of effector recognition (Coll et al. 2011).

To better understand the molecular basis of AWR-caused necrosis, we investigated subcellular localization of yellow fluorescent protein (YFP)-tagged AWR proteins. Agroinfiltration of some YFP-tagged AWR proteins in *N. benthamiana* leaves resulted in tissue collapse in early time points (24 h), indicating that YFP-tagged AWR proteins are functional. Confocal microscopy pictures taken at short intervals postinduction (8 h) are presented in Figure 5D. The images clearly show that fluorescence from all effector fusions was evenly localized in the cytoplasm, with some association to membranes (e.g., AWR4). In contrast to the free YFP protein, which is partially retained in the nucleus, none of the effectors targeted this compartment.

AWR5 causes an HR when transiently expressed in tobacco species.

To determine whether the cell death observed after AWR5 production in planta corresponded to an HR, we performed additional experiments by expressing this effector or the control AvrA protein at various levels. AvrA was previously described as triggering an HR response (Poueymiro et al. 2009). Serial infiltrations of different concentrations of *Agrobacterium* cells carrying either AWR5 or AvrA were performed on *N. tabacum* leaves, because the phenotypes were sharper in this plant and appeared earlier. Expression of both AWR5 or AvrA generated necrosis to the same level at similar time point (<24 h) (Fig. 6A). To further compare cell death phenotypes caused by AvrA and AWR5, we performed trypan blue staining of the infected leaf tissues to visualize dead cells (Keogh et al. 1980), and diaminobenzidine (DAB) staining that results in brown deposits upon reaction with H202 (Thordal-Christensen et al. 1997). Agroinfiltration of AWR5 triggered a cell-death phenotype and induced higher accumulation of H202 compared with AvrA in *N. benthamiana* (Fig. 6A, right panels). These results imply that the AWR5-triggered cell death response in nonhost tobacco plants resembles classical HR (Torres, 2010). To better characterize the observed responses at the molecular level, we measured the expression of defense-related marker genes that are induced during development of HR in *N. benthamiana*. *HIN1* was chosen as a specific molecular marker of HR in tobacco, because its expression is highly induced during incompatible interactions and strictly restricted to the challenged tissue (Gopalan et al. 1996; Kiba et al. 2003). Transcript levels of *HIN1* and pathogen-response (PR) genes were measured by real-time quantitative reverse-transcription-mediated polymerase chain reaction (RT-PCR) by using total RNA samples isolated from agroinfiltrated *N. benthamiana* leaves. The results of these experiments are presented in Figure 6B as fold-induction with respect to basal expression levels from leaves expressing the control GUS transcripts. A marked increase of the *HIN1* transcripts was already apparent 3 h after estradiol induction of effectors, causing clear HR-like phenotypes (AvrA or AWR5), and this high expression extended to 6 and 9 h postinduction. At these late time points, *HIN1* was also induced at levels comparable with those caused by AvrA and by AWR2 or AWR1, which caused milder necrosis on tobacco. The AWR effectors (AWR3 and AWR4) producing no macroscopic phenotype when agroinfiltrated did not activate HR-responsive genes (Fig. 6B). By contrast, expression of the PR1a defense gene was almost unaltered (<twofold changes compared with *AvrA*) for any of the strains tested. For AWR2, AWR5, and the control strains, RNA levels of the defense-responsive PR1b or the HR-responsive *hsr203j* (Kiba et al. 2003; Pontier et al. 1998) were comparable with *HIN1* and *PR1a* (data not shown). Gene *hsr203j* was tested because it had been described as specifically induced in tobacco tissues inoculated with strain GMI1000 (incompatible interaction) and undetectable upon challenge with strain K60 (compatible interaction) or a nonpathogenic *hrp* mutant strain (Pontier et al. 1998). Thus, induction of the specific molecular markers perfectly correlated with the phenotypes observed in planta.

From our results, we infer that an HR only appears when an expression threshold of marker genes is reached. This threshold implies a minimum transcript level at a certain time (approximately 30-fold before 6 h for *HIN1*), so that lower levels or even comparable levels but at later times are not sufficient to mount programmed cell death. Along the same line, it has been suggested that common genes are involved in both compatible and incompatible responses against pathogens, with the differential timing determining the outcome (Hu et al. 2008; Tao et al. 2003). Taken together, our phenotypic and molecular analyses prove that AWR5 can trigger an HR when overexpressed in *Nicotiana* spp. It is noteworthy that this response is equivalent to that caused on tobacco leaves with AvrA or with the whole bacterial strain GMI1000 (Kiba et al. 2003), suggesting that AWR effectors can play a role in restriction of the *R. solanacearum* host range.

Conclusion.

R. solanacearum is a devastating pathogen that requires T3SS to successfully infect plants (Boucher et al. 1987). It is one of the bacterial pathogens with the highest number of predicted T3E (Cunnac et al. 2010; Kay and Bonas, 2009; Mukaihara et al. 2010) but most of their functions remain unknown, contrary to other pathogens such as *P. syringae* or the xanthomonads. Among all putative effectors found in *R. solanacearum*, we have focused here on the characterization of a multigenic family called AWR. Our results demonstrate that the encoded proteins in GMI1000 are secreted through the T3SS and are required for full virulence of the pathogen on natural hosts. It is interesting to note that AWR1 translocation to plant cells had been undetected using a *cyaA* reporter fusion but it was proven here through protein secretion studies. This discrepancy is unlikely due to the fact that proteins from different strains (RS1000 and GMI1000) were analyzed, because the N terminal (first 50 amino acids) of the two proteins, where secretion signals lay, is 94% identical. Rather, we favor the hypothesis that type III-dependent secretion studies are a more sensitive test than translocation of *cyaA* fusions, which may be prone to false negatives.

The high redundancy of effector repertoires has been interpreted as a means to use particular combinations for effective colonization of different hosts (Cunnac et al. 2004a; Kvitko et

al. 2009). In the case of AWR, one of them (AWR2) plays a major role in pathogenicity, regardless of the plant host, whereas the other members of the family act synergistically, reinforcing this function. Our deletion and complementation experiments suggest that the role of each family member in virulence is somewhat redundant. For example, a single AWR (AWR2) confers wild-type pathogenicity on eggplant whereas a single mutant for the same AWR shows higher pathogenicity than a mutant deleted for all the *awr* genes. These features of the AWR family suggest that *R. solanacearum* virulence involves a small number of effectors with a key effect and many effectors with a weak, additive contribution. This seems to be true for the whole GMI1000 effector repertoire, out of which only AWR2 and RSp0304 deletion mutants showed decreased pathogenicity on tomato (Cunnac et al. 2004b).

Contrary to the similar contribution of AWR to pathogenicity on diverse hosts, we have found a high degree of specificity in the responses triggered by AWR in different plants. AWR5—and, to a lesser extent, AWR2 and AWR1—triggered the major responses in nonhost tobacco plants, whereas *Arabidopsis* plants showed some recognition of AWR5 and AWR4. Thus, AWR exhibit functional diversification, as was recently described by another *R. solanacearum* type III effector family showing specialized roles in pathogenicity on different plant hosts (Remigi et al. 2011). Our results in *A. thaliana* are especially interesting. In this plant host, the presence of AWR seems to restrict *R. solanacearum* virulence, as revealed by the increased pathogenicity and multiplication of the Δ*awr1*-5 strain. It seems logical that the bacterium is not fully pathogenic in this plant, which is never confronted with the pathogen in nature. However, when the role of each AWR was analyzed separately by a gain-of function approach in the heterologous pathogen *P. syringae*, we obtained somehow conflicting results. As mentioned, AWR5 and AWR4 showed this capacity to restrict bacterial multiplication but AWR2 expression clearly promoted the pathogenicity of *P. syringae*. Thus, the outcome of the interaction of *R. solanacearum* with *A. thaliana* is the result of antagonistic interactions specific for each effector.

AWR2 is one of the main contributors to *R. solanacearum* virulence on different hosts, suggesting conservation in its targets, but it is also recognized by the plant surveillance system. This dual role in virulence and resistance has already been documented for some bacterial effector proteins and been interpreted in the light of plant–pathogen coevolution, which results in compatible and incompatible interactions (Schulze-Lefert and Panstruga 2010). For instance, AvrBsT from *X. campestris* pv. *vesicatoria* is recognized in pepper and *N. benthamiana* plants whereas it enhances bacterial growth in tomato plants (Kim et al. 2010). Similarly, evolutionary and virulence–avirulence studies with effectors of the YopJ/HopZ effector superfamily have shown their functional diversification in wide-ranging coevolutionary interactions (Lewis et al. 2011). The distinct functions of each AWR in virulence and avirulence likely contribute to host adaptation, explaining the high degree of conservation of these effectors in *R. solanacearum*.

AWR are also present in other plant-pathogenic strains with emerging importance such as the rice pathogen *B. glumae*, other *Burkholderia* strains, *Acidovorax avenae* infecting cucurbitaceae or poaceae and some *Xanthomonas* pathovars causing disease in rice, pepper, tomato, brasicaceae, citrus, or even a bacterial wilt in banana (Ham et al. 2010; Mole et al. 2007; Smith et al. 2008; Viallard et al. 1998; Willems et al. 1992). The long evolution suffered by this ancestral family and the disparate contexts in which it functions may have facilitated the functional diversification that we have observed for its members. In addition, AWR homologues are also present in the mammal pathogen *B. pseudomallei*, the causal agent for melioidosis (Wuthiekanun and Peacock 2006), whose T3SS is similar to that of *R. solanacearum* (Rainbow et al. 2002). It would be interesting to evaluate the role of AWR in this pathogen also capable of infecting tomato plants (Lee et al. 2010) because, in *P. aeruginosa*, some virulence factors are important for pathogenesis on both plant and animal hosts (Rahme et al. 1997). Indeed, effectors from plant pathogens such as HopAO1 from *P. syringae* have already been shown to share the same function with their homologues in *Salmonella* and *Shigella* spp. (Shan et al. 2007).

In this work, we characterized the physiological impact of AWR on different plant species. Plant localization did not give clues to the events that follow effector translocation in planta. Experiments are under way to identify and biochemically characterize the molecular targets of AWR in host and nonhost plants to broaden our knowledge of the virulence strategies developed by *R. solanacearum* to provoke bacterial wilt disease.

MATERIALS AND METHODS

DNA cloning and molecular biology techniques.

TOPO or GATEWAY BP/LR recombinational clonings were achieved according to the supplier's manuals (Invitrogen Life Technologies Ltd. Paisley, U.K.). Some of the genes were amplified with and without STOP codon or, alternatively, this codon was inserted or deleted afterward with the QuikChange XL-Site-directed mutagenesis kit (Stratagene, La Jolla, CA, U.S.A.). PCR amplifications were typically performed with the proofreading Pfx DNA polymerase (Invitrogen) in a 50 µl-mix containing 0.3 mM each dNTP, 0,6 mM each primer, 2 mM $MgSO_4$, 2× Pfx amplification buffer, 2× enhancer solution, 0.2 µg of DNA, and 1.25 U of Pfx DNA polymerase. Amplification cycles were always performed approximately 5°C below the melting temperature of the primers employed. To clone in pGEM-T, 5′ A-overhangs were added to PCR products by incubating 6 µl of the PCR with 1 µl of 10× reaction buffer containing $MgCl_2$, 0.2 mM dATP, and 5 U of GoTaq polymerase at 70°C for 20 min. Verification of PCR was routinely carried out with the nonproofreading GoTaq DNA polymerase, as recommended by the supplier (Promega Corp.). For all clonings, DNA fragments were electrophoresed in agarose gels in Tris-acetate EDTA containing SYBR Safe DNA gel stain (Invitrogen), and bands were excised and purified with the Expin GEL SV (GeneAll Biotechnology Co., Ltd Seoul, Korea), introduced to the final vector by Gateway recombination or ligation, and transformed into *Escherichia coli*. Plasmids were then recovered with the Exprep Plasmid SV kit (GeneAll) for clone verification with restriction enzymes (New England) and sequencing with BigDye terminator v3.1 (Life Technologies Ltd., Paisley, U.K.) followed by further cloning if required.

For the generation of the *R. solanacearum* deletion mutant strains with the *cre*-lox system, we amplified 1 Kb-long 5′ (L) and 3′ (R) flanking regions of the coding sequence of interest and cloned the fragments in pGEM-T (Invitrogen). Inner *Eco*RI and *Sac*I restriction sites in 2139L (GAATTC>GATTTC) and 0099R (GAGCTC>GAGCAC) were mutagenized with the QuikChange XL site-directed mutagenesis kit before cloning into the final pCM351 vector. All generated plasmids are described in Supplementary Table S2. Clones without stop codons were used for expression with C-terminal fusions, unless otherwise stated. All primers used in this study for cloning or RT-PCR are listed in Supplementary Table S3.

Bacterial strains, plant material, and growth conditions.

E. coli cells were routinely grown in Luria-Bertani (LB) medium at 37°C. *Agrobacterium tumefaciens* and *P. syringae*

were grown in YEB or L-media, respectively, at 30°C. *R. solanacearum* cells were grown in complete B medium or in minimal medium (MM) supplemented with 20 mM glutamate at 28°C (Boucher et al. 1987). For secretion studies, bacteria were grown at 25°C in MM containing 10 mM glutamate and 10 mM sucrose as a carbon source. Congo red was also added to the cultures, at 100 µg/ml, because it is known to promote or stabilize secretion (Bahrani et al. 1997; Gueneron et al. 2000). Antibiotics were used for selection at the following concentrations: ampicillin at 100 µg/ml, chloramphenicol at 30 µg/ml, gentamicin at 15 µg/ml (10 in plates or 5 in liquid cultures for *Ralstonia* spp.), kanamycin at 50 µg/ml, rifampicin at 25 µg/ml, spectinomycin at 40 µg/ml, and tetracycline at 10 µg/ml (5 in *Ralstonia* liquid cultures).

The plants used for this work were 5-week-old *Arabidopsis thaliana* Columbia 0; 4-week-old *N. benthamiana;* 5-week-old *N. glutinosa*; 6-week-old *N. tabacum* 'Bottom special'; 4- to 5-week-old *Lycopersicon esculentum* Marmande, 'Bonnie Best', and Hawaii 7996; and 5-week-old *Solanum melongena* Zebrina. All plants were grown in long-day light conditions, except for *A. thaliana*, grown in short-day conditions with constant temperature at 22°C and humidity approximately 60%. After *Agrobacterium* sp. infiltrations, plants were kept in the same conditions whereas, after *Ralstonia* or *Pseudomonas* sp. inoculations, they were incubated in a chamber with constant light conditions and a fixed temperature of 28 and 25°C, respectively.

Bacterial transformation.

RbCl-chemically competent E. coli cells were transformed by the heat-shock method, as described by Sambrook and Russell (2001). MACH-1 cells (Invitrogen) were used as recipients for all clonings except for the GATEWAY-carrying plasmids, which were always transformed in the ccdB-resistant *E. coli gyrA462* mutant strain (Bernard et al. 1994). *Agrobacterium tumefaciens* GV3103 was transformed by electroporation in a 2-mm cuvette (2.5 Kev, 25 µF, 186 Ω) with 2 µl of DNA, incubated for phenotypic expression during 3 to 6 h, plated, and then incubated overnight in LB with suitable antibiotics. A standard triparental mating procedure (Sohn et al. 2007) was used to transfer plasmids from *E. coli* to *P. syringae* DC3000 using the *E. coli*-carrying pRK2013 as a helper strain. *R. solanacearum* GMI1000 natural transformations were performed as described (Boucher et al. 1985). For deletion mutagenesis in *R. solanacearum* with the *cre*-lox system (Marx and Lidstrom 2002), pCM351-derived plasmids were introduced in *R. solanacearum* by natural transformation and mutants resistant to gentamicin were recovered. The resistance gene flanked by *lox*P sites was finally excised by electroporating the strain (2.5 Kv, 50 µF, 129 Ω, 2-mm cuvettes) with pSG15, which harbors the *cre* recombinase, and growing the transformants for 2 days at 30°C without antibiotics to cure the pSG15 plasmid. Deletion of all AWR genes was confirmed by hybridization of genomic DNA extracted from the different mutant strains onto the genomic microarray from strain GMI1000 as described by Guidot and associates (2007). For each mutant, T3SS functionality was validated by infiltration in *N. benthamiana* plants to verity HR caused by ETI.

***Agrobacterium*-mediated protein expression in planta.**

Transient *Agrobacterium*-mediated protein expression was performed in *N. benthamiana, N. tabacum*, and *N. glutinosa*. For this, *A. tumefaciens* overnight-cultured cells were centrifuged and resuspended in 10 mM $MgCl_2$, 10 mM MES, and 150 µM acetosyringone for inoculation at an optical density at 600 nm of 0.5 to 0.8, then incubated for 1 to 2 h at room temperature. A strain harboring the P19 vector was co-infiltrated in most cases to avoid plant-silencing mechanisms. Bacterial strains were hand inoculated with a needle-free syringe in plant leaves from different plants. If required, protein expression was induced by painting the leaves 36 h postinfiltration with 5 µM estradiol and some Silwet L-77. For protein detection, three leaf discs of 6 mm were harvested at 3 to 6 h postinduction and homogenized in liquid nitrogen. Samples were subjected to standard Western-blot analysis as described by Sambrook and Russell (2001) using polyvinylidene difluoride (PVDF) membranes, an already HRP-conjugated anti-HA antibody (1:4000; F. Hoffmann, La Roche Ltd., Basel, Switzerland), Amersham Hypercassette films (GE Healthcare, Piscataway, NJ, U.S.A.), and Immobilon ECL (Billerica, MA, U.S.A.). For AWR subcellular localization, disc samples mounted in water were observed under a confocal microscope (Leica DMIRE2, Ryswyk, The Netherlands) with the 525- to 550-nm laser for YFPv and the 610- to 700-nm laser for chloroplasts. Images were taken with the ×40 objective (Leica confocal software) and processed with the Fiji software. For trypan blue staining, *Agrobacterium*–infiltrated leaves were boiled in a trypan blue-lactophenol solution with ethanol and cleared in chloral hydrate solution as described (Keogh et al. 1980). For DAB staining, *Agrobacterium*–infiltrated leaves were incubated overnight at room temperature with DAB as previously described (Thordal-Christensen et al. 1997).

Pathogenesis assays in planta.

R. solanacearum multiplication in planta was measured similarly to what is used in the *Pseudomonas* community to assay the effect of T3E proteins in bacterial virulence (Sohn et al. 2007), with a procedure adapted from Macho and associates (2010). Briefly, plant leaves were hand inoculated with fresh bacteria at 10^5 CFU/ml (tomato and eggplant) or 10^6 CFU/ml (col-0) with a 1-ml blunt syringe. *Pseudomonas* strains were inoculated at 5×10^5 CFU/ml in *Arabidopsis* plants. Bacteria were recovered in 200 µl of water at 0 and 3 dpi (4 dpi for *Arabidopsis* and Hawaii tomato plants inoculated with *Ralstonia* spp.). For each strain, two biological replicates were taken at 0 dpi and four at 3 to 4 dpi (each containing four discs of 5 mm in diameter from independent leaves). Bacterial suspensions were serially 10-fold diluted and plated in replicas on rich B medium plates. CFU were counted and bacterial growth calculated as the recovered CFU per square centimeter with respect to the original inoculums. Results were validated with the one-way analysis of variance test (Tukey post-analysis test) with the GraphPad software statistics package. HR assays were performed as described (Poueymiro et al. 2009) by infiltrating solutions of 1.5×10^8 bacteria/ml obtained from fresh colonies on adult *Nicotiana* plants grown in a greenhouse.

For *R. solanacearum* pathogenicity tests by soil inoculation, 5-week-old *Arabidopsis* plants grown in Jiffy-7 peat pellets were root cut, incubated with a bacterial solution at 10^8 CFU/ml for 30 min, and transferred to the growth chamber again. Symptom appearance was recorded independently for each plant according to a wilting scale of 0 to 4 (0 = no wilting; 1 = 25, 2 = 50, and 3 = 75% leaves wilted; and 4 = death).

RNA obtention and quantitative RT-PCR.

Two independent biological replicas of six tubes containing six leaf discs from six different plants expressing each AWR and control proteins were harvested at different time points after induction and they were homogenized in liquid nitrogen. RNA was extracted from the samples (NucleoSpin RNA plant; Macherey-Nagel, Düren, Germany) according to the manufacturer's protocol and quantified afterward. Approximately 2 µg of total RNA was subjected to retrotranscription with anchored oligo-$(dT)_{18}$ primers (Transcriptor first strand cDNA synthesis

kit; Roche). For quantitative real-time PCR, a Light Cycler 480 (Roche) with SYBR Green chemistry was used with two technical replicas. Tubulin was used as a housekeeping gene to normalize samples for the amount of RNA. The results were presented with respect to the transcript levels of the *gus* control gene that should not interfere with expression of the genes assessed.

Protein purification, immunodetection, and secretion studies.

For secretion studies, overnight-grown *R. solanacearum* bacteria were inoculated at 2×10^8 cells/ml in 20 ml of MM containing 10 mM glutamate and 10 mM sucrose as a carbon source. Congo red was also added to the cultures at 100 µg/ml to promote or stabilize secretion (Gueneron et al. 2000). Cultures were grown at 25°C for 12 to 18 h and bacteria were separated from the medium by centrifugation at 4,000 × *g* for 10 min at room temperature. Cells were resuspended in 1 ml of phosphate-buffered saline (PBS) buffer, lysed by sonication, and mixed 1:1 with 2× Laemmli sample loading buffer. Culture supernatants were filtered through a 0.22-µm-pore membrane to eliminate residual cells, which was confirmed by plating 200 µl into a rich agar plate. Proteins were then precipitated from the medium by adding one volume of 25% trichloroacetic acid and incubating overnight at 4°C. Precipitated proteins were pelleted by centrifugation at 6,000 × *g* for 30 min at 4°C, washed twice in cold 90% acetone, dried, resuspended in 100 µl PBS, mixed 1:1 with 2× Laemmli buffer, and subjected to Western-blot analysis.

Sodium dodecyl sulfate polyacrylamide gel electrophoresis and Western-blot analysis.

Samples were routinely mixed 1:1 with Laemmli buffer (0.2 M dithiothreitol, 0.125 Tris-HCl [pH 7.5], 4% sodium dodecyl sulfate, and 20% glycerol), loaded into 1-mm-wide 7.5% acrylamide gels, and migrated for 1 to 3 h at 120 to 170 V (Bio-Rad, Munich). Proteins were transferred to PVDF membranes (Amersham, Bucks, U.K.) overnight at 4°C (30 V) or 1 h at room temperature (100 V). For HA-tag detection, membranes were incubated overnight at 4°C or 3 to 5 h at room temperature with anti-HA rat monoclonal antibody (clone 3F10; Roche) already conjugated to HRP (diluted 1/4000). For YFP detection, membranes were incubated for 1 h at room temperature with anti-green fluorescent protein rabbit polyclonal antibody (Santa Cruz Biotechnology Inc., Santa Cruz, CA, U.S.A.) already conjugated to HRP (diluted 1/1000). For detection, immobilon ECL (Millipore) and a LAS-4000 mini system (Fujifilm, Tokyo) were used, or Amersham Hypercassette films (GE Healthcare) developed with silver nitrate in a Medical Film Processor FPM-100A (Fujifilm).

In silico analysis of the AWR gene family.

DNA and protein BLAST analyses were performed separately for all AWR sequences (nonredundant protein sequences) to find related members in other *Ralstonia* strains or other bacterial species. InterPro scan was used as an integrated database for protein "signatures" prediction of AWR. The PHYRE database was used for three-dimensional predictions. To obtain similarity and identity values between AWR proteins and their representative homologs in other species, we used the EMBOSS Needle online software that performs a global alignment of two given sequences. Protein sequences that showed similarity to AWR (*e* value < 0.01 with a sequence coverage ≥30% or sequence identity ≥20% with higher *e* values) were aligned using the MAFFT program (E-INS-i parameter suitable for sequences with multiple conserved domains and long gaps) and edited with GBlocks (allowing smaller final blocks, smaller gap position, and less strict flanking positions). Phylogenetic analysis was performed by the MrBayes program (Huelsenbeck and Ronquist 2001), based in a Bayesian estimation, with a stringency convergence <0.01, and contrasted with PhyML, based in a maximum-likelihood estimation (100 trials performed). All sequences used for tree constructions and their access number are described in Supplementary Table S2.

ACKNOWLEDGMENTS

We thank C. Boucher, S. Rivas, and N. Sánchez-Coll for their advice, support, and stimulating discussions; A. Sebé and M. Riutort for their valuable assistance with phylogenetic analyses; and E. Washington for kindly providing plasmid pMDC7-Citrine. M. Solé held a Formación de Personal Investigador Ph.D. fellowship from the Ministerio de Ciencia, Tecnología e Innovación (MICINN) and an EMBO (European Molecular Biology Organization) short-term fellowship. This work was supported by grants SGR0052 and CONES2010-0030 from the Comissionat per Universitats i Recerca of the Generalitat de Catalunya and HF2008-0021, BIO2006-09019 and AGL2010-21870 from the MICINN.

LITERATURE CITED

Alfano, J. R., and Collmer, A. 2004. Type III secretion system effector proteins: Double agents in bacterial disease and plant defense. Annu. Rev. Phytopathol. 42:385-414.

Angot, A., Peeters, N., Lechner, E., Vailleau, F., Baud, C., Gentzbittel, L., Sartorel, E., Genschik, P., Boucher, C., and Genin, S. 2006. *Ralstonia solanacearum* requires F-box-like domain-containing type III effectors to promote disease on several host plants. Proc. Natl. Acad. Sci. U.S.A. 103:14620-14625.

Arnold, D. L., Pitman, A., and Jackson, R. W. 2003. Pathogenicity and other genomic islands in plant pathogenic bacteria. Mol. Plant Pathol. 4:407-420.

Attree, O., and Attree, I. 2001. A second type III secretion system in *Burkholderia pseudomallei*: Who is the real culprit? Microbiology 147:3197-3199.

Bahrani, F. K., Sansonetti, P. J., and Parsot, C. 1997. Secretion of Ipa proteins by *Shigella flexneri*: Inducer molecules and kinetics of activation. Infect. Immun. 65:4005-4010.

Bernard, P., Gabant, P., Bahassi, E. M., and Couturier, M. 1994. Positive-selection vectors using the F plasmid ccdB killer gene. Gene 148:71-74.

Block, A., Li, G., Fu, Z. Q., and Alfano, J. R. 2008. Phytopathogen type III effector weaponry and their plant targets. Curr. Opin. Plant Biol. 11:396-403.

Boucher, C., Barberis, P., Trigalet, A., and Demery, D. 1985. Transposon mutagenesis of *Pseudomonas solanacearum*: Isolation of TnS-induced virulent mutants. J. Gen. Microbiol. 131:2449-2457.

Boucher, C. A., Van Gijsegem, F., Barberis, P. A., Arlat, M., and Zischek, C. 1987. *Pseudomonas solanacearum* genes controlling both pathogenicity on tomato and hypersensitivity on tobacco are clustered. J. Bacteriol. 169:5626-5632.

Buttner, D., and He, S. Y. 2009. Type III protein secretion in plant pathogenic bacteria. Plant Physiol. 150:1656-1664.

Carney, B. F., and Denny, T. P. 1990. A cloned avirulence gene from *Pseudomonas solanacearum* determines incompatibility on *Nicotiana tabacum* at the host species level. J. Bacteriol. 172:4836-4843.

Castresana, J. 2000. Selection of conserved blocks from multiple alignments for their use in phylogenetic analysis. Mol. Biol. Evol. 17:540-552.

Coll, N. S., Epple, P., and Dangl, J. L. 2011. Programmed cell death in the plant immune system. Cell Death Differ. 18:1247-1256.

Cui, H., Xiang, T., and Zhou, J. M. 2009. Plant immunity: A lesson from pathogenic bacterial effector proteins. Cell Microbiol. 11:1453-1461.

Cunnac, S., Boucher, C., and Genin, S. 2004a. Characterization of the cis-acting regulatory element controlling HrpB-mediated activation of the type III secretion system and effector genes in *Ralstonia solanacearum*. J. Bacteriol. 186:2309-2318.

Cunnac, S., Occhialini, A., Barberis, P., Boucher, C., and Genin, S. 2004b. Inventory and functional analysis of the large Hrp regulon in *Ralstonia solanacearum*: Identification of novel effector proteins translocated to plant host cells through the type III secretion system. Mol. Microbiol. 53:115-128.

Cunnac, S., Chakravarthy, S., Kvitko, B. H., Russell, A. B., Martin, G. B., and Collmer, A. 2010. Genetic disassembly and combinatorial reassembly identify a minimal functional repertoire of type III effectors in *Pseudomonas syringae*. Proc. Natl. Acad. Sci. U.S.A. 108:2975-2980.

Dean, P. 2011. Functional domains and motifs of bacterial type III effector proteins and their roles in infection. FEMS (Fed. Eur. Microbiol. Soc.) Microbiol. 35:1100-1125.

Deslandes, L., Olivier, J., Peeters, N., Feng, D. X., Khounlotham, M., Boucher, C., Somssich, I., Genin, S., and Marco, Y. 2003. Physical interaction between RRS1-R, a protein conferring resistance to bacterial wilt, and PopP2, a type III effector targeted to the plant nucleus. Proc. Natl. Acad. Sci. U.S.A. 100:8024-8029.

Fabro, G., Steinbrenner, J., Coates, M., Ishaque, N., Baxter, L., Studholme, D. J., Korner, E., Allen, R. L., Piquerez, S. J., Rougon-Cardoso, A., Greenshields, D., Lei, R., Badel, J. L., Caillaud, M. C., Sohn, K. H., Van den Ackerveken, G., Parker, J. E., Beynon, J., and Jones, J. D. 2011. Multiple candidate effectors from the oomycete pathogen *Hyaloperonospora arabidopsidis* suppress host plant immunity. PLoS Pathog. 7:e1002348. Published online.

Galan, J. E., and Collmer, A. 1999. Type III secretion machines: Bacterial devices for protein delivery into host cells. Science 284:1322-1328.

Gopalan, S., Wei, W., and He, S. Y. 1996. *hrp* gene-dependent induction of hin1: A plant gene activated rapidly by both harpins and the avrPto gene-mediated signal. Plant J. 10:591-600.

Gueneron, M., Timmers, A. C., Boucher, C., and Arlat, M. 2000. Two novel proteins, PopB, which has functional nuclear localization signals, and PopC, which has a large leucine-rich repeat domain, are secreted through the *hrp*-secretion apparatus of *Ralstonia solanacearum*. Mol. Microbiol. 36:261-277.

Guidot, A., Prior, P., Schoenfeld, J., Carrere, S., Genin, S., and Boucher, C. 2007. Genomic structure and phylogeny of the plant pathogen *Ralstonia solanacearum* inferred from gene distribution analysis. J. Bacteriol. 189:377-387.

Guidot, A., Coupat, B., Fall, S., Prior, P., and Bertolla, F. 2009. Horizontal gene transfer between *Ralstonia solanacearum* strains detected by comparative genomic hybridization on microarrays. ISME J 3:549-562.

Ham, J. H., Melanson, R. A., and Rush, M. C. 2010. *Burkholderia glumae*: Next major pathogen of rice? Mol. Plant Pathol. 12:329-339.

Hann, D. R., Gimenez-Ibanez, S., and Rathjen, J. P. 2010. Bacterial virulence effectors and their activities. Curr. Opin. Plant Biol. 13:388-393.

Hayward, A. C. 2000. *Ralstonia solanacearum*. Pages 32-42 in: Encyclopedia of Microbiology. J. Lederberg, ed. Academic Press, Dordrecht, The Netherlands.

He, S. Y., Nomura, K., and Whittam, T. S. 2004. Type III protein secretion mechanism in mammalian and plant pathogens. Biochim. Biophys. Acta 1694:181-206.

Hogenhout, S. A., Van der Hoorn, R. A., Terauchi, R., and Kamoun, S. 2009. Emerging concepts in effector biology of plant-associated organisms. Mol. Plant-Microbe Interact. 22:115-122.

Hong, J., Ji, P., Momol, M. T., Jones, J. B., Olson, S. M., Pradhanang, P., and Guven, K. 2005. *Ralstonia solanacearum* detection in tomato irrigation ponds and weeds. Pages 309-311 in: Proceedings of the First International Symposium on Tomato Diseases. International Society for Horticultural Science, Orlando, FL, U.S.A.

Hu, J., Barlet, X., Deslandes, L., Hirsch, J., Feng, D. X., Somssich, I., and Marco, Y. 2008. Transcriptional responses of *Arabidopsis thaliana* during wilt disease caused by the soil-borne phytopathogenic bacterium, *Ralstonia solanacearum*. PLoS ONE 3:e2589. Published online.

Huelsenbeck, J. P., and Ronquist, F. 2001. MRBAYES: Bayesian inference of phylogenetic trees. Bioinformatics 17:754-755.

Jones, J. D., and Dangl, J. L. 2006. The plant immune system. Nature 444:323-329.

Katoh, K., Misawa, K., Kuma, K., and Miyata, T. 2002. MAFFT: A novel method for rapid multiple sequence alignment based on fast Fourier transform. Nucleic Acids Res. 30:3059-3066.

Kay, S., and Bonas, U. 2009. How *Xanthomonas* type III effectors manipulate the host plant. Curr. Opin. Microbiol. 12:37-43.

Keogh, R. C., Deverall, B. J., and McLeod, S. 1980. Comparison of histological and physiological responses to *Phakopsora pachyrhizi* in resistant and susceptible soybean. Trans. Br. Mycol. Soc. 74:329-333.

Kiba, A., Tomiyama, H., Takahashi, H., Hamada, H., Ohnishi, K., Okuno, T., and Hikichi, Y. 2003. Induction of resistance and expression of defense-related genes in tobacco leaves infiltrated with *Ralstonia solanacearum*. Plant Cell Physiol. 44:287-295.

Kim, N.H., Choi, H.W., and Hwang, B.K. 2010. *Xanthomonas campestris* pv. *vesicatoria* effector AvrBsT induces cell death in pepper, but suppresses defense responses in tomato. Mol. Plant-Microbe Interact. 23:1069-1082.

Kvitko, B. H., Park, D. H., Velasquez, A. C., Wei, C. F., Russell, A. B., Martin, G. B., Schneider, D. J., and Collmer, A. 2009. Deletions in the repertoire of *Pseudomonas syringae* pv. tomato DC3000 type III secretion effector genes reveal functional overlap among effectors. PLoS Pathog. 5:e1000388. Published online.

Lavie, M., Shillington, E., Eguiluz, C., Grimsley, N., and Boucher, C. 2002. PopP1, a new member of the YopJ/AvrRxv family of type III effector proteins, acts as a host-specificity factor and modulates aggressiveness of *Ralstonia solanacearum*. Mol. Plant-Microbe Interact. 15:1058-1068.

Lee, P. C., Stopford, C. M., Svenson, A. G., and Rietsch, A. 2010. Control of effector export by the *Pseudomonas aeruginosa* type III secretion proteins PcrG and PcrV. Mol. Microbiol. 75:924-941.

Lewis, J. D., Guttman, D. S., and Desveaux, D. 2009. The targeting of plant cellular systems by injected type III effector proteins. Semin. Cell Dev. Biol. 20:1055-1063.

Lewis, J. D., Lee, A., Ma, W., Zhou, H., Guttman, D. S., and Desveaux, D. 2011. The YopJ superfamily in plant-associated bacteria. Mol. Plant Pathol. 12:928-937.

Lin, Y. M., Chou, I. C., Wang, J. F., Ho, F. I., Chu, Y. J., Huang, P. C., Lu, D. K., Shen, H. L., Elbaz, M., Huang, S. M., and Cheng, C. P. 2008. Transposon mutagenesis reveals differential pathogenesis of *Ralstonia solanacearum* on tomato and *Arabidopsis*. Mol. Plant-Microbe Interact. 21:1261-1270.

Macho, A. P., Guidot, A., Barberis, P., Beuzon, C. R., and Genin, S. 2010. A competitive index assay identifies several *Ralstonia solanacearum* type III effector mutant strains with reduced fitness in host plants. Mol. Plant-Microbe Interact. 23:1197-1205.

Marlovits, T., and Stebbins, C. 2009. Type III secretion systems shape up as they ship out. Curr. Opin. Microbiol. 13:1-6.

Marx, C. J., and Lidstrom, M. E. 2002. Broad-host-range cre-lox system for antibiotic marker recycling in gram-negative bacteria. Biotechniques 33:1062-1067.

Milling, A., Babujee, L., and Allen, C. 2011. *Ralstonia solanacearum* extracellular polysaccharide is a specific elicitor of defense responses in wilt-resistant tomato plants. PLoS One 6:e15853. Published online.

Mole, B. M., Baltrus, D. A., Dangl, J. L., and Grant, S. R. 2007. Global virulence regulation networks in phytopathogenic bacteria. Trends Microbiol. 15:363-371.

Monteiro, F., Sole, M., van Dijk, I., and Valls, M. 2012. A chromosomal insertion toolbox for promoter probing, mutant complementation and pathogenicity studies in *Ralstonia solanacearum*. Mol. Plant-Microbe Interact. 25: 557-568.

Mukaihara, T., and Tamura, N. 2009. Identification of novel *Ralstonia solanacearum* type III effector proteins through translocation analysis of *hrpB*-regulated gene products. Microbiology 155:2235-2244.

Mukaihara, T., Tamura, N., and Iwabuchi, M. 2010. Genome-wide identification of a large repertoire of *Ralstonia solanacearum* type III effector proteins by a new functional screen. Mol. Plant-Microbe Interact. 23:251-262.

Naum, M., Brown, E. W., and Mason-Gamer, R. J. 2009. Phylogenetic evidence for extensive horizontal gene transfer of type III secretion system genes among enterobacterial plant pathogens. Microbiology 155:3187-3199.

Pontier, D., Tronchet, M., Rogowsky, P., Lam, E., and Roby, D. 1998. Activation of hsr203, a plant gene expressed during incompatible plant-pathogen interactions, is correlated with programmed cell death. Mol. Plant-Microbe Interact. 11:544-554.

Poueymiro, M., and Genin, S. 2009. Secreted proteins from *Ralstonia solanacearum*: A hundred tricks to kill a plant. Curr. Opin. Microbiol. 12:44-52.

Poueymiro, M., Cunnac, S., Barberis, P., Deslandes, L., Peeters, N., Cazale-Noel, A.C., Boucher, C., and Genin, S. 2009. Two type III secretion system effectors from *Ralstonia solanacearum* GMI1000 determine host-range specificity on tobacco. Mol. Plant-Microbe Interact. 22:538-550.

Preston, G. M. 2007. Metropolitan microbes: Type III secretion in multihost symbionts. Cell Host Microbe 2:291-294.

Rahme, L. G., Tan, M. W., Le, L., Wong, S. M., Tompkins, R. G., Calderwood, S. B., and Ausubel, F. M. 1997. Use of model plant hosts to identify *Pseudomonas aeruginosa* virulence factors. Proc. Natl. Acad. Sci. U.S.A. 94:13245-13250.

Rainbow, L., Hart, C. A., and Winstanley, C. 2002. Distribution of type III secretion gene clusters in *Burkholderia pseudomallei*, *B. thailandensis* and *B. mallei*. J. Med. Microbiol. 51:374-384.

Remigi, P., Anisimova, M., Guidot, A., Genin, S., and Peeters, N. 2011. Functional diversification of the GALA type III effector family contributes to *Ralstonia solanacearum* adaptation on different plant hosts. New Phytol. 192:976-987.

Robertson, A. E., Wechter, W. P., Denny, T. P., Fortnum, B. A., and Kluepfel, D. A. 2004. Relationship between avirulence gene (avrA) diversity in *Ralstonia solanacearum* and bacterial wilt incidence. Mol. Plant-Microbe Interact. 17:1376-1384.

Salanoubat, M., Genin, S., Artiguenave, F., Gouzy, J., Mangenot, S., Arlat, M., Billault, A., Brottier, P., Camus, J. C., Cattolico, L., Chandler, M., Choisne, N., Claudel-Renard, C., Cunnac, S., Demange, N., Gaspin, C.,

Lavie, M., Moisan, A., Robert, C., Saurin, W., Schiex, T., Siguier, P., Thebault, P., Whalen, M., Wincker, P., Levy, M., Weissenbach, J., and Boucher, C. A. 2002. Genome sequence of the plant pathogen *Ralstonia solanacearum*. Nature 415:497-502.

Sambrook, J., and Russell, D. 2001. Molecular Cloning: A Laboratory Manual, 3rd ed. Cold Spring Harbor Laboratory Press, Cold Spring Harbor, NY, U.S.A.

Schulze-Lefert, P., and Panstruga, R. 2010. A molecular evolutionary concept connecting nonhost resistance, pathogen host range, and pathogen speciation. Trends Plant Sci. 16:117-125.

Segonzac, C., and Zipfel, C. 2011. Activation of plant pattern-recognition receptors by bacteria. Curr. Opin. Microbiol. 14:54-61.

Shan, L., He, P., and Sheen, J. 2007. Intercepting host MAPK signaling cascades by bacterial type III effectors. Cell Host Microbe 1:167-174.

Smith, J. J., Jones, D. R., Karamura, E. B., Blomme, G., and Turyagyenda, F. L. 2008. An analysis of the risk from *Xanthomonas campestris* pv. *musacearum* to banana cultivation in Eastern, Central and Southern Africa, Montpellier, France.

Sohn, K. H., Lei, R., Nemri, A., and Jones, J. D. 2007. The downy mildew effector proteins ATR1 and ATR13 promote disease susceptibility in *Arabidopsis thaliana*. Plant Cell 19:4077-4090.

Song, C., and Yang, B. 2010. Mutagenesis of 18 type III effectors reveals virulence function of XopZ(PXO99) in *Xanthomonas oryzae* pv. *oryzae*. Mol. Plant-Microbe Interact. 23:893-902.

Stavrinides, J., McCann, H. C., and Guttman, D. S. 2008. Host-pathogen interplay and the evolution of bacterial effectors. Cell Microbiol. 10:285-292.

Tao, Y., Xie, Z., Chen, W., Glazebrook, J., Chang, H.-S., Han, B., Zhu, T., Zou, G., and Katagiri, F. 2003. Quantitative Nature of *Arabidopsis* Responses during Compatible and Incompatible Interactions with the Bacterial Pathogen *Pseudomonas syringae*. Plant Cell Online 15:317-330.

Tasset, C., Bernoux, M., Jauneau, A., Pouzet, C., Briere, C., Kieffer-Jacquinod, S., Rivas, S., Marco, Y., and Deslandes, L. 2010. Autoacetylation of the *Ralstonia solanacearum* effector PopP2 targets a lysine residue essential for RRS1-R-mediated immunity in *Arabidopsis*. PLoS Pathog. 6:e1001202. Published online.

Tayeb, L. A., Lefevre, M., Passet, V., Diancourt, L., Brisse, S., and Grimont, P. A. D. 2008. Comparative phylogenies of *Burkholderia*, *Ralstonia*, *Comamonas*, *Brevundimonas* and related organisms derived from *rpoB, gyrB* and *rrs* gene sequences. Res. Microbiol. 159:169-177.

Thordal-Christensen, H., Zhang, Z., Wei, Y., and Collinge, D. B. 1997. Subcellular localization of H_2O_2 in plants. H_2O_2 accumulation in papillae and hypersensitive response during the barley–powdery mildew interaction. Plant J. 11:1187-1194.

Torres, M. A. 2010. ROS in biotic interactions. Physiol. Plant. 138:414-429.

Tsuda, K., and Katagiri, F. 2010. Comparing signaling mechanisms engaged in pattern-triggered and effector-triggered immunity. Curr. Opin. Plant Biol. 13:459-465.

Turner, M., Jauneau, A., Genin, S., Tavella, M. J., Vailleau, F., Gentzbittel, L., and Jardinaud, M. F. 2009. Dissection of bacterial wilt on *Medicago truncatula* revealed two type III secretion system effectors acting on root infection process and disease development. Plant Physiol. 150:1713-1722.

Viallard, V., Poirier, I., Cournoyer, B., Haurat, J., Wiebkin, S., Ophel-Keller, K., and Balandreau, J. 1998. *Burkholderia graminis* sp. nov., a rhizospheric *Burkholderia* species, and reassessment of *Pseudomonas* phenazinium, *Pseudomonas pyrrocinia* and *Pseudomonas glathei* as *Burkholderia*. Int. J. Syst. Bacteriol. 48:549-563.

Wang, J.-F., Olivier, J., Thoquet, P., Mangin, B., Sauviac, L., and Grimsley, N. H. 2000. Resistance of tomato line Hawaii7996 to *Ralstonia solanacearum* Pss4 in Taiwan is controlled mainly by a major strain-specific locus. Mol. Plant-Microbe Interact. 13:6-13.

Willems, A., Goor, M., Thielemans, S., Gillis, M., Kersters, K., and De Ley, J. 1992. Transfer of several phytopathogenic *Pseudomonas* species to *Acidovorax* as *Acidovorax avenae* subsp. *avenae* subsp. *nov.*, comb. nov., *Acidovorax avenae* subsp. *citrulli*, *Acidovorax avenae* subsp. *cattleyae*, and *Acidovorax konjaci*. Int. J. Syst. Bacteriol. 42:107-119.

Wroblewski, T., Caldwell, K. S., Piskurewicz, U., Cavanaugh, K. A., Xu, H., Kozik, A., Ochoa, O., McHale, L. K., Lahre, K., Jelenska, J., Castillo, J. A., Blumenthal, D., Vinatzer, B. A., Greenberg, J. T., and Michelmore, R. W. 2009. Comparative large-scale analysis of interactions between several crop species and the effector repertoires from multiple pathovars of *Pseudomonas* and *Ralstonia*. Plant Physiol. 150:1733-1749.

Wu, M., and Eisen, J.A. 2008. A simple, fast, and accurate method of phylogenomic inference. Genome Biol. 9:R151.

Wuthiekanun, V., and Peacock, S. J. 2006. Management of melioidosis. Expert Rev. Anti-Infe. 4:445-455.

Zhou, J. M., and Chai, J. 2008. Plant pathogenic bacterial type III effectors subdue host responses. Curr. Opin. Microbiol. 11:179-185.

AUTHOR-RECOMMENDED INTERNET RESOURCES

National Center for Biotechnology Information BLAST database: blast.ncbi.nlm.nih.gov/Blast.cgi
European Bioinformatics Institute (EBI) InterPro server: www.ebi.ac.uk/Tools/pfa/iprscan
EBI EMBOSS needle server: www.ebi.ac.uk/Tools/psa/emboss_needle
GBlocks server: molevol.cmima.csic.es/castresana/Gblocks_server.html
MAFFT server: mafft.cbrc.jp/alignment/server
PhyM server: www.atgc-montpellier.fr/phyml
PHYRE database: www.sbg.bio.ic.ac.uk/~phyre

Cell Death and Differentiation (2014), 1–10

www.nature.com/cdd

The plant metacaspase AtMC1 in pathogen-triggered programmed cell death and aging: functional linkage with autophagy

NS Coll*[,1,2], A Smidler[1,8], M Puigvert[2], C Popa[2], M Valls[2,3] and JL Dangl[1,4,5,6,7]

Autophagy is a major nutrient recycling mechanism in plants. However, its functional connection with programmed cell death (PCD) is a topic of active debate and remains not well understood. Our previous studies established the plant metacaspase AtMC1 as a positive regulator of pathogen-triggered PCD. Here, we explored the linkage between plant autophagy and AtMC1 function in the context of pathogen-triggered PCD and aging. We observed that autophagy acts as a positive regulator of pathogen-triggered PCD in a parallel pathway to AtMC1. In addition, we unveiled an additional, pro-survival homeostatic function of AtMC1 in aging plants that acts in parallel to a similar pro-survival function of autophagy. This novel pro-survival role of AtMC1 may be functionally related to its prodomain-mediated aggregate localization and potential clearance, in agreement with recent findings using the single budding yeast metacaspase YCA1. We propose a unifying model whereby autophagy and AtMC1 are part of parallel pathways, both positively regulating HR cell death in young plants, when these functions are not masked by the cumulative stresses of aging, and negatively regulating senescence in older plants.
Cell Death and Differentiation advance online publication, 2 May 2014; doi:10.1038/cdd.2014.50

An emerging theme in cell death research is that cellular processes thought to be regulated by linear signaling pathways are, in fact, complex. Autophagy, initially considered merely a nutrient recycling mechanism necessary for cellular homeostasis, was recently shown to regulate cell death, mechanistically interacting with components that control apoptosis. Deficient autophagy can result in apoptosis[1–3] and autophagy hyper-activation can also lead to programmed cell death (PCD).[4] In addition, the pro-survival function of autophagy is mediated by apoptosis inhibition and apoptosis mediates autophagy, although this cross-regulation is not fully understood.[5]

In plants, autophagy can also have both pro-survival and pro-death functions. Autophagy-deficient plants exhibit accelerated senescence,[6–8] starvation-induced chlorosis,[6,7,9] hypersensitivity to oxidative stress[10] and endoplasmic reticulum stress.[11] Further, autophagy-deficient plants cannot limit the spread of cell death after infection with tissue-destructive microbial infections.[12,13] The plant phytohormone salicylic acid (SA) mediates most of these phenotypes.[8] Autophagy has an essential, pro-survival role in situations where there is an increasing load of damaged proteins and organelles that need to be eliminated, that is, during aging or stress. Autophagy has an opposing, pro-death role during developmentally regulated cell death[14,15] or during the pathogen-triggered hypersensitive response PCD (hereafter, HR) that occurs locally at the site of attempted pathogen attack.[16,17] The dual pro-death/pro-survival functions of plant autophagy remain a topic of active debate.

Also under scrutiny are possible novel functions of caspases and caspase-like proteins as central regulators of pro-survival processes. Caspases were originally defined as executioners of PCD in animals, but increasing evidence indicates that several caspases have non-apoptotic regulatory roles in cellular differentiation, motility and in the mammalian immune system.[18–20]

Yeast, protozoa and plants do not have canonical caspases, despite the occurrence of morphologically heterogeneous PCDs.[21] More than a decade ago, distant caspase homologs termed metacaspases were identified in these organisms using structural homology searches.[22] Metacaspases were classified into type I or type II metacaspases based on the presence or absence of an N-terminal prodomain, reminiscent of the classification in animals into initiator/inflammatory or executioner caspases, respectively. Despite the architectural analogy between caspases and metacaspases, differences in their structure, function, activation and mode of action exist.[23–25]

Metacaspases mediate PCD in yeast,[26–31] leishmania,[32,33] trypanosoma[34] and plants.[24] We demonstrated that two type I metacaspases, AtMC1 and AtMC2, antagonistically regulate HR in *Arabidopsis thaliana*.[35] Our work showed that AtMC1 is

[1]Department of Biology, University of North Carolina, Chapel Hill, NC 27599, USA; [2]Centre for Research in Agricultural Genomics, Barcelona, Spain; [3]Department of Genetics, Universitat de Barcelona, Barcelona, Spain; [4]Howard Hughes Medical Institute, University of North Carolina, Chapel Hill, NC 27599, USA; [5]Curriculum in Genetics and Molecular Biology, University of North Carolina, Chapel Hill, NC 27599, USA; [6]Department of Microbiology and Immunology, University of North Carolina, Chapel Hill, NC 27599, USA and [7]Carolina Center for Genome Sciences University of North Carolina, Chapel Hill, NC, USA
*Corresponding author: NS Coll, Centre for Research in Agricultural Genomics, Campus UAB, Edifici CRAG, Bellaterra 08193, Barcelona, Spain. Tel: + 34 93 5636600; Fax: +34 93 5636601; E-mail: nuria.sanchez-coll@cragenomica.es
[8]Current address: Department of Immunology and Infectious Diseases, Harvard School of Public Health, Boston, MA 02115, USA.
Abbreviations: PCD, programmed cell death; HR, hypersensitive response cell death; SA, salicylic acid; ROS, reactive oxygen species; FB1, fumonisin B1; NLR, nucleotide-binding domain and leucine-rich repeat containing; BTH, benzo(1,2,3)thiadiazole-7-carbothioic acid *S*-methyl ester
Received 06.2.14; revised 11.3.14; accepted 13.3.14; Edited by G Salvesen

a positive regulator of HR and that this function is mediated by its catalytic activity and negatively regulated by the AtMC1 N-terminal prodomain. AtMC2 antagonizes AtMC1-mediated HR.

Besides AtMC2, new examples of metacaspases with a pro-life/non-PCD role are emerging. Protozoan metacaspases are involved in cell cycle dynamics[34,36–38] and cell proliferation.[39] The yeast metacaspase Yca1 alters cell cycle dynamics[40] and interestingly, is required for clearance of insoluble protein aggregates, thus contributing to yeast fitness.[41]

Here, we explore the linkage between plant autophagy and AtMC1 function in the context of pathogen-triggered HR and aging. Our data support a model wherein autophagy and AtMC1 are part of parallel pathways, both positively regulating HR cell death in young plants and negatively regulating senescence in older plants.

Results

Autophagy components and AtMC1 act additively to positively regulate HR. Autophagy is induced by activation of plant intracellular NLR (nucleotide-binding domain and leucine-rich repeat containing) immune receptors upon pathogen recognition, and thus can be a positive regulator of HR in Arabidopsis young leaves.[16,17] To ascertain whether AtMC1- and autophagy-mediated HR are part of the same pathway, we crossed Arabidopsis *atmc1* knockout plants[35] to two different autophagy-deficient knockout mutants: *atg5*[42] and *atg18a*.[13] ATG5 and ATG18a are each required for autophagosome formation at different points of the autophagic pathway.[7,43] We infected 2-week-old wild-type Col-0, *atmc1*, *atg5*, *atg18a*, *atmc1 atg5* and *atmc1 atg18a* plants with *Pseudomonas syringae* pathovar tomato strain (*Pto* DC3000 expressing the type III effector *avrRpm1 Pto* DC3000(*avrRpm1*)). Recognition of AvrRpm1 triggers HR mediated by the intracellular NLR receptor RPM1.[44] We quantified HR using a single-cell death assay,[35] and we observed suppression of RPM1-mediated HR both in *atmc1*[35] and in autophagy-deficient mutant plants. When combined, autophagy and *atmc1* deficiencies had an additive effect on HR suppression (Figure 1a). Thus, autophagy and AtMC1 mediate independent pathways triggered by NLR activation that contribute to HR.

Using the same assay, we observed that the lack of AtMC2, a negative regulator of AtMC1-mediated HR cell death,[35] has no effect on autophagy-mediated HR cell death (Supplementary Figure 1). In *atmc1* and autophagy-deficient mutants, HR suppression does not result in increased susceptibility to *Pto* DC3000(*avrRpm1*), uncoupling HR and pathogen growth restriction.[35] Thus, the additive HR suppression in *atmc1 atg18a* double mutants did not result in enhanced pathogen proliferation (Figure 1b).

We also investigated whether *atmc1* mutants were defective in autophagy. Figure 1c and Supplementary Figure 2 show Col-0 and *atmc1* transgenic plants expressing the autophagosome marker GFP-ATG8a with or without concanamycin A treatment.[43] Plants lacking *atg18a* (or *atg5*) are defective in autophagosome formation.[10,17,43] *Atmc1* mutants displayed normal autophagosome formation (Figure 1c).

Recently, the plant cargo receptor NBR1 was demonstrated to be a selective autophagy marker that constitutively over-accumulates in autophagy-deficient plants.[45] We performed immunoblot analysis of mock- or *Pto* DC3000 (*avrRpm1*)-treated plants using anti-NBR1 antisera to address whether selective autophagy was induced during HR. We observed slightly increased NBR1 accumulation 12-h post-inoculation in all lines tested (Figures 1d and e), indicating that selective autophagy is not induced after RPM1 activation at a time point when the HR cell death is complete (Figure 1). *Atmc1* plants expressed wild-type NBR1 levels in either uninfected controls or following RPM1 activation, indicating that AtMC1 deficiency alone did not result in NBR1-mediated selective autophagy defects. As expected, *atg18a* and *atmc1 atg18a* mutants express higher NBR1 levels than wild-type plants because of defective selective autophagy.[45] This NBR1 over-accumulation is more pronounced in *atmc1 atg18* double mutants, indicating that AtMC1 may have a role in selective autophagy when bulk autophagy is defective.

SA accumulation negatively regulates the contribution of autophagy, but not of AtMC1, to RPM1-mediated HR. SID2 encodes the chloroplastic isochorismate synthase 1, the rate-limiting SA biosynthetic enzyme required for the increased accumulation of this phytohormone observed following pathogen recognition.[46] To investigate if the HR suppression phenotypes observed in young autophagy- and *atmc1*-deficient plants were SA dependent, we quantified HR in wild-type, *atmc1*, *atg18a, sid2*, *atmc1 atg18a*, *atmc1 sid2* and *atg18a sid2* and *atmc1 atg18a sid2* plants (Figure 2). *Sid2* plants supported wild-type HR cell death levels, indicating that SA accumulation is dispensable for RPM1-mediated HR.[47] Interestingly, we observed that the loss of SA accumulation restores nearly wild-type levels of HR in *atg18a*, but not in *atmc1* plants (Figure 2). This suggests that SA accumulation negatively regulates the contribution of autophagy to RPM1-mediated HR in *atg18a sid2*, but does not significantly regulate the AtMC1 contribution in *atmc1 sid2*. This observation also reinforces our hypothesis that autophagy and AtMC1 participate in separate HR signaling pathways. In *atmc1 atg18a sid2* plants, the lack of SA accumulation reverts only partially HR suppression, indicating that the additive effects on HR observed in *atmc1 atg18a* cannot be solely explained by the sum of both deficiencies. It is worth noting that at the developmental stage used for the single-cell HR assay, *atmc1*, *atg18a* and *atmc1 atg18a* expressed essentially equivalent basal SA levels (Supplementary Figure 3).

The plant respiratory burst NADPH oxidase encoded by AtrbohD is required for the reactive oxygen species (ROS) burst downstream of RPM1 activation, but contributes only modestly to regulation of RPM1-mediated HR (Supplementary Figure 4).[48] Consistent with these data, the lack of an NADPH-dependent ROS burst did not alter HR suppression in *atmc1*, *atg18a* or *atmc1 atg18a* mutants (Supplementary Figure 4), indicating that this ROS burst acts independently or upstream of AtMC1 and autophagy.

Autophagy components and AtMC1 act additively to negatively regulate senescence. Autophagy-deficient plants exhibit an early senescence phenotype, evidenced by premature leaf chlorosis.[6–9] Interestingly, *atmc1* mutants

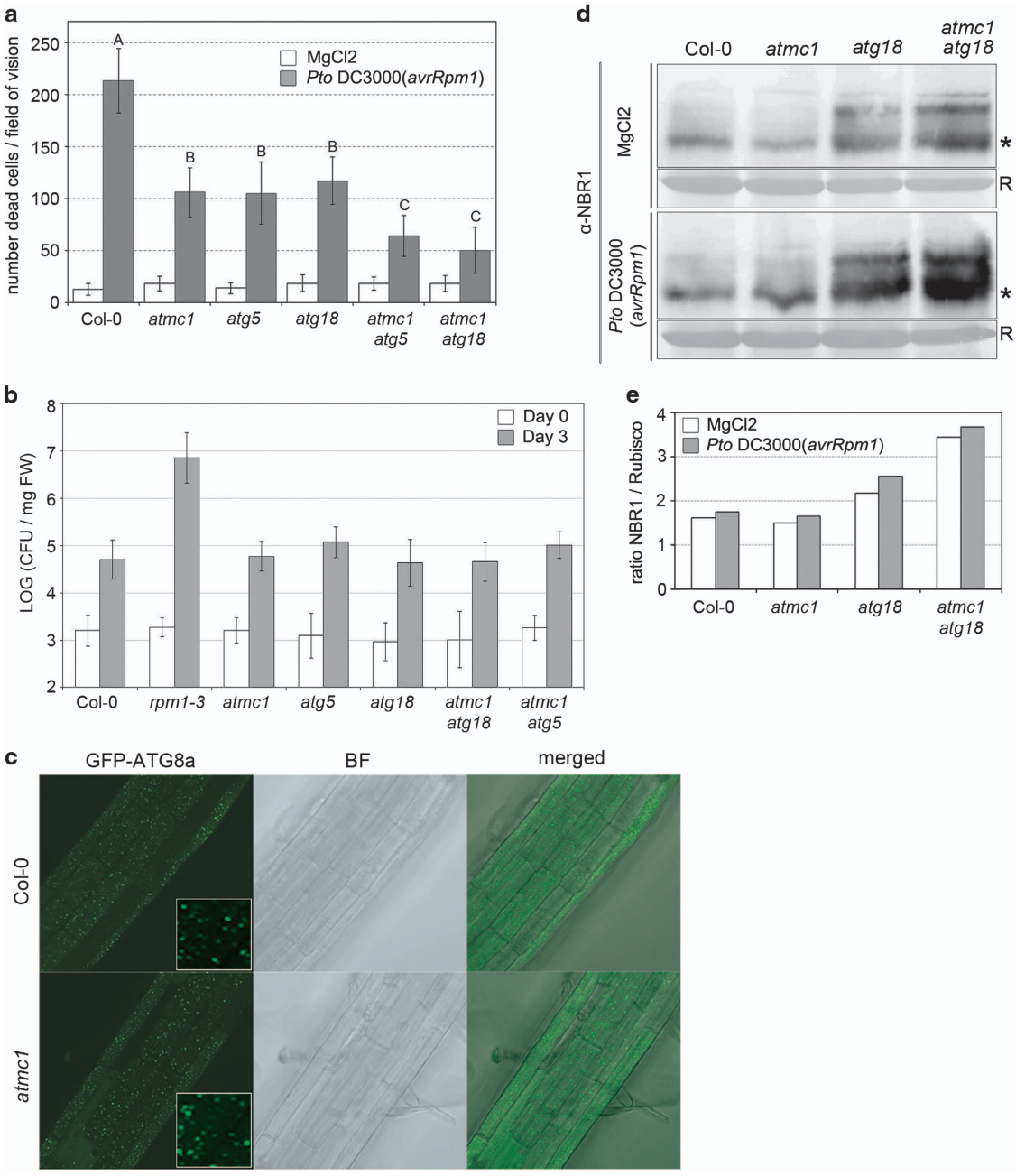

Figure 1 Autophagy components and AtMC1 act additively to positively regulate HR. (**a**) Two-week-old plants of the indicated phenotypes were vacuum infiltrated with 500 000 colony-forming units (CFU)/ml of *Pto* DC3000(*avrRpm1*) or $MgCl_2$. After 12 h, plants were stained with the cell death dye Trypan blue. To quantify cell death, all dead cells per field of vision ($\times$ 10 magnification) were counted. Values correspond to the average of 20 leaves per genotype and treatment $\pm 2 \times$ S.E. Letters indicate a significant difference following post-ANOVA Student's *t*-test ($\alpha = 0.05$). The experiment is representative of three independent replicates. (**b**) Two-week-old plants of the indicated phenotypes were dip inoculated with 2.5×10^7 CFU/ml of *Pto* DC3000(*avrRpm1*). Bacterial growth was monitored at days 0 and 3 after infection. Values indicate the average of four samples per genotype $\pm 2 \times$ S.E. The experiment was repeated three times. (**c**) One-week-old transgenic Col-0 and *atmc1* plants constitutively expressing GFP-ATG8 were treated with 1 μM concanamycin A to allow autophagosome visualization in the vacuole of root cells using confocal microscopy. BF, bright field. Inlets show $\times$ 16 magnifications of the central part of each root shown. (**d**) Western blot analysis of the NBR1 cargo receptor protein using plants of the noted genotypes treated as in (**a**). The band corresponding to NBR1 is marked with an asterisk. Coomassie-stained Rubisco (R) was used as a loading control. (**e**) Densitometry analysis of the samples in (**d**) using Multi Gauge (Fujifilm, ScienceLab 2005, version 3.0, Minato, Tokyo, Japan)

also senesce prematurely (Figure 3a). In *atmc1 atg18a*, this early senescence phenotype is enhanced and progresses faster than in either Col-0, *atmc1* or *atg18a* plants (Supplementary Figure 5). These observations indicate that similar to autophagy, AtMC1 is also required for correctly timed leaf senescence and that autophagy and AtMC1 act additively on these processes.

Quantitative PCR analysis using the senescence marker *SAG12*[49] confirmed the early senescence phenotype in 5-week-old *atmc1*, *atg18a* and *atmc1 atg18a* plants at the

transcriptional level (Figure 3b). We did not detect any differences in *SAG12* expression in 2-week-old plants. This indicates that the HR suppression phenotypes observed in *atmc1*, *atg18a* and *atmc1 atg18a* mutants cannot be explained by the early senescence onset, which occurs later.

Early senescence in autophagy-deficient plants, but not in *atmc1* plants, requires SA accumulation. It was previously shown that the onset of early senescence and growth retardation in autophagy-deficient plants is correlated with SA hyper-accumulation.[8] We confirmed and extended this result, showing that the lack of SA accumulation in *sid2 atg18a* largely reverts the early senescence phenotype of *atg18* (Figure 3a). In contrast, AtMC1-regulated senescence processes occur independently of SA accumulation, as evidenced by the *sid2 atmc1* early senescence phenotype. In addition, the fact that the lack of SA cannot fully revert the extreme early senescence phenotype of *atmc1 atg18a* indicates that the additive effects on this phenotype cannot be solely explained by the sum of both deficiencies and that other – yet unknown – factors likely mediate this additivity.

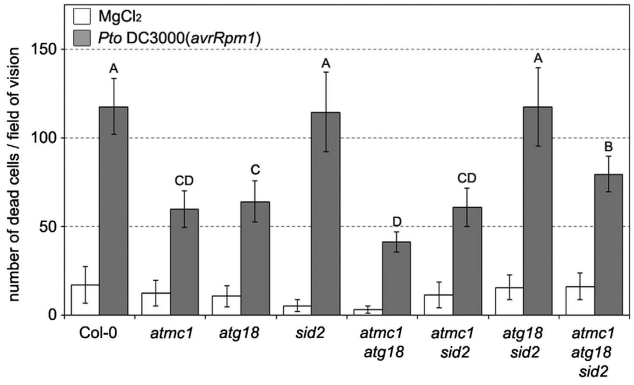

Figure 2 SA accumulation negatively regulates the autophagy contribution to RPM1-mediated HR, but does not significantly regulate the AtMC1 contribution. Two-week-old plants of the indicated phenotypes were vacuum infiltrated with 500 000 colony-forming units (CFU)/ml of *Pto* DC3000(*avrRpm1*) or $MgCl_2$. After 12 h, plants were stained with the cell death dye Trypan blue. To quantify cell death, all dead cells per field of vision ($\times$ 10 magnification) were counted. Values indicate the average of 20 samples per genotype and treatment $\pm$ 2 $\times$ S.E. Letters indicate a significant difference following post-ANOVA Student's *t*-test ($\alpha = 0.05$). The experiment is representative of three independent replicates

***atmc1* and *atg18a* mutants are hypersensitive to the SA agonist BTH and to externally generated ROS.** We next treated *atmc1*, *atg18a* and *atmc1 atg18a* with either the SA agonist benzo(1,2,3)thiadiazole-7-carbothioic acid *S*-methyl ester (BTH) or different ROS-generating agents. BTH treatment resulted in leaf chlorosis in both *atmc1* and *atg18a*, and this phenotype was enhanced in *atmc1 atg18a* but not in wild-type plants (Figure 4a). Leaf chlorosis was accompanied by increased ROS production and cell death (Figures 4b and c). The phenotype caused by BTH on these plants, grown under short-day conditions, is reminiscent of untreated plants grown 4 weeks under short-day conditions and then transferred to long-day conditions (Figure 3a). This suggests that light-dependent increases in SA accumulation trigger autophagy and AtMC1-mediated processes important for the proper remobilization of resources to reach a timely senescence.

To study the effect of ROS on autophagy or *AtMC1*-regulated processes, plants were treated with rose bengal, methyl viologen or the fungal toxin fumonisin B1 (FB1) and cell death progression was visualized using Trypan blue (Figures 4d and e). Methyl viologen treatment resulted in confined cell death in wild-type plants, modestly enhanced cell death in *atmc1* and *atg18a*, and runaway cell death in *atmc1 atg18a*. These results suggest that both AtMC1 and autophagy have a function in downregulating the toxicity of ROS. Similar results were observed using rose bengal and FB1 as ROS accumulation triggers (Figure 4b). Together, these results indicate that the primary roles of autophagy and AtMC1 in older plants may be to protect the cells against the consequences of increasing ROS and SA levels during aging. Furthermore, aging autophagy- and *atmc1*-deficient plants cannot restrict cell death caused by the necrotrophic fungus *Botrytis cinerea* (Supplementary Figure 6).[50] We infer from these results that autophagy and AtMC1 also act additively to limit cell death following necrotroph infection.

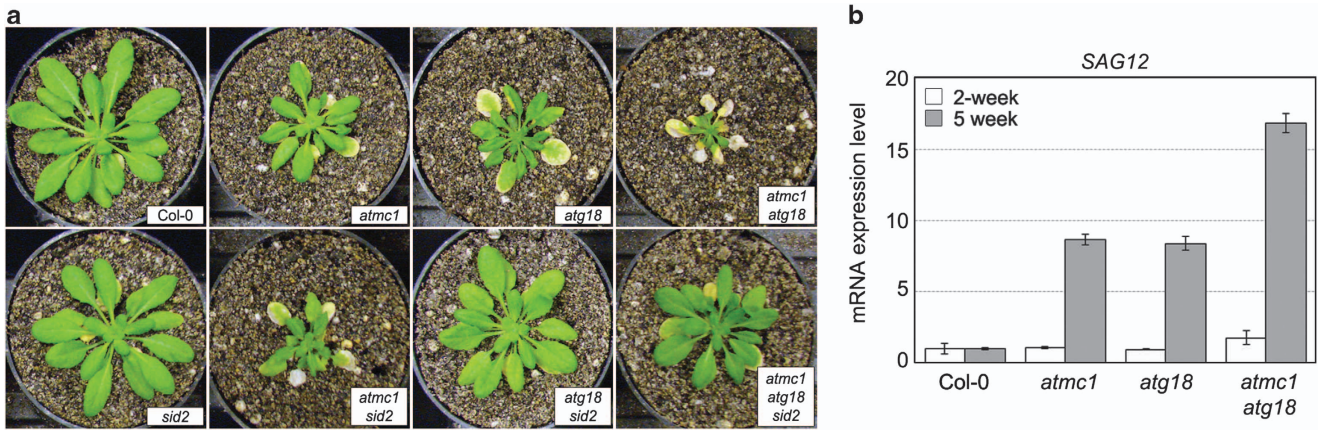

Figure 3 Autophagy components and AtMC1 act additively to negatively regulate senescence. (**a**) Early senescence was SA-dependent in autophagy-deficient plants but SA-independent in *atmc1* mutants. Pictures show plants grown for 3 weeks under short-day conditions and then transferred to long-day conditions for 4 additional weeks. (**b**) Quantitative real-time PCR analysis of the senescence marker gene SAG12 in 2- and 5-week-old plants of the indicated genotypes, normalized to EF-1α. The S.E. was calculated from three samples per genotype and the experiment was performed three times

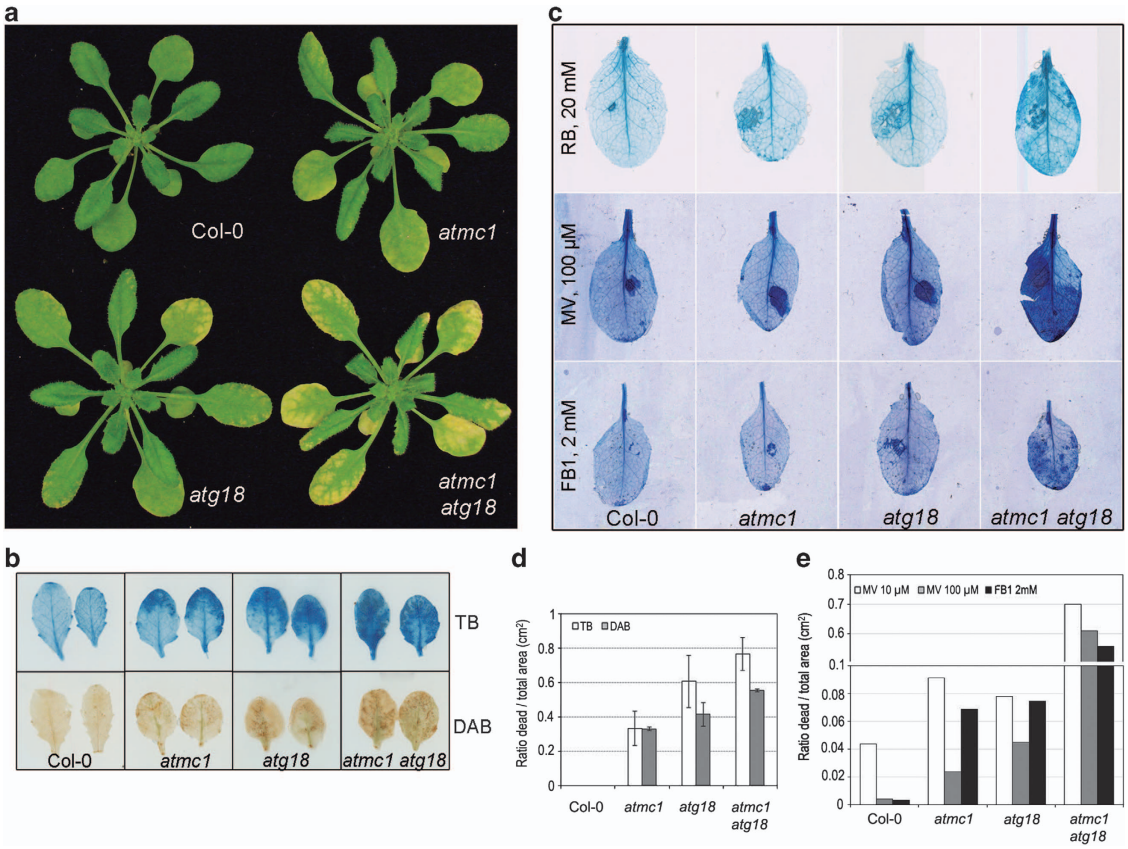

Figure 4 *Atmc1* and *atg18a* mutants are hypersensitive to the SA agonist BTH and to externally generated ROS. (**a**) Pictures of representative 4-week-old plants grown under short-day conditions, 4 days after 300 μM BTH treatment. (**b**) Representative leaves of plants treated as in (**a**) were stained with Trypan blue (TB, upper panel) or with 3,3-diamino-benzidine (DAB, lower panel) to visualize cell death and H_2O_2 accumulation, respectively. (**c**) Quantification of cell death and H_2O_2 accumulation in (**b**) by measuring the stained area (excluding the central vein) relative to the whole area of the leaf. (**d**) Pictures of representative 4-week-old plants 24 h after treatment with the ROS donors rose bengal (RB), methyl viologen (MV), the fungal toxin FB1, stained with Trypan blue to visualize cell death. (**d** and **e**) Quantification of cell death in (**d**) performed as in (**c**)

A fraction of full-length AtMC1 localizes to insoluble aggregates. The budding yeast *Saccharomyces cerevisiae* expresses a single type I metacaspase (Yca1), which mediates catalytic site-dependent PCD in this organism.[26–31] However, Yca1 also can be localized to insoluble protein aggregates where it promotes aggregate clearance independent of the Yca1 catalytic site.[41] Yca1 localization in protein aggregates is mediated by its N-terminal putative prodomain. We hypothesized that AtMC1 may also target protein aggregates and mediate its clearance, independent of its pro-death role during HR. Such a function could explain the early senescence and ROS/SA hypersensitivity of *atmc1* plants. Furthermore, it could account for the observed enhancement of the SA and ROS sensitivity phenotypes of *atmc1 atg18a*, since those plants would lack two complementary pro-life processes required to cope with the strains of aging.

We studied AtMC1 subcellular localization in plants conditionally overexpressing AtMC1-HA (Figure 5a).[35] Total protein extract (T) contained equal amounts of full-length and cleaved, presumably active AtMC1 (Figure 5a, left). Most of the cleaved AtMC1 localized in the soluble fraction (S), whereas full-length AtMC1 was also present in the microsomal/insoluble fraction (M + A). Subsequent solubilization of the microsomal/insoluble fraction revealed that AtMC1, in particular the full-length form, was insoluble (A). This indicates that a fraction of full-length AtMC1 likely localizes to insoluble protein aggregates. We performed the same fractionation using plants expressing the catalytic dead version of AtMC1 (AtMC1-C99A-C220A-HA).[35] The catalytic dead AtMC1 protein remained mostly insoluble. Taken together, these data indicate that at least part of the full-length AtMC1 localizes to insoluble aggregates independently of its catalytic activity, similar to yeast Yca1.

We also tested AtMC1 localization when expressed under the control of its native promoter (*atmc1 pAtMC1::AtMC1-HA*) using untreated or pathogen-treated young plants and older plants. Figure 5b shows that natively expressed AtMC1 protein accumulation is induced by pathogen-triggered HR cell death and aging. As expected, AtMC1 aggregate localization reaches its maximum in aging plants.

Subsequently, we analyzed aggregate content in Col-0, *atmc1*, *atg18a* and *atmc1 atg18a* under basal (Figure 5d), pathogen-induced cell death and aging conditions using the total and soluble fractions as a loading control (Figure 5c). Early senescing *atmc1* and *atg18a* mutants showed a higher aggregate content than wild-type plants. In *atmc1 atg18a* plants, aggregate over-accumulation was even more marked as expected from their additive phenotypes (Figure 5d). We hypothesize that localization mediates clearance of insoluble

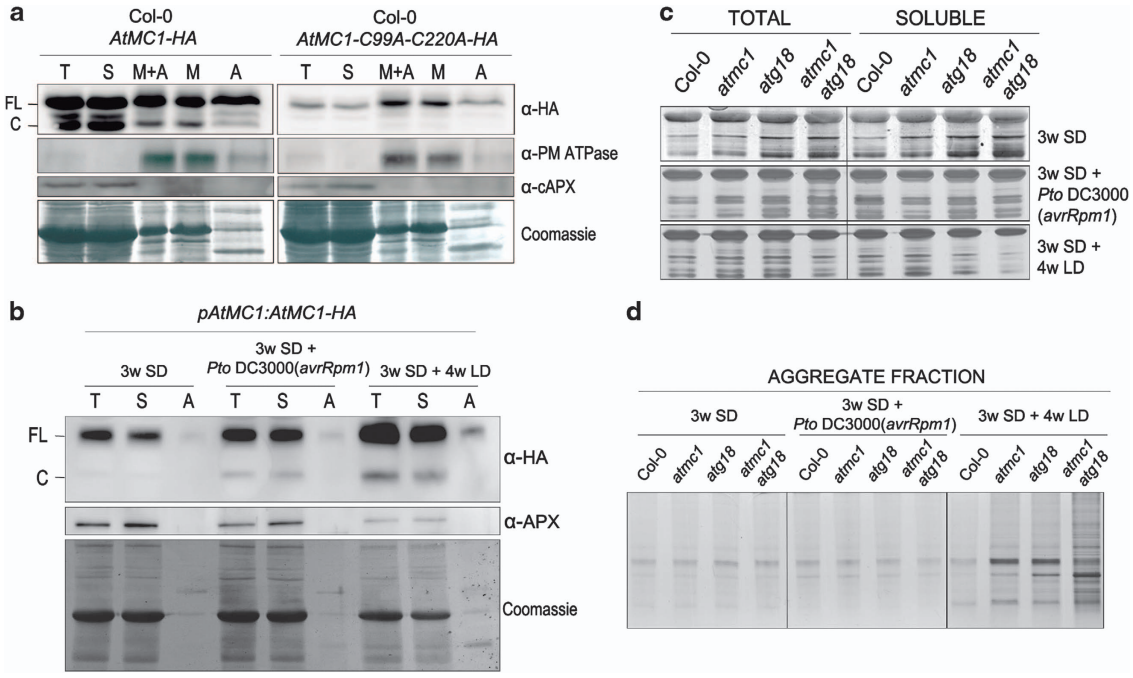

Figure 5 A fraction of full-length AtMC1 localizes to insoluble aggregates independent of its catalytic activity, contributing to aggregate clearance. (**a**) Protein extracts of 4-week-old Col-0 plants conditionally overexpressing AtMC1-HA (left) and AtMC1-C99AC220A-HA (right) were subjected to cellular fractionation. Total protein extract (T) was fractionated into a supernatant containing the soluble proteins (S) and a pellet, containing microsomal proteins and aggregates (S + A). This pellet was further fractionated into a supernatant, containing most of the microsomal proteins (M), and a pellet, containing insoluble protein aggregates (A). After separation on an SDS-PAGE gel, the fractions were either Coomassie-stained or analyzed by immunoblot using anti-HA, anti-cytosolic ascorbate peroxidase (cAPX) and anti-plasma membrane (PM) H^+ ATPase. The HA antibody recognized full-length AtMC1 (FL) and cleaved, putatively active AtMC1 (C). (**b**) *atmc1 pAtMC1::AtMC1-HA* plants were grown for 3 weeks under short-day conditions (3w SD), treated with 500 000 CFU/ml of *Pto* DC3000(*avrRpm1*) (3w SD + *Pto* DC3000(*avrRpm1*)) or transferred to long-day conditions (3w SD + 4w LD) and western blot analysis using anti-HA antibody or anti-cAPX was performed after fractionation into total (T), soluble (S) and insoluble aggregate (A) fractions. (**c** and **d**) Silver stains of total, soluble (**c**) and insoluble aggregate fractions (**d**) of plants of the indicated genotypes treated as in (**b**)

aggregates and thus contributes to cellular homeostasis and stress responses in a process that acts genetically in parallel to autophagy. This function is independent of, and does not preclude, the pro-death catalytic activity-dependent function of AtMC1 during HR cell death, which is most evident in young, non-stressed tissues.

Discussion

Autophagy and AtMC1 act in separate pathways as positive regulators of pathogen-triggered HR cell death. We previously demonstrated that AtMC1 is a positive regulator of HR cell death triggered by activation of different plant intracellular NLR innate immune receptors.[35] A similar pro-death function was reported for autophagy.[16,17] These findings were in sharp contrast to other studies, where autophagy was proposed as a pro-survival mechanism during HR cell death in plants.[8,51,52] These apparent discrepancies can be reconciled in a model where autophagy has a pro-death role locally in the HR site, whereas in the surrounding uninfected tissue, autophagy promotes survival, protecting cells beyond the HR site from unnecessary damage.[53,54] Signaling gradients that establish cell death control borders at sites of pathogen recognition have been demonstrated in plants.[48,55–58] Importantly, the studies that reported a pro-survival role of autophagy during pathogen-triggered HR cell death used relatively old plants.[8,51,52] With age, autophagy mutants become prematurely senescent and accumulate high levels of ROS that can drive accumulation of SA, potentially increasing their vulnerability to ER stress. Activation of defense responses upon infection may further destabilize the already altered homeostasis in autophagy mutants, rendering them unable to restrict cell death. Consistent with this proposal, prevention of SA accumulation suppresses premature senescence and runaway cell death after pathogen infection in *atg5*.[8]

We therefore assayed young autophagy mutant plants treated with low-dose bacterial inocula more closely mimicking natural infections to avoid the unwanted effects of combinatorial stresses. Our data confirm previous findings defining autophagy as a positive regulator of HR.[16,17] Autophagy and AtMC1 act separately to contribute to HR, as evidenced by the further suppression of cell death in *atmc1 atg18a*. However, the independent pathways thus defined cannot account for full HR, as cell death suppression in the double mutant is incomplete. Hence, there must exist (an)other pathway(s), which account for the remaining HR.

The idea that AtMC1 and autophagy function in separate pathways during HR is supported by the fact that they are differentially regulated. The metacaspase AtMC2 negatively regulates AtMC1[35] but not autophagy. SA mediates the pro-death function of autophagy, but not of AtMC1. In fact, SA is a negative regulator of the combined contributions to HR regulated by AtMC1 and undefined contributors to HR, as

illustrated by the nearly complete recovery of HR in *atg18a sid2* and the partial recovery of HR in *atmc1 atg18a sid2*. The recovery of HR in *atg18a sid2* is not due to altered basal SA levels in these mutants. Our data are in agreement with previous findings establishing that SA can act as a negative regulator of HR.[59] Furthermore, our results are consistent with the idea that autophagy can be both a positive and a negative regulator of HR depending on the spatio-temporal context (HR site *versus* adjacent tissues or young *versus* old tissue).[17,54] Finally, our data also show that HR suppression phenotypes in *atmc1*, *atg18a* and *atmc1 atg18a* is not accompanied by altered bacterial growth in any of these lines, further decoupling HR from pathogen growth restriction.[35]

The suppressed cell death phenotype in plants lacking AtMC1 is not due to defective autophagy. In order to explore the role of selective autophagy in pathogen-triggered HR and the possible linkage of AtMC1 to this process, we used the recently identified NBR1 autophagosome cargo protein marker.[45] Autophagy-deficient mutants accumulate higher NBR1 basal levels than wild-type,[45] which are further increased during the HR onset after RPM1 activation. This indicates that NBR1-mediated degradation of target proteins by autophagy may have an important role in HR cell death, perhaps contributing to vacuolar collapse.

Autophagy and AtMC1 independently control timely senescence in aging plants. Considering that autophagy has a main role in nutrient recycling,[6,7,9] it is not surprising that autophagy-deficient plants are prematurely senescent.[6–8] Furthermore, SA levels increase during senescence; this increase has been proposed to accelerate senescence once initiated.[60] Autophagy mutants start accumulating SA at an earlier developmental stage than the wild-type[8,13] and this over-accumulation underlies their premature senescent phenotype, as SA removal in these mutants results in normal timing of senescence.[8]

Besides its role in senescence, SA, in conjunction with ROS, is a potent defense regulator during infection.[61,62] Treatment with the SA analog BTH causes chlorosis, ROS hyper-accumulation and cell death in autophagy-deficient plants, but not in wild-type plants. This hypersensitivity could result from accumulation of damaged proteins and organelles in these plants because of impaired autophagy-dependent recycling, which renders them less able to cope with further stress. Like autophagy-deficient plants, *atmc1* plants are prematurely senescent and hypersensitive to BTH, ROS and necrotrophic fungi. In *atmc1 atg18a* plants, this phenotype is enhanced, indicating that the proteins act independently to downregulate these responses. Thus, AtMC1 has an additional, pro-survival homeostatic function in aging plants that acts in parallel to a similar pro-survival function of autophagy in aging.

A possible role of AtMC1 in protein aggregate clearance. Our data show that a fraction of the total full-length AtMC1 localizes to insoluble protein aggregates and this accumulation increases with age. Similar to yeast, aggregate localization of AtMC1 is also mediated by its N-terminal prodomain, and AtMC1 localization to protein aggregates does not require its catalytic activity. Furthermore, *atmc1* and *atg18a* plants, and to a further extent *atmc1 atg18a*, over-accumulate insoluble protein aggregates with age, which may be the cause of their premature senescence. The observed additive effects corroborate our notion that both pathways act independently to restrict insoluble protein aggregate accumulation.

Our hypothesis that AtMC1 functions in aggregate clearance is supported by the autophagy-like phenotypes of aging *atmc1* null mutants: premature senescence and ROS hypersensitivity AtMC1-mediated aggregate clearance and autophagy could constitute two complementary processes controlling cellular homeostasis during stress responses and aging by virtue of their ability to eliminate accumulated cellular debris.

A proposed model integrating the dual pro-death/pro-survival functions of AtMC1 and autophagy at different developmental stages. In young plants, we defined pro-death functions for autophagy and AtMC1 in HR control, as these functions were not masked by the cumulative stresses of aging. Figure 6a schematically shows a young plant cell undergoing HR after pathogen recognition. Under basal conditions, AtMC1 activation is prevented by the action of several negative regulators (AtMC2, LSD1[35] and probably other, unknown). Pathogen recognition leads to activation of intracellular NLR innate immune receptors, which results in local HR. In these circumstances, AtMC1 contributes to HR. Alternatively, enhanced auto-processing or processing by other metacaspases may contribute to accumulation of active AtMC1 in the cell. We speculate that the pro-death function of autophagy could be mediated by an active overload of the vacuole because of autophagy induction during HR, ultimately leading to vacuolar lysis. Interestingly, it has been recently reported that in Norway spruce the programmed vacuolar cell death that normally occurs in the

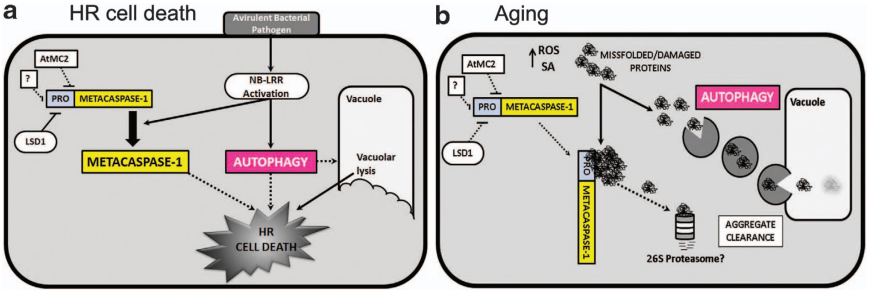

Figure 6 Proposed model integrating the dual pro-death/pro-survival functions of AtMC1 and autophagy at different developmental stages. (**a**) Pro-death functions of autophagy and AtMC1 in HR control in young plants. (**b**) Pro-survival role of autophagy and AtMC1 in aging cells

embryo suspensor requires autophagy, which lies downstream of a type II metacaspase,[15] indicating that the interactions between the various cell death regulators may vary depending on the cellular scenario.

In aging cells, the pro-survival functions of AtMC1 and autophagy are revealed by the constant increase of damaged proteins and organelles that accumulate in the cell and require clearance (Figure 6b). In this developmental scenario, autophagy is induced to clear aggregates via their autophagosome-mediated delivery to the vacuole. We hypothesize that AtMC1 also contributes to this process by independently targeting aggregates and facilitating their degradation. Our genetic framework sets the stage for the elucidation of these mechanisms.

Materials and Methods

Plant materials and growth. All experiments were performed using *Arabidopsis thaliana* accession Col-0. Single mutant lines have been previously described elsewhere: *atmc1* and *atmc2*,[35] *atg5* (SALK_020601),[42] *atg18a* (GABI651D08),[13] *atrbohD*,[59] *rpm1-3*[63] and *sid2/eds16*.[46] Transgenic Col-0 *35S::GFP-ATG8a* plants are described in Thompson *et al.*[43] and *atmc1 35S::GFP-ATG8a* plants were obtained by transformation using the floral dip method.[64]

Plants were grown under short-day conditions (9-h light, 21 °C; 15-h dark, 18 °C) for most experiments. To study senescence, plants were transferred to long-day conditions (15-h light, 21 °C; 8-h dark, 18 °C) 3 or 4 weeks after germination.

Cell death assay and bacterial growth. Single HR cell death events after infection with *Pto* DC3000(*avrRpm1*) were quantified according to Coll *et al.*[35]

Growth of *Pto* DC3000(*avrRpm1*) was tested using dip inoculations as previously described.[65]

Chemical treatments. Plants were grown 4 weeks under short-day conditions before treatment. For BTH treatment, plants were sprayed 300 μM BTH supplemented with 0.005% Silwett.

To monitor oxidative stress, a 2 μl drop of 100 μM Methyl viologen, a 10 μl drop of 2 mM rose bengal or a 5 μl drop of the necrotrophic fungal toxin FB1 were applied onto the abaxial surface of the leaf.

Stains. In order to visualize dead cells after chemical treatments, leaves were stained with Trypan blue as described.[66,67] H_2O_2 accumulation in leaves treated with BTH was visualized using 3,3′-diaminobenzidine staining as previously described.[59] To quantify cell death and H_2O_2 accumulation from the pictures, total leaf area and cell death or stained area was measured using ImageJ (Bethesda, MD, USA), and the ratio (area of cell death/ total leaf area) was calculated.

Infection with the necrotroph *Botrytis cinerea*. Five-week-old plants were sprayed with 1×10^6 spores/ml of *Botrytis cinerea*. Symptoms were visually followed for 1 week.

Total SA measurement. Total SA (free SA + glucose-conjugated SA, SAG) was measured as previously described,[68] using as starting material 100 mg of leaves from 2-week-old plants grown under short-day conditions (untreated).

RT-qPCR. Plant RNA was obtained from 2-week-old plants grown under short-day conditions or 5-week-old plants grown for 3 weeks under short-day and then transferred to long-day conditions. RNA was extracted using TRIzol (Life Technologies, Carlsbad, CA, USA) according to the manufacturer's instructions. RNA was treated 30 min with Ambion TURBO DNase (Life Technologies) to eliminate DNA contamination. Two microgram RNA was reverse transcribed using the Ambion RETROscript kit random decamers (Life Technologies).

RT-qPCR was performed using the Life Technologies SYBR Green PCR Master Mix in a total volume of 25 μl: 12.5 μl SYBR Green PCR Master Mix, 1 μl cDNA, 1 μl forward primer (10 μM), 1 μl reverse primer 2 (10 μM) and 9.5 μl H_2O. The reaction was run at 95 °C for 5 min, followed by 40 cycles at 95 °C for 15 s, 55 °C for 30 s and 72 °C for 30 s. Relative expression of SAG12 was calculated using the $\Delta\Delta$Ct method.[69] SAG12 (At5g45890) expression was first normalized to expression of the housekeeping gene elongation factor1α (At5g60390).

Confocal laser scanning microscopy. Seeds from transgenic lines expressing 35S::GFP-ATG8a in the Col-0 wild-type or *atmc1* mutant backgrounds were surface sterilized in a 50% bleach and 0.2% Triton X-100 solution for 10 min. Sterile seeds were plated onto solid MS medium plates (Murashige-Skoog Vitamin and Salt Mixture (Life Technologies), 2.4 mM MES (pH 5.7) and 0.9% Phyto Agar (Duchefa Biochemie, Haarlem, The Netherlands)). After 3 days vernalization at 4 °C in the dark, seedlings were grown for 1 week under short-day conditions. Seedlings were subsequently transferred to MS liquid medium (Murashige-Skoog Vitamin and Salt Mixture (Life Technologies), 2.4 mM MES (pH 5.7)) with or without 1 μM concanamycin A and incubated for 15 h in the dark.

Roots were imaged using a Zeiss LSM 710 confocal laser scanning microscope (Zeiss, Oberkochen, Germany). All images were collected using a 40x/1.2NA C-Apochromat water immersion objective. Imaging of cells expressing GFP was performed using 480 nm excitation Scan parameters including pinhole, gain and offset were identical for each experiment to ensure image accuracy. Images were analyzed using the ZEN 2009 software (Zeiss).

Protein analysis. For the analysis of NBR1 protein accumulation, 2-week-old plants were vacuum infiltrated with ~250 000 colony-forming units/ml of *Pto* DC3000(*avrRpm1*). Leaf samples were snap frozen in liquid nitrogen 12 h after infection and mechanically ground in 250 μl of plant extraction buffer (20 mM Tris (pH 7.5), 150 mM NaCl, 1 mM EDTA, 1% Triton X-100 and 0.1% SDS, 5 mM DTT and 1 : 100 dilution of Protease Inhibitor Cocktail (Sigma, St. Louis, MO, USA)). Protein extract was centrifuged 15 min at 10 000 $\times$ *g* at 4 °C. The supernatants were collected, boiled on SDS-loading buffer (120 mM Tris, pH 6.8, 50% glycerol, 6% SDS, 3 mM DTT and 1% Bromophenol blue) and separated on 7.5% SDS-PAGE gels. Immunoblot analysis was performed using a 1 : 1000 dilution of anti-NBR1 polyclonal antibody.

Cell fractionation. Plants were grown 4 weeks under short-day conditions. In all, 200 mg of leaf tissue was ground in 4 ml sucrose buffer (20 mM Tris (pH 8), 0.33 M sucrose, 1 mM EDTA (pH 8) and 1 : 100 dilution of Protease Inhibitor Cocktail (Sigma)) and filtered through Miracloth (Millipore, Billerica, MA, USA). Samples were centrifuged 5 min at 4 °C at 2000 $\times$ *g* to remove large particles. The supernatants were subsequently centrifuged 10 min at 4 °C at 6000 $\times$ *g*. An aliquot of the supernatant was collected representing the total protein fraction (T) and the rest was centrifuged at 100 000 $\times$ *g* at 4 °C for 90 min. The supernatant (S) of this centrifugation was the soluble fraction. To separate microsomal proteins from protein aggregates in the pellet (M + A), sucrose buffer containing 0.3% Triton X-100 was added. The pellet was redissolved by pipetting and incubation at 4 °C for 1 h. Triton X-100-treated M + A was then centrifuged 50 000 $\times$ *g* at 4 °C for 90 min. The supernatant (M) of this centrifugation represented the microsomal fraction, whereas the pellet (A) corresponded to insoluble protein aggregates. Protein extracts were boiled on SDS-loading buffer and separated on 12% SDS-PAGE gels. Gels were either Coomassie-stained or subjected to immunoblot analysis using a 1 : 5000 dilution of anti-HA monoclonal antibody (3F10, Roche, Basel, Switzerland), 1 : 10 000 anti-cAPX (Agrisera, Vännäs, Sweden) and anti-plasma membrane H^+ ATPase (Agrisera).

Alternatively, we used a modified version of the protocol described in Lee *et al.*[41] obtaining similar results. Essentially, 1 g of plant tissue was ground in liquid nitrogen and 2 ml of buffer B was added (Buffer B: 50 mM Tris, pH 7.5, 1 mM EDTA, 1% glycerol, 0.1% Nonidet P-40 and protease inhibitor cocktail (Roche)). Cell debris was eliminated by passing the protein extract through a Miracloth filter (Millipore) and two sequential spins of 2000 and 3000 $\times$ *g* at 4 °C. Equal amounts of supernatant were collected (total) and centrifuged at 100 000 $\times$ *g* at 4 °C for 90 min. The supernatant of this centrifugation corresponded to the soluble (S) fraction. The pellet was washed three times by adding buffer B supplemented with 2% Nonidet P-40 and centrifugation at 15 000 $\times$ *g* for 30 min. The resulting insoluble protein aggregate fractions were resuspended in an equal volume of buffer B (10 $\times$ concentrated relative to the total and soluble fractions) and sonicated using a Bioruptor (Diagenode, Seraing, Belgium). In all, 6 $\times$ loading buffer was then added and after boiling the samples for 10 min they were loaded on SDS-PAGE gels.

Silver staining. For silver staining, 40 μl of cell equivalents of the total, soluble and aggregate fractions (10 $\times$ concentrated) were loaded on 12% SDS-PAGE gels. Gels were fixed for 1 h in a 50% methanol, 37% formaldehyde and 12% acetic acid

solution. After three washes with 50% ethanol, gels were pre-treated 1 min with a 0.02% sodium thiosulfate solution, washed three times with water and stained 20 min in the dark with a 0.2% silver nitrate, 0.03% formaldehyde solution. Gels were then washed three times with water and treated with a 6% sodium carbonate, 0.02% formaldehyde, 0.0005% sodium thiosulfate solution until the bands became visible. Gels were then washed for 5 s with water and a stop solution (50% methanol and 12% acetic acid) was added for 10 min. Once the reaction was stopped, gels were transferred to water for short-term storage.

Conflict of Interest

The authors declare no conflict of interest.

Acknowledgements. We thank S Svenning (University of Tromsø, Norway) for the NBR1 antisera, T Nürnberger (University Tübingen, Tübingen, Germany) for the *atg18a* mutant seeds and S Dinesh-Kumar (University California-Davis, CA, USA) for the *atg5* mutant. We kindly thank R Vierstra (University Wisconsin-Madison, WI, USA) for critical reading of the manuscript and for sharing the Col-0 35S::GFP-ATG8a seeds with us. We also thank JL Crespo (Instituto de Bioquímica Vegetal y Fotosíntesis, Spain) for sharing the ATG8 antisera and for valuable advices. This research was supported by NIH grant RO1GM057171 JLD and PCDMC-321738 from EU-Marie Curie Actions and BP_B 00030 from the Catalan Government and to NSC. JLD is an HHMI investigator and this work was funded in part by the Howard Hughes Medical Institute and the Gordon and Betty Moore Foundation (GBMF3030).

1. Hara T, Nakamura K, Matsui M, Yamamoto A, Nakahara Y, Suzuki-Migishima R *et al.* Suppression of basal autophagy in neural cells causes neurodegenerative disease in mice. *Nature* 2006; **441**: 885–889.
2. Komatsu M, Waguri S, Chiba T, Murata S, Iwata J, Tanida I *et al.* Loss of autophagy in the central nervous system causes neurodegeneration in mice. *Nature* 2006; **441**: 880–884.
3. Takacs-Vellai K, Vellai T, Puoti A, Passannante M, Wicky C, Streit A *et al.* Inactivation of the autophagy gene bec-1 triggers apoptotic cell death in *C. elegans*. *Curr Biol* 2005; **15**: 1513–1517.
4. Gonzalez-Polo RA, Boya P, Pauleau AL, Jalil A, Larochette N, Souquere S *et al.* The apoptosis/autophagy paradox: autophagic vacuolization before apoptotic death. *J Cell Sci* 2005; **118**(Pt 14): 3091–3102.
5. Gordy C, He YW. The crosstalk between autophagy and apoptosis: where does this lead? *Protein Cell* 2012; **3**: 17–27.
6. Doelling JH, Walker JM, Friedman EM, Thompson AR, Vierstra RD. The APG8/12-activating enzyme APG7 is required for proper nutrient recycling and senescence in *Arabidopsis thaliana*. *J Biol Chem* 2002; **277**: 33105–33114.
7. Xiong Y, Contento AL, Bassham DC. AtATG18a is required for the formation of autophagosomes during nutrient stress and senescence in *Arabidopsis thaliana*. *Plant J* 2005; **42**: 535–546.
8. Yoshimoto K, Jikumaru Y, Kamiya Y, Kusano M, Consonni C, Panstruga R *et al.* Autophagy negatively regulates cell death by controlling NPR1-dependent salicylic acid signaling during senescence and the innate immune response in Arabidopsis. *Plant Cell* 2009; **21**: 2914–2927.
9. Hanaoka H, Noda T, Shirano Y, Kato T, Hayashi H, Shibata D *et al.* Leaf senescence and starvation-induced chlorosis are accelerated by the disruption of an Arabidopsis autophagy gene. *Plant Physiol* 2002; **129**: 1181–1193.
10. Xiong Y, Contento AL, Nguyen PQ, Bassham DC. Degradation of oxidized proteins by autophagy during oxidative stress in Arabidopsis. *Plant Physiol* 2007; **143**: 291–299.
11. Liu Y, Burgos JS, Deng Y, Srivastava R, Howell SH, Bassham DC. Degradation of the endoplasmic reticulum by autophagy during endoplasmic reticulum stress in Arabidopsis. *Plant Cell* 2012; **24**: 4635–4651.
12. Lai Z, Wang F, Zheng Z, Fan B, Chen Z. A critical role of autophagy in plant resistance to necrotrophic fungal pathogens. *Plant J* 2011; **66**: 953–968.
13. Lenz HD, Haller E, Melzer E, Kober K, Wurster K, Stahl M *et al.* Autophagy differentially controls plant basal immunity to biotrophic and necrotrophic pathogens. *Plant J* 2011; **66**: 818–830.
14. Kwon SI, Cho HJ, Jung JH, Yoshimoto K, Shirasu K, Park OK. The Rab GTPase RabG3b functions in autophagy and contributes to tracheary element differentiation in Arabidopsis. *Plant J* 2010; **64**: 151–164.
15. Minina EA, Filonova LH, Fukada K, Savenkov EI, Gogvadze V, Clapham D *et al.* Autophagy and metacaspase determine the mode of cell death in plants. *J Cell Biol* 2013; **203**: 917–927.
16. Hofius D, Schultz-Larsen T, Joensen J, Tsitsigiannis DI, Petersen NH, Mattsson O *et al.* Autophagic components contribute to hypersensitive cell death in Arabidopsis. *Cell* 2009; **137**: 773–783.
17. Kwon SI, Cho HJ, Kim SR, Park OK. The Rab GTPase RabG3b positively regulates autophagy and immunity-associated hypersensitive cell death in Arabidopsis. *Plant Physiol* 2013; **161**: 1722–1736.
18. Feinstein-Rotkopf Y, Arama E. Can't live without them, can live with them: roles of caspases during vital cellular processes. *Apoptosis* 2009; **14**: 980–995.
19. Portela M, Richardson HE. Death takes a holiday—non-apoptotic role for caspases in cell migration and invasion. *EMBO Rep* 2013; **14**: 107–108.
20. Rodrigue-Gervais IG, Saleh M. Caspases and immunity in a deadly grip. *Trends Immunol* 2013; **34**: 41–49.
21. van Doorn WG, Beers EP, Dangl JL, Franklin-Tong VE, Gallois P, Hara-Nishimura I *et al.* Morphological classification of plant cell deaths. *Cell Death Differ* 2011; **18**: 1241–1246.
22. Uren AG, O'Rourke K, Aravind LA, Pisabarro MT, Seshagiri S, Koonin EV *et al.* Identification of paracaspases and metacaspases: two ancient families of caspase-like proteins, one of which plays a key role in MALT lymphoma. *Mol Cell* 2000; **6**: 961–967.
23. McLuskey K, Rudolf J, Proto WR, Isaacs NW, Coombs GH, Moss CX *et al.* Crystal structure of a Trypanosoma brucei metacaspase. *Proc Natl Acad Sci USA* 2012; **109**: 7469–7474.
24. Tsiatsiani L, Van Breusegem F, Gallois P, Zavialov A, Lam E, Bozhkov PV. Metacaspases. *Cell Death Differ* 2011; **18**: 1279–1288.
25. Wong AH, Yan C, Shi Y. Crystal structure of the yeast metacaspase Yca1. *J Biol Chem* 2012; **287**: 29251–29259.
26. Gonzalez IJ, Desponds C, Schaff C, Mottram JC, Fasel N. Leishmania major metacaspase can replace yeast metacaspase in programmed cell death and has arginine-specific cysteine peptidase activity. *Int J Parasitol* 2007; **37**: 161–172.
27. Ivanovska I, Hardwick JM. Viruses activate a genetically conserved cell death pathway in a unicellular organism. *J Cell Biol* 2005; **170**: 391–399.
28. Khan MA, Chock PB, Stadtman ER. Knockout of caspase-like gene, YCA1, abrogates apoptosis and elevates oxidized proteins in *Saccharomyces cerevisiae*. *Proc Natl Acad Sci USA* 2005; **102**: 17326–17331.
29. Madeo F, Herker E, Maldener C, Wissing S, Lachelt S, Herlan M *et al.* A caspase-related protease regulates apoptosis in yeast. *Mol Cell* 2002; **9**: 911–917.
30. Mazzoni C, Herker E, Palermo V, Jungwirth H, Eisenberg T, Madeo F *et al.* Yeast caspase 1 links messenger RNA stability to apoptosis in yeast. *EMBO Rep* 2005; **6**: 1076–1081.
31. Silva RD, Sotoca R, Johansson B, Ludovico P, Sansonetty F, Silva MT *et al.* Hyperosmotic stress induces metacaspase- and mitochondria-dependent apoptosis in *Saccharomyces cerevisiae*. *Mol Microbiol* 2005; **58**: 824–834.
32. Lee N, Gannavaram S, Selvapandiyan A, Debrabant A. Characterization of metacaspases with trypsin-like activity and their putative role in programmed cell death in the protozoan parasite Leishmania. *Eukaryot Cell* 2007; **6**: 1745–1757.
33. Zalila H, Gonzalez IJ, El-Fadili AK, Delgado MB, Desponds C, Schaff C *et al.* Processing of metacaspase into a cytoplasmic catalytic domain mediating cell death in Leishmania major. *Mol Microbiol* 2011; **79**: 222–239.
34. Laverriere M, Cazzulo JJ, Alvarez VE. Antagonic activities of Trypanosoma cruzi metacaspases affect the balance between cell proliferation, death and differentiation. *Cell Death Differ* 2012; **19**: 1358–1369.
35. Coll NS, Vercammen D, Smidler A, Clover C, Van Breusegem F, Dangl JL *et al.* Arabidopsis type I metacaspases control cell death. *Science* 2010; **330**: 1393–1397.
36. Ambit A, Fasel N, Coombs GH, Mottram JC. An essential role for the Leishmania major metacaspase in cell cycle progression. *Cell Death Differ* 2008; **15**: 113–122.
37. Helms MJ, Ambit A, Appleton P, Tetley L, Coombs GH, Mottram JC. Bloodstream form Trypanosoma brucei depend upon multiple metacaspases associated with RAB11-positive endosomes. *J Cell Sci* 2006; **119**(Pt 6): 1105–1117.
38. Proto WR, Castanys-Munoz E, Black A, Tetley L, Moss CX, Juliano L *et al.* Trypanosoma brucei metacaspase 4 is a pseudopeptidase and a virulence factor. *J Biol Chem* 2011; **286**: 39914–39925.
39. Szallies A, Kubata BK, Duszenko M. A metacaspase of Trypanosoma brucei causes loss of respiration competence and clonal death in the yeast *Saccharomyces cerevisiae*. *FEBS Lett* 2002; **517**: 144–150.
40. Lee RE, Puente LG, Kaern M, Megeney LA. A non-death role of the yeast metacaspase: Yca1p alters cell cycle dynamics. *PLoS One* 2008; **3**: e2956.
41. Lee RE, Brunette S, Puente LG, Megeney LA. Metacaspase Yca1 is required for clearance of insoluble protein aggregates. *Proc Natl Acad Sci USA* 2010; **107**: 13348–13353.
42. Wang Y, Nishimura MT, Zhao T, Tang D. ATG2, an autophagy-related protein, negatively affects powdery mildew resistance and mildew-induced cell death in Arabidopsis. *Plant J* 2011; **68**: 74–87.
43. Thompson AR, Doelling JH, Suttangkakul A, Vierstra RD. Autophagic nutrient recycling in Arabidopsis directed by the ATG8 and ATG12 conjugation pathways. *Plant Physiol* 2005; **138**: 2097–2110.
44. Debener T, Lehnackers H, Arnold M, Dangl JL. Identification and molecular mapping of a single *Arabidopsis thaliana* locus determining resistance to a phytopathogenic Pseudomonas syringae isolate. *Plant J* 1991; **1**: 289–302.
45. Svenning S, Lamark T, Krause K, Johansen T. Plant NBR1 is a selective autophagy substrate and a functional hybrid of the mammalian autophagic adapters NBR1 and p62/SQSTM1. *Autophagy* 2011; **7**: 993–1010.
46. Wildermuth MC, Dewdney J, Wu G, Ausubel FM. Isochorismate synthase is required to synthesize salicylic acid for plant defence. *Nature* 2001; **414**: 562–565.
47. Tsuda K, Sato M, Glazebrook J, Cohen JD, Katagiri F. Interplay between MAMP-triggered and SA-mediated defense responses. *Plant J* 2008; **53**: 763–775.
48. Torres MA, Jones JD, Dangl JL. Pathogen-induced, NADPH oxidase-derived reactive oxygen intermediates suppress spread of cell death in *Arabidopsis thaliana*. *Nat Genet* 2005; **37**: 1130–1134.

49. Noh YS, Amasino RM. Identification of a promoter region responsible for the senescence-specific expression of SAG12. *Plant Mol Biol* 1999; **41**: 181–194.
50. Govrin EM, Levine A. The hypersensitive response facilitates plant infection by the necrotrophic pathogen Botrytis cinerea. *Curr Biol* 2000; **10**: 751–757.
51. Liu Y, Schiff M, Czymmek K, Talloczy Z, Levine B, Dinesh-Kumar SP. Autophagy regulates programmed cell death during the plant innate immune response. *Cell* 2005; **121**: 567–577.
52. Patel S, Dinesh-Kumar SP. Arabidopsis ATG6 is required to limit the pathogen-associated cell death response. *Autophagy* 2008; **4**: 20–27.
53. Hayward AP, Dinesh-Kumar SP. What can plant autophagy do for an innate immune response? *Annu Rev Phytopathol* 2011; **49**: 557–576.
54. Hofius D, Munch D, Bressendorff S, Mundy J, Petersen M. Role of autophagy in disease resistance and hypersensitive response-associated cell death. *Cell Death Differ* 2011; **18**: 1257–1262.
55. Costet L, Cordelier S, Dorey S, Baillieul F, Fritig B, Kauffmann S. Relationship between localized acquired resistance (LAR) and the hypersensitive response (HR): HR is necessary for LAR to occur and salicylic acid is not sufficient to trigger LAR. *Mol Plant Microbe Interact* 1999; **12**: 655–662.
56. Dorey S, Baillieul F, Pierrel MA, Saindrenan P, Fritig B, Kauffmann S. Spatial and temporal induction of cell death, defense genes, and accumulation of salicylic acid in tobacco leaves reacting hypersensitively to a fungal glycoprotein elicitor. *Mol Plant Microbe Interact* 1997; **10**: 646–655.
57. Roberts M, Tang S, Stallmann A, Dangl JL, Bonardi V. Genetic requirements for signaling from an autoactive plant NB-LRR intracellular innate immune receptor. *PLoS Genet* 2013; **9**: e1003465.
58. Shirasu K, Nakajima H, Rajasekhar VK, Dixon RA, Lamb C. Salicylic acid potentiates an agonist-dependent gain control that amplifies pathogen signals in the activation of defense mechanisms. *Plant Cell* 1997; **9**: 261–270.
59. Torres MA, Dangl JL, Jones JD. Arabidopsis gp91phox homologues AtrbohD and AtrbohF are required for accumulation of reactive oxygen intermediates in the plant defense response. *Proc Natl Acad Sci USA* 2002; **99**: 517–522.
60. Abreu ME, Munne-Bosch S. Photo- and antioxidant protection and salicylic acid accumulation during post-anthesis leaf senescence in Salvia lanigera grown under Mediterranean climate. *Physiol Plant* 2007; **131**: 590–598.
61. Lawton KA, Friedrich L, Hunt M, Weymann K, Delaney T, Kessmann H *et al.* Benzothiadiazole induces disease resistance in Arabidopsis by activation of the systemic acquired resistance signal transduction pathway. *Plant J* 1996; **10**: 71–82.
62. Yang Y, Shah J, Klessig DF. Signal perception and transduction in plant defense responses. *Genes Dev* 1997; **11**: 1621–1639.
63. Grant MR, Godiard L, Straube E, Ashfield T, Lewald J, Sattler A *et al.* Structure of the Arabidopsis RPM1 gene enabling dual specificity disease resistance. *Science* 1995; **269**: 843–846.
64. Clough SJ, Bent AF. Floral dip: a simplified method for Agrobacterium-mediated transformation of *Arabidopsis thaliana*. *Plant J* 1998; **16**: 735–743.
65. Tornero P, Dangl JL. A high-throughput method for quantifying growth of phytopathogenic bacteria in *Arabidopsis thaliana*. *Plant J* 2001; **28**: 475–481.
66. Keogh RC, Deverall BJ, McLeod S. Comparison of histological and physiological responses to Phakopsora pachyrhizi in resistant and susceptible soybean. *Trans Br Mycol Soc* 1980; **74**: 329–333.
67. Koch E, Slusarenko A. Arabidopsis is susceptible to infection by a downy mildew fungus. *Plant Cell* 1990; **2**: 437–445.
68. Bonardi V, Tang S, Stallmann A, Roberts M, Cherkis K, Dangl JL. Expanded functions for a family of plant intracellular immune receptors beyond specific recognition of pathogen effectors. *Proc Natl Acad Sci USA* 2011; **108**: 16463–16468.
69. Livak KJ, Schmittgen TD. Analysis of relative gene expression data using real-time quantitative PCR and the 2(-delta delta C(T)) method. *Methods* 2001; **25**: 402–408.

Supplementary Information accompanies this paper on Cell Death and Differentiation website (http://www.nature.com/cdd)